Agrociencia

eISSN: 2521-9766

VOLUME 59, NUMBER 6 | August 16 - September 30, 2025 | MÉXICO

In Memoriam

Julieta Norma Fierro Gossman

1948 – 2025

AGRICULTURA
SECRETARIA DE AGRICULTURA

COPYRIGHT AND RELATED RIGHTS, **Volume 59, Number 6, August 16 - September 30, 2025**, Agrociencia is a semi-monthly publication edited by Colegio de Postgraduados. Carretera Mexico-Texcoco, Km 36.5, Montecillo, Texcoco, State of Mexico. C. P. 56264. Phone: 5959284427. www.colpos.mx. Editor in chief: Dr. Fernando Carlos Gómez Merino. Reservations of Rights to Exclusive Use 04-2021-031913431800-203. eISSN: 2521-9766, granted by the National Copyright Institute. Last modification date, **September 30, 2025**.

All correspondence (subscription information, sales, advertising, author contributions, etc.) should be addressed to:

Central Office:

Agrociencia
Guerrero No. 9, Esquina con Avenida Hidalgo,
San Luis Huexotla, Texcoco 56220,
State of Mexico. MEXICO
Tel.: +52-595 92 84427

https://agrociencia-colpos.org/index.php/agrociencia

Cover: Dra. Julieta Norma Fierro Gossman
(Mexico City, February 24th, 1948 – Mexico City, September 19th, 2025)
Distinguished Mexican physicist, astronomer, and science communicator

AGRICULTURA
SECRETARÍA DE AGRICULTURAY DESARROLLO RURAL

Contents

Volume 59, Number 6 | August 16 - September 30, 2025

Applied Mathematics-Statistics-Computer Science

Biotechnology

Crop Science

Agrociencia

INTERNET OF THINGS SENSOR DATA AND META-ALGORITHMIC APPROACHES FOR ADVANCED CLIMATE CHANGE-RELATED NATURAL DISASTER PREDICTION

Thirumalaimuthu **Babu**[1], Karuppaiya Sathaiah **Balamurugan**[2], Kanmani Pappa **Chandramohan**[3], Surendran **Rajendran**[4*]

[1]St. Joseph's College of Engineering. Department of Electrical and Electronic Engineering. Chennai, Tamil Nadu, India. 600119.
[2]Karpaga Vinayaga College of Engineering and Technology. Department of Electronics and Communication Engineering. Chengalpattu, Tamil Nadu, India. 603308.
[3]Vel Tech Rangarajan Dr. Sagunthala R&D Institute of Science and Technology. Department of Electronics and Communication Engineering. Chennai, Tamil Nadu, India. 600062.
[4]Saveetha Institute of Medical and Technical Sciences. Department of Computer Science and Engineering. Chennai, Tamil Nadu, India. 602105.
* Author for correspondence: dr.surendran.cse@gmail.com

Citation: Babu T, Balamurugan KS, Chandramohan KP, Rajendran S. 2025. Internet of things sensor data and meta-algorithmic approaches for advanced climate change-related natural disaster prediction. **Agrociencia** 59(6): 784-799. https://doi.org/ 10.47163/agrociencia.v59i6.3427

Editor in Chief:
Dr. Fernando C. Gómez Merino

Received: March 19, 2025.
Approved: September 12, 2025.
Published in Agrociencia: September 23, 2025.

ABSTRACT

Natural disasters are catastrophic events caused by natural phenomena such as earthquakes, floods, hurricanes, and wildfires, resulting in severe damage, destruction, and human suffering. Existing methods for predicting natural disasters often lack precision because of the complexity and variability of natural processes, limited data availability, and the unpredictable cascading effects of initial events such as earthquakes. In this work, a range of machine learning techniques was applied for predicting various natural disasters under climate change: Long Short-Term Memory (LSTM) networks for earthquakes, Support Vector Machines (SVM) for tsunamis, Convolutional Neural Networks (CNN) for cyclones, and Random Forest (RF) for extreme temperatures. These models were integrated into a comprehensive meta-algorithm, enhanced by the Internet of Things (IoT) for real-time data collection and analysis. Performance evaluation against traditional models, including the Ensemble Decision Tree model and the Logistic Discriminant model, showed that the meta-algorithm achieved 5 % greater accuracy, highlighting its effectiveness in natural disaster prediction.

Keywords: machine learning, Meta Algorithm, data collection, data analysis.

INTRODUCTION

The Internet of Things (IoT) incorporates several enabling technologies, including 5G connectivity, advanced sensors, intelligent actuators, and software applications, and has become a crucial component of modern information technology and smart communications (Balamurugan *et al*., 2024). These technologies together establish a framework for smart connectivity that addresses key challenges such as data transfer

in cloud-edge services, functional performance, availability, and quality of service (QoS) metrics.

Intelligent sensors and actuators in the IoT environment are constrained by limited storage capacity and short battery life, which restrict their ability to retain large volumes of data for intelligent networking (Vinuja and Devi, 2024). Efficient information broadcasting is essential for transferring data from the IoT layer to the distributed computing layer for processing and storage. Several studies have shown that the IoT framework is increasingly applied to safety-critical situations, such as wildfires, earthquakes, floods, blizzards, hurricanes, seasonal tornadoes, and landslides, where it supports disaster management and response. Due to global warming, natural disasters occur with increasing frequency and intensity. It is essential to implement preventive measures prior to such events, collect and analyze information in real time during their occurrence, and conduct accurate post-event assessments. The fatalities and injuries from these disasters not only cause long-term societal trauma but also result in significant economic losses. Voosen et al (2025) discussed according to the National Oceanic and Atmospheric Administration (NOAA), the global average temperature increased by approximately 1 °C between 1901 and 2020. This rise has contributed to sea levels rising at nearly twice their historical rate, while melting glaciers faster.

The National Aeronautics and Space Administration (NASA) has reported that climate-related changes intensify the natural disasters experienced worldwide, increasing both their frequency and diversity. Natural disasters have a profound impact on people's lives, causing displacement, loss of housing, and disruption of livelihoods. They also cause physical injuries, emotional trauma, and severe psychological distress. According to the International Monetary Fund (IMF), the negative consequences are most severe for low-income countries. The lack of access to critical resources such as safe drinking water, food, and healthcare exacerbates these issues. Communities frequently face long-term economic hardship and recovery barriers as a result of severe damage to support systems and infrastructure.

IoT and artificial intelligence (AI) are increasingly intertwined, transforming various sectors. IoT devices collect massive amounts of data, which AI algorithms analyze to produce actionable insights and support autonomous decision-making (Umamaheswari *et al*., 2025). This combination improves efficiency in industries like manufacturing, healthcare, and transportation by enabling predictive maintenance, personalized medicine, and self-driving vehicles. AI strengthens IoT by increasing data processing speed, accuracy, and security, while IoT extends AI's reach by collecting real-time data from interconnected devices. Together, these technologies foster smarter, more adaptive, and responsive systems across diverse applications. Despite significant advances in AI and IoT, predicting specific natural disasters, particularly earthquakes, remains a major scientific challenge. Their inherently unpredictable nature, absence of reliable precursors, and the complexity of subsurface processes make long-term forecasting extremely difficult. In seismically active regions such as Mexico, traditional prediction approaches remain virtually unfeasible. Suárez *et al*.

(2022) developed the early warning systems, such as the Mexican Seismic Alert System (SASMEX), provide only seconds to a few minutes of lead time by detecting initial seismic waves. This emphasizes the need to develop hybrid frameworks that integrate real-time sensing, rapid alerts, and efficient communication with communities, rather than relying exclusively on long-term predictions.

Urban floods, caused by the unpredictable intensity of rainfall, can cause significant damage and are highly nonlinear events that are difficult to analyze. Keum *et al*. (2020) proposed a real-time flood prediction system based on classification by utilizing linear and nonlinear regression techniques. The system incorporated screening methods such as Probabilistic Neural Networks (PNN) and Latin Hypercube Sampling (LHS) to enhance forecasting accuracy, achieving 85 % accuracy with a processing time of 1 min and 12 s. Additionally, instruments designed according to the disaster management framework were developed to ensure alignment with actual emergency response procedures (Elshami *et al*., 2025). The integration of expert evaluations and statistical validation techniques, including factor analysis and consistency assessments, enhances the reliability and practical applicability of these tools across diverse healthcare settings. Suhardono *et al*. (2025) highlighted the importance of integrating community education, early warning systems, and infrastructure planning to strengthen disaster resilience in coastal regions. Using a choice experiment methodology, researchers assessed public preferences and the economic valuation of preparedness strategies. Multi-scenario frameworks that integrate educational, logistical, and ecological components have proven to be effective models for comprehensive disaster management.

Duraisamy and Natarajan (2024) applied an enhanced Bidirectional Encoder Representations from Transformers (BERT) model with Twitter data for disaster prediction, showing superior performance compared to Gated Recurrent Unit (GRU) and Memory-Augmented Neural Networks (MANN). Khan *et al*. (2024) introduced a non-intrusive, cost-effective geophysical approach that integrates regional-scale geology for detecting and forecasting rock bursts in coal mines in northwestern China. Yang *et al*. (2023) proposed a hybrid model combining Long Short-Term Memory (LSTM), Random Forest (RF), and Multitask Deep Belief Networks (MDBN) for landslide prediction. Overall, the combined model achieved high predictive reliability for landslide vulnerability. Sathianarayanan *et al.* (2024) introduced a Convolutional Neural Network (CNN) detection model along with multi-digit phone number data and street view house numbers, and achieved over 79 % of average precision, 82 % aggregated average precision, and an overlap coefficient of 0.5. Zheng *et al*. (2024) proposed a multi-factor geographic game restoration approach for forecasting mineral water inrush catastrophes, using Principal Component Analysis (PCA), a Whale Optimization Algorithm-Random Forest-Geographic Information System (WOA-RF-GIS), and Collaborative Kriging Interpolation to address data dimensionality. Özen and Souri (2024) introduced a method combining Analysis of Variance (ANOVA)-based feature selection with the Optimized Ensemble Bagged Tree (OEBT) algorithm, integrated with cloud-based prediction and 5G technology. Their approach achieved

a reliability of 97.9 %, precision of 98.7 %, recall of 78.9 %, and an F1-score of 78.3 %. Park and Lee (2024) developed new hybrid fuzzy-Deep Neural Network (DNN) method for urban floods with high accuracy. Chai and Wu (2023) proposed a method with AI and multi-criteria decision-making (MCDM) for the early prediction of earth quakes through continuous monitoring. Powers *et al*. (2023) introduced a method for sending emergency messages on social media during natural disasters using deep learning techniques, including CNNs, BERT, and XLNet, with CNNs demonstrating the highest accuracy. Similarly, Wu *et al*. (2023) developed a conceptual model based on Data Envelopment Analysis (DEA) to assess regional disaster susceptibility across mainland China, using annual data from official Chinese statistics spanning 2006 to 2021. The model incorporated five input factors: population density, gross domestic product (GDP) per square kilometer, per capita GDP, total regional population, and regional investments in water conservation, environmental management, and public services. Zhu *et al*. (2021) proposed a flood forecasting technique that integrates the Ensemble Decision Tree model with Geographic Information System (GIS) technologies, demonstrating that the combination of the RF algorithm and GIS is effective for analyzing the spatial distribution and underlying patterns of flood risk. Anbarasan *et al*. (2020) developed a flood detection approach using IoT, Big Data, and Convolutional Deep Neural Networks (CDNNs), which outperformed established algorithms such as Feedforward Neural Networks (FNNs) and Hierarchical Neural Networks (HNNs) in terms of accuracy. These studies highlight the value of integrating advanced computational methods and diverse data sources to improve natural disaster prediction under varying conditions.

MATERIALS AND METHODS

An integrated system for natural disaster prediction was developed using IoT sensors and advanced machine learning models (Figure 1). Sensors such as seismometers, buoys, barometers, and climate stations collect real-time environmental data, which is transmitted to a cloud-based infrastructure for processing. In the cloud, machine learning models such as LSTM for earthquakes, SVM for tsunamis, CNNs for cyclones, and RF for extreme temperatures analyze incoming data to generate predictive insights.

Data preparation

Sensors continuously collect environmental data to support the prediction of earthquakes, tsunamis, cyclones, and extreme temperature events. Seismometers detect ground vibrations for earthquake forecasting, while ocean buoys and pressure sensors monitor sea level changes for tsunami detection. Climate stations measure wind speed, atmospheric pressure, and temperature to track cyclones and extreme heat or cold events, enabling timely and informed disaster preparedness.

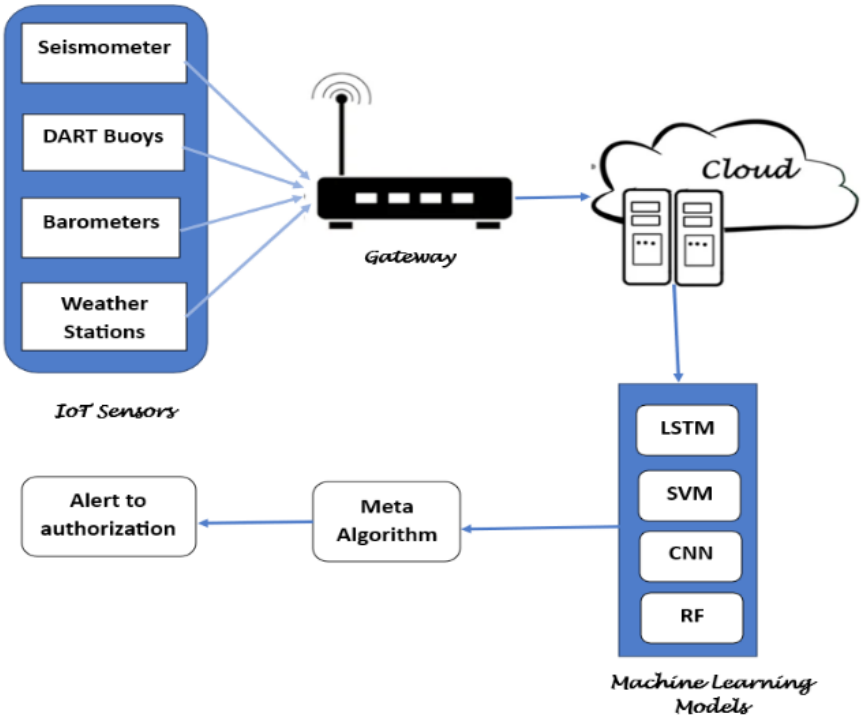

Figure 1. Proposed integrated Internet of Things (IoT) and machine learning model for real-time natural disaster prediction.

Datasets for this study were obtained from Kaggle, a platform providing curated data across multiple domains to support data-driven research and analysis. The earthquake dataset includes approximately three million records of seismic events worldwide from 1990 to 2023, with each entry detailing attributes such as timestamp, geographic coordinates (latitude and longitude), magnitude, epicenter depth, magnitude measurement type, affected area, and other relevant information.

The Global Historical Tsunami Database catalogs over 2400 tsunami events from 2100 BC to the present, covering the Atlantic, Indian, and Pacific Oceans, as well as the Mediterranean and Caribbean Seas. The National Hurricane Center (NHC) maintains the HURDAT historical tropical cyclone database, which includes Atlantic HURDAT2 and Northeast/North Central Pacific HURDAT2 datasets. These records, which are updated every six hours, include cyclone positions, peak wind speeds, central pressures, and storm dimensions for all tropical and subtropical cyclones.

For extreme temperatures, the Land Max Temperature and Land Min Temperature datasets were used, containing the highest and lowest average global land temperatures, respectively, each with associated uncertainty intervals. Additionally, the Land and Ocean Average Temperature dataset provides combined global land and ocean temperatures in Celsius, along with its corresponding uncertainty measurements.

Preprocessing

Data preprocessing was performed prior to transmission to the cloud to reduce bandwidth usage, improve data quality, minimize false alarms, enhance processing efficiency, and lower costs. Sensor data noise was mitigated using the moving average technique, which smooths measurements by averaging values within a sliding window:

$$MA_i = \frac{1}{\omega}\sum_{i=t-\omega+1}^{t} x_i$$

where MA_i represents moving average value at time t, ω is the size of window, and x_i represents data points within the window.

To reduce the volume of data transmitted to the cloud, downsampling was applied, decreasing the frequency of data points by selecting a representative subset. For a time series $X + \{x_1, x_2, \ldots x_n\}$ and a down sampling factor k:

$$X' = \{x_1, x_{1+k}, x_{1+2k}, \ldots\}$$

where X' is the down sampling dataset, and k is the down sampling factor.

The processed data is transmitted to the cloud via a cloud gateway, which serves as an intermediary between the sensors and the cloud storage platform. In the cloud, data is securely stored in a scalable infrastructure, enabling efficient access, management, and analysis. Machine learning models are then applied to process the data, train predictive models, and generate actionable insights for different types of natural disasters (Santhanaraj *et al*., 2023). This integration of cloud storage and machine learning allows large-scale processing of sensor data, supporting real-time decision-making and analytics.

Hyperparameter tuning

Every machine learning model requires careful parameter tuning to achieve optimal performance. The systematic search technique was employed for this purpose, specifically using Grid Search, which evaluates a predefined set of parameters to identify the configuration that maximizes model performance (Surendran *et al*., 2023). The process involves several sequential steps to determine the best hyperparameters. First, the machine learning model M must be defined. A decision tree classifier $M(\theta)$ uses a parameter set θ that includes the maximum tree depth (d), the minimum number of samples required to split an internal node (s), and the minimum number of samples required at a leaf node (l). Hyperparameters along with their range of values need to be defined next. For example, let θ={d,s,l} where:

$d \in \{3,5,7,10\};\ s \in \{2,5,10\};\ l \in \{1,2,4\}$

A parameter grid Θ is created as the Cartesian product of all hyperparameter values:

$$\Theta = \{ (d, s, l) \mid d \in \{3,5,7,10\}, s \in \{2,5,10\}, l \in \{1,2,4\} \}$$

To evaluate system performance, an appropriate scoring metric S is selected. For classification tasks, this is typically accuracy (A), calculated as:

$$A = \frac{\text{Number of correct predictions}}{\text{Number of test cases}}$$

The dataset D was partitioned into training and testing sets, and k-fold cross-validation was employed to ensure robust performance evaluation. The model is trained and validated k times, each time using a different subset as the validation set and the remaining k-1 subsets for training. The overall performance is calculated as the average across all k iterations:

$$S_{cv} = \frac{1}{k} \sum_{i=1}^{k} S_i$$

Grid search is implemented by iterating over each combination of hyperparameters $\theta \in \Theta$, training the model M(θ) on the training dataset, and evaluating its performance using the selected scoring metric on the validation set. The optimal set of model parameters is denoted as θ^*:

$$\theta^* = \arg max_{\theta \in \Theta} S_{cv}(\theta)$$

After determining the optimal hyperparameters θ^*, the model M(θ^*) is retrained on the full training dataset and its performance is evaluated on an independent test set T to assess generalization capability:

$$S_{test} = S(M(\theta^*), T)$$

After completing hyperparameter tuning and cross-validation, each machine learning model was trained for validation. The selected algorithms for predicting each natural disaster are as follows: Earthquakes, Tsunami, Cyclone, and Extreme Temperature.
The likelihood and magnitude category of future earthquake events were predicted using time-series data, including seismic wave velocity, magnitude, and depth. A three-layer LSTM network with 64, 32, and 16 units was used, followed by a dense

layer with sigmoid activation for binary classification. The input shape was *(batch_size, time_steps, features)*, with features comprising magnitude, depth, and timestamp intervals. The model was compiled using binary cross-entropy loss and the Adam optimizer.

Model 1. Long Short-Term Memory (LSTM) earthquake prediction

The input to the LSTM model is a multivariate time series, where each sequence represents seismic activity over time. Each time step includes magnitude of the earthquake (float), depth of the event (float), latitude and longitude (float), and timestamp (converted to a numerical or cyclic format).

The final input shape for the LSTM model is:

$$X_{train} \in R^{(N,T,F)}$$

where N is the number of samples, T represents time steps, and F represents number of features per step.

The output is a single predicted magnitude of the next earthquake event:

$$y_{train} \in R^{(N,1)}$$

The model learns temporal patterns to forecast the magnitude of the next event based on previous sequences.

Model 2. Support Vector Machine (SVM) for tsunami prediction

A Support Vector Machine (SVM) classifier with a radial basis function (RBF) kernel was employed to determine whether a seismic or oceanic event would trigger a tsunami. Input features included wave height (1–30 m), sea-level pressure, water displacement, sea surface temperature, earthquake magnitude, and geographic coordinates (latitude and longitude). Hyperparameters C and γ were optimized using grid search. The target variable y was a binary label indicating tsunami occurrence (1 = tsunami, 0 = no tsunami).

Model 3. Convolutional Neural Networks (CNN) for cyclone prediction

Convolutional Neural Networks (CNN) for cyclone prediction to classify the risk level of extreme temperature events (hot or cold) based on historical temperature, humidity, and pressure data, used a RF classifier with 100 estimators and gini criterion. Input features included land max temp, min temp, and surface pressure. Hyperparameters were tuned using GridSearchCV.

Model 4. Random Forest (RF) for prediction of extreme temperatures

Random Forest (RF) for prediction of extreme temperatures used after the completion of training and validation for each model using grid search, a meta-algorithm can be utilized to add the outputs of these individual models to achieve higher accuracy and robustness.

Meta Algorithm

Ensemble learning combines multiple models to achieve predictive performance superior to any single model (Zheng *et al*., 2024). By leveraging a diverse set of models, ensemble methods can correct individual errors, improving overall accuracy. In this study, the Adaptive Boosting (AdaBoost) algorithm was employed, a technique recently applied in cloud–IoT disaster management systems for enhanced reliability and precision (Sathianarayanan *et al*., 2024). Each model in the sequence is trained on a reweighted dataset, emphasizing previously misclassified instances, and the final prediction is obtained as a weighted aggregate of the individual model outputs.

AdaBoost is an ensemble learning method that combines multiple weak classifiers, typically decision stumps, into a strong predictive model. It trains models while reweighting misclassified instances, allowing subsequent classifiers to focus on harder cases. This iterative process reduces bias and improves the overall accuracy of the final model. Mathematically, the following is a description of the AdaBoost algorithm:

Initialization

All training instances are initially assigned equal weights. Given a training dataset $\{(x_1, y_1), (x_2, y_2), \ldots (x_m, y_m)\}$, where x_i are the input features and $y_i \in \{-1,1\}$ are the class labels, the initial weight $w_1(i)$ for each instance i is:

$$w_1(i) = \frac{1}{m} \; for \; i = 1,2, \ldots, m$$

During each boosting iteration $t = 1, 2, \ldots, T$, a weak learner $h_t(x)$ is trained on the weighted dataset. The performance of each learner is evaluated by computing its weighted error rate ($\in_t$):

$$\epsilon_t = \sum_{i=1}^{m} w_t(i).I\left(y_i \neq h_t(x_i)\right)$$

where I is the indicator function, returning one if the condition is met and zero otherwise. Based on this error rate, the weight α_t of the weak learner is determined as:

$$\alpha_t = \frac{1}{2}\ln\left(\frac{1-\epsilon_t}{\epsilon_t}\right)$$

This weight reflects the contribution of each weak learner to the final ensemble, with lower-error learners receiving higher influence in the aggregated prediction.

Updating instance weights

For the following iteration, modify the training entities' sizes. Accurately identified cases are assigned a lower value than occurrences that are misclassified by the present weak learner:

$$w_{i+1}(i) = w_t(i).\exp\left(\alpha_t.I(y_i \neq h_t(x_i)\right)$$

To maintain a valid probability distribution, the updated weights are normalized so that they sum to one:

$$w_{t+1}(i) = \frac{w_{t+1}(i)}{\sum_{j=1}^{m} w_{t+1}(j)}$$

Final classifier

After completing all iterations, the final classifier $H(x)$ is obtained as a weighted sum of the individual weak learners:

$$H(x) = sign \sum_{t=1}^{T} \left(\alpha_t h_t(x)\right)$$

The class label is determined by the sign of the weighted sum, where the *sign* function assigns the predicted class based on whether the sum is positive or negative.

The ensemble algorithm integrates the outputs of multiple predictive models to determine the type of impending natural disaster, enhancing both accuracy and reliability. Once generated, predictions are transmitted through the Emergency Alert System (EAS) to authorities and emergency management agencies, enabling timely response, efficient resource allocation, and the issuance of public warnings. By continuously updating with new data, the system strengthens disaster preparedness and response.

Experimental Setup

The models were implemented in Python (version 3.9) with several open-source libraries. NumPy (v1.23.5) was used for numerical computation, matrix operations, and data manipulation. Keras (v2.11.0), a high-level neural network API, was used to build and train the LSTM and CNN models. Scikit-learn (v1.2.2) was used to implement the SVM, RF, and AdaBoost classifiers, as well as to compute evaluation metrics including accuracy, precision, and recall. Pandas (v1.5.3) facilitated dataset loading, preprocessing, and structuring. All tests were carried out on a system with an

Intel i5 processor and 64 GB of RAM to meet the computational demands of training and evaluation.

Given the scale and complexity of real-time disaster prediction, characterized by high-frequency sensor streams and large spatiotemporal datasets, advanced infrastructure is required. The proposed system is intended for deployment on cloud-based platforms that provide scalable computing resources, distributed storage, and real-time analytics capabilities. Future implementation will leverage services such as Amazon Web Services (AWS), Google Cloud Platform (GCP), or Microsoft Azure to ensure feasibility and robustness under production workloads.

The dataset covers a broad spectrum of natural disasters and their associated parameters (Table 1). The established thresholds reveal the wide range of excessive and unpredictable conditions that natural disasters impose on different global regions. Threshold values for each natural disaster were defined using historical records, official monitoring agency datasets such as the United States Geological Survey (USGS), the National Oceanic and Atmospheric Administration (NOAA), and the World Meteorological Organization (WMO), and extreme events reported in the literature. These values represent the lower limits where impacts become significant and the upper limits corresponding to the most severe documented cases.

Table 1. Minimum and maximum threshold values of various natural disasters.

Natural Disaster	Minimum Threshold	Maximum Threshold
Earthquake	Magnitude 2.5 on Richter Scale	Magnitude 9.5 on Richter Scale
Tsunami	Wave height 0.5 m	Wave height 30 m
Cyclone	Wind speed 74 mph	Wind speed 157+ mph
Extreme Temperature	Below -30 °C (Extreme Cold)	Above 45 °C (extreme hot)

Machine learning models require performance metrics to assess their effectiveness across different tasks. Forecasting accuracy is evaluated using metrics such as the F1-score, recall, precision, and overall reliability. The general consistency of predictions is primarily measured through accuracy, calculated as the proportion of correct predictions to total predictions:

$$Accurateness = \frac{Correct\ predictions}{Total\ predictions}$$

Precision measures the percentage of accurate positive projections:

$$Precision = \frac{True\ positives}{True\ positives + False\ positives}$$

Recall assesses the fraction of actual positives correctly identified:

$$Recall = \frac{True\ positives}{True\ positives + False\ negatives}$$

The F1-score provides an equilibrium across precision and recall by taking the harmonic mean of the two criteria:

$$F1\ score = 2 \times \frac{Precision \times recall}{Precision + recall}$$

RESULTS AND DISCUSSION

Five machine learning algorithms were used, including LSTM combined with SVM, CNN, and RF for natural disaster prediction models, as well as the AdaBoost Ensemble method to bring them together. The AdaBoost ensemble model demonstrates a balanced improvement across all disaster types, effectively leveraging the strengths of individual models (Table 2). This confirms the advantage of using a meta-algorithm for integrated disaster prediction.

Table 2. Performance evaluation of the machine learning models for natural disaster classification.

Model	Disaster type	Accuracy	Precision	Recall	F1-score
LSTM	Earthquake	0.94	0.91	0.90	0.96
SVM	Tsunami	0.95	0.95	0.96	0.91
CNN	Cyclone	0.93	0.98	0.92	0.95
RF	Extreme temperatures	0.97	0.93	0.94	0.96
AdaBoost Ensemble	Combined disaster	0.96	0.97	0.95	0.97

LSTM: Long Short-Term Memory; SVM: Support Vector Machine; CNN: Convolutional Neural Network; RF: Random Forest.

This research evaluated the performance of LSTM, SVM, CNN, RF, and the Ensemble Method using the metrics of accuracy, precision, recall, and F1-score (Figure 2). The LSTM model achieved strong accuracy and F1-score but showed comparatively lower precision and recall. The SVM model excelled in precision but had a lower recall, while accuracy and F1-score remained balanced. The CNN model showed high recall but slightly lower precision and accuracy than the others. The RF model achieved the highest precision with balanced accuracy, though recall was lower. Finally, the Ensemble Method produced consistently strong results across all metrics, demonstrating its effectiveness in capitalizing on the strengths of individual models.
From 1990 to 2003, global disaster data (Figure 3) indicates that small-scale and large-

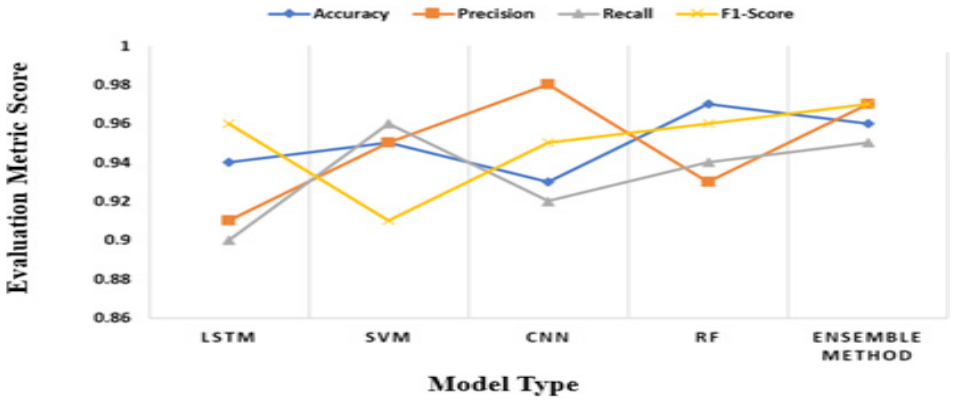

Figure 2. Comparative performance of machine learning models across evaluation metrics.

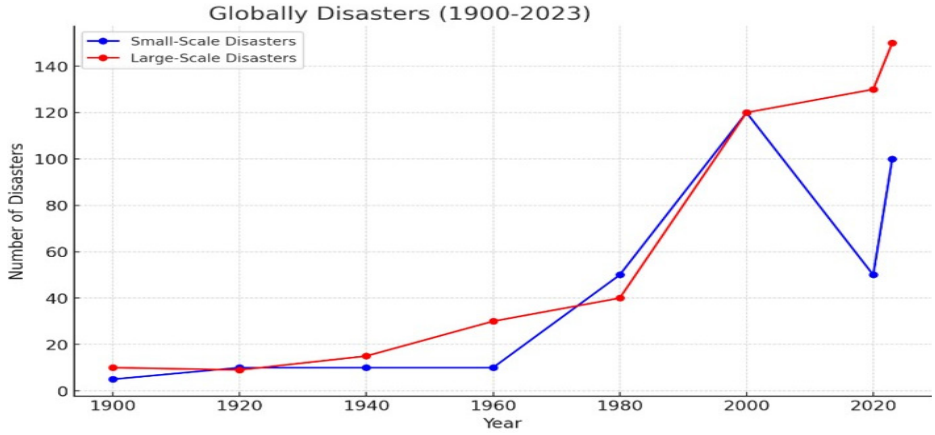

Figure 3. Global number of reported disasters by size, 1900 to 2023 (Small and Large -scale disasters events).

scale disasters events are characterized by a specific set of criteria. Small-scale disasters events involve five or fewer fatalities, affecting fewer than 1500 people, or resulting in economic losses below USD 13 million. Large-scale disasters events involving at least 50 fatalities, affecting more than 150 000 individuals, or causing economic damages of at least USD 320 million. This categorization provides a framework for understanding the severity and impact of such events over the analyzed period.

The study presents a comparative analysis of various earthquake prediction methods and their reported performance (Table 3). Keum *et al*. (2020) and Yang *et al*. (2023) both achieved 85 % accuracy using linear and non-linear regression techniques and the LSTM-RF-MDBN model, respectively. Sathianarayana *et al*. (2024) used CNNs, reaching 79 % accuracy. Özen and Souri (2024) used Bagged Tree and ANOVA techniques, achieving 95.5 % accuracy. Park and Lee (2024) implemented the Hybrid

fuzzy and DNN model achieved 96 % accuracy. The proposed Ensemble AdaBoost method demonstrated the highest performance, reaching 96 % accuracy.

Table 3. Comparative performance of earthquake prediction methods.

Author	Methods	Performance
Keum *et al*. (2020)	Linear and Non-Linear Regression Techniques	85 %
Yang *et al*. (2023)	LSTM-RF-MDBN	85 %
Sathianarayana *et al*. (2024)	Convolutional Neural Networks	79 %
Özen and Souri (2024)	Bagged Tree and ANOVA techniques	95.5 %
Park and Lee (2024)	Hybrid fuzzy and DNN	95 %
Proposed method	Ensemble AdaBoost	96 %

CONCLUSIONS

A meta-algorithm-based framework was developed for predicting multiple natural disasters by integrating IoT sensor data with machine learning models. Combined using the AdaBoost ensemble technique, the system achieved high accuracy, precision, recall, and F1-scores, demonstrating its effectiveness for disaster forecasting and real-time alert generation. Despite the promising results, the proposed system has certain limitations. The model's performance heavily depends on the availability and quality of historical datasets, which may be sparse or inconsistent for certain regions or disaster types. Moreover, it has so far been validated only using historical data in a simulation environment. Real-time field deployment and integration with government-level emergency response systems remain untested. Future work includes enabling real-time data ingestion from IoT networks, implementing geospatial visualization and decision-support dashboards, incorporating deep learning-based anomaly detection, and conducting field trials with disaster management authorities to validate the system under operational conditions.

ACKNOWLEDGEMENTS

Data availability

https://www.kaggle.com/datasets/alessandrolobello/the-ultimate-earthquake-dataset-from-1990-2023

https://www.kaggle.com/datasets/andrewmvd/tsunamidataset?select= tsunami_dataset.csv

https://www.kaggle.com/datasets/noaa/hurricane-database

https://www.kaggle.com/datasets/berkeleyearth/climate-change-earth-surface-temperature-data

REFERENCES

Anbarasan M, Muthu B, Sivaparthipan CB, Sundarasekar R, Kadry S, Krishnamoorthy S, Samuel RDJ, Dasel AA. 2020. Detection of flood disaster system based on IoT, big data and convolutional deep neural network. Computer Communications 150: 150–157. https://doi.org/10.1016/j.comcom.2019.11.022

Balamurugan M, Sathesh M, Ramakrishnan K, Raja M, Kalaiarasi K. 2024. Integrating Remote sensing technologies for real-time disaster management, mitigation, and decision support systems. *In* 2024 International Conference on Recent Advances in Science and Engineering Technology. Institute of Electrical and Electronics Engineers: Nagara, India. https://doi.org/10.1109/icraset63057.2024.10895763

Chai J, Wu HZ. 2023. Prevention/mitigation of natural disasters in urban areas. Smart Construction and Sustainable Cities 1 (1). https://doi.org/10.1007/s44268-023-00002-6

Duraisamy P, Natarajan Y. 2024. Twitter disaster prediction using different deep learning models. SN Computer Science 5 (1). https://doi.org/10.1007/s42979-023-02520-7

Elshami S, Ibrahim MIM, Abdel-Rahman ME, Rahim HA, Mukhalalati B. 2025. Developing and evaluating a disaster management assessment tool for health care practitioners. BMC Emergency Medicine 25 (1). https://doi.org/10.1186/s12873-025-01199-8

Keum HJ, Han KY, Kim HI. 2020. Real-time flood disaster prediction system by applying machine learning technique. KSCE Journal of Civil Engineering 24 (9): 2835–2848. https://doi.org/10.1007/s12205-020-1677-7

Khan M, He X, Guo J, Song D. 2024. Accurate prediction of indicators for engineering failures in complex mining environments. Engineering Failure Analysis 155: 107736. https://doi.org/10.1016/j.engfailanal.2023.107736

Özen F, Souri A. 2024. Cloud-based disaster management architecture using hybrid machine learning approach in IoT. Multimedia Tools and Applications 83 (29): 72357–72370. https://doi.org/10.1007/s11042-024-18333-6

Park K, Lee EH. 2024. Urban flood vulnerability analysis and prediction based on the land use using Deep Neural Network. International Journal of Disaster Risk Reduction, 101: 104231. https://doi.org/10.1016/j.ijdrr.2023.104231

Powers CJ, Devaraj A, Ashqeen K, Dontula A, Joshi A, Shenoy J, Murthy D. 2023. Using artificial intelligence to identify emergency messages on social media during a natural disaster: A deep learning approach. International Journal of Information Management Data Insights 3 (1): 100164. https://doi.org/10.1016/j.jjimei.2023.100164

Santhanaraj RK, Rajendran S, Tavera-Romero CA, Murugaraj SS. 2023. Internet of Things enabled energy aware metaheuristic clustering for real time disaster management. Computer Systems Science and Engineering 45 (2): 1561–1576. https://doi.org/10.32604/csse.2023.029463

Sathianarayanan M, Hsu PH, Chang CC. 2024. Extracting disaster location identification from social media images using deep learning. International Journal of Disaster Risk Reduction 104: 104352. https://doi.org/10.1016/j.ijdrr.2024.104352

Suhardono S, Lee CH, Suryawan IWK. 2025. Valuation of marine integrated disaster management amidst global warming in Southern Coast of Java, Indonesia. Marine Pollution Bulletin 211: 117446. https://doi.org/10.1016/j.marpolbul.2024.117446

Suárez, G., 2022. The seismic early warning system of Mexico (SASMEX): A retrospective view and future challenges. Frontiers in Earth Science, 10, p.827236.

Surendran R, Alotaibi Y, Subahi AF. 2023. Lens-oppositional wild geese optimization based clustering scheme for wireless sensor networks assists real time disaster management.

Computer Systems Science and Engineering 46 (1): 835–851. https://doi.org/10.32604/csse.2023.036757

Umamaheswari U, Suneel S, Ravikumar K, Baburao D, Upadhyay S, Swapna B. 2025. Design and development of a rescue robot to identify human presence in disaster scenarios by using artificial intelligence assisted sensor support. *In* 2025 6th International Conference on Mobile Computing and Sustainable Informatics. Institute of Electrical and Electronics Engineers: Goathgaun, Nepal. https://doi.org/10.1109/icmcsi64620.2025.10883140

Vinuja G, Devi NB. 2024. Leveraging 6G networks for disaster monitoring and management in remote sensing. *In* Development of 6G Networks and Technology, pp.115-143.

John Wiley and Sons: Hoboken, NJ, USA, pp: 115–143. https://doi.org/10.1002/9781394230686.ch5

Voosen, P., 2025. NASA, NOAA face major climate science cuts. Science (New York, NY), 388(6744), pp.237-238.

Wu L, Ma D, Li J. 2023. Assessment of the regional vulnerability to natural disasters in China based on DEA model. Sustainability 15 (14): 10936. https://doi.org/10.3390/su151410936

Yang X, Fan X, Wang K, Zhou Z. 2023. Research on landslide susceptibility prediction model based on LSTM-RF-MDBN. Environmental Science and Pollution Research 31 (1): 1504–1516. https://doi.org/10.1007/s11356-023-31232-x

Zheng Q, Wang C, Zhu Z. 2024. Research on the prediction of mine water inrush disasters based on multi-factor spatial game reconstruction. Geomechanics and Geophysics for Geo-Energy and Geo-Resources 10 (1). https://doi.org/10.1007/s40948-024-00761-1

Zhu Z, Zhang Y. 2021. Flood disaster risk assessment based on random forest algorithm. Neural Computing and Applications 34 (5): 3443–3455. https://doi.org/10.1007/s00521-021-05757-6

Agrociencia

CHARACTERIZATION OF AN AQUEOUS EXTRACT OBTAINED FROM *Pleurotus ostreatus* PROTEIN CONCENTRATE BY-PRODUCT

Angélica **Cruz-Solorio**[1*], Yazmin **Lara-Salinas**[1], Leticia **Aguilar-Doroteo**[1], María Eugenia **Garín-Aguilar**[2], Gustavo **Valencia-del Toro**[1]

[1]Instituto Politécnico Nacional. Unidad Profesional Interdisciplinaria de Biotecnología, Laboratorio de Cultivos Celulares de la Sección de Estudios de Posgrado e Investigación. La Laguna Ticoman SN, Mexico City, Mexico. C. P. 07340.
[2]Universidad Nacional Autónoma de México. Facultad de Estudios Superiores Iztacala, Laboratorio de Farmacobiología. Tlalnepantla de Baz, State of Mexico, Mexico. C. P. 54090.
* Author for correspondence: ancruzs@ipn.mx

Citation: Cruz-Solorio A, Lara-Salinas Y, Aguilar-Doroteo L, Garín-Aguilar ME, Valencia-del Toro G. 2025. Characterization of an aqueous extract obtained from *Pleurotus ostreatus* protein concentrate by-product. **Agrociencia** 59(6): 800-811. https://doi.org/ 10.47163/agrociencia.v59i6.3119

Editor in Chief:
Dr. Fernando C. Gómez Merino

Received: January 15, 2025.
Approved: September 2, 2025.
Published in Agrociencia: September 10, 2025.

ABSTRACT

Recently, the antioxidant activity of the *Pleurotus* genus has been associated with the content of polysaccharides, particularly in crude extracts, since they have the capacity to trap free radicals and inhibit lipid peroxidation. On the other hand, during the processing of protein concentrates obtained from these fungi, by-products rich in carbohydrates and proteins are produced. The present study focused on the determination of the antioxidant activity and the electrophoretic characterization of proteins present in the by-products obtained from the aqueous extract of protein concentrates of two parental strains (PCM and POS) and a hybrid strain (PCM × POS) of *Pleurotus ostreatus*. The hybrid strain had a higher total protein content (25.29 %) compared to the parental strains PCM (23.93 %) and POS (22.6 %). The electrophoretic profile of the aqueous extracts of *Pleurotus ostreatus* revealed protein bands with molecular weights between 14 and 99 kDa. In relation to the antioxidant capacity, strains POS and PCM showed higher mean inhibitory concentration (ED50), with values of 11.84 and 20.57 mg mL^{-1}, respectively, while the hybrid strain PCM × POS had an ED50 of 4.67 mg mL^{-1}. The results suggest that the hybrid strain extract with the lowest mean inhibitory concentration (ED50) has potential as an antioxidant and biological material for the production of metabolites for other biological functions.

Keywords: antioxidant, fungal hybrid.

INTRODUCTION

Oxidative stress damages important biomolecules due to an imbalance between the production of reactive oxygen species (ROS) and the antioxidant defense system (Pisoschi *et al*., 2021). High concentrations of ROS or an unbalanced defense system can lead to protein oxidation, lipid peroxidation, and nucleic acid destruction, and in turn, have an impact on cellular functions, causing health problems such as cancer, inflammation, and cardiovascular diseases. Therefore, there is currently great interest in the search for biomolecules with antioxidant activity (Zhang *et al*., 2020).

Macrofungal fruiting bodies are rich in dietary proteins and contain significant amounts of carbohydrates, fats, vitamins, fiber, and minerals (Mwangi *et al*., 2022). Characteristic fungal compounds, known as mycochemicals, include polysaccharides (β-glucans), peptides, proteins, lectins, phenolic compounds, polyketides, glycoproteins, terpenoids, and enzymes, which are generally isolated from fruiting bodies. Changes in substrate composition or culture conditions can increase the concentration and type of fungal compounds (Krishnamoorthi *et al*., 2022).

The genus *Pleurotus* is considered a functional food due to its organoleptic characteristics and high nutritional and medicinal properties (Raman *et al*., 2021). In addition, it is highly valued for its simple cultivation procedures, which are adaptable to a variety of substrates, including agroforestry residues, and can be used to produce food, enzymes, and nutraceuticals. This genus is widely used in the production of by-products, recognized for their therapeutic properties, such as antihypercholesterolemic, antihypertensive, antidiabetic, antiobesity, hepatoprotective, antiaging, antimicrobial, and antioxidant activities (Lesa *et al*., 2022).

Phenolic compounds are key contributors to the antioxidant activity of macromycetes; however, this activity has also been linked to the presence of polysaccharides, particularly in crude extracts (Carrasco-González *et al*., 2017), due to their ability to trap free radicals and inhibit lipid peroxidation (Barbosa *et al*., 2020). Industrial production of fungal by-products, such as broken fruiting bodies or stipes, accounts for approximately 20 % of total fruiting body weight and has a high recycling potential (Prandi *et al*., 2023). Moreover, when obtaining protein concentrates, highly enriched by-products are generated, especially in carbohydrates and proteins (Meganaharshini *et al*., 2023). Therefore, the objective of this research was to determine the antioxidant activity and to characterize electrophoretically the proteins of the by-products obtained from the aqueous extract of protein concentrates of *Pleurotus ostreatus* fruiting bodies.

MATERIALS AND METHODS

Fungal material

The study used three *Pleurotus* strains: PCM (collection strain), POS (commercial strain), and PCM × POS (hybrid generated from PCM and POS). The fungal strains belonged to the strain bank of the Cell Culture Laboratory of the Interdisciplinary Professional Unit of Biotechnology of the National Polytechnic Institute (IPN) in Mexico City, Mexico.

Preparation of aqueous extracts

The *Pleurotus* strains were grown on pasteurized wheat straw substrate. After harvesting, the fruiting bodies were dried at 40 °C and ground using a homogenizer (Osterizer, Mexico) at 9000 rpm. The resulting flour was sieved through a number 50 mesh (Montinox, Mexico). The flour was then defatted with hexane at a 1:5 (w/v) ratio

under continuous agitation for 8 h at 4 °C. The hexane was removed by decanting, and the defatted flour was placed in an extraction cabinet for 24 h. Finally, the flour was again sieved through a number 80 mesh (Montinox, Mexico) and stored at 4 °C. To obtain the aqueous extract of *Pleurotus*, the isoelectric precipitation method described by Cruz-Solorio *et al*. (2018) was used (Figure 1).

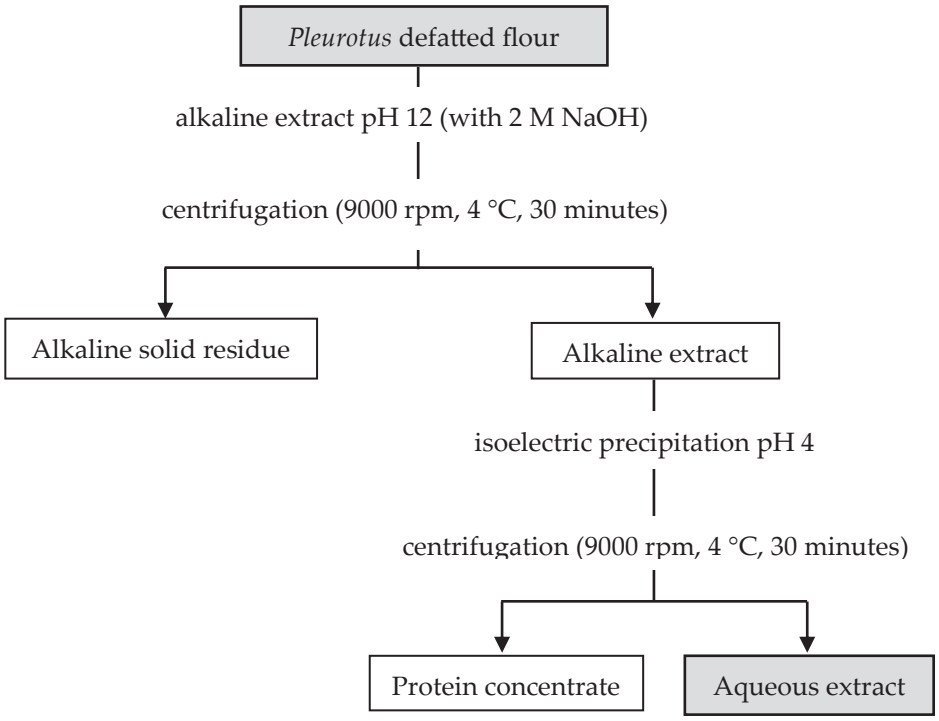

Figure 1. Schematic diagram for the preparation of *Pleurotus ostreatus* protein concentrate.

The aqueous extracts were spray dried using a Mini Spray Dryer B-290 (Buchi, Switzerland) under the following conditions: inlet temperature (Te) of 110 °C, outlet temperature (Ts) of 50 °C, and air flow (Fa) of 10 %. The powders obtained were stored at room temperature for later use.

Determination of total protein content

Crude protein content was determined using the micro-Kjeldahl method (AOAC, 1984). A total of 0.02 g of dry, defatted sample was weighed, and 0.25 g of a catalytic mixture of copper sulfate and potassium sulfate was added. The samples were placed in Micro-Kjeldahl flasks with 2 mL of concentrated sulfuric acid and subjected to the digestion process. The digested samples were processed in a K-350 distillation unit (Buchi, Switzerland), and the distillate was titrated with 0.1 N HCl. The protein content

of the *P. ostreatus* aqueous extracts was calculated by multiplying the percentage of protein nitrogen obtained by a factor of 4.38.

Determination of soluble protein content

Soluble protein content was quantified using the Bradford method (Bradford, 1976) with some modifications. From each sample, 100 µL were taken, and 1500 µL of Bradford's reagent was added. The mixture was stirred gently and allowed to stand for 5 min. Finally, the absorbance of the samples was measured at 595 nm using a spectrophotometer (Thermo Genesys 10UV, USA). For analysis, a standard curve was prepared with bovine serum albumin (BSA).

Determination of total carbohydrates content

The total sugar content was measured by the modified phenol-sulfur technique (Dubois *et al*., 1956). From each sample, 200 µL were mixed with 200 µL of 5 % phenol, followed by the addition of 1000 µL of concentrated sulfuric acid. The mixture was allowed to stand for 10 min. Subsequently, distilled water was added until a total volume of 2.5 mL was reached. The samples were shaken and incubated at 30 °C for 30 min. Finally, the absorbance of the samples was measured at 490 nm using a spectrophotometer (Thermo Genesys 10UV, USA). For analysis, a sucrose standard curve was prepared.

Determination of reducing sugar content

A stock solution was prepared from each of the extracts, with a concentration of 2 g L^{-1}. Then, 100 µL of the stock solution were mixed with 900 µL of distilled water. From this mixture, 250 µL were taken and combined with 250 µL of the 3,5-dinitrosalicylic acid (DNS) reagent in an Eppendorf tube. The samples were heated for 15 min in a boiling bath at 80–90 °C, and then cooled on ice for 5 min. Subsequently, distilled water was added until a final volume of 3 mL was reached. The absorbance of the samples was measured at 540 nm using a spectrophotometer (Thermo Genesys 10UV, USA). For analysis, a fructose standard curve was used as described by Miller (1972).

Electrophoretic profile

The determination of the molecular weights of the proteins present in the aqueous extracts was carried out by the method of Laemmli (1970) using sodium dodecyl sulfate–polyacrylamide gel electrophoresis (SDS-PAGE) under reducing conditions. A 12.5 % separating gel (pH 8.8) and a 5 % stacking gel (pH 6.8) were used. The run buffer contained 0.025 M Tris, 0.1 % SDS, 0.192 M glycine, and had a pH of 8.3. A 15 µL sample of 2 % (w/v) was prepared and mixed in a 1:1 ratio with Laemmli sample buffer (Bio-RAD, USA).

The assay was performed with a Mini PROTEAN-3 electrophoresis chamber (Bio-RAD, USA). The proteins were stained with Coomassie brilliant blue R-250. Electrophoresis was carried out at 200 V and 60 mA for 45 min. Subsequently, the gel was stained

with 0.125 % Coomassie brilliant blue R-250 and decolorized with a solution of 25 % methanol and 10 % acetic acid until the background was transparent. The molecular weight of the protein bands was estimated using a standard Mark 12 protein marker with a weight range of 2.5 to 200 kDa (Invitrogen, USA).

Infrared spectroscopy analysis

Aqueous extracts of *P. ostreatus* were examined by Fourier transform infrared (FTIR) spectroscopy in a range from 400 to 4000 cm^{-1}, with a resolution of 8 cm^{-1} and a total of 12 scans, using a 16F polycarbonate (PC) FTIR spectrometer (Perkin-Elmer, Germany). Interpretation of the results was performed using Spekwin32 software.

Antioxidant activity

The ability of the aqueous extracts to scavenge free radicals was evaluated by the 1,1-diphenyl-2-picrylhydrazyl (DPPH) method (Blois, 1958). Solutions with a concentration of 0.016 g mL^{-1} of the aqueous fractions were prepared as a starting point; subsequently, 500 µL of each sample were placed in test tubes, and 2500 µL of the DPPH reagent were added. The mixtures were shaken for 30 min, and the absorbance was measured in a spectrophotometer at 517 nm. Ascorbic acid was used as a positive control, and the percentage of free radicals was calculated from a standard curve prepared with different concentrations of ascorbic acid.

Statistical analysis

The results were analyzed by two-way analysis of variance (ANOVA) using Statistical Package for the Social Sciences (SPSS) version 22. Differences between means were evaluated using Duncan's multiple comparison test ($p < 0.05$). Data presented in tables and figures are expressed as the average of three replicates ± standard deviation (SD).

RESULTS AND DISCUSSION

Total protein, soluble protein, total carbohydrates, and reducing sugar content

The hybrid strain presented 25.29 % total protein, while the parental strains were 23.94 % for PCM and 22.6 % for POS (Table 1). The protein content the aqueous extracts was higher than that reported for solid alkaline residues obtained from *Vicia faba* L., which presented 6.9 % total protein (Vioque *et al*., 2012).

Regarding soluble protein content (Table 1), values ranged from 1.24 to 1.25 g L^{-1}. The proteins present in the aqueous extract did not precipitate at pH 4. Cruz-Solorio *et al*. (2014) indicated that defatted meals of *Pleurotus* spp. exhibited values between 0.2 and 0.24 g L^{-1}, while for defatted meals of *P. ostreatus,* it remained between 0.035 and 0.51 g L^{-1} (González *et al*., 2021).

The total carbohydrate content ranged (Table 1) between 27.26 and 37.11 µg $µL^{-1}$, which partially agrees with that reported by Santhosharajan and Sarawathy (2014)

Table 1. Contents of protein and carbohydrates in Pleurotus ostreatus aqueous extracts.

	PCM	POS	PCM × POS
Total protein (%)	23.94 ± 0.52[a]	22.60 ± 0.44[a]	25.29 ± 1.02[a]
Soluble protein (g L^{-1})	1.24 ± 0.01[a]	1.24 ± 0.01[a]	1.25 ± 0.01[a]
Total carbohydrates (μg μL^{-1})	37.11 ± 0.01[b]	34.48 ± 0.01[a]	27.26 ± 0.02[a]
Reducing sugar content (μg μL^{-1})	3.72 ± 0.00[a]	7.44 ± 0.01[c]	5.81 ± 0.00[b]

Values are expressed as mean ± standard deviation (n = 3). Means with different letters within a row differ significantly ($p < 0.05$).

for *Pleurotus* polysaccharide extracts (15–30 μg μL^{-1}). In contrast, the concentration of reducing sugars was lower in aqueous extracts than that reported by the same authors (18–20 μg μL^{-1}). On the other hand, Shukla and Jaitly (2011) reported a range of reducing sugars between 0.26 and 0.35 μg μL^{-1} lower than that of total soluble sugars (130.5 to 192.8 μg μL^{-1}) for species of the *Pleurotus* genus. Beltrán-Delgado *et al.* (2021) reported that, in edible fungi, carbohydrates are present in greater proportion, while reducing sugars constitute only a minor fraction of their total content.

The alkali extraction method contributes to a higher release of polysaccharides, attributable to the possibility of disrupting the existing ester and hydrogen bonding, which increases the rate of polysaccharide extraction (Janardhanan *et al*., 2024). Furthermore, it has been observed that carbohydrate composition depends on the strain, the substrate used in its cultivation, and its conditions (Yadav and Negi, 2021).

Electrophoretic profile

The electrophoretic profile of the aqueous extracts of *P. ostreatus* (Figure 2) revealed the presence of protein bands with molecular weights between 14 and 99 kDa, with six representative bands standing out in each extract, with greater intensity in the range of 20 to 30 kDa. The bands detected in the aqueous extracts could correspond to different proteins previously reported for the genus *Pleurotus*. Liao *et al*. (2020) found polypeptides with molecular weights of 27, 30, 55, 88, and 115 kDa, with antioxidant activity in *P. geesteranus*. Likewise, Jin *et al*. (2022) reported five representative proteins in the protein extract of *P. geesteranus*, obtained by isoelectric precipitation, with molecular weights >15, 27~31, 46~50, 15~16, and 42~43 kDa, highlighting their physicochemical and functional properties.

Bands with molecular weights in the range of 17 to 94 kDa correspond to proteins from *Pleurotus eryngii*. These proteins are an alternative resource with applications in the food industry due to their functional properties and antioxidant activity (Wu *et al*., 2023). Likewise, a ribotoxin-like protein has been purified from *Pleurotus ostreatus* fruiting bodies, with a molecular weight of 15 kDa (Landi *et al*., 2020). The results obtained in the present investigation are consistent with molecular weights previously reported for this genus.

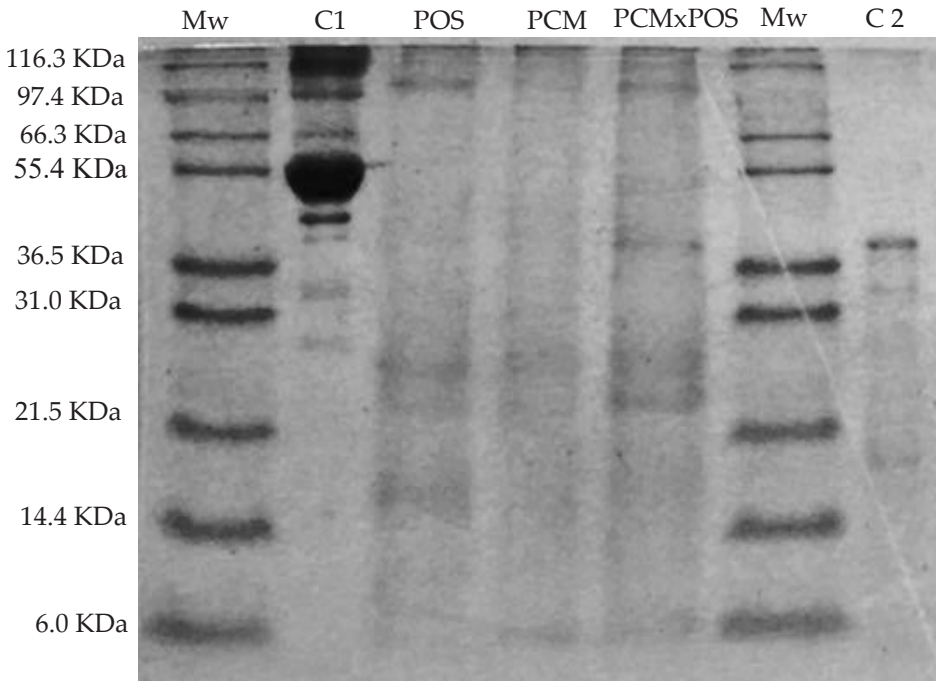

Figure 2. Sodium dodecyl sulfate–polyacrylamide gel electrophoresis (SDS-PAGE) pattern of *Pleurotus ostreatus* aqueous extracts. Mw: standard marker Invitrogen; C1: albumin; C2: pepsine.

Infrared spectroscopy analysis

A similar pattern was observed for all fungal extracts (Figure 3). All three spectra showed a C-H bond around 2932 cm^{-1}, carboxyl groups in absorption peaks near 1642

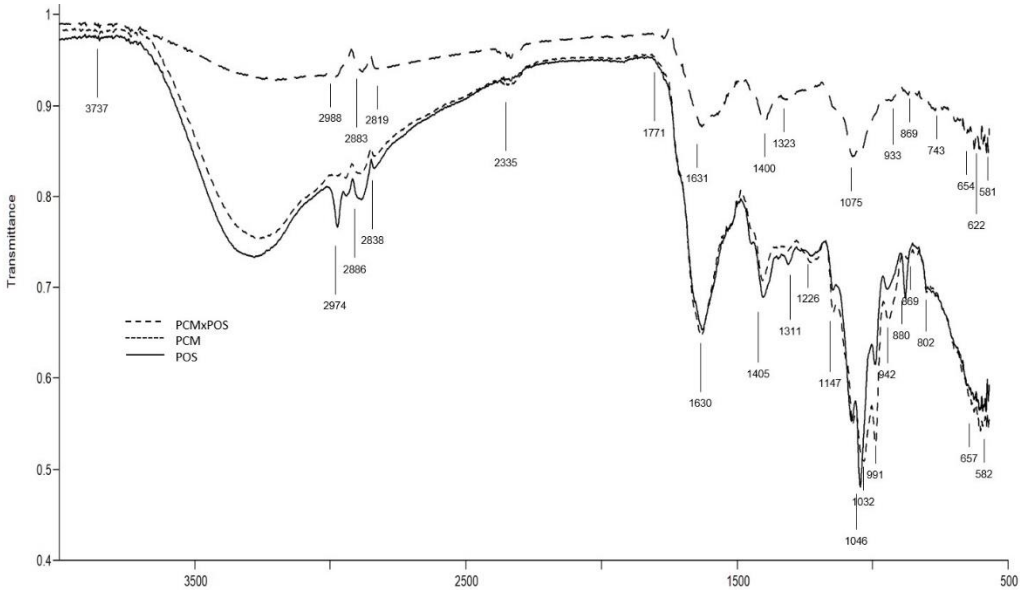

Figure 3. Infrared spectrum of *Pleurotus ostreatus* aqueous extracts.

cm^{-1}, and α-configuration in sugar units at 847 cm^{-1} (Wang *et al*., 2020). Peaks at 1000–1200 cm^{-1} were attributed to C-O glycosidic bonds, while pyranose rings were found at 500–1000 cm^{-1} (Ji *et al*., 2019).

According to Jin *et al*. (2022), the absorption peaks in the 1650–1660, 1610–1642, 1660–1680, 1680–1700, and 1642–1650 cm^{-1} regions corresponded to secondary structures of proteins α-helix, β-strand, β-turns, β-antiparallel, and random coil, respectively. On the other hand, peaks at 1375, 1312, 1100, 1065, 1038, and 890 cm^{-1} were associated with the presence of β-D-glucans (Bikmurzin *et al*., 2022). Based on these results, the present study confirms the presence of polysaccharides and proteins in the aqueous extracts of the fungal strains by infrared spectroscopy.

Antioxidant activity

The free radical scavenging activity assay by DPPH is one of the most widely used methods to evaluate antioxidant capacity. The hybrid strain PCM × POS showed 93.97 % antioxidant activity (percentage of inhibition) at a concentration of 54.79 μg μL^{-1}, being the highest activity recorded compared to the parental strains PCM and POS, which presented 64.29 % at 44.63 μg μL^{-1} and 79.73 % at 44.63 μg μL^{-1}, respectively (Figure 4). Aqueous extracts of PCM × POS evidenced higher DPPH radical scavenging capacity compared to extracts of the parental *P. ostreatus* strains, which could be attributed to their high affinity for DPPH radicals.

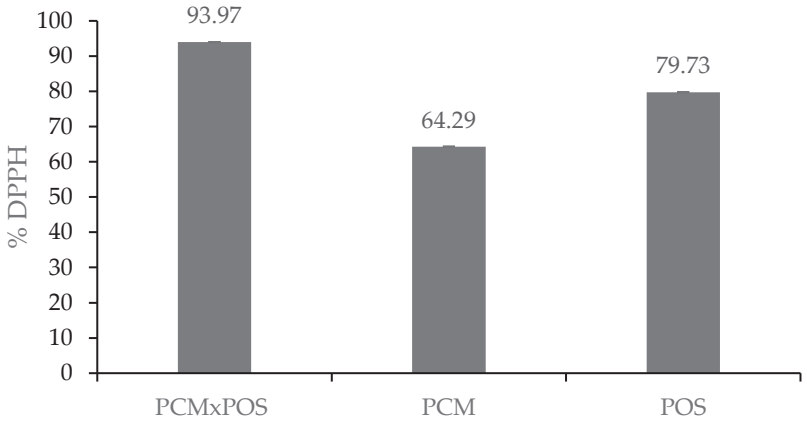

Figure 4. 1,1-diphenyl-2-picrylhydrazyl (DPPH) radical scavenging activity (%) of *Pleurotus ostreatus* aqueous extracts.

On the other hand, IC50 is defined as the amount of an antioxidant-containing material required to scavenge 50 % of a radical. In addition, an antioxidant substance or extract is considered more effective in scavenging radicals when it has a lower IC50 value. Therefore, a lower IC50 indicates higher antioxidant activity (Effiong *et al*., 2024). The

results showed that aqueous extracts of PCM × POS had an IC50 of 4.67 mg mL^{-1}, higher than aqueous extracts of PCM and POS (11.84 and 20.57 mg mL^{-1}, respectively). A previous study showed that *P. ostreatus* protein hydrolysates presented antioxidant activity between 16.55 and 31 %, with a minimum IC50 value of 5.24 mg mL^{-1} (Goswami *et al*., 2021). For their part, Beltrán-Delgado *et al*. (2021) reported the antioxidant activity of the aqueous extract of the fruiting body of *P. ostreatus*, with DPPH uptake percentages between 16 % and 26 %, and an IC50 of 1.72 mg mL^{-1}. These results suggest the presence of proteins, reducing sugars, carbohydrates, and flavonoids.

Phenolic compounds have an impact on the antioxidant activity of macromycetes. However, recent studies have associated this activity with the content of polysaccharides, especially in crude extracts (Carrasco-González *et al*., 2017), due to their ability to trap free radicals and inhibit lipid peroxidation (Barbosa *et al*., 2020). The antioxidant effectiveness of these polysaccharides is influenced by factors such as their molecular weight, glycosidic bond type, uronic acid content, water solubility, and monosaccharide composition (Wang *et al*., 2018). For example, a polysaccharide isolated from *P. djamor* showed DPPH free radical scavenging activity with percentages of 27.4 and 52.3 %, and IC50 of 3.83 mg mL^{-1} (Maity *et al*., 2021).

Likewise, fungal antioxidant agents, such as proteins and peptides, have been identified. Liao *et al*. (2020) reported a DPPH free radical inhibition of 91.2 % using protein hydrolysates from *P. geesteranus* when evaluating the antioxidant activity of this primary metabolite. On the other hand, Huang *et al*. (2023) found that proteins and uronic acid present in polysaccharides can enhance their ability to scavenge free radicals.

CONCLUSIONS

Aqueous extracts of *Pleurotus ostreatus* from parental and hybrid strains exhibit antioxidant activity. Soluble sugars, polysaccharides, and proteins were found in lower proportions, potentially contributing to their biological activity. In addition, the hybrid strain, which had the lowest average inhibitory concentration (IC50), represented a promising extract with antioxidant properties.

ACKNOWLEDGEMENTS

The valuable support to projects SIP20200412, SIP20210805, SIP20221162, and SIP20231843 is greatly acknowledged.

REFERENCES

AOAC (Association of Official Analytical Chemists). 1984. Official methods of analysis (14th edition). Arlington, TX, USA.

Barbosa JR, dos Santos MMF, da Silva LHM, de Carvalho RNJ. 2020. Polysaccharides of mushroom *Pleurotus* spp.: New extraction techniques, biological activities, and development

of new technologies. Carbohydrate Polymers 229: 115550. https://doi.org/10.1016/j.carbpol.2019.115550

Beltrán-Delgado Y, Morris-Quevedo HJ, Dominguez DO, Batista-Corbal P, Llaurado-Maury G. 2021. Composición micoquímica y actividad antioxidante de la seta *Pleurotus ostreatus* en diferentes estados de crecimiento. Acta Biologica Colombiana 26 (1): 89–98.

Bikmurzin R, Bandzevičiūtė R, Maršalka A, Maneikis A, Kalėdienė L. 2022. FT-IR method limitations for β-glucan analysis. Molecules 27 (14): 4616. https://doi.org/10.3390/molecules27144616

Blois MS. 1958. Antioxidant determinations by the use of a stable free radical. Nature 181 (4617): 1199–1200. https://doi.org/10.1038/1811199a0

Bradford MM. 1976. A rapid and sensitive method for the quantitation of microgram quantities of protein utilizing the principle of protein–dye binding. Analytical Biochemistry 72 (1–2): 248–254. https://doi.org/10.1016/0003-2697(76)90527-3

Carrasco-González JA, Serna-Saldívar SO, Gutiérrez-Uribe JA. 2017. Nutritional composition and nutraceutical properties of the *Pleurotus* fruiting bodies: Potential use as food ingredient. Journal Food Composition and Analysis 58: 69–81. https://doi.org/10.1016/j.jfca.2017.01.016

Cruz-Solorio A, Garín-Aguilar ME, Leal-Lara H, Ramírez-Sotelo MG, Valencia-del Toro G. 2014. Proximate composition of *Pleurotus* fruit body flour and protein concentrate. Journal Chemical, Biological and Physical Sciences 5: 52–60.

Cruz-Solorio A, Villanueva-Arce R, Garín-Aguilar ME, Leal-Lara H, Valencia-del Toro G. 2018. Functional properties of flours and protein concentrates of 3 strains of the edible mushroom *Pleurotus ostreatus*. Journal of Food Science and Technology 55 (10): 3892–3901. https://doi.org/10.1007/s13197-018-3312-x

Dubois K, Giles J, Hamilton P, Smith F. 1956. Colorimetric method for determination of sugars and related substances. Analytical Chemistry 28 (3): 350–356. https://doi.org/10.1021/ac60111a017

Effiong ME, Umeokwochi CP, Afolabi IS, Chinedu SN. 2024. Comparative antioxidant activity and phytochemical content of five extracts of *Pleurotus ostreatus* (oyster mushroom). Scientific Reports 14 (1): 3794. https://doi.org/10.1038/s41598-024-54201-x

González A, Nobre C, Simões LS, Cruz M, Loredo A, Rodríguez-Jasso RM, Contreras J, Texeir J, Belmares R. 2021. Evaluation of functional and nutritional potential of a protein concentrate from *Pleurotus ostreatus* mushroom. Food Chemistry 346: 128884. https://doi.org/10.1016/j.foodchem.2020.128884

Goswami B, Majumdar S, Das A, Barui A, Bhowal J. 2021. Evaluation of bioactive properties of *Pleurotus ostreatus* mushroom protein hydrolysate of different degree of hydrolysis. LWT 149: 111768. https://doi.org/10.1016/j.lwt.2021.111768

Huang Y, Xie W, Tang T, Chen H, Zhou X. 2023. Structural characteristics, antioxidant and hypoglycemic activities of polysaccharides from Mori Fructus based on different extraction methods. Frontiers in Nutrition 10: 1125831. https://doi.org/10.3389/fnut.2023.1125831

Janardhanan A, Govindan S, Moorthy A, Prashanth KVH, Savitha Prashanth MR, Ramani P. 2024. An alkali-extracted polysaccharide from *Pleurotus eous* and exploration of its antioxidant and immunomodulatory activities. Journal of Food Measurement and Characterization 18 (4): 2489–2504. https://doi.org/10.1007/s11694-023-02318-4

Ji HY, Chen P, Yu J, Feng YY, Liu AJ. 2019. Effects of heat treatment on the structural characteristics and antitumor activity of polysaccharides from *Grifola frondosa*. Applied Biochemistry and Biotechnology 188 (2): 481–490. https://doi.org/10.1007/s12010-018-02936-5

Jin M, Xie Y, Xie P, Zheng Q, Wei T, Guo L, Lin J, Ye Z, Zou Y. 2022. Physicochemical and functional properties of *Pleurotus geesteranus* proteins. Food Research International 162: 111978. https://doi.org/10.1016/j.foodres.2022.111978

Krishnamoorthi R, Srinivash M, Mahalingam PU, Malaikozhundan B. 2022. Dietary nutrients in edible mushroom, *Agaricus bisporus* and their radical scavenging, antibacterial, and antifungal effects. Process Biochemistry 121: 10–17. https://doi.org/10.1016/j.procbio.2022.06.021

Laemmli UK. 1970. Cleavage of structural proteins during the assembly of the head of bacteriophage T4. Nature 227 (5259): 680–685. https://doi.org/10.1038/227680a0

Landi N, Ragucci S, Russo R, Valletta M, Pizzo E, Ferreras JM, Di Maro A. 2020. The ribotoxin-like protein ostreatin from *Pleurotus ostreatus* fruiting bodies: Confirmation of a novel ribonuclease family expressed in basidiomycetes. International Journal of Biological Macromolecules 161: 1329–1336. https://doi.org/10.1016/j.ijbiomac.2020.07.267

Lesa KN, Khandaker MU, Mohammad RIF, Sharma R, Islam F, Mitra S, Emran TB. 2022. Nutritional value, medicinal importance, and health-promoting effects of dietary mushroom (*Pleurotus ostreatus*). Journal of Food Quality 2022 (1): 2454180. https://doi.org/10.1155/2022/2454180

Liao X, Zhu Z, Wu S, Chen M, Huang R, Wang J, Wang J, Wu Q, Ding Y. 2020. Preparation of antioxidant protein hydrolysates from *Pleurotus geesteranus* and their protective effects on H_2O_2 oxidative damaged PC12 cells. Molecules 25 (22): 5408. https://doi.org/10.3390/molecules25225408

Maity GN, Maity P, Khatua S, Acharya K, Dalai S, Mondal S. 2021. Structural features and antioxidant activity of a new galactoglucan from edible mushroom *Pleurotus djamor* International Journal of Biological Macromolecules 168: 743–749. https://doi.org/10.1016/j.ijbiomac.2020.11.131

Meganaharshini M, Sudhakar V, Bharathi ND, Deepak S. 2023. Review on recent trends in the application of protein concentrates and isolates–A food industry perspective. Food and Humanity 1: 308–325. https://doi.org/10.1016/j.foohum.2023.05.022

Miller GL. 1972. Use of dinitrosalicyclic acid reagent for determination of reducing sugar. Analytical Chemistry 31 (3): 426–428. https://doi.org/10.1021/ac60147a030

Mwangi RW, Macharia JM, Wagara IN, Bence RL. 2022. The antioxidant potential of different edible and medicinal mushrooms. Biomedicine and Pharmacotherapy 147: 112621. https://doi.org/10.1016/j.biopha.2022.112621

Pisoschi AM, Pop A, Iordache F, Stanca L, Predoi G, Serban AI. 2021. Oxidative stress mitigation by antioxidants-an overview on their chemistry and influences on health status. European Journal of Medicinal Chemistry 209: 112891. https://doi.org/10.1016/j.ejmech.2020.112891

Prandi B, Cigognini IM, Faccini A, Zurlini C, Rodríguez Ó, Tedeschi T. 2023. Comparative study of different protein extraction technologies applied on mushrooms by-products. Food and Bioprocess Technology 16 (7): 1570–1581. https://doi.org/10.1007/s11947-023-03015-2

Raman J, Jang KY, Oh YL, Oh M, Im JH, Lakshmanan H, Sabaratnam V. 2021. Cultivation and nutritional value of prominent *Pleurotus* spp.: An overview. Mycobiology 49 (1): 1–14. https://doi.org/10.1080/12298093.2020.1835142

Santhosharajan N, Sarawathy N. 2014. Studies on nutritional and medicinal characteristics of some edible mushrooms. *In* Singh M. (ed.), 8th International Conference on Mushroom Biology and Mushroom Products. New Delhi, India.

Shukla S, Jaitly AK. 2011. Morphological and biochemical characterization of different oyster mushroom (*Pleurotus* spp.). Journal of Phytology 3 (8): 18–20.

Vioque J, Alaiz M, Girón-Calle J. 2012. Nutritional and functional properties of *Vicia faba* protein isolates and related fractions. Food Chemistry 132 (1): 67–72. https://doi.org/10.1016/j.foodchem.2011.10.033

Wang W, Li X, Chen K, Yang H, Jialengbieke B, Hu X. 2020. Extraction optimization, characterization, and the antioxidant activities *in vitro* and *in vivo* of polysaccharide from *Pleurotus ferulae.* International Journal of Biological Macromolecules 160: 380–389. https://doi.org/10.1016/j.ijbiomac.2020.05.158

Wang Y, Jia J, Ren X, Li B, Zhang Q. 2018. Extraction, preliminary characterization and *in vitro* antioxidant activity of polysaccharides from *Oudemansiella radicata* mushroom. International Journal of Biological Macromolecules 120: 1760–1769. https://doi.org/10.1016/j.ijbiomac.2018.09.209

Wu D, Jia X, Zheng X, Mo Y, Teng J, Huang L, Xia N. 2023. Physicochemical and functional properties of *Pleurotus eryngii* proteins with different molecular weight. LWT 184: 115102. https://doi.org/10.1016/j.lwt.2023.115102

Yadav D, Negi PS. 2021. Bioactive components of mushrooms: Processing effects and health benefits. Food Research International 148: 110599. https://doi.org/10.1016/j.foodres.2021.110599

Zhang B, Li Y, Zhang F, Linhardt RJ, Zengand G, Zhang A. 2020. Extraction, structure, and bioactivities of the polysaccharides from *Pleurotus eryngii*: A review. International Journal of Biological Macromolecules 150: 1342–1347. https://doi.org/10.1016/j.ijbiomac.2019.10.144

Agrociencia

INDUCTION, MULTIPLICATION, AND ELONGATION OF *IN VITRO* SHOOTS OF ADVANCED LINES OF *Phaseolus vulgaris* L., *Phaseolus coccineus* L., AND *Vigna radiata* L.

Jesús Iván **Ruiz-Terrazas**[1], María Cristina Guadalupe **López-Peralta**[1*], Serafín **Cruz-Izquierdo**[1], Andrés Adolfo **Estrada-Luna**[2]

[1]Colegio de Postgraduados. Recursos Genéticos y Productividad-Genética. Carretera México-Texcoco km 36.5, Montecillo, Texcoco, State of Mexico, Mexico. C. P. 56264.
[2]Centro de Investigación y de Estudios Avanzados del IPN (Cinvestav), Unidad Irapuato. Departamento de Ingeniería Genética. Libramiento Norte Carretera Irapuato-León km 9.6, Irapuato, Guanajuato, Mexico. C. P. 36824.
* Author for correspondence: cristy@colpos.mx

Citation: Ruiz-Terrazas JI, López-Peralta MCG, Cruz-Izquierdo S, Estrada-Luna AA. 2025. Induction, multiplication, and enlargement of *in vitro* buds of advanced lines of *Phaseolus vulgaris* L., *Phaseolus coccineus* L., and *Vigna radiata* L. **Agrociencia** 59(6): 812-824. https://doi.org/ 10.47163/agrociencia.v59i6.3433

Editor in Chief:
Dr. Fernando C. Gómez Merino

Received: March 18, 2025.
Approved: September 24, 2025.
Published in Agrociencia: September 25, 2025.

ABSTRACT

Beans are the second most important crop in Mexico and the most consumed legume in the human diet. Advances in the knowledge of its genetic diversity have allowed the identification of lines with resistance to biotic and abiotic factors. To exploit this variability, the use of *in vitro* culture techniques aimed at the multiplication of germplasm with economic, cultural, and nutritional value is proposed. In this research, conditions for the induction, multiplication, and shoot elongation of three advanced lines of *Phaseolus vulgaris* L., *Phaseolus coccineus* L., and *Vigna radiata* L. by direct organogenesis were determined. Seeds were disinfected by a sequential treatment that reached 93 % asepsis. Germination was achieved in Murashige and Skoog (MS) medium at 50 % inorganic salts after scarifying the seeds in 1 % hydrogen peroxide for 30 min. To induce organogenesis, explants were grown on MS medium with a full concentration of inorganic salts. The best results were obtained in cotyledonary nodes, with 72 µM of 6-benzyladenine (BA) for *P. vulgaris* (4.1 shoots) and *V. radiata* (6.8 shoots), and with 90 µM of BA for *P. coccineus* (27.9 shoots). Multiplication was most efficient in groups of 3 to 4 shoots per explant, using 72 µM of BA for *P. vulgaris* (6.1 shoots), 54 µM of BA for *P. coccineus* (30.7 shoots), and 90 µM of thidiazuron (TDZ) for *V. radiata* (24.6 shoots). Shoot elongation was achieved on MS medium without regulators for *P. vulgaris* (0.22 cm), with 5.6 µM gibberellic acid (AG_3) for *P. coccineus* (5.53 cm), and with 2.8 µM AG_3 for *V. radiata* (0.8 cm).

Keywords: bean, regeneration, cotyledonary nodes, growth regulators.

INTRODUCTION

Mexico is the center of origin of several crop species with global economic importance. Beans are a legume that, since its domestication, has been an important part of the Mexican people's daily diet and, when combined with corn, provides practically all of

the necessary proteins consumed by the lowest-interest social strata (INEGI, 2024). In 2023, bean production in Mexico was recorded at 724 thousand Mg, which represents a 25 % decrease compared to 2022, mainly due to the drought caused by the delay in rainfall. This figure represents the lowest production in 30 years (SIAP, 2024). More than 85 % of the total area cultivated with beans is worked under rainfed conditions, so the crop is affected by the incidence of biotic and abiotic factors that decrease its production (Pandey *et al*., 2017).

Genetic variability is the foundation for survival and adaptation (Schmitz *et al*., 2023) and is essential in a breeding program, which allows the selection of cultivars for higher yield, higher protein or oil content, and tolerance to biotic or abiotic factors (Morales-Soto and Lamz-Piedra, 2020). *In vitro* culture consists of the isolation of explants (cells, tissues, or organs) from the mother plant and their development in defined culture media under aseptic conditions. These techniques allow the rapid propagation of disease-free and genetically uniform plants in a short time, which benefits production (Segura *et al*., 2024). Direct organogenesis plays an important role in the process of plant tissue culture for common bean regeneration (Yu *et al*., 2021).

The creation of an efficient *in vitro* propagation protocol for *Phaseolus* and *Vigna* species represents a strategic tool in breeding programs, as it overcomes many limitations imposed by traditional breeding methods. Furthermore, it facilitates the rapid and massive multiplication of elite genotypes, especially those with desirable agronomic traits, and the conservation of valuable germplasm, including lines resistant or tolerant to adverse conditions. As a result of research on genetic diversity in the genera *Phaseolus* and *Vigna* and the interest in the creation and use of a germplasm base in breeding programs for the creation of varieties, lines with resistance to abiotic and biotic factors have been developed, while including other favorable attributes such as nutritional quality, earliness, growth habits, and tolerance to high temperatures.

The objective of this research was to characterize the induction, multiplication, and shoot elongation capacity of advanced lines of *Phaseolus vulgaris*, *P. coccineus,* and *Vigna radiata* by direct organogenesis. For this purpose, different culture media, as well as different combinations and concentrations of plant growth regulators, were evaluated in order to exploit and utilize available genetic variation, as well as the capacity to multiply and preserve potential germplasm.

MATERIALS AND METHODS

Advanced lines of *Phaseolus vulgaris* L. (white bean variety), *Phaseolus coccineus* L., and *Vigna radiata* L. provided by the Bean Breeding Program of the Postgraduate Program in Genetic Resources and Productivity (PREGEP-Genetics) of the Postgraduate College were used.

Culture medium and incubation conditions

Murashige and Skoog (1962) basic culture medium (MS medium), supplemented with sucrose (30 g L^{-1}) and solidified with agar (Merck, Mexico, 7 g L^{-1}), was used.

The pH of the medium was adjusted to 5.7 with NaOH or 1N HCl using an Orion 3 Star potentiometer (Thermo Fisher Scientific, Mexico City, Mexico) before adding the agar. The sterilization was carried out in a vertical autoclave (AESA 300, Mexico City, Mexico) at 121 °C and 1.5 kg cm^{-2} pressure for 20 min. The culture flasks with the seeded plant material were kept in an incubation room with a photoperiod of 16/8 h of light/darkness provided by 75 W LED cold white light lamps and luminous intensity of 45 μmol m^{-2} s^{-1}, or in darkness, at a temperature of 25 ± 1 °C sustained by a mini-split (Carrier Mexico, Mexico City, Mexico) and relative humidity of 40 %.

Establishment of the aseptic culture

Seeds were washed with commercial detergent (Roma, Mexico) and tap water for 10 min under continuous agitation. Two disinfection treatments were tested: 1) seeds were immersed in ethanol (70 %) for 1 min, then in commercial sodium hypochlorite (NaOCl; 0.5 % v/v) (Cloralex, Alen del Norte, Mexico City, Mexico) + Tween 20 (five drops per 100 mL of solution) (Thermo Fisher Scientific, Mexico City, Mexico) + colloidal silver-based bactericide (1 % v/v, 0.2 % active ingredient) (Microdyn, Alen del Norte, Mexico City, Mexico) dissolved in sterilized water, and finally, in a fungicide solution (4 g L^{-1} Benlate and 4 g L^{-1} Captan) (Sigma Aldrich, USA); 2) using the same treatment with a variation in NaOCl concentration (1 % v/v).

In both treatments, seeds were shaken continuously and rinsed five times with sterilized distilled water before depositing them in each solution. Three seeds were sown in 250 mL capacity glass vials with 30 mL of MS culture medium with 50 and 100 % concentrations of inorganic salts. After 17 d, the germination rate (%), days to germination, bacterial contamination (%), and fungal contamination (%) were determined. The experiment was set up in a completely randomized design with 12 replicates per treatment. The experimental unit was one seed in each jar.

In vitro germination

Seeds of three bean species were subjected to different scarification times (4, 2, and 1.5 h, plus a control without scarification) using hydrogen peroxide (H_2O_2) at concentrations of 0, 1, and 3 % (v/v). Subsequently, they were seeded on MS medium with 50 % of the concentration of inorganic salts. After three weeks, germination rate (%), days to germination, and seedling height (cm) were quantified. The experiment was set up in a simple completely randomized design with 10 replicates per variety, with five seeds in each jar as the experimental unit.

Shoot induction

Evaluation of different explant types and culture media

Cotyledonary nodes (Cn), cotyledonary axis (Ca), cotyledons (C), and embryonic axis (Ea) were dissected from 14-d-old *in vitro* germinated seedlings of the three species. They were planted on MS and B5 culture medium (Gamborg *et al*., 1968). The latter

is composed of inorganic salts, thiamine (10 mg L^{-1}), and organic components of MS medium. Both culture media were supplemented with 6-benzyladenine (BA, 72 μM). At three weeks, sprouting (percentage of explants that generated shoots), number of shoots per explant, and shoot length were quantified. The experiment followed a completely randomized design with 15 replicates per treatment, using a single explant per culture flask as the experimental unit.

Evaluation of different concentrations of 6-benzyladenine (BA) and thidiazuron (TDZ)

The two types of explants that yielded the best results (cotyledon and cotyledonary node) were sown on MS medium supplemented with 54, 72, and 90 μM 6-benzyladenine (BA) and thidiazuron (TDZ), in addition to a medium without plant growth regulators as a control. After three weeks, sprouting (percentage of explants that generated shoots), number of shoots per explant, and shoot length were quantified. The experiment followed a completely randomized design with 10 replicates per treatment, considering a single explant per culture flask as the experimental unit.

Shoot multiplication

To increase the number of shoots, groups of 3 to 4 shoots with an average length of 0.1 to 0.15 cm, obtained from cotyledon and cotyledonary node explants during the induction stage, were sown in MS medium supplemented with the same BA and TDZ concentrations used previously (54, 72, and 90 μM). At three weeks, sprouting (percentage of explants that generated shoots), number of shoots per explant, and shoot length were quantified. The experiment was set up in a simple completely randomized design with 10 replicates per treatment, considering a single explant per culture flask as the experimental unit.

Shoot elongation

Groups of 3 to 4 shoots from the cotyledon and cotyledonary node of the multiplication stage, with a uniform average length (between 0.05 and 0.1 cm depending on the species), were sown in MS medium with two concentrations of inorganic salts (50 and 100 %) and different concentrations of gibberellic acid (AG_3) (0.0, 1.4, 2.8, 4.2, 5.6, and 7 μM). Each treatment included 12 replicates, with one explant per culture flask serving as the experimental unit. The experiment followed a completely randomized design.

Statistical analysis

With the data of the quantified variables, an analysis of variance was performed with the statistical program R (R Core Team, 2022) using Tukey's test ($p \leq 0.05$) for comparison of means.

RESULTS AND DISCUSSION

Establishment of the aseptic culture

Two weeks after *in vitro* sowing, the treatment with 20 % NaOCl prevented the growth of fungi and bacteria ($p \leq 0.05$). In addition, this treatment showed the best response for aseptic culture, achieving germination rates of 50, 87.5, and 95.33 % in *P. vulgaris*, *P. coccineus*, and *V. radiata*, respectively. After 17 d, the seedlings reached 1.08, 4.64, and 5.15 cm in height. These results are similar to those obtained by Yu *et al*. (2021), who disinfected *P. vulgaris* seeds with 20 % sodium hypochlorite for 10 min. On the other hand, Santalla *et al*. (1998) successfully disinfected *P. coccineus* seeds with 95 % ethanol for 1 min and 1 % sodium hypochlorite for 20 min, while Nupur (2025) established an effective seed disinfection protocol for *V. radiata*, using 0.1 % sodium hypochlorite for 15 min.

In vitro germination

Vigna radiata germinated faster (2.65 d after sowing) than *P. vulgaris* (3.25 d after sowing) and *P. coccineus* (4.01 d after sowing). It was found that 30 min of immersion in hydrogen peroxide caused a decrease in germination time of 3.12 d after sowing in all three species, compared to other treatments (1, 2, and 4 h). The scarification of seeds from all species with hydrogen peroxide caused an increase in germination due to the softening of the seed coat, and germination rates of 85.13, 95.9, and 91.79 % were achieved in *P. vulgaris*, *P. coccineus*, and *V. radiata*, respectively, with a considerable increase in *P. vulgaris* (from 50 to 85.13 %). This is consistent with the findings of Rajashekar and Baek (2014), who accelerated the imbibition of *P. vulgaris* seeds and facilitated seed coat removal by immersing them in peroxide.

Shoot induction

Evaluation of different types of explants and culture media

Significant differences in sprouting were detected among species ($p \leq 0.05$). *Phaseolus coccineus* showed superior sprouting (100 %) and a higher number of explants with shoots (9.08 in MS) in both culture media (MS and B5) (Figure 1). Results for *P. vulgaris* were significantly lower (30.77 % sprouting in MS and 46.15 % in B5) in contrast to *P. coccineus* and *V. radiata* (Table 1). The main cause of this is recalcitrance, which limits the *in vitro* regeneration of this species (Song *et al*., 2020).

In *P. vulgaris*, the explant that showed the best results was the cotyledon axis planted in MS medium supplemented with 72 μM BA. However, its response was not significantly higher than that of cotyledonary nodes, which produced up to 1.23 shoots per explant on MS medium, although with shorter shoot length. These results are lower than those obtained by Yu *et al*. (2021), who generated 2.91 shoots with a length of at least 2 cm per explant in cotyledon nodes sown in MS medium. This difference may be attributable to the variety used in the present study. On the other hand, sprouting reached 64.29 %

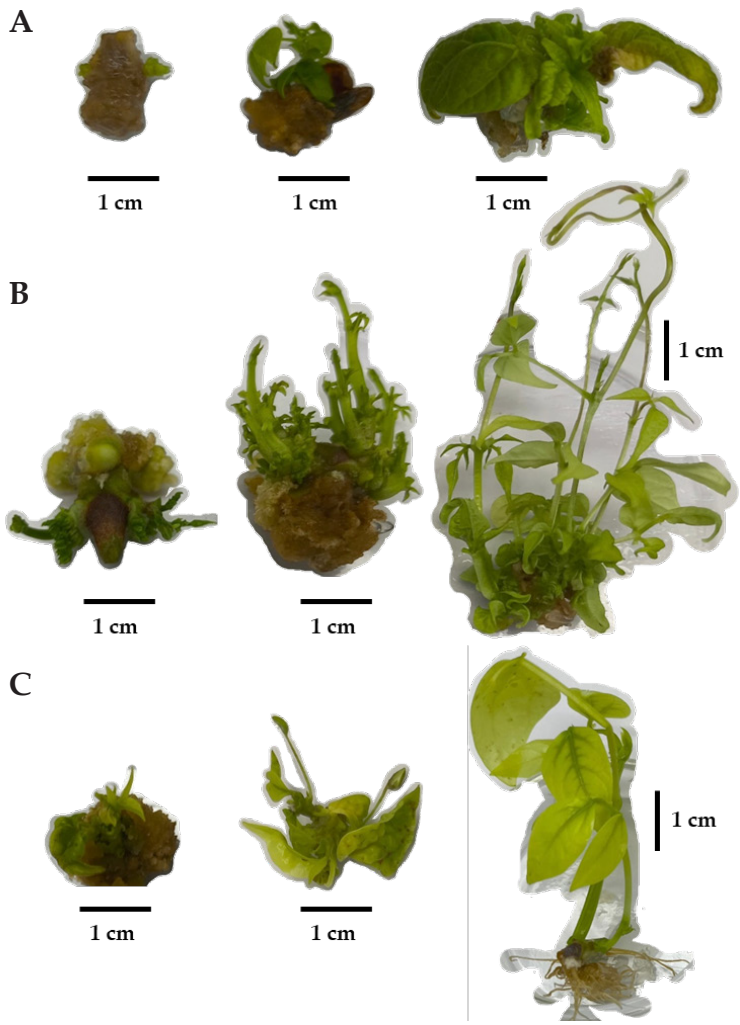

Figure 1. Induction, multiplication, and elongation of shoots *in vitro*. A: *Phaseolus vulgaris* L.; B: *Phaseolus coccineus* L.; C: *Vigna radiata* L.

in MS medium, exceeding the 46.15 % obtained in B5 medium. This contrasts with the findings of Quintero-Jiménez *et al*. (2010), who achieved greater shoot regeneration in B5 medium (98–100 %) compared to MS medium (15–73 %). For *P. coccineus*, the best results were achieved in cotyledon nodes in MS medium supplemented with 72 µM BA, with 12.36 shoots per explant (Table 1). This was similar to that obtained by Malik and Saxena (1992), who obtained up to 11 shoots per explant in *P. coccineus* cotyledons in MS medium supplemented with 30 µM BA.

In the case of *V. radiata*, the highest number of shoots per explant (7.27) was obtained in cotyledons sown in MS medium supplemented with 72 µM BA. In contrast, Avenido and Hattori (2021) found that the cotyledon node had the highest potential for shoot

Table 1. Effect of the interaction between the cotyledon axis, cotyledon node, cotyledon, and embryonic axis of *Phaseolus vulgaris* L., *Phaseolus coccineus* L., and *Vigna radiata* L. in Murashige and Skoog (1962) and B5 (Gamborg *et al*., 1968) culture media on *in vitro* shoot induction after three weeks of culture.

Species	Culture media						
		MS			B5		
	Explant (Type)	Sprouting (%)	Number of shoots per explant	Shoot length (cm)	Sprouting (%)	Number of shoots per explant	Shoot length (cm)
P. vulgaris	Cn	30.77 cde	1.23 bcde	0.04 cd	46.15 abcde	1.15 bcde	0.11 bcd
	Ca	64.29 abcd	1.71 bcde	0.05 cd	46.15 abcde	0.62 de	0.03 d
	C	13.33 de	0.13 e	0.01 d	7.33 e	0.93 cde	0.01 d
	Ea	0.00 e	0.00 e	0.00 d	0.00 e	0.00 e	0.00 d
P. coccineus	Cn	85.71 ab	12.36 a	0.31 a	85.71 ab	8.71 abcd	0.19 abc
	Ca	100.00 a	9.08 abc	0.10 bcd	100.00 a	2.69 bcde	0.22 ab
	C	33.33 bcde	9.13 ab	0.18 abc	6.67 a	0.20 e	0.01 d
	Ea	14.29 cde	2.69 bcde	0.06 cd	14.29 cde	0.79 cde	0.04 cd
V. radiata	Cn	53.33 abcde	3.27 bcde	0.07 cd	40.00 bcde	1.33 bcde	0.09 bcd
	Ca	93.33 a	2.60 bcde	0.09 bcd	93.33 a	1.33 bcde	0.11 bcd
	C	66.67 abc	7.27 abcde	0.06 cd	60.00 abcd	6.20 abcd	0.06 cd
	Ea	20.00 cde	1.00 cde	0.01 cd	20.00 cde	0.67 de	0.02 d

Means with a common letter are not significantly different (Tukey, $\alpha \leq 0.05$). MS: Murashige and Skoog basic culture medium; B5: Gamborg culture medium; Cn: cotyledon node; Ca: cotyledon axis; C: cotyledon; Ea: embryonic axis.

induction by direct organogenesis in *V. radiata*, with 3.3 to 10.4 shoots per explant. In this work, the longest shoots were obtained from the cotyledon axis (0.09 cm in MS medium and 0.11 cm in B5 medium, both supplemented with 72 µM BA). These results are much lower than those reported by Bhajan *et al*. (2024), who obtained shoots of up to 5 cm in cotyledons in MS medium supplemented with 5 µM BA.

Evaluation of different concentrations of 6-benzyladenine (BA) and thidiazuron (TDZ)

To evaluate the effect of BA and TDZ on shoot induction, cotyledon nodes and cotyledons were used as explants due to their quantitative and qualitative results. In this case, *P. coccineus* and *V. radiata* showed a higher percentage ($p \leq 0.05$) of sprouting than *P. vulgaris* (Table 2).

In the case of *P. vulgaris*, the most efficient responses were obtained with cotyledonary nodes planted in MS medium supplemented with 72 µM BA (Table 2), where the highest number of shoots per explant (4.1) was obtained, as well as the longest shoots (0.09 cm). These results are superior in terms of number of shoots per explant (2.91) and inferior in terms of shoot length (2 cm) to those obtained by Yu *et al*. (2021) in cotyledon nodes sown in MS medium supplemented with 7 mg L^{-1} BA and 0.2 mg

Table 2. Effect of the interaction between cotyledon (C), cotyledon node (Cn), 6-benzyladenine (BA), and thidiazuron (TDZ) on the induction of *in vitro* shoots of *Phaseolus vulgaris* L., *Phaseolus coccineus* L., and *Vigna radiata* L. after three weeks of cultivation.

Species	Explant							
			Cotyledon			Cotyledonary node		
	BA (μM)	TDZ (μM)	Sprouting (%)	Number of shoots per explant	Shoot length (cm)	Sprouting (%)	Number of shoots per explant	Shoot length (cm)
P. vulgaris	0	0	30 abc	0.5 f	0.02 d	40 abc	0.8 f	0.03 d
	54	0	10 c	0.6 f	0.01 d	40 abc	1.1 f	0.04 d
	72	0	40 abc	3.1 f	0.05 cd	100 a	4.1 f	0.09 cd
	90	0	10 c	0.6 f	0.01 d	50 abc	1.1 f	0.05 cd
	0	54	60 abc	2.9 f	0.03 d	40 abc	2.2 f	0.04 d
	0	72	10 c	2.3 f	0.01 d	70 abc	2.5 f	0.07 cd
	0	90	20 bc	2.1 f	0.01 d	40 abc	1.0 f	0.04 d
P. coccineus	0	0	60 abc	1.5 f	0.59 abc	100 a	12.2 bcdef	0.83 ab
	54	0	70 abc	10.7 cdef	0.10 cd	100 a	27.3 a	0.37 abcd
	72	0	40 abc	3.6 f	0.09 cd	90 ab	22.3 abcd	0.28 cd
	90	0	60 abc	9.7 def	0.24 cd	100 a	27.9 a	0.44 abcd
	0	54	60 abc	10.4 def	0.17 cd	80 abc	25.9 ab	0.17 cd
	0	72	70 abc	20.6 abcde	0.26 cd	100 a	25.6 abc	0.28 cd
	0	90	70 abc	14.2 abcdef	0.16 cd	90 ab	28.2 a	0.23 cd
V. radiata	0	0	10 c	0.2 f	0.02 d	100 a	5.7 ef	0.86 a
	54	0	40 abc	2.5 f	0.08 cd	80 abc	5.1 f	0.16 cd
	72	0	50 abc	5.5 f	0.04 d	100 a	6.8 ef	0.31 bcd
	90	0	30 abc	3.5 f	0.04 d	80 abc	6.2 ef	0.13 cd
	0	54	70 abc	7.9 def	0.05 cd	90 ab	7.1 ef	0.10 cd
	0	72	40 abc	2.6 f	0.03 d	90 ab	4.3 f	0.17 cd
	0	90	60 abc	8.2 def	0.04 d	100 a	6.2 ef	0.13 cd

Means with a common letter are not significantly different (Tukey, $\alpha \leq 0.05$).

L^{-1} 1-naphthaleneacetic acid (ANA). It is likely that this balance of auxins (ANA) and cytokinins (BA) favored the growth in shoot length.

For *P. coccineus*, the best sprouting response was obtained in cotyledon nodes planted in MS medium supplemented with 90 μM BA (Table 2), where 100 % sprouting and 27.9 shoots per explant with an average length of 0.44 cm were achieved. The number of shoots per explant obtained was higher than that reported by Santalla *et al*. (1998), who achieved up to 13.5 shoots per explant in cotyledon nodes sown in MS medium supplemented with 15 μM BA and 2 μM AG_3. The shoots of *P. coccineus*, both in cotyledon nodes and cotyledons, were significantly superior in size and vigor compared to *P. vulgaris* and *V. radiata* (Figure 1).

Finally, in *V. radiata*, the most efficient response was obtained with cotyledon nodes planted in MS medium supplemented with 72 μM BA, with 100 % sprouting, up to 6.8 shoots per explant, and measuring 0.31 cm in length. These results were superior

to those reported by Bhajan *et al*. (2024), who achieved 5.36 shoots per explant in cotyledon nodes planted in MS medium supplemented with 5 mg L^{-1} BA. This reflects that a higher concentration of BA in the MS medium caused greater shoot regeneration.

Shoot multiplication

Groups of 3 to 4 shoots from cotyledonary nodes and cotyledons of the three species were dissected and sown in MS medium supplemented with the same concentrations of BA and TDZ as in the induction stage. The sprouting behavior showed significant differences ($p \leq 0.05$), with *P. coccineus* (84.29 %) and *V. radiata* (72.86 %) showing a higher sprouting percentage compared to *P. vulgaris* (42.86 %) (Table 3). The unsatisfactory responses in *P. vulgaris* could be mainly due to the recalcitrance of this species, which causes limitations for its *in vitro* cultivation (Chero-Ayay *et al*., 2019).

Table 3. Effect of the interaction between shoots from the cotyledon, cotyledon node, 6-benzyladenine (BA), and thidiazuron (TDZ) on the *in vitro* multiplication of shoots of *Phaseolus vulgaris* L., *Phaseolus coccineus* L., and *Vigna radiata* L. after four weeks of cultivation.

Species	BA (μM)	TDZ (μM)	Original explant					
			Cotyledon			Cotyledon nodes		
			Sprouting (%)	Number of shoots per explant	Shoot length (cm)	Sprouting (%)	Number of shoots per explant	Shoot length (cm)
P. vulgaris	0	0	30 abc	0.6 h	0.03 c	50 abc	1.2 h	0.03 c
	54	0	30 abc	1.5 h	0.03 c	50 abc	1.6 gh	0.06 c
	72	0	40 abc	3.4 gh	0.10 c	100 a	6.1 fgh	0.11 c
	90	0	10 c	0.0 h	0.01 c	50 abc	1.3 h	0.06 c
	0	54	60 abc	3.0 gh	0.05 c	40 abc	3.4 gh	0.05 c
	0	72	10 c	2.3 gh	0.03 c	70 abc	4.0 gh	0.08 c
	0	90	20 bc	2.8 gh	0.03 c	40 abc	1.0 h	0.04 c
P. coccineus	0	0	60 abc	4.0 gh	0.77 abc	100 a	16.7 bcdefgh	1.22 a
	54	0	70 abc	14.7 cdefgh	0.25 bc	100 a	36.9 a	0.64 abc
	72	0	60 abc	8.6 defgh	0.52 abc	90 ab	27.4 abcde	0.57 abc
	90	0	80 abc	14.2 cdefgh	0.76 abc	100 a	30.7 abc	0.64 abc
	0	54	90 ab	21.7 abcdfg	0.54 abc	80 abc	28.2 abcd	0.34 abc
	0	72	80 abc	31.0 abc	0.91 abc	100 a	28.0 abcde	0.54 abc
	0	90	80 abc	27.1 abcde	0.55 abc	90 ab	35.5 ab	0.44 abc
V. radiata	0	0	20 bc	0.8 h	0.04 c	100 a	6.5 fgh	1.17 ab
	54	0	50 abc	5.4 fgh	0.15 c	80 abc	8.3 defgh	0.18 c
	72	0	50 abc	6.7 fgh	0.03 c	100 a	8.0 efgh	0.39 abc
	90	0	40 abc	6.4 fgh	0.12 c	80 abc	9.6 defgh	0.17 c
	0	54	80 abc	15.2 cdefgh	0.08 c	90 ab	11.6 cdefgh	0.12 c
	0	72	50 abc	6.6 fgh	0.07 c	90 ab	9.4 defgh	0.24 bc
	0	90	90 ab	24.6 abcdef	0.13 c	100 a	9.5 defgh	0.18 c

Means with a common letter are not significantly different (Tukey, $\alpha \leq 0.05$).

For *P. vulgaris*, superior sprouting was achieved with shoots from cotyledonary nodes planted in MS medium supplemented with 72 µM BA (Table 3), with the highest increase in shoots per explant (6.1), in addition to shoots with greater length (0.11 cm). This was lower than that reported by Quintero-Jiménez *et al*. (2010), who obtained up to 20 shoots per explant from embryonic axis sown in MS medium supplemented with 10 mg L^{-1} BA.

Explants from cotyledon nodes in MS medium with 54 µM BA showed the most efficient response for *P. coccineus* (Table 3), with 100 % sprouting and an increase of 30.7 shoots per explant with an average length of 0.64 cm. The increase in shoots, considering that four shoots per explant were used as a starting point, was almost 800 %. These results greatly exceeded those obtained by Vaquero *et al*. (1993), who achieved a multiplication of between 200 and 300 % in *P. coccineus* in MS medium supplemented with 1 µM BA, 0.1 µM ANA, and AG_3.

In *V. radiata*, the highest increase in shoots per explant (24.6) was observed in shoots from cotyledons sown in MS medium with 90 µM TDZ, greatly exceeding the results of Patra *et al*. (2018), who achieved up to 7.8 shoots per explant in cotyledon nodes sown in MS medium supplemented with 1.5 mg L^{-1} BA and 1 mg L^{-1} kinetin. It can be deduced that, in *V. radiata*, high concentrations of TDZ are preferable for effective *in vitro* shoot multiplication.

Shoot elongation

In order to accelerate the growth of shoots of the three species, groups of 3 to 4 shoots with an average length of 0.1 to 0.15 cm from cotyledon nodes (Cn) and cotyledons (C) were dissected. Significant differences were detected between the different levels of AG_3 ($p \leq 0.05$) (Table 4).

The shoots of *P. coccineus*, with an average length of 3.19 cm, elongated to a greater extent than those of *P. vulgaris* (0.12 cm) and *V. radiata* (0.18 cm) (Figure 1), with a concentration of 5.6 µM of AG_3 in shoots from cotyledonary nodes, causing maximum elongation (5.533 cm). This is similar to the results obtained by Vaquero *et al*. (1993), who achieved effective shoot elongation of up to 91 % of the explants (cotyledon nodes) planted in MS medium supplemented with 3 µM AG_3. Shoot elongation in MS medium with 100 % inorganic salts was higher (1.35 cm) compared to that obtained in MS medium with 50 % inorganic salts (1.24 cm). This is similar to what was reported by Doğan (2022), who obtained the greatest shoot elongation of *Staurogyne repens* (2.27 cm) with 100 % inorganic salts in MS medium.

On the other hand, in *P. vulgaris*, greater elongation (0.222 cm) was achieved in shoots from cotyledonary nodes sown in MS medium with 100 % inorganic salts without AG_3 (control). This is consistent with the methodology followed by Mohamed *et al*. (1993), who achieved at least 0.5 cm elongation in *P. vulgaris* shoots sown in MS medium without plant growth regulators.

In the case of *V. radiata*, shoots from cotyledon nodes planted in MS medium with 100 % inorganic salts and supplemented with 2.8 µM AG_3 were those that increased their

Table 4. Effect of the interaction between shoots from cotyledon nodes (Cn), cotyledons (C), and gibberellic acid (AG_3) sown *in vitro* in Murashige and Skoog (1962) basic medium (MS) with 50 and 100 % inorganic salts on the elongation of *in vitro* shoots of *Phaseolus vulgaris* L., *Phaseolus coccineus* L., and *Vigna radiata* L. after four weeks of cultivation.

Species	AG_3 (µM)	MS inorganic salts (%)			
		100 Increase in shoot length (cm)		50 Increase in shoot length (cm)	
		C Shoots	Cn Shoots	C Shoots	Cn Shoots
P. vulgaris	0.0	0.117 hi	0.222 ghi	0.106 hi	0.161 hi
	1.4	0.211 ghi	0.089 hi	0.039 i	0.094 hi
	2.8	0.139 hi	0.206 ghi	0.117 hi	0.083 i
	4.2	0.044 i	0.117 hi	0.194 ghi	0.056 i
	5.6	0.039 i	0.056 i	0.067 i	0.033 i
	7.0	0.211 ghi	0.078 i	0.011 i	0.044 i
P. coccineus	0.0	1.854 defghi	2.008 defghe	2.460 cdefgh	5.208 a
	1.4	3.187 abdcef	2.675 bcdef	2.608 bcdefg	4.125 abcd
	2.8	5.192 ab	2.025 cdefghi	1.429 defghi	3.967 abcd
	4.2	4.842 ab	4.025 abcd	2.237 cdefghi	2.808 abcdef
	5.6	3.754 abcde	5.533 a	1.125 efghi	2.512 bcdefgh
	7.0	1.475 defghi	5.450 a	2.825 abcdef	4.592 abc
V. radiata	0.0	0.083 i	0.236 ghi	0.056 i	0.161 hi
	1.4	0.071 i	0.617 fghi	0.076 i	0.083 i
	2.8	0.083 i	0.804 fghi	0.050 i	0.075 i
	4.2	0.092 hi	0.042 i	0.104 hi	0.204 ghi
	5.6	0.046 i	0.129 hi	0.058 i	0.129 hi
	7.0	0.100 hi	0.129 hi	0.067 i	0.129 hi

Means with a common letter are not significantly different (Tukey, $\alpha \leq 0.05$).

length to a greater extent (0.804 cm). This elongation was lower than that reported by Bhajan *et al*. (2019), who managed to increase shoots taken from cotyledon nodes grown in MS medium supplemented with 2 µM BA by up to 4 cm.

CONCLUSIONS

The induction, multiplication, and elongation of shoots from advanced lines of *Phaseolus vulgaris*, *Phaseolus coccineus*, and *Vigna radiata* were established using explants from dissected cotyledonary nodes of *in vitro* germinated seedlings. Shoot induction was achieved in Murashige and Skoog (MS) medium with 100 % inorganic salts and 72 µM (*P. vulgaris* and *V. radiata*) or 90 µM (*P. coccineus*) 6-benzyladenine (BA). Multiplication was effective in MS medium with 100 % salts and 72 µM BA (*P. vulgaris*), 54 µM BA (*P. coccineus*), or 90 µM thidiazuron (TDZ) (*V. radiata*). Elongation was achieved in MS

medium at 100 % salts without growth regulators (*P. vulgaris*), 5.6 µM gibberellic acid (AG_3) (*P. coccineus*), or 2.8 µM AG_3 (*V. radiata*).

ACKNOWLEDGEMENTS

To the Postgraduate College Campus Montecillo for the facilities made available for the development of this research, and to the Ministry of Science, Humanities, Technology, and Innovation (SECIHTI) for the national scholarship awarded under CVU number 1232178 to the first author to pursue postgraduate studies.

REFERENCES

Avenido RA, Hattori K. 2021. Differences in shoot regeneration response from cotyledonary node explants in Asiatic *Vigna* species support genomic grouping within subgenus *Ceratotropis* (Piper) Verdc. Plant Cell, Tissue and Organ Culture 144 (1): 99–110.

Bhajan SK, Begum S, Islam MN, Hoque MI, Sarker RH. 2019. *In vitro* regeneration and *Agrobacterium*-mediated genetic transformation of local varieties of mungbean (*Vigna radiata* (L). Wilczek). Plant Tissue Culture and Biotechnology 29 (1): 81–97. https://doi.org/10.3329/ptcb.v29i1.41981

Bhajan SK, Hasan MM, Rahman MA, Sarker RH, Islam MN. 2024. An efficient approach of *in vitro* plant regeneration and propagation of mungbean [*Vigna radiata* L. (Wilczek)]. Plant Trends 2 (3): 46–56. https://doi.org/10.5455/pt.2024.05

Chero-Ayay J, Rojas-Idrogo C, Delgado-Paredes GEG. 2019. Indirect organogenesis in common bean: Other model of recalcitrant species? Journal of Global Biosciences 8 (4): 6146–6159.

Doğan M. 2022. Influence of different concentrations of Murashige and Skoog medium on multiple shoot regeneration of *Staurogyne repens* (Nees) Kuntze. Journal of Engineering Technology and Applied Sciences 7 (1): 61–67. https://doi.org/10.30931/jetas.1055833

Gamborg OL, Miller RA, Ojima K. 1968. Nutrient requirements of suspension cultures of soybean root cells. Experimental Cell Research 50 (1): 151–158. https://doi.org/10.1016/0014-4827(68)90403-5

INEGI (Instituto Nacional de Estadística y Geografía). 2024. Abasto y comercialización de productos básicos: frijol. Ciudad de México, México. 20 p.

Malik KA, Saxena PK. 1992. Regeneration in *Phaseolus vulgaris* L.: High-frequency induction of direct shoot formation in intact seedlings by N6-benzylaminopurine and thidiazuron. Planta 186 (3): 384–389. https://doi.org/10.1007/bf00195319

Mohamed MF, Coyne DP, Read PE. 1993. Shoot organogenesis in callus induced from pedicel explants of common bean (*Phaseolus vulgaris* L.). Journal of the American Society for Horticultural Science 118 (1): 158–162.

Morales-Soto A, Lamz-Piedra A. 2020. Métodos de mejora genética en el cultivo del frijol común (*Phaseolus vulgaris* L.) frente al Virus del Mosaico Dorado Amarillo del Frijol (BGYMV). Cultivos Tropicales 41 (4).

Murashige T, Skoog F. 1962. A revised medium for rapid growth and bio assays with tobacco tissue cultures. Physiologia Plantarum 15: 473–497. https://doi.org/10.1111/j.1399-3054.1962.tb08052.x

Nupur AK. 2025. *In-vitro* evaluation on the germination potential and seedling growth of *Vigna radiata* (L.) under heavy metal stress. Environment and Ecology 43 (1): 16–23. https://doi.org/10.60151/envec/GUSZ8343

Pandey P, Irulappan V, Bagavathiannan MV, Senthil-Kumar M. 2017. Impact of combined abiotic and biotic stresses on plant growth and avenues for crop improvement by exploiting physio-morphological traits. Frontiers in Plant Science 8 (53). https://doi.org/10.3389/fpls.2017.00537

Patra A, Samal KC, Rout GR, Jagadev PN. 2018. *In vitro* regeneration of recalcitrant green gram (*Vigna radiata* L.) from immature cotyledons for genetic improvement. International Journal of Current Microbiology and Applied Sciences 7 (1): 3072–3080. https://doi.org/10.20546/ijcmas.2018.701.364

Quintero-Jiménez A, Espinosa-Huerta E, Acosta-Gallegos JA, Guzmán-Maldonado HS, Mora-Avilés MA. 2010. Enhanced shoot organogenesis and regeneration in the common bean (*Phaseolus vulgaris* L.). Plant Cell, Tissue and Organ Culture 102 (3): 381–386. https://doi.org/10.1007/s11240-010-9744-2

R Core Team. 2022. R: A language and environment for statistical computing. R Foundation for Statistical Computing, Vienna, Austria. https://www.R-project.org/

Rajashekar CB, Baek KH. 2014. Hydrogen peroxide alleviates hypoxia during imbibition and germination of bean seeds (*Phaseolus vulgaris* L.). American Journal of Plant Sciences 5 (24): 3572–3584. https://doi.org/10.4236/ajps.2014.524373

Santalla M, Power J, Davey M. 1998. Efficient *in vitro* shoot regeneration responses of *Phaseolus vulgaris* and *P. coccineus*. Euphytica 102 (2): 195–202. https://doi.org/10.1023/a:1018317327302

Schmitz S, Barrios R, Dempewolf H, Guarino L, Lusty C, Muir J. 2023. Crop diversity, its conservation and use for better food systems. *In* von Braun J, Afsana K, Fresco LO, Hassan MHA. (eds.), Science and Innovations for Food Systems Transformation. Springer: Cham, Switzerland, pp: 545–555. https://doi.org/10.1007/978-3-031-15703-5_29

Segura J, Ballester A, Barceló A. 2024. Cultivo *in vitro* de plantas: herramienta fundamental para la investigación básica y aplicada. Encuentros Multidisciplinares 26 (77).

SIAP (Servicio de Información Agroalimentaria y Pesquera). 2024. Panorama Agroalimentario 2018-2024. Gobierno de México. Secretaría de Agricultura y Desarrollo Rural. Servicio de Información Agroalimentaria y Pesquera. Ciudad de México, México. 210 p.

Song G, Han X, Wiersma A, Zong X, Awale HE, Kelly JD. 2020. Induction of competent cells for *Agrobacterium tumefaciens*-mediated stable transformation of common bean (*Phaseolus vulgaris* L.). PLOS ONE 15 (3): e0229909. https://doi.org/10.1371/journal.pone.0229909

Vaquero F, Robles C, Ruiz ML. 1993. A method for long-term micropropagation of *Phaseolus coccineus* L. Plant Cell Reports 12: 395–398. https://doi.org/10.1007/bf00234699

Yu Y, Liu D, Liu C, Yan Z, Yang X, Feng G. 2021. *In vitro* regeneration of *Phaseolus vulgaris* L. via direct and indirect organogenesis. Plant Biotechnology Reports 15 (3): 279–288. https://doi.org/10.1007/s11816-021-00681-6

Agrociencia

YELLOW PEARL POPCORN IS A VIABLE ALTERNATIVE TO IMPROVE MEXICAN POPCORN VARIETIES

Hugo **García-Perea**[1], Amalio **Santacruz-Varela***[1], Iris Grisel **Galván-Escobedo**[2], J. Jesús **García-Zavala**[1]

[1]Colegio de Postgraduados Campus Montecillo. Postgrado en Recursos Genéticos y Productividad-Genética. Carretera México-Texcoco km 36.5, Montecillo, Texcoco, State of Mexico, Mexico. C. P. 56264.
[2]Colegio de Postgraduados Campus Montecillo. Postgrado Botánica. Carretera México-Texcoco km 36.5, Montecillo, Texcoco, State of Mexico, Mexico. C. P. 56264.
* Author for correspondence: asvarela@colpos.mx

Citation: García-Perea H, Santacruz-Varela A, Galván-Escobedo IG, García-Zavala JJ. 2025. Yellow pearl popcorn is a viable alternative to improve Mexican popcorn varieties. **Agrociencia** 59(6): 825-839. https://doi.org/ 10.47163/agrociencia.v59i6.3108

Editor in Chief:
Dr. Fernando C. Gómez Merino

Received: November 08, 2024.
Approved: August 12, 2025.
Published in Agrociencia: August 15, 2025.

ABSTRACT

The deacclimatization of introduced maize varieties or races (*Zea mays* L.) limits their use. The effects of deacclimatization on the ability to produce pollen from introduced varieties are unknown. Therefore, the purpose of this study was to determine if the weather conditions in the High Valleys of central Mexico limit the ability to produce pollen from the North American Yellow Pearl Popcorn race for use as a male parent in popcorn breeding. Eight genotypes, including two from the Corn Belt of the United States, were evaluated in two sites. The morphological characteristics of tassel, pollen grain, ear, and viability were registered. Additionally, intervarietal and plant-to-plant crossing were used to observe the effect of pollen on the characteristics of the ears. Differences were found in the number of branches of the tassel, pollen grain diameter, ear diameter, and viability. There were no differences in ear characteristics between the types of crosses used. It was concluded that the climate conditions of the high valleys of central Mexico do affect the morphological characteristics of the race studied but do not limit their ability to produce pollen. Therefore, North American Yellow Pearl Popcorn race can be used as a pollen donor in the breeding of local popcorn varieties.

Keywords: introduced variety, deacclimatization, breeding, intervarietal cross.

INTRODUCTION

Plant breeding uses a variety of methodologies to produce improved varieties, including recurrent selection and hybridization with either local or exotic varieties. Exotic varieties are introduced to incorporate desirable characteristics into improved or native varieties. The disadvantage of the latter procedure is that the introduced varieties can undergo deacclimatization, which may cause problems with the reproductive ability of the introduced variety (Santiago-López *et al*., 2020; López-Morales *et al*., 2021).

Diverse studies have been conducted, including the introduction of an exotic variety to incorporate desired characteristics. Ramírez-Díaz *et al*. (2007) proposed a breeding

method to introduce genes from exotic varieties into native varieties through crosses. They concluded that this method is more efficient than other methods like reciprocal selection or conventional backcross. According to Gómez-Espejo *et al*. (2015), introducing exotic varieties from warm to temperate climates can promote the development of varieties with alleles of interest for the Mexican High Valleys region. Velasco-García *et al*. (2020) suggest using the variability of native and exotic varieties in the High Valleys of Mexico in maize breeding programs to increase heterosis. In turn, Santiago-López *et al*. (2020) mentioned that the use of adapted tropical germplasm as a source of variation for the maize of the High Valleys is feasible.

In the High Valleys of Mexico, Palomero Toluqueño is the popcorn race with the greatest popping volume, although breeding developed on this variety is limited (Bautista-Ramírez *et al*., 2020). Research on this race has focused on conservation, management, and use Gámez-Vázquez *et al. (*2014) highlight a focus on tortilla production, and propose an standardization of popping methods (de la O-Olán *et al*., 2018; Trejo-Pastor *et al*., 2023), yield, and expansion ability (Bautista-Ramírez *et al*., 2020), as well as conditions and factors of its distribution (Bautista-Ramírez *et al*., 2018). Bautista-Ramírez *et al*. (2020) found an average grain expansion volume of 2.73 cm^3 g^{-1} in 47 accessions of the Palomero Toluqueño race held at the National Institute of Forestry, Agricultural and Livestock Research (INIFAP) germplasm bank. However, the Yellow Pearl North American popcorn race has a much greater ability for popping than the Mexican variety, with expansion volumes of 40 cm^3 g^{-1} (Santacruz-Varela *et al*., 2004). Thus, the North American Yellow Pearl Popcorn race could be introduced into Mexican popcorn breeding programs to boost Palomero Toluqueño expansion.

Although numerous studies have been conducted to investigate the effects of introducing an exotic variety in order to incorporate desirable characteristics, there has been little research on this topic for popcorn. The extent to which the environment of the High Valleys in central Mexico can influence the morphological characteristics of the tassel, pollen grain, and ear, as well as whether these can have a negative influence on pollen production, is unknown, and thus whether or not it can be effective when introduced in breeding programs of Mexican popcorn programs is unclear. As a result, the goal of this research was to determine to what extent the environmental conditions of Mexican High Valleys influence the development of plants and pollen production in the North American Yellow Pearl popcorn race, allowing it to participate, at least as a male parent, in local popcorn breeding programs.

MATERIALS AND METHODS

Study locations

In the 2022 spring-summer season, two experiments were established: one in San Salvador Atenco and the other in Montecillo, Texcoco, both in the State of Mexico, Mexico, at an altitude of 2250 m with a mean annual temperature of 15 °C and a mean annual rainfall of 645 mm.

Genetic material

The plant material consisted of eight genotypes: two populations corresponding to advanced generations of hybrids of the North American Yellow Pearl Popcorn (NAYPP; Jack Superior and Iowa Pop 12), a variety of the Palomero Toluqueño race (Criollo Plaza), a synthetic variety derived from the cross between Palomero Toluqueño and the North American Yellow Pearl, a variety of the Chalqueño, Cacahuacintle, and Cónico races, which are native to the High Valleys, and a population of teosinte (*Zea mays* ssp. *mexicana*) of the Chalco race, which only participated in the viability and pollen morphology studies.

Phenotypic characterization in the field

A completely randomized experimental design with six repetitions was used in both locations. The experimental unit consisted of two rows (5 m long and spaced by 0.8 m). Each row contained 11 plants, resulting in a total of 44 plants per experimental plot.

The following phenological and morphological variables were evaluated: 1) Days to male flowering (DMF), determined by counting the number of days from planting until 50 % of the plants in each experimental plot exhibited anthesis; 2) Peduncle length (PL, cm), measured with a measuring tape from the last internode to the beginning of the tassel ramifications; 3) Length of the ramified part of the tassel (LRAP, cm), measured from the tassel (LMA, cm), measured from the end of the branches to the tip of the tassel; and 5) Number of primary branches (NB), determined by counting the primary branches present on the tassel.

In addition, five ears formed by open pollination, representative of each experimental unit, were evaluated for the following ear-related morphological variables: 6) Ear length (EL, cm), measured with a measuring tape from the base to the tip of the ear; 7) Ear diameter (ED, cm), measured at the midpoint of the ear using a caliper; 8) Number of kernel rows per ear (NR); 9) Number of kernels per row (NKR), determined by counting the kernels in two rows per ear and calculating the average; and 10) Shelling factor (SHF), calculated as the ratio of maize grain weight to total sample weight, evaluated by treatment and cross type.

Reproductive ability of the pollen in the field

Intervarietal and plant-to-plant crosses were conducted within each experimental unit using the same experimental setup established for the characterization of the genotypes. Plant-to-plant crosses were performed in row 1, while intervarietal crosses were conducted in row 2. This design aimed to assess potential differences in the effects of pollen from the same genotype (plant-to-plant crosses) compared to pollen from an exotic genotype belonging to the North American Yellow Pearl Popcorn race (intervarietal crosses using Jack Superior as the pollen donor) on ear morphological traits. The evaluated variables included ear length (EL, cm), ear diameter (ED, cm), number of kernel rows (NR), number of kernels per row (NKR), and shelling factor (SHF).

Pollen variables determined in the laboratory

Pollen grain viability was assessed by collecting pollen from 10 plants per treatment. The ears were placed in wax paper bags (No. 12 pollination bags), and after 10 min, the bags were shaken and removed from the tassels. The contents of the individual bags were pooled into a single bag to obtain a representative mixture of pollen grains for each treatment. The pollen was collected in the morning, when air temperatures ranged between 18 and 22 °C (Escobar and Pardey, 2020).

The impurities were removed from the pollen using a sieve (No. 120). Once it was clean, 0.5 g was weighed using a digital scale (Uline® brand, model H-9884, Pleasant Prairie, WI, USA) and emptied into an Eppendorf tube for microcentrifugation with a capacity of 1 mL, into which 0.5 mL of a 0.5 % 2,3,5-triphenyltetrazolium chloride solution was added. The tubes were wrapped in metal foil to avoid contact with light and then set aside for 4 h (Martins *et al*., 2017). Then, permanent mounts were made on four slides per treatment. Glycerinated gelatin was used, and they were dried for 24 h. The preparations were sealed with clear nail polish and left to dry for 24 h (Martins *et al*., 2017).

Using the AmScope software and microscope with a built-in camera, 10 photographs (40 per treatment) of the pollen grains were taken. The stained, non-stained, and total pollen grains were then counted using the "cell counter" tool in ImageJ. The result was calculated as a percentage of viability using the stained, non-stained, and total grains counted. Using the AmScope "line" tool, the diameter of the pollen grain (μm) was measured from end to end, along with the diameter of the pore (μm) and the thickness of the exine (μm) from the internal part of the last layer of the pollen grain to the external part. These variables were measured in 15 pollen grains from each treatment.

Statistical analysis

All statistical analyses were carried out using SAS/STAT v9.0 (SAS Institute, Cary, NC, USA). A completely randomized block experimental design was used to analyze the variables of days to male flowering and morphological variables of the tassel for genotype characterization. The statistical model was as follows:

$$Y = \mu + Gen + Loc + Gen\ x\ Loc + e$$

where Y is the response variable, μ is the general mean, *Gen* is the effect of the genotypes, *Loc* is the effect of the locations, *Gen* × *Loc* is the effect of the Genotype-Environment interaction, and e is the experimental error.

The morphological variables used to evaluate the crosses underwent an analysis of variance and Tukey means comparison test ($p \leq 0.05$). The following statistical model was used:

$$Y = \mu + Gen + Loc + TC/Gen + Loc\ x\ (TC/Gen) + e$$

where Y is the variable of response, μ is the general mean, *Gen* is the effect of the genotypes, *Loc* is the effect of the locations, *TC/GEN* is the effect of the cross types within genotypes, *Loc × (TC/GEN)* is the effect of the interaction of locations by type of cross within genotypes, and e is the experimental error.

In the case of pollen, for the percentage of grain viability, the data were transformed using the arc sine function, given the percentage scale with which the information was obtained. This variable, along with the morphological variables of the pollen grain, was analyzed using a completely randomized experimental design, with analysis of variance and Tukey means comparison ($p \leq 0.05$). The statistical model used was as follows:

$$Y = \mu + Gen + e$$

where Y is the response variable, μ is the general mean, *Gen* is the effect of the genotypes, and e is the experimental error.

RESULTS AND DISCUSSION

Phenotypic characteristics of the genotypes

Significant differences were observed in the variables of days to male flowering, ear length, ear diameter, number of kernel rows, number of kernels per row, and shelling factor between genotypes (Table 1). For the variables corresponding to the morphology of the tassel, there were no statistically significant differences.

Table 1. Analysis of variance, mean squares, and significance of the variables and characteristics of the tassel and the ears in the popcorn maize (*Zea mays* L.) populations evaluated.

Variable	Variation factor									
	Gen		*Loc*		*Gen × Loc*		Error	CV (%)		
DMF	172.07	**	581.440	**	228.30	**	48.230	8.57		
EL	21.18	**	0.102	ns	3.36	ns	4.224	17.44		
ED	9.02	**	3.313	*	1.50	ns	0.853	26.16		
NR	157.77	**	0.154	ns	27.35	**	3.800	16.23		
NKR	297.46	**	41.005	ns	107.49	**	14.636	18.88		
SHF	0.04	**	0.002	ns	0.03	**	0.004	8.22		
LS	16.37	ns	77.500	*	11.04	ns	15.180	17.33		
LRAP	6.59	ns	169.940	**	15.10	*	5.070	24.14		
LMA	26.02	ns	267.580	**	9.86	ns	13.170	13.75		
NB	27.52	ns	295.570	**	16.75	ns	12.85	34.51		

**: significant at $p \leq 0.01$; *: significant at $p \leq 0.05$; ns: not significant; Loc: location; *Gen × Loc*: Genotype × Location; DMF: days to male flowering; EL: ear length; ED: ear diameter; NR: number of kernel rows; NKR: number of kernels per row; SHF: shelling factor; LS: length of peduncle; LRAP: length of the ramified part of the tassel; LMA: length of main axis; NB: number of branches.

Fonseca *et al.* (2003) mentioned that deacclimatization of a variety can affect the pollen availability and floral synchrony. Uribelarrea *et al.* (2002) also mentioned that pollen production is affected by the delay in planting dates. In this investigation, the North American Yellow Pearl Popcorn (NAYPP) race showed a difference in terms of days to male flowering, resulting in one of the latest, leading to the results supporting the theory, since differences were observed with the group of adapted genotypes (Cónico, Chalqueño, and Cacahuacintle).

No differences were found in three of the four morphological variables of the tassel evaluated among races (Table 2). The Iowa Pop variety, which corresponds to the NAYPP race, was the only one to show a difference in the variable of number of branches (NB). The results indicate that the NAYPP race, despite being an introduced variety, displays similar morphological tassel characteristics to the popcorn races that predominate in the highlands of central Mexico and related native races of this region. Vidal-Martínez *et al.* (2004) highlight that the most important components for production are the total of male flowers, flowers per branch, flowers on the main axis, and the number of branches of the tassel. Fonseca *et al.* (2003) observed that the number of branches also positively affects the production of pollen per tassel. As the number of branches per tassel decreases, so will the production of pollen (Tranel *et al*., 2009). The present work supports this statement since the Jack Superior variety, derived from the NAYPP, as in the controls used, had the highest number of branches

Table 2. Days to male flowering and morphological variables means of the ear and tassel of seven popcorn maize (*Zea mays* L.) genotypes introduced and native to the High Valleys in San Salvador Atenco and Montecillo, Mexico.

Genotype	Race	DMF	EL (cm)	ED (cm)	NR	NKR	SHF	LS (cm)	LRAP (cm)	LMA (cm)	NB (cm)
Jack Superior	PPAN	87 a	11 b	2.5 b	10.65 c	16 d	0.72 c	23 a	9.3 a	9 a	10 a
Iowa Pop	PPAN	80 a	10 c	2.8 b	13.20 b	20 b	0.79 a	23 a	7.8 a	8 a	7 b
Chalqueño	Chalqueño	77 b	13 a	4.2 a	11.51 c	22 a	0.84 a	23 a	9.3 a	9 a	9 a
Criollo Plaza	Palomero Toluqueño	81 a	12 a	3.7 a	15.6 a	24 a	0.83 a	21 a	9.7 a	9 a	12 a
Criollo Plaza × Iowa Pop 12	Palomero Toluqueño × PPAN	77 b	12 a	3.7 a	14.66 a	24 a	0.81 a	23 a	9.8 a	9 a	10 a
Cacahuacintle	Cacahuacintle	79 a	12 a	3.8 a	9.60 d	16 d	0.76 b	22 a	9.1 a	9 a	11 a
Cónico	Cónico	85 a	12 a	3.9 a	8.82 e	18 d	0.83 a	21 a	10 a	10 a	10 a
HSD (0.05)		8	2	0.7	1.6	3	0.05	4	2.7	2	4

Means with the same letter are statistically equal (Tukey, $p \leq 0.05$). HSD: honest significant difference; DMF: days to male flowering; EL: ear length; ED: ear diameter; NR: number of kernel rows; NKR: number of kernels per row; SHF: shelling factor; LS: length of peduncle; LRAP: length of the ramified part of the tassel; LMA: length of main axis; NB: number of branches.

per tassel, implying that it can produce the same amount of pollen. The number of branches conditions the number of anthers produced, which, in turn, conditions the amount of pollen produced.

Velasco-García *et al.* (2020) mentioned that the introduction of exotic varieties without prior adaptation may present greater changes in plant morphology characteristics, such as height, earliness, and morphological changes in the ear. The results support this statement, since differences were observed in all the morphological ear variables evaluated of the NAYPP race compared to the genotypes adapted to the weather conditions of the Mexican highlands (Table 2). Therefore, it can be considered that this North American race differs completely in morphological characteristics from the rest of the genotypes. Schoper *et al.* (1987) mentioned that the grain viability and amount of pollen released limit the production of grains on the ear when the tassels are exposed to heat stress, which occasionally occurs in the spring and summer in the area under study.

Pollen production by location

The differences in days to male flowering and morphological tassel characteristics between locations (Table 3) may indicate a difference in pollen productivity for the varieties studied. Humidity and warm temperatures, combined with a well-distributed rainfall, favor pollen production (Rácz *et al.*, 2006). Another aspect worth considering is the genetic component. Vidal-Martinez *et al*. (2004) consider that phenotypic plasticity plays an important role in the production of pollen in maize. Likewise, Fonseca *et al*. (2003) found that pollen production is conditioned by genotypic and environmental variations.

Table 3. Comparison of means between locations for the variables of days to male flowering, ear morphology, and tassel characteristics evaluated in popcorn maize (*Zea mays* L.) genotypes.

Loc	DMF	EL (cm)	ED (cm)	NR	NKR	SHF	LS (cm)	LRAP (cm)	LMA (cm)	NB (cm)
Atenco	78.40 a	11.75 a	3.39 a	12.04 a	19.76 a	0.79 a	23.4 a	7.90 b	28 a	9 b
Montecillo	83.66 b	11.80 a	3.67 a	11.98 a	20.75 a	0.80 a	21.5 b	11.0 a	25 b	12 a
HSD	3.03	0.62	0.28	0.59	1.16	0.2	1.69	1	1.6	2

Means with the same letter are statistically equal (Tukey, $p \leq 0.05$). HSD: honest significant difference; DMF: days to male flowering; EL: ear length; ED: ear diameter; NR: number of kernel rows; NKR: number of kernels per row; SHF: shelling factor; LS: length of peduncle; LRAP: length of the ramified part of the tassel; LMA: length of main axis; NB: number of branches.

Ear characteristics by location

There no statistical differences in the means of the variables corresponding to the ear characteristics between locations (Table 4).

Table 4. Comparison of means between locations of the ear morphology variables evaluated in popcorn maize (*Zea mays* L.) genotypes.

Location	EL (cm)	ED (cm)	NR	NGH	FDES
Atenco	11.75 a	3.39 a	11.98 a	19.76 a	0.79 a
Montecillo	11.80 a	3.67 a	12.04 a	20.75 a	0.80 a
DMS	0.62	0.28	0.59	1.16	0.02

Means with the same letter are statistically equal (Tukey; $p \leq 0.05$); HSD: honest significant difference; EL: ear length; DM: ear diameter; NR: number of kernel rows; NKR: number of grains per row; SHF: shelling factor.

Effect of pollen origin on ear characteristics (crosses)

The combined analysis of variance across locations for the morphological ear variables (Table 5) showed differences between phenotypes for all morphological variables of the ear.

Table 5. Mean squares and their significance from the combined analysis of variance across locations for ear-related variables in popcorn (*Zea mays* L.) genotypes.

Variable	*Gen*		*Loc*		TC/*Gen*		*Loc*/(*TC*/*Gen*)		CV (%)
EL	21.18	**	0.100	*	6.920	ns	3.36	ns	17.44
ED	9.02	**	3.310	*	1.810	*	1.0	ns	26.16
NR	157.77	**	0.150	ns	12.800	*	14.58	**	16.23
NKR	297.46	**	41.000	ns	30.110	ns	56.78	**	18.88
SHF	0.04	**	0.002	ns	0.004	ns	0.01	**	8.22

**: Significant at $p \leq 0.01$; *: significant at $p \leq 0.05$; ns: not significant; Loc: location; Gen: genotype; TC: type of cross (plant-to-plant and intervarietal cross); EL: ear length; ED: ear diameter; NR: number of kernel rows; NKR: number of kernels per row; SHF: shelling factor.

Diverse studies point out yield as the main adaptation indicator (Gómez-Espejo *et al.,* 2015; Santiago-López *et al.,* 2020; López-Morales *et al.,* 2021). The difference in yield usually determines if an introduced variety adapts and becomes a candidate for breeding programs. In contrast to this study, where variables such as pollen viability were included, the ear characteristics resulting from intervarietal crosses in comparison to those obtained with plant-to-plant crosses act as indicators of the potential of the NAYPP race to produce pollen and act as a male parent under the weather conditions of the central Mexico highlands.

The comparison of means for the morphological ear variables for different maize genotypes (Table 6) showed differences in all variables. The NAYPP race presented a slight reduction in the values of ear length, ear diameter, and number of kernel rows. There were differences in the morphology of the ear of the NAYPP race in comparison to the remaining races, showing that it was negatively affected.

Table 6. Comparison of means of the variables of ears from different popcorn (*Zea mays* L.) genotypes.

Genotype	Race	EL (cm)	ED (cm)	NR	NKR	SHF
Jack Superior	PPAN	11.06 c	2.53 b	10.65 d	15.83 d	0.72 c
Iowa Pop 12	PPAN	10.28 c	2.81 b	13.20 b	20.45 b	0.79 b
Chalqueño	Chalqueño	13.20 a	4.20 a	11.51 c	22.41 b	0.84 a
Criollo Plaza	Palomero Toluqueño	11.51 b	3.70 a	15.60 a	24.16 a	0.83 a
Criollo Plaza × Iowa Pop 12	Palomero Toluqueño × PPAN	11.93 b	3.71 a	14.66 b	24.29 a	0.81 b
Cacahuacintle	Cacahuacintle	12.22 b	3.80 a	9.60 d	16.54 d	0.76 b
Cónico	Cónico	12.25 b	3.93 a	8.82 e	18.08 c	0.83 a
HSD (0.05)		1.77	0.79	1.68	3.3	0.05

Means with the same letters are statistically equal (Tukey; $p \leq 0.05$); HSD: honest significant difference; EL: ear length; ED: ear diameter; NR: number of kernel rows; NKR: number of kernels per row; SHF: shelling factor.

Within the varieties, no differences were observed in the characteristics of the ears from plant-to-plant crosses or intervarietal crosses (Table 7). Criollo Plaza variety statistically displayed the same ear length with both crossing methods when using the Jack Superior genotype as a pollen source. The results show that comparing the means of the types of crossing of the morphological variables indicates that they are equal and that an intervarietal cross leads to the risk of winning or losing 2.51 cm. In the case of ear length, such a difference is not statistically significant. The values of the intervarietal crosses, in comparison with the plant-to-plant crosses, were equal for ear characteristics, indicating that there is a sufficient ability of the pollen of the introduced NAYPP variety to produce normal ears.

In general terms, the NAYPP race displayed different and inferior morphological tassel and ear characteristics to those of the native varieties under the weather conditions of the central Mexican highlands. However, these differences did not limit its ability to produce pollen with characteristics comparable to the Palomero Toluqueño race. Therefore, its use is possible in the breeding programs for local popcorn varieties. The separation between original populations without any adaptation and those selected in the High Valleys has been previously reported (Velasco-García *et al.*, 2020).

Table 7. Comparison of means of the ear variables depending on the type of the crossing method used in popcorn (*Zea mays* L.) genotypes evaluated.

Genotype	Type of cross	EL (cm)	ED (cm)	NR	NKR	SHF
Jack Superior	Plant-to-plant	11.60 a	2.53 a	10 a	16 a	0.72 a
	Intervarietal	11.60 a	2.53 a	10 a	15 a	0.73 a
Iowa Pop 12	Plant-to-plant	9.85 a	2.67 a	12 a	20 a	0.79 a
	Intervarietal	10.71 a	2.95 a	13 a	20 a	0.80 a
Chalqueño	Plant-to-plant	13.12 a	3.94 a	11 a	21 a	0.85 a
	Intervarietal	13.28 a	4.46 a	11 a	23 a	0.83 a
Criollo Plaza	Plant-to-plant	11.77 a	3.66 a	15 a	24 a	0.83 a
	Intervarietal	11.25 a	3.75 a	15 a	24 a	0.83 a
Criollo Plaza × Iowa Pop 12	Plant-to-plant	11.60 a	3.25 a	13 b	22 a	0.80 a
	Intervarietal	12.26 a	4.18 a	16 a	25 a	0.82 a
Cacahuacintle	Plant-to-plant	10.99 a	3.34 a	8 a	14 a	0.73 a
	Intervarietal	13.45 a	4.26 a	10 a	18 a	0.79 a
Cónico	Plant-to-plant	11.87 a	8.50 a	8 a	16 a	0.82 a
	Intervarietal	12.63 a	4.06 a	9 a	19 a	0.83 a
HSD (0.05)		2.51	1.13	2	4	0.08

Means with the same letter are statistically equal (Tukey; $p \leq 0.05$); HSD: honest significant difference; EL: ear length; ED: ear diameter; NR: number of rows; NKR: number of grains per row; SHF: shelling factor.

However, when carrying out intervarietal crosses, the NAYPP pollen had no negative effect on the characteristics of the ears and can therefore be used as a male parent for intervarietal crosses.

The introduction of exotic varieties has not yet been fully studied in popcorn, so more investigations are required to help to determine their potential to be used as parents in breeding programs or as varieties after undergoing an adaptation process through recurrent selection in the new target environment. This would help generate new varieties that help boost production in order to reduce the imports of this grain and the conservation of the Palomero Toluqueño race in Mexico.

Study of pollen grains

The analysis of variance for the variables of viability and morphology of the pollen grain (Table 8) showed highly significant differences in the variables of viability and diameter of the grain (Figure 1). However, for the variables of pore diameter and thickness of exine, significant differences were only observed in the genotype variation factor.

The pollen grain viability is negatively affected by deacclimatization (Fonseca *et al.*, 2003). The results contrast with the above statement, since the viability of the pollen grain from the NAYPP race is different from some genotypes but had the same viability as the group of genotypes adapted to the weather conditions of the High Valleys of Mexico (Table 9).

Table 8. Analysis of variance of the characteristics evaluated in the pollen of maize (*Zea mays* L.) genotypes.

Variable	df	Genotype		Error	CV (%)
VIA	7	333.15	**	55.62	12.32
DPG	14	1457.89	**	55.93	8.30
DP	14	8.23	*	0.81	15.55
EXT	14	0.21	*	0.08	27.77

**: Significant at $p \leq 0.01$; *: significant at $p \leq 0.05$; ns: not significant; df: degrees of freedom; CV: coefficient of variation; VIA: viability; DPG: diameter of the pollen grain; DP: diameter of pore; EXT: exine thickness.

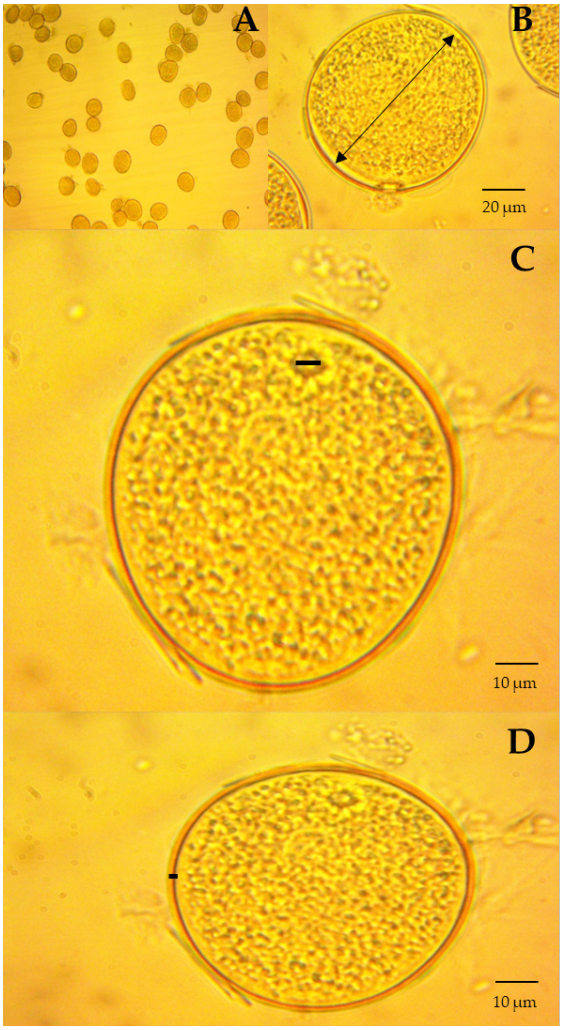

Figure 1. Maize (*Zea mays* L.) pollen grain dimensions. A: pollen grains; B: pollen grain diameter; C: pore diameter; D: exine thickness.

Table 9. Comparison of means for viability and morphology of the pollen grains of maize (*Zea mays* L.) genotypes.

Genotype	Race	VIA	DGP (μm)	PD (μm)	EXT (μm)
Jack Superior	NAYPP	65 a	92 a	5.7 b	1.0 a
Iowa Pop 12	NAYPP	63 a	95 a	5.0 c	1.0 a
Chalqueño	Chalqueño	56 c	92 a	6.4 a	1.0 a
Criollo Plaza	Palomero Toluqueño	59 b	88 b	5.7 b	1.2 a
Criollo Plaza × Iowa Pop 12	Palomero Toluqueño × NAYPP	60 a	90 a	5.6 c	1.0 a
Cacahuacintle	Cacahuacintle	59 b	95 a	6.6 a	1.1 a
Cónico	Cónico	60 a	91 a	5.7 b	1.0 a
Teosinte	Chalco	59 b	67 c	5 d	0.9 b
HSD (0.05)		5	6.2	0.7	0.2

Means with the same letter are statistically equal (Tukey; $p \leq 0.05$); HSD: honest significant difference; VIA: percentage of viability; DPG: diameter of the pollen grain; DP: diameter of pore; EXT: exine thickness; NAYPP: North American Yellow Pearl Popcorn.

Pollen is an important vector in the genetic flow of maize (Luna *et al.*, 2001). The NAYPP race did not differ with three of the genotypes studied (Table 9). Its viability behaved in the same way as the Cónico race and did not show an evolutionary tendency towards the loss or gain of viability of the pollen grain, since the teosinte that represents the basal position in the evolutionary scale has an intermediate pollen viability, with races of higher or lower pollen viability. The pollen grain viability of the North American race was not affected by the weather conditions of the High Valleys of Mexico, possibly as a survival mechanism against the lack of adaptation for grain yield.

Regarding pollen morphology, an increase stands out in the dimensions of the grain diameter, pore diameter, and exine thickness in the planted maize races in comparison to the wild relative. A slight tendency was observed towards the increase in the viability of the pollen as the dimensions of the morphology variables increase, particularly the variable of the pollen grain diameter, since the viability of the pollen is highly conditioned by the temperature and relative humidity of the environment (Kaefer *et al.*, 2016; Razzaq *et al.*, 2019). The size of the pollen grain is related to the amount of water it contains (Aylor, 2003); therefore, the smallest grains are less visible. Teosinte and Criollo Plaza are among the genotypes with the least viability, as well as the smallest size (Table 9).

Results show that pollen grain characteristics depended more on the variety, reflecting previous breeding work. For example, the Jack Superior and Iowa Pop varieties, despite deriving from the same maize race, are different for the pore diameter variable, whereas for the rest of the variables, they were equal. Taking the diameter of the

pollen grain (DPG) as a reference, the varieties that showed the most breeding work displayed a greater grain diameter in relation to the oldest maize varieties, such as Palomero Toluqueño (Kato-Yamakake, 2023) or teosinte itself. This was also observed for the diameter of the pore (DP) and exine thickness (EXT), where teosinte displayed the lowest values. It is possible that the smallest diameter of the grain is caused by a tolerance to desiccation (Table 10), since, at flowering, the pollen grains are larger when they undergo intense stress due to desiccation (Ejsmond *et al.*, 2011).

Comparison of means from locations

Table 10. Comparison of the means of the pollen grain morphology of different maize (*Zea mays* L.) genotypes.

Location	DPG (μm)	DP (μm)	EXT (μm)
Atenco	92.81 a	5.74 a	1.09 a
Montecillo	87.70 b	5.85 a	0.97 b
HSD (0.05)	1.97	0.23	0.59

Means with the same letter are statistically equal (Tukey; $p \leq 0.05$); HSD: honest significant difference. DPG: pollen grain diameter; DP: pore diameter; EXT: exine thickness.

CONCLUSIONS

Deacclimatization in the highlands of central Mexico reduces the agronomic yield of the North American Yellow Pearl Popcorn race in traits such as earliness, tassel, and ear morphology. However, these changes do not limit the ability of the pollen produced, since its viability and morphology have no effect on its role as a male parent, allowing for the production of ears with the same characteristics as when pollen from native varieties is used. Therefore, the North American Yellow Pearl Popcorn race is an alternative that can be used in breeding for local popcorn varieties.

ACKNOWLEDGEMENTS

Our thanks go to the farmer Luis Sánchez from San Salvador Atenco for the access to his fields for the realization of this study.

REFERENCES

Aylor DE. 2003. Rate of dehydration of corn (*Zea mays* L.) pollen in the air. Journal of Experimental Botany 54 (391): 2307–2312. https://doi.org/10.1093/jxb/erg242

Bautista-Ramírez E, Cuevas-Sánchez JA, Santacruz-Varela A, Hernández-Leal E, Hernández-Galeno CA, Hernández- Bautista A, Gómez-Maldonado R. 2018. Conditioning factors in the distribution of Palomero Toluqueño maize and alternatives for its conservation. Revista Bio Ciencias 5 (2): e476. https://doi.org/10.15741/revbio.05.03.03

Bautista-Ramírez E, Santacruz-Varela A, Córdova-Téllez L, Muñoz Orozco A, López-Sánchez H, Esquivel-Esquivel G. 2020. Rendimiento y capacidad de expansión del grano de maíz en la raza Palomero Toluqueño. Revista Mexicana de Ciencias Agrícolas 11 (7): 1607–1618. https://doi.org/10.29312/remexca.v11i7.2130

de la O-Olán M, Santacruz-Varela A, Sangermán-Jarquín DM, Gámez-Vázquez AJ, Arellano-Vázquez JL, Valadez-Bustos MG, Ávila-Perches MÁ. 2018. Estandarización del método de reventado para la evaluación experimental del maíz palomero. Revista Mexicana de Ciencias Agrícolas 9 (7): 1471–1482. https://doi.org/10.29312/remexca.v9i7.1675

Ejsmond MJ, Wrońska-Pilarek D, Ejsmond A, Dragosz-Kluska D, Karpińska-Kołaczek M, Kołaczek P, Kozłowski J. 2011. Does climate affect pollen morphology? Optimal size and shape of pollen grains under various desiccation intensity. Ecosphere 2 (10): 1–15. https://doi.org/10.1890/es11-00147.1

Escobar PRS, Pardey RC. 2020. Evaluación de la germinación del polen de *Zea mays* a través de metodologías *in vitro* en Santa Marta, Colombia. Intropica 15 (2): 137–143. https://doi.org/10.21676/23897864.3565

Fonseca AE, Westgate ME, Grass L, Dornbos Jr DL. 2003. Tassel morphology as an indicator of potential pollen production in maize. Crop Management 2 (1): 1–15, https://doi.org/10.1094/CM-2003-0804-01-RS

Gámez-Vázquez AJ, de la O-Olán M, Santacruz-Varela A, López-Sánchez H. 2014. Conservación *in situ*, manejo y aprovechamiento de maíz Palomero Toluqueño con productores custodios. Revista Mexicana de Ciencias Agrícolas 5 (8): 1519–153. https://doi.org/10.29312/remexca.v5i8.832

Gómez-Espejo AL, Molina-Galán JD, García-Zavala JJ, Mendoza-Castillo MC, de la Rosa-Loera A. 2015. Poblaciones exóticas originales y adaptadas de maíz. I: Variedades de clima templado × variedades tropicales. Revista Fitotecnia Mexicana 38 (1): 57–66. https://doi.org/10.35196/rfm.2015.1.57

Kaefer KAC, Chiapetti R, Figasca L, Muller AL, Calixto GB, Chaves EID. 2016. Viability of maize pollen grains *in vitro* collected at different times of the day. African Journal of Agricultural Research 11 (12): 1040–1047. https://doi.org/10.5897/ajar2015.10181

Kato-Yamakake TA. 2023. Caracterización y origen genético de tres razas de maíz a partir de datos de nudos cromosómicos. Revista Fitotecnia Mexicana 46 (3): 219–227. https://doi.org/10.35196/rfm.2023.3.219

López-Morales F, Vázquez-Carrillo MG, García-Zavala JJ, Reyes-López D, Bonilla-Barrientos O, Esquivel-Esquivel G, García L, Hernández-Salinas G, Pérez-Jiménez G, Herrera-Pérez L, Molina-Galán JD. 2021. Rendimiento y calidad del maíz Tuxpeño V-520C adaptado con selección masal a Valles Altos, México. Revista Fitotecnia Mexicana 44 (2): 231–239. https://doi.org/10.35196/rfm.2021.2.231

Luna SV, Figueroa JM, Baltazar BM, Gómez RL, Townsend R, Schoper JB. 2001. Maize pollen longevity and distance isolation requirements for effective pollen control. Crop Science 41 (5): 1551–1557. https://doi.org/10.2135/cropsci2001.4151551x

Martins ES, Davide LMC, Miranda GJ, Barizon JO, Souza FAJ, de Carvalho RP, Gaoncalves MC. 2017. *In vitro* viability of maize cultivars at different times of collections. Ciencia Rural 47 (2). https://doi.org/10.1590/0103-8478cr20151077

Rácz F, Hidvégi S, Zaborszky S, Pál M, Marton C. 2006. Pollen production of new generation inbred maize lines. Cereal Research Communications 34 (1): 633–636. https://doi.org/10.1556/crc.34.2006.1.158

Ramírez-Díaz JL, Chuela-Bonaparte M, Vidal-Martínez VA, Ron-Parra J, Caballero-Hernández F. 2007. Propuesta para formar híbridos de maíz combinando patrones hetéroticos. Revista Fitotecnia Mexicana 30 (4): 453–461. https://doi.org/10.35196/rfm.2007.4.453

Razzaq MK, Rauf S, Khurshid M, Iqbal S, Bhat JA, Farzand A, Riaz A, Xing G, Gai J. 2019. Pollen viability an index of abiotic stresses tolerance and methods for the improved pollen viability. Pakistan Journal of Agricultural Research 32 (2): 609–624 https://doi.org/10.17582/journal.pjar/2019/32.4.609.624

Santacruz-Varela A, Widrlechner MP, Ziegler KE, Salvador RJ, Millard MJ, Bretting PK. 2004. Phylogenetic relationships among North American popcorns and their evolutionary links to Mexican and South American popcorns. Crop Science 44 (4): 1456–1467. https://doi.org/10.2135/cropsci2004.1456

Santiago-López N, García-Zavala JJ, Espinoza-Banda A, Santiago-López U, Esquivel-Esquivel G, Molina-Galán JD. 2020. Adaptación de maíz Tuxpeño a valles altos de México mediante selección masal. Revista Fitotecnia Mexicana 43 (3): 259–265. https://doi.org/10.35196/rfm.2020.3.259

Schoper JB, Lambert RJ, Vasilas BL. 1987. Pollen viability, pollen shedding, and combining ability for tassel heat tolerance in maize. Crop Science 27 (1): 27–31. https://doi.org/10.2135/cropsci1987.0011183X002700010007x

Tranel D, Knapp A, Perdomo A. 2009. Chilling effects during maize tassel development and lack of compensational plasticity. Crop Science 49 (5): 1852–1858. https://doi.org/10.2135/cropsci2008.10.0593

Trejo-Pastor V, Santacruz-Varela A, Córdova-Téllez L, López-Sánchez H, Costich DE, de la C, Díaz-Juárez R. 2023. Popping patterns in F_2 segregant progenies from popcorn × non-popcorn crosses. Emirates Journal of Food and Agriculture 35 (7). https://doi.org/10.9755/ejfa.2023.3106

Uribelarrea M, Cárcova J, Otegui ME, Wesrgate ME. 2002. Pollen production, pollination dynamics, and kernel set in maize. Crop Science 42 (6): 1910–1918. https://doi.org/10.2135/cropsci2002.1910

Velasco-García AM, García-Zavala JJ, Sahagún-Castellanos J, Lobato-Ortiz R, Sánchez-Abarca C, Marín-Montes IM. 2020. Análisis de la variabilidad morfológica de maíces nativos y exóticos en valles altos de México. Revista Fitotecnia Mexicana 43(4A): 517–524. https://doi.org/10.35196/rfm.2020.4-A.517

Vidal-Martínez VA, Clegg MD, Jonhson BE, Osuna-García JA, Coutiño-Estrada B. 2004. Phenotypic plasticity and pollen production components in maize. Agrociencia 38 (3): 273–284.

Agrociencia

BLOSSOM-END ROT CONTROL IN TOMATO (*Solanum lycopersicum* L.) FRUIT USING PLANT GROWTH REGULATORS

Ana Bell **Sánchez-Aguilar**[1], Manuel **Sandoval-Villa**[1]*, Libia Iris **Trejo-Téllez**[1], Javier **Suárez-Espinosa**[1], Yolanda Leticia **Fernández-Pavía**[1]

[1]Colegio de Postgraduados Campus Montecillo. Carretera México-Texcoco km 36.5, Montecillo, Texcoco, State of Mexico, Mexico. C. P. 56264.
* Author for correspondence: msandoval@colpos.mx

Citation: Sánchez-Aguilar AB, Sandoval-Villa M, Trejo-Téllez LI, Suárez-Espinosa J, Fernández-Pavía YL. 2025. Blossom-end rot control in tomato (*Solanum lycopersicum* L.) fruit using plant growth regulators. **Agrociencia** 59(6): 840-856. https://doi.org/ 10.47163/agrociencia.v59i6.3331

Editor in Chief:
Dr. Fernando C. Gómez Merino

Received: March 21, 2025.
Approved: September 19, 2025.
Published in Agrociencia: September 23, 2025.

ABSTRACT

The tomato (*Solanum lycopersicum* L.) is the second most produced vegetable worldwide. Mexico ranks eighth as a producer and is the main exporter. This crop adapts to diverse climates and soil types, although it is susceptible to diseases and physiological disorders. Blossom-end rot (BER) is the most relevant, with damage that can reach up to 50 % of greenhouse production. This study aimed to evaluate the effect of foliar application of abscisic acid (ABA) combined with 24-epibrassinolide (EBL) to assess BER of tomato fruit in plants fed with low calcium (Ca) concentration (45 mg L^{-1}) in the supplied nutrient solution. Likewise, the physiological and metabolic changes that these growth regulators generate *in planta* were determined. A 4 × 4 factorial experiment was established in a completely randomized design. Four concentrations of ABA (0, 60, 100, and 140 mg L^{-1}) and four of EBL (0, 0.0024, 0.0048, and 0.0096 mg L^{-1}) were evaluated as factors, with four replications. The percentage of BER and fruit set, photosynthesis, stomatal conductance, intercellular CO_2, transpiration, Ca concentration in leaves and fruits, and the concentration of amino acids and proteins were determined. In the first evaluation (20 d of treatment), treatments ABA3EBL2 and ABA3EBL0 showed a lower incidence of BER (80 and 66 %). In the second evaluation, EBL decreased transpiration by 50.6 %. ABA1EBL1 (35.7 %) and ABA3EBL0 (30.5 %) increased fruit Ca, while ABA2EBL1 increased leaf Ca by 62.2 %. ABA0EBL1, ABA1EBL1, ABA3EBL0, and ABA1EBL3 increased total amino acids more than twofold, and ABA2EBL2 increased protein by up to 13.6 %. These results indicate that the early application of ABA and EBL reduces BER and improves physiological and metabolic parameters in tomato plants.

Keywords: abscisic acid, calcium, physiological disorder, environmental factors, 24-epibrassinolide.

INTRODUCTION

The tomato (*Solanum lycopersicum* L., Solanaceae family) is one of the most cultivated plant species in the world (Caruso *et al*., 2022). It is the second most important horticultural crop worldwide. In 2023, Mexico ranked as the eighth largest producer

and exporter of tomatoes. The main producing states are Sinaloa, San Luis Potosi, Michoacan, Jalisco, Morelos, Baja California Sur, Sonora, Puebla, and Zacatecas (SIAP, 2023). Tomatoes are the most important vegetables exported from Mexico and provide a significant economic benefit to farmers and marketers. In 2023, the production volume in Mexico was approximately 3.6 million Mg (SIAP, 2023).

Climate change and extreme weather events are causing significant negative impacts on crop production. Tomatoes are adaptable to almost all climatic regions; however, environmental stresses are the main limitations on yield and potential quality (Gerszberg and Hnatuszko-Konka, 2017). Abiotic stress can lead to the alteration of multiple processes in the plant, such as increased transpiration, decreased photosynthesis and photosynthetic pigments, decreased stomatal conductance, decreased turgor, and the production of reactive oxygen species (Sharma *et al*., 2020).

Blossom-end rot is a physiological disorder that causes significant losses in many horticultural crops, including tomato, watermelon, and pepper. It occurs in all tomato-producing areas worldwide and results in unmarketable fruits and decreased supply, resulting in significant economic losses (Hagassou *et al*., 2019). On the other hand, calcium (Ca) deficiency in tomato fruits can cause cell membrane rupture, followed by solute extravasation and cellular plasmolysis, resulting in the formation of blossom-end rot symptoms (Saure, 2014). Phytohormones play an important role in the onset of Ca deficiency disorders (de Freitas *et al*., 2018). Growth regulators such as abscisic acid (ABA) and 24-epibrassinolide (EBL) help plants tolerate different types of biotic and abiotic stresses.

The objective of this study was to evaluate the effect of foliar applications of ABA and EBL with a limited Ca content in the supplied nutrient solution on blossom-end rot in tomato fruit, as well as to determine the physiological and metabolic changes these compounds cause in tomato plants. The hypothesis was that tomato plants fed with a low dose of Ca and treated with foliar applications of ABA and EBL would show a significant decrease in blossom end rot while also causing beneficial physiological and metabolic changes in the plant.

MATERIALS AND METHODS

Location of the experiment

This study was conducted at the Postgraduate College Campus Montecillo, located at 19° 27′ 51″ N and 98° 54′ 15″ W, at an altitude of 2250 m. The experiment was carried out under greenhouse conditions in an area of 96 m^2. Two side curtains and a zenithal curtain protected with anti-aphid mesh at 25 threads per inch were used for ventilation. The average minimum temperature was 5.7 °C and the maximum was 41.9 °C, with a relative humidity of 33 %. The greenhouse and tutoring material (rings and hooks) were disinfested with quaternary ammonium salts (Aniba Plus, Mexico) at a dose of 0.2 mL L^{-1} of water.

Genetic material

Tomato (*Solanum lycopersicum* L.) hybrid 'El Cid' seeds were sown in a 200-well styrofoam tray filled with peat (Kekkilä, Finland) as a substrate. The irrigation water used to prepare the Steiner nutrient solution (SNS) recorded an electrical conductivity (EC) of 0.44 dS m^{-1} throughout the crop cycle. In addition, it contained the following ions, expressed in milligrams per liter (mg L^{-1}): K = 3.519, Ca = 15.831, Mg = 16.659, Na = 60.49, PO_4 = 1.267, SO_4 = 0.912, HCO_3 = 306.22, Cl = 0.01, B = 0.08, Cu = 0.022, and Zn = 0.004. The EC indicated for the different SNS concentrations refers only to the fertilizer input.

The seedlings were irrigated with SNS at 0.69 dS m^{-1} EC, with the pH adjusted to 5.5. The complete SNS contained the following macronutrients, expressed in milliequivalents per liter (meq L^{-1}): NO_3^- = 12, $H_2PO_4^-$ = 1, SO_4^{-2} = 7, K^+ = 7, Ca^{2+} = 9, and Mg^{2+} = 4. The concentrations of SNS applied during the different phenological stages of the crop were adjusted based on this complete solution. The fertilizers used for SNS preparation at the various concentrations included calcium nitrate ($Ca(NO_3)_2.4H_2O$) (YaraTera, CALCINIT; Madrid, Spain), potassium sulfate (K_2SO_4) (Ultrasol NKS 46, SQM, Chile), monopotassium phosphate (KH_2PO_4) (Ultrasol MKP, SQM, Chile), magnesium sulfate ($MgSO_4.7H_2O$) (Sulmag Sal Epsom, Peñoles, Mexico), and a microelements mixture (Tradecorp AZ, Tradecorp, Spain).

Transplanting was carried out 40 d after planting. The irrigation regime was adjusted according to the phenological stage of the plant: during early growth, irrigation was applied for 1 min every hour; during the vegetative stage, for 2 min every 2 h; during flowering and fruiting, for 3 min every 2 h; and during ripening, for 4 min every 2 h. The average water output per dripper was 23.8 mL per minute.

Experimental design and treatments

The experiment had a 4 × 4 augmented factorial arrangement in a completely randomized experimental design. The assessed factors were abscisic acid (ABA) from a commercial product (PC) (5 %, Nutrigota; Guanajuato, Mexico) and 24-epibrassinolide (EBL) (85 %, Sigma-Aldrich; MO, USA), each evaluated at four levels. The ABA concentrations used were 0 (ABA0, 0 mg L^{-1} PC), 60 (ABA1, 1200 mg L^{-1} PC), 100 (ABA2, 2000 mg L^{-1} PC), and 140 mg L^{-1} (ABA3, 2800 mg L^{-1} PC). In the case of EBL, the concentrations were 0 mg L^{-1} (EBL0), 0.0024 mg L^{-1} (EBL1), 0.0048 mg L^{-1} (EBL2), and 0.0096 mg L^{-1} (EBL3).

The experimental unit consisted of a single tomato plant in a 13 L black polyethylene bag. Sixteen treatments, corresponding to the combinations of ABA and EBL levels, were applied to plants receiving a low Ca concentration in the nutrient solution (45 mg L^{-1}) plus Ca from irrigation water (15.8 mg L^{-1}) at 99, 106, and 113 d after transplant (dat). An augmented control was included, consisting of plants supplied with an adequate Ca concentration in the nutrient solution (180 mg L^{-1}) in addition to the Ca from water (15.8 mg L^{-1}), without foliar application of growth regulators. Each treatment was replicated four times, for a total of 68 plants.

Experiment development

From transplantation onwards, plants were irrigated with 25 % SNS (EC 0.5 dS m^{-1} and pH 5.5). Past 23 dat, the SNS concentration increased to 50 % (EC 1 dS m^{-1}). At 43 dat, a nearly complete SNS was prepared (except for Ca concentration). Half of the nutrients required for a complete SNS was supplied with fertilizers (90 mg L^{-1}) plus Ca supplied from water (15.8 mg L^{-1}). The remaining macro- and micronutrients were supplied according to the requirements of a complete SNS.

Three months after transplanting, the amount of Ca supplied through fertilizers was reduced (45 mg L^{-1}). The complete SNS had an EC of 2 dS m^{-1}; however, when modifying the amount of Ca in the solution, the EC varied. With Ca at 50 % of the requirement, the EC decreased to 1.9 dS m^{-1}, and with Ca at 25 % of the requirement, the EC decreased to 1.8 dS m^{-1}.

After 10 d of irrigating the plants with 45 mg L^{-1} of Ca, that is, at 99 dat, when the fifth fruit cluster was in anthesis, the treatments were applied with a spray bottle, using 125 mL of the solution per plant. The liquid was sprayed onto the stem, leaves, and opening flowers. To prevent the product from drifting to other plants during application, a plastic curtain was used to cover the target plant.

Variables evaluated

Twenty days after each application, the plant was evaluated for flower number, flower set percentage, blossom-end rot percentage, net photosynthetic rate, CO_2 assimilation, stomatal conductance, and transpiration. Total soluble protein, total free amino acids, and Ca concentration were determined in fruits from clusters 5, 6, and 7. Two fruits per cluster were considered for fresh-harvest analysis. Fruits were weighed and stored at -70 °C in an ultra-low temperature freezer (Thermo Scientific S/819442-162, USA). For dried fruit analysis, two fruits per cluster from each plant were dried at 72 °C for 72 h in a forced-air oven (Riossa HCF-125D, Mexico). Furthermore, a leaf was taken from the seventh cluster in each plant and dried for 48 h under the same conditions as the fruits. Before analyzing fresh fruits, they were ground in a porcelain mortar with a pestle using liquid nitrogen.

Evaluation of physiological parameters

A portable meter (LI-6400, LiCOR; Lincoln, NE, USA) was used to measure CO_2 assimilation rates, stomatal conductance, transpiration, and net photosynthetic rate. Readings were taken from the first leaf immediately following the fifth and seventh clusters, 20 d after each ABA and EBL application.

Nutritional analysis, primary and secondary metabolites

Calcium was determined in fruits and leaves by wet digestion according to Alcántar-González and Sandoval-Villa (1999). The extracts were analyzed using an induction plasma optical emission spectroscopy (ICP-OES 725-ES, Agilent; Santa Barbara, CA, USA). Antioxidant activity, free amino acids, total protein, and hydrogen peroxide

were analyzed in fruits. Antioxidant activity was measured according to Castañeda-Castañeda *et al*. (2008). Extracts were read at a wavelength of 517 nm. Total free amino acids were determined using the ninhydrin method (Moore and Stein, 1954) and read at a wavelength of 570 nm. Total protein determination was based on the methodology of Bradford (1976) with some modifications, at an absorbance of 595 nm. For hydrogen peroxide quantification, the methodology of Sergiev *et al*. (1997) was used, at an absorbance of 390 nm. All readings were measured using a spectrophotometer (Synergy 2 Microplate Reader, Biotek, USA).

Statistical analysis

Data from the greenhouse and laboratory were analyzed using analysis of variance (ANOVA), logistic regression, or Poisson regression, depending on the data type. For ANOVA, when the null hypothesis was rejected, *post hoc* comparisons were performed with Tukey's test at a significance level of 0.05. When the null hypothesis was not rejected, pairwise comparisons were conducted using the Bonferroni adjustment. All analyses were performed using the R software v4.3.1 (R Core Team, 2023).

RESULTS AND DISCUSSION

Effect of growth regulators on flower number, flower set percentage, and blossom-end rot percentage

The results obtained from the statistical tests to compare the effect of the application of abscisic acid (ABA) and 24-epibrassinolide (EBL) or their combinations showed effects on the number of flowers, percentage of setting, and percentage of apical rot (Table 1).

Table 1. Results of statistical tests of the effect of the application of abscisic acid (ABA) and 24-epibrassinolide (EBL) on the variables number of flowers, percentage of setting, and percentage of blossom-end rot in tomato (*Solanum lycopersicum* L.).

Evaluation (days after starting treatment)	Variable/statistical test	*p* value
	Number of flowers	
2 (27)	Poisson regression	0.148
3 (34)	Poisson regression	0.126
	Fruit set percentage	
1 (20)	Kruskal-Wallis	0.546
2 (27)	ANOVA	0.604
3 (34)	ANOVA	0.691
	Blossom-end rot percentage	
1 (20)	ANOVA	0.019
2 (27)	Logistic regression	0.067
3 (34)	Logistic regression	0.684

For the number of flowers, tests were conducted 27 and 34 d after the start of treatment (dast); in both cases, no significant differences were recorded between the factor levels and between the factor combinations (p = 0.148 and 0.126). This may be due to factors such as temperature, since maximum temperatures of up to 41.9 °C were recorded. Temperatures above 27 °C negatively affect tomato flower formation. In greenhouse production, the optimal relative humidity ranges between 50 and 80 % (Castellanos, 2009; Shamshiri *et al*., 2018); however, in this experiment it averaged only 33 %. The mean number of flowers per plant was 7.8 at the second evaluation and 7 at the third. Similar results to those obtained in this study have been reported. Verma *et al*. (2014) applied three doses of gibberellic acid (GA; 20, 30, and 40 ppm) and naphthaleneacetic acid (NAA; 15, 30, and 45 mg L^{-1}) in tomato and obtained significant differences in the number of flowers. Kumar *et al*. (2018), when evaluating three doses of GA (20, 30, and 40 ppm), found that the application increased the number of flowers by 10, 12, and 15 %, respectively, compared to the control. Likewise, Tepkaew *et al*. (2022) indicated that the application of brassinosteroid type 7,8-dihydro-8α-20-hydroxyecdysone (DHECD, 0.1 μM L^{-1}) increased up to 225 % the number of flowers per inflorescence compared to the control in mango (*Mangifera indica* L.).

Similarly, growth regulators did not affect fruit set percentage across factor levels or factor combinations in the three evaluations conducted in this study. This could have been due to the temperature spikes and low relative humidity during the experiment, which interfered with pollination and fruit set, despite the fact that EBL promotes tolerance to environmental stress (Ahammed *et al*., 2015). Likewise, Riboldi *et al*. (2018) found no significant differences in fruit set after applying three growth regulators (GA, ABA, and EBL) to tomato plants without Ca supplementation. However, in *Annona squamosa* L., EBL application at a dose of 2 mg L^{-1} was found to promote fruit set, surpassing the control by up to 97 % (Aly *et al*., 2021).

On the other hand, the treatments evaluated had significant differences in blossom-end rot (BER) in the first evaluation carried out on fruits from the fifth cluster (Figure 1). In the case of ABA, the concentration of 140 mg L^{-1} (ABA3) significantly reduced BER by 45.2 % compared to ABA0 and 77.6 % compared to ABA1, which had a higher percentage of incidence. Furthermore, the ABA3EBL0 and ABA3EBL2 combinations induced a significant reduction in BER (66 and 80 %, respectively), compared to the combination without applying ABA0EBL0 regulators, and up to 88 and 93 %, in the same order, compared to ABA1EBL0, which presented the highest incidence of BER (90 %).

Based on the comparison of the effects of the combinations of growth regulators, considering the amount of Ca offered (45 mg L^{-1}), it is recommended to use the combination ABA3EBL0 since, although the BER is higher (10.7 %) than that obtained in ABA3EBL2 (6.3 %), the difference between both was not significant, which indicates that the difference was not due to the effect of the combinations; likewise, both treatments have significantly different effects than ABA1EBL0, while the rest of the combinations do not exceed the effect of any other combination (Figure 1).

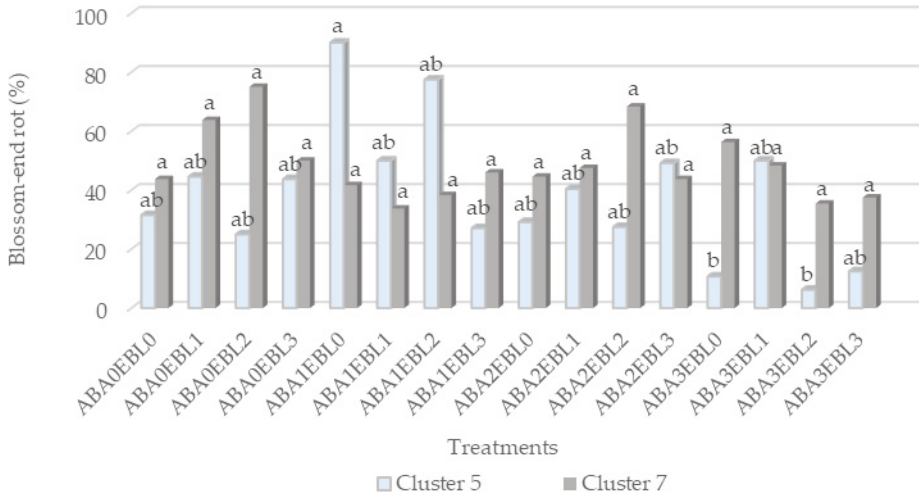

Figure 1. Effects of abscisic acid (ABA) levels and ABA × 24-epibrassinolide (EBL) combinations on blossom-end rot percentage (first and third evaluations 20 and 34 d after treatment initiation and 119 and 133 d after transplanting, respectively). ABA0: 0 mg L^{-1}; ABA1: 60 mg L^{-1}; ABA2: 100 mg L^{-1}; ABA3: 140 mg L^{-1}; EBL0: 0 mg L^{-1}; EBL1: 0.0024 mg L^{-1}; EBL2: 0.0048 mg L^{-1}; EBL3: 0.0096 mg L^{-1}. Values with the same letters are not statistically different (Tukey, $p \leq 0.05$).

When comparing BER across sampling times, incidence was higher in the third evaluation than in the first for 12 of the 17 treatments (Figure 1). The augmented control (180 mg Ca^{2+} L^{-1}, without ABA and EBL) showed no BER in the fifth cluster but reached 41.7 % in the seventh (data not shown). In contrast, the ABA0EBL0 treatment exhibited 31.5 % BER in the fifth cluster, increasing to 43.8 % in the seventh.

The decrease in BER in tomato with the use of ABA has been documented in various studies. Balate *et al*. (2018) reported an 86 % reduction compared to untreated plants. In contrast, de Freitas *et al*. (2014) indicated that 15 d after pollination, the application of ABA completely prevented BER, while the control presented an incidence of up to 19 %. Barickman *et al*. (2014) found that ABA treatments decreased BER incidence by 26.6 %. On the other hand, the use of EBL in tomato plants under abiotic stress with low Ca supply decreased the incidence of BER by 44.2 % (Riboldi *et al*., 2019).

The response of BER to ABA is attributed to its ability to activate specific mechanisms in both the plant and the fruit. These mechanisms may reduce xylem Ca transport to the leaves, enhancing Ca movement and uptake in the fruit. As a result, the apoplastic Ca concentration increases, leading to reduced membrane permeability and a lower incidence of blossom-end rot in fruit tissue (Barickman *et al*., 2014; de Freitas *et al*., 2014, 2011).

In the third evaluation (cluster 7), high percentages of BER were observed (Figure 1). This can be explained by the prolonged period of insufficient Ca supply, which extended beyond the requirements for commercial production (Steiner, 1984). At this

stage, the plants were also at an advanced phenological phase (3.5 months). As noted by Alcántar-González *et al*. (2016), during tomato ripening, premature root senescence and lignification of conductive tissues can restrict nutrient transport to developing fruits. In addition, during the second and third evaluations, greenhouse temperatures reached 40 °C with a relative humidity of 20 %, conditions that further limited nutrient uptake and transport, which intensified BER incidence.

According to Saure (2014), blossom-end rot occurs more frequently under conditions of low relative humidity, high light intensity, and elevated temperature, as these factors inhibit calcium transport to the rapidly growing distal fruit tissues. Moreover, insufficient Ca supply alone does not always induce BER symptoms; rather, the disorder is primarily driven by abiotic stress. In this experiment, unfavorable environmental conditions, including Ca deficiency, low relative humidity, and high temperature, were present, which contributed to the increased incidence of BER.

Effect of growth regulators on physiological variables

In the first evaluation (119 dat, 20 dast) there was no effect of growth regulators on the physiological variables (Table 2), between the levels of the factors, or between their combinations. On the other hand, in the second evaluation (133 dat, 34 dast), the treatment with 0.0048 mg L^{-1} of EBL significantly reduced plant transpiration up to 50.6 % (Table 2) compared to the treatment without growth regulators (ABA0EBL0).

The effect observed with 0.0048 mg L^{-1} of EBL (EBL2) (Table 2) coincides with that reported by Riboldi *et al*. (2019), who indicate that when exogenous applications of EBL were made in tomato plants exposed to abiotic stress (low Ca supply), transpiration (7.6 %) and Ca concentration in the leaf (9 %) decreased. In turn, de Freitas *et al*. (2014) mention that the concentration of Ca in the fruit is not the primary cause of BER, but rather the combined action of several factors favors its appearance. Furthermore, reducing leaf transpiration can potentially decrease the movement of xylem Ca to the leaves and increase its movement to the fruit. Although in this study there was a decrease in transpiration and foliar Ca concentration after the application of EBL, the Ca concentration in the fruit (Table 3) was not affected.

Regarding transpiration (Table 2), the treatment that showed the greatest reduction over time was ABA2EBL2, with a decrease of 73.7 %, a net photosynthesis of 81.3 %, and stomatal conductance of up to 85.7 %. In contrast, the combination that showed the smallest decrease over time was ABA0EBL1, with 21 % in transpiration, 29.7 % net photosynthesis, and 8.3 % stomatal conductance. These results demonstrated a high correlation between net photosynthesis, stomatal conductance, and transpiration. On the other hand, intercellular carbon decreased by up to 49 %, with ABA2EBL3 showing the greatest reduction in this variable. However, several treatments had an increase in intercellular CO_2 concentration at the last measurement: ABA0EBL2 (30.6 %), Control A (22.5 %), ABA3EBL3 (19.1 %), ABA1EBL1 (17.4 %), ABA2EBL0 (15.5 %), ABA3EBL2 (9.5 %), and ABA0EBL1 (4.5 %).

Table 2. Statistical analysis of the effects of abscisic acid (ABA) and 24-epibrassinolide (EBL) on the physiological response of tomato leaves at 119 (evaluation 1) and 133 d (evaluation 2) after transplantation.

Variables		Evaluation 1				Evaluation 2			
		ABA	EBL	ABA*EBL	COMB	ABA	EBL	ABA*EBL	COMB
Np	Pr(>F)	0.130	0.934	0.890	0.753	0.468	0.054	0.121	0.086
Sc	Pr(>F)	0.113	0.401	0.493	0.318	0.276	0.186	0.166	0.147
Ci	Pr(>F)	0.398	0.213	0.550	0.436	0.512	0.770	0.948	0.950
T	Pr(>F)	0.158	0.730	0.843	0.692	0.453	0.035	0.252	0.122

Combination	Np^5	Np^7	Sc^5	Sc^7	CO_2i^5	CO_2i^7	T^5	T^7
	mmol CO_2 m^{-2} s^{-1}		mol H_2O m^{-2} s^{-1}		mmol CO_2 mol^{-1}		mmol H_2O m^{-2} s^{-1}	
ABA0EBL0	21.56	7.76	0.19	0.06	186.02	133.83	10.13	3.89
ABA0EBL1	17.33	12.19	0.12	0.11	132.80	138.74	5.75	4.54
ABA0EBL2	17.51	3.04	0.11	0.02	116.78	152.54	7.08	1.92
ABA0EBL3	16.25	10.33	0.13	0.07	172.29	117.29	6.11	3.10
ABA1EBL0	20.77	8.65	0.18	0.07	188.88	135.31	8.11	3.30
ABA1EBL1	19.50	6.11	0.12	0.04	118.19	138.78	7.54	3.04
ABA1EBL2	22.47	7.96	0.15	0.05	126.60	101.89	8.53	3.69
ABA1EBL3	22.01	6.33	0.23	0.04	210.21	111.98	10.43	2.80
ABA2EBL0	20.64	9.29	0.13	0.08	104.87	121.2	7.95	4.88
ABA2EBL1	20.21	6.99	0.15	0.05	136.98	128.96	7.69	2.92
ABA2EBL2	20.14	3.75	0.14	0.02	129.10	105.75	7.75	2.04
ABA2EBL3	19.04	8.61	0.15	0.06	164.00	83.68	7.26	3.24
ABA3EBL0	17.38	9.31	0.14	0.07	162.56	126.21	6.94	4.33
ABA3EBL1	19.39	8.71	0.13	0.07	139.39	127.05	6.86	3.78
ABA3EBL2	17.34	8.47	0.11	0.08	106.30	116.35	5.52	3.68
ABA3EBL3	18.70	9.15	0.12	0.08	120.01	142.99	6.96	3.48
Control A	19.22	6.76	0.14	0.07	119.00	145.73	6.65	3.53

Np: net photosynthesis; Sc: stomatal conductance; Ci: intercellular CO_2; T: transpiration; COMB: combination; ^{5}: readings from leaves located above the fifth cluster. ^{7}: Readings from leaves located above the seventh cluster. ABA0: 0 mg L^{-1}; ABA1: 60 mg L^{-1}; ABA2: 100 mg L^{-1}; ABA3: 140 mg L^{-1}; EBL0: 0 mg $L^{-1;}$ EBL1: 0.0024 mg L^{-1}; EBL2: 0.0048 mg L^{-1}; EBL3: 0.0096 mg L^{-1}; Control A: augmented control.

In the first evaluation (Table 2), stomatal conductance remained between 0.11 and 0.15 mol H_2O m^{-2} s^{-1} in treatments where only EBL was applied (ABA0EBL1, ABA0EBL2, and ABA0EBL3), which represented between 21 and 42 % of the value observed in the treatment without growth regulators (ABA0EBL0). However, no statistically significant differences were detected either between factor levels or their interactions (Table 2), indicating that the observed variations were attributable to random variation rather than the effect of the growth regulators.

Table 3. Calcium concentration in fruits and leaves of tomato (*Solanum lycopersicum* L.) treated with abscisic acid (ABA) and 24-epibrassinolide (EBL).

Combination	Ca F1	Ca F2	Ca F3	Ca H
	(mg kg^{-1} dry biomass)			
ABA0EBL0	990.54 abc	804.11 cd	938.76 a	8075.57 efg
ABA0EBL1	1147.28 a	782.06 d	845.89 ab	6896.31 g
ABA0EBL2	997.38 abc	978.39 abc	775.76 ab	7750.75 fg
ABA0EBL3	1091.48 abc	830.79 cd	698.64 b	6969.1 g
ABA1EBL0	1143.6 a	863.43 bcd	784.84 ab	8958.40 def
ABA1EBL1	1060.54 abc	1091.26 a	762.52 ab	9339.46 cdef
ABA1EBL 2	1079.26 abc	937.48 bcd	764.23 ab	9131.32 def
ABA1EBL3	1116.98 ab	756.84 d	853.48 ab	11127.59 bc
ABA2EBL0	1052.10 abc	1019.83 ab	857.36 ab	11922.40 ab
ABA2EBL1	1035.30 abc	776.80 d	811.65 ab	13095.8 a
ABA2EBL2	885.60 bc	973.72 abc	764.90 ab	8835.2 def
ABA2EBL3	842.84 c	934.28 abcd	776.66 ab	9771.65 cde
ABA3EBL0	1051.19 abc	1049.62 a	810.60 ab	10324.95 bcd
ABA3EBL1	1029.19 abc	908.64 abcd	708.66 b	7938.13 efg
ABA3EBL2	1111.44 ab	856.52 bcd	668.46 b	9647.85 cde
ABA3EBL3	1034.91 abc	857.72 bcd	669.88 b	8712.93 defg

ABA0: 0 mg L^{-1}; ABA1: 60 mg L^{-1}; ABA2: 100 mg L^{-1}; ABA3: 140 mg L^{-1}; EBL0: 0 mg L^{-1}; EBL1: 0.0024 mg L^{-1}; EBL2: 0.0048 mg L^{-1}; EBL3: 0.0094 mg L^{-1}; Ca: calcium; F: fruit; 1: first evaluation (20 d after the start of treatments); 2: second evaluation (27 d after the start of treatments); 3: third evaluation (34 d after the start of treatments); H: leaf. Values with the same letters in each column are not statistically different (Tukey, $p \leq 0.05$).

The stomatal conductance values obtained in this study are consistent with those reported by Riboldi *et al*. (2019), who found no significant differences between EBL-treated tomato plants (0.15 mol H_2O m^{-2} s^{-1}) and the control (0.17 mol H_2O m^{-2} s^{-1}). Likewise, transpiration did not differ significantly between EBL treatment (2.32 mmol H_2O m^{-2} s^{-1}) and the control (2.51 mmol H_2O m^{-2} s^{-1}). In a previous study, Riboldi *et al*. (2018) also reported that the application of EBL in tomato plants did not produce significant differences in transpiration, although they observed a difference in stomatal conductance, with an increase of 6 to 9 %. In the second evaluation, both stomatal conductance and transpiration recorded lower values than those obtained in the first evaluation.

The decrease in photosynthesis across evaluations (Table 2) can be attributed to factors such as the use of growth regulators. ABA plays an important role in inducing stomatal closure (Engineer *et al*., 2016), which was observed in leaves located above the seventh cluster. Similarly, Hao *et al*. (2021) reported that foliar application of ABA in *Emmenopterys henryi* Oliv. under excess light stress reduced not only the

net photosynthetic rate but also stomatal conductance and transpiration, while simultaneously increasing intercellular CO_2 concentration.

In this study, photosynthesis, stomatal conductance, and transpiration showed similar behavior to that described above. While intercellular CO_2 concentration showed this trend in seven combinations, when growth regulators were used separately or at medium or high doses, intercellular CO_2 concentrations increased over time, with the exception of the ABA1EBL1 treatment. It was observed that different types of stress (biotic and abiotic) negatively affect gas exchange in the plant. Li *et al*. (2020) showed that tomato plants, when competing in high planting densities, tend to decrease stomatal conductance, transpiration, and net photosynthesis.

A second reason for the decrease in photosynthesis may be attributable to the plant's phenological phase (fruiting), combined with the climatic conditions (high temperature and low relative humidity), which caused a decrease in overall metabolism. Shamshiri *et al*. (2018) report that the optimal relative humidity range during all stages of tomato growth is between 50 and 70 %. Furthermore, under greenhouse conditions, when plant leaves are exposed to excessively hot air, transpiration is ineffective. These conditions were present during the experiment.

In contrast, Trouwborst *et al*. (2011) reported that in vertically trained crops such as tomato, the combined effects of leaf aging and reduced light intensity are associated with a decline in photosynthetic capacity. While leaf age alone significantly influences photosynthesis, the greatest impact is attributed to the reduction in photosynthetically active photon flux. As tomato plants grow under vertical training, lower leaves become progressively shaded, leading to reduced photosynthesis. The plants in this study were exposed to these conditions (vertical training and leaf aging), which was reflected in an overall decline in photosynthetic activity.

Effect of growth regulators on calcium concentration

In all treatments evaluated, fruit Ca concentration decreased as the number of harvested clusters increased (Table 3). Looking at the results of the first evaluation (20 d), treatments ABA0EBL1 and ABA1EBL0 had higher fruit Ca concentrations, exceeding the treatment without applying regulators (ABA0EBL0) by 15.8 and 15.5 %, respectively. However, no statistically significant differences were found between ABA1EBL0, ABA3EBL0, and ABA3EBL2. In the same first evaluation, the BER percentage of ABA1EBL0 was the highest (90 %), while in ABA3EBL0 and ABA3EBL2 it was significantly the lowest.

The differences in BER percentage cannot be explained by Ca deficiencies in the fruit. In the second evaluation, treatments ABA1EBL1 and ABA3EBL0 exceeded treatment ABA0EBL0 by 35.7 and 30.5 %, while in the second and third evaluations (27 and 34 d), Ca concentration in fruits of plants treated with ABA1EBL0 decreased by 24.5 and 31.4 %, respectively. This reduction is likely due to the increasing distance of the developing fruits from the nutrient supply points as the plant grows. These findings are consistent with those reported by Coolong *et al*. (2014), who state that as the number of harvested

clusters increases, not only does the concentration of Ca decrease (up to 18.8%), but so does the concentration of most nutrients.

In the third evaluation (34 dast), the combination without applied growth regulators (ABA0EBL0) recorded the highest Ca concentration in fruit, presenting significant differences with ABA0EBL3, ABA3EBL1, ABA3EBL2, and ABA3EBL3 (25.6, 24.5, 28.8, and 28.6 %, respectively). However, no significant differences were found for BER percentage. Although ABA0EBL0 had the highest concentration, it was lower than those recorded in the first evaluations. In the first evaluation (fifth cluster), the combinations of growth regulators ABA3EBL0 and ABA3EBL2 gave the best results. Riboldi *et al*. (2018) reported that Ca concentration in tomato fruit, compared to the control, increased from 57 to 67 % when ABA was applied, while with EBL it increased from 38 to 72 %. On the other hand, Riboldi *et al*. (2019) mentioned a Ca concentration in fruits treated with EBL and harvested 15 d after pollination (dap) had 3000 mg kg^{-1} of dry biomass, while the control presented 3760 mg kg^{-1} of dry biomass.

In this study, in fruits from the fifth cluster, the Ca concentration ranged from 840 to 1150 mg kg^{-1} of dry biomass in the different combinations. Meanwhile, for the sixth and seventh clusters, the Ca concentration was below 1090 and 940 mg kg^{-1} of dry biomass, respectively. Overall, the concentrations recorded in the three evaluations were lower than those reported by Riboldi *et al*. (2019), who found higher Ca levels even in fruits harvested at 15 dap. This discrepancy may be explained by the abiotic stress experienced by the plants in the present study. This result is similar to that reported by Maia *et al*. (2019), who found that nutrient concentration and accumulation were influenced by the imposed nutritional deficiencies.

Leaf Ca concentration was only measured in the third evaluation and showed significant differences between factor levels and factor combinations (Table 3). Treatment with ABA2EBL1 showed an increase of up to 62.2 % in leaf Ca concentration compared to the treatment without regulations (ABA0EBL0). Balate *et al*. (2018), working with tomato plants in soil, found a leaf Ca concentration of 30 620 mg kg^{-1} (control), while plants treated with 500 mg ABA L^{-1} had a Ca concentration of 37 000 mg kg^{-1} of dry biomass.

Riboldi *et al*. (2018), when evaluating the effect of growth regulators on Ca concentration in tomato leaves under hydroponic conditions, reported that foliar application of ABA (136.2 μM) increased Ca concentration to 23 800 mg kg^{-1} of dry matter. In contrast, a lower ABA dose resulted in 17 950 mg kg^{-1} of dry biomass, representing decreases of 28.1 and 3.6 % relative to the control, respectively. Regarding the use of brassinolides, Riboldi *et al*. (2019) reported that the application of EBL to leaves (0.01 μM) generated a concentration of Ca in leaves of 35 900 mg kg^{-1} of dry biomass, 9.1 % lower than in the control.

The lower Ca concentrations in leaves, compared with both the cited literature and the present maximum value of 13 095.8 mg kg^{-1} of dry biomass (ABA2EBL1) obtained in this study, can be explained by two main factors: 1) Riboldi *et al*. (2019) measured Ca in leaves located above the first cluster, whereas in this study, measurements were

taken from leaves above the sixth cluster; and 2) the experiment was conducted under conditions of reduced Ca availability. These results indicate that the limited Ca supply in the nutrient solution negatively affected all treatments.

Effect of growth regulators on amino acids and proteins

The concentration of total free amino acids in tomato fruits (Table 4) was influenced by most treatments. However, ABA0EBL1, ABA1EBL1, ABA3EBL0, and ABA1EBL3 showed statistically significant differences with the ABA0EBL0 treatment, surpassing it by 187.9, 151.5, 139.4, and 136.4 %, respectively. ABA0EBL1 had the highest amino acid concentration (0.95 mg g^{-1} of fresh biomass), followed by the augmented control (0.94 mg g^{-1} of fresh biomass) (data not shown). However, no significant differences were found between the aforementioned treatments with higher amino acid concentrations. Rouphael *et al.* (2021) found an amino acid concentration of 6.14 mg g^{-1} BF in tomato fruits (control), which increased by 11.4 % with the application of a biostimulant (Auxym, Rivoli Veronese, Italy). In contrast, the highest amino acid concentration

Table 4. Concentration of total free amino acids and total proteins in tomato (*Solanum lycopersicum* L.) fruits (seventh cluster) on the third evaluation (133 d after transplantation) from plants treated with abscisic acid (ABA) and 24-epibrassinolide (EBL).

Combination	Total free amino acids (mg g^{-1} BF)	Total soluble proteins (mg g^{-1} BF)
ABA0EBL0	0.33 b	0.22 ab
ABA0EBL1	0.95 a	0.09 de
ABA0EBL2	0.65 ab	0.16 bcd
ABA0EBL3	0.67 ab	0.07 e
ABA1EBL0	0.55 ab	0.17 abc
ABA1EBL1	0.83 a	0.15 bcde
ABA1EBL2	0.70 ab	0.12 cde
ABA1EBL3	0.78 a	0.17 bc
ABA2EBL0	0.36 b	0.21 ab
ABA2EBL1	0.69 ab	0.12 cde
ABA2EBL2	0.55 ab	0.25 a
ABA2EBL3	0.59 ab	0.19 abc
ABA3EBL0	0.79 a	0.14 bcde
ABA3EBL1	0.65 ab	0.11 cde
ABA3EBL2	0.76 ab	0.12 cde
ABA3EBL3	0.67 ab	0.18 abc

ABA0: 0 mg L^{-1}; ABA1: 60 mg L^{-1}; ABA2: 100 mg L^{-1}; ABA3: 140 mg L^{-1}; EBL0: 0 mg L^{-1}; EBL1: 0.0024 mg L^{-1}; EBL2: 0.0048 mg L^{-1}; EBL3: 0.0094 mg L^{-1}; BF: Fresh biomass. Values with equal letters are not statistically different (Tukey, $p \leq 0.05$).

recorded in this study, under the ABA0EBL1 treatment, was considerably lower, likely because the fruits were harvested at only 20 dap. This suggests that amino acid levels rise as fruits ripen. Moreover, the application of growth regulators, either individually or in the combinations ABA0EBL1, ABA1EBL1, ABA1EBL3, and ABA3EBL0, enhanced amino acid accumulation in tomato fruits grown under nutritional stress.

The treatments showed wide variability in total protein concentration (Table 4). Only ABA2EBL2 recorded higher protein concentrations than the treatment without the application of regulators (ABA0EBL0, 13.6 %). The ABA1EBL0, ABA2EBL0, ABA2EBL3, and ABA3EBL3 treatments did not show significant differences. The highest average concentrations of total soluble protein were observed either with ABA alone (ABA1EBL0 and ABA2EBL0) or with combined applications of ABA and EBL at medium to high doses (ABA2EBL2, ABA2EBL3, and ABA3EBL3), whereas EBL applied alone did not enhance protein concentration.

Dalyan (2023) mentions that foliar application of EBL in tomato plants under abiotic stress (fungicide) favored the increase of total proteins in the leaf up to 21.9 % compared to the control. Choi *et al*. (2011), when analyzing the protein concentration in 11 tomato varieties grown without abiotic stress under greenhouse conditions, found that the concentration remained in the range of 0.59 to 1.05 % in red fruit and 1.3 % in green fruit. Similarly, Rouphael *et al.* (2021) found a protein concentration of 2.4 % in ripe tomato fruits between 60 and 90 dat. The highest concentration in the present study was 0.025 % (0.25 mg g^{-1} of fresh biomass). This may be explained by the conditions under which the tomato plants were grown and harvested (abiotic stress due to low Ca supply, high temperatures, and low relative humidity).

The exogenous application of ABA enhances cell viability under stress by increasing the capacity of cells to scavenge reactive oxygen species (Liu *et al*., 2009). This effect is mediated by elevated antioxidant enzyme activity and the synthesis of antioxidant compounds, such as ascorbic acid, which also promotes the production of osmolytes, including amino acids like proline and glycine-betaine (Ahmad *et al*., 2017). Foliar application of ABA promotes antioxidant production (de Freitas *et al*., 2018). This explains why amino acid concentrations increased after the application of growth regulators.

CONCLUSIONS

The combined application of abscisic acid (ABA) and 24-epibrassinolide (EBL), particularly treatments ABA3EBL0 and ABA3EBL2 at the early phenological stage of the tomato plant, effectively mitigated the stress caused by low Ca supply, thereby significantly decreasing the incidence of blossom-end rot. The application of ABA and EBL did not affect stomatal conductance, net photosynthesis, and intercellular carbon, but it did affect transpiration. Treatments ABA0EBL1, ABA1EBL1, ABA1EBL3, and ABA3EBL0 favored the concentration of amino acids, while ABA2EBL increased the concentration of total proteins.

REFERENCES

Ahammed JG, Xia XJ, Li X, Shi K, Yu JQ, Zhou YH. 2015. Role of brassinosteroid in plant adaptation to abiotic stresses and its interplay with other hormones. Current Protein and Peptide Science 16 (5): 462–473. https://doi.org/10.2174/1389203716666150330141427

Ahmad P, Ahanger MA, Egamberdieva D, Alam P, Alyemeni MN, Ashraf M. 2017. Modification of osmolytes and antioxidant enzymes by 24-epibrassinolide in chickpea seedlings under mercury (Hg) toxicity. Journal of Plant Growth Regulation 37 (1): 309–322. https://doi.org/10.1007/s00344-017-9730-6

Alcántar-González G, Sandoval-Villa M. 1999. Manual de análisis químico de tejido vegetal. Publicación especial 10. Sociedad Mexicana de la Ciencia del Suelo. Chapingo, México. 156 p.

Alcántar-González G, Trejo-Téllez L, Gómez-Merino FC. 2016. Nutrición de cultivos. Colegio de Postgraduados. Texcoco, México. 443 pp.

Aly MA, Ezz TM, Mahmoud G, Khadeejah HN. 2021. Effect of some growth regulators on productivity, fruit quality and storability of sugar apple *Anona squamosa* L. Natural Volatiles and Essential Oils Journal 8 (5): 12298–12316.

Balate CA, de Souza DC, Resende LV, de Freitas ST. 2018. Effect of abscisic acid on the calcium content for controlling blossom-end rot in tomato under water stress. Pesquisa Agropecuária Tropical 48 (4): 414–419. https://doi.org/10.1590/1983-40632018v4852048

Barickman TC, Kopsell DA, Sams CE. 2014. Foliar applications of abscisic acid decrease the incidence of blossom-end rot in tomato fruit. Scientia Horticulturae 179: 356–362. https://doi.org/10.1016/j.scienta.2014.10.004

Bradford MM. 1976. A rapid and sensitive method for the quantitation of microgram quantities of protein utilizing the principle of protein-dye binding. Analytical Biochemistry 72 (1–2): 248–254. https://doi.org/10.1016/0003-2697(76)90527-3

Caruso AG, Bertacca S, Parrella G, Rizzo R, Davino S, Panno S. 2022. Tomato brown rugose fruit virus: A pathogen that is changing the tomato production worldwide. Annals of Applied Biology 181 (3): 258–274. https://doi.org/10.1111/aab.12788

Castañeda-Castañeda B, Ramos-Llica E, Ibáñez-Vasquez L. 2008. Evaluación de la capacidad antioxidante de plantas medicinales peruanas. Revista Horizonte Médico 8 (1): 56–72. https://doi.org/10.24265/horizmed.2008.v8n1.04

Castellanos JZ. 2009. Manual de producción de tomate en invernadero. Intagri S.C. Guanajuato, México. 460 p.

Choi SH, Kim HR, Kim HJ, Lee IS, Kozukue N, Levin CE, Friedman M. 2011. Free amino acid and phenolic contents and antioxidative and cancer cell-inhibiting activities of extracts of 11 greenhouse-grown tomato varieties and 13 tomato-based foods. Journal of Agricultural and Food Chemistry 59 (24): 12801–12814. https://doi.org/10.1021/jf202791j

Coolong T, Mishra S, Barickman C, Sams C. 2014. Impact of supplemental calcium chloride on yield, quality, nutrient status, and postharvest attributes of tomato. Journal of Plant Nutrition 37 (14): 2316–2330. https://doi.org/10.1080/01904167.2014.890222

Dalyan E. 2023. Amelioration of the adverse effects of thiram by 24-epibrassinolide in tomato (*Solanum lycopersicum* Mill.). Archives of Biological Sciences 75 (2): 187–197. https://doi.org/10.2298/abs230201015d

de Freitas ST, Martinelli F, Feng B, Reitz NF, Mitcham EJ. 2018. Transcriptome approach to understand the potential mechanisms inhibiting or triggering blossom-end rot development in tomato fruit in response to plant growth regulators. Journal of Plant Growth Regulation 37 (1): 183–198. https://doi.org/10.1007/s00344-017-9718-2

de Freitas ST, McElrone AJ, Shackel KA, Mitcham EJ. 2014. Calcium partitioning and allocation and blossom-end rot development in tomato plants in response to whole-plant and fruit-specific abscisic acid treatments. Journal of Experimental Botany 65 (1): 235–247. https://doi.org/10.1093/jxb/ert364

de Freitas ST, Shackel KA, Mitcham EJ. 2011. Abscisic acid triggers whole-plant and fruit-specific mechanisms to increase fruit calcium uptake and prevent blossom end rot development in tomato fruit. Journal of Experimental Botany 62 (1): 2645–2656. https://doi.org/10.1093/jxb/erq430

Engineer CB, Hashimoto-Sugimoto M, Negi J, Israelsson-Nordström M, Azoulay-Shemer T, Rappel WJ, Iba K, Schroeder JI. 2016. CO_2 sensing and CO_2 regulation of stomatal conductance: Advances and open questions. Trends in Plant Science 21 (1): 16–30. https://doi.org/10.1016/j.tplants.2015.08.014

Gerszberg A, Hnatuszko-Konka K. 2017. Tomato tolerance to abiotic stress: A review of most often engineered target sequences. Plant Growth Regulation 83 (2): 175–198. https://doi.org/10.1007/s10725-017-0251-x

Hagassou D, Francia E, Ronga D, Buti M. 2019. Blossom end-rot in tomato (*Solanum lycopersicum* L.): A multi-disciplinary overview of inducing factors and control strategies. Scientia Horticulturae 249: 49–58. https://doi.org/10.1016/j.scienta.2019.01.042

Hao YF, Feng YY, Cai LJ, Wu Q, Song LL. 2021. Effect of ABA on photosynthesis and chlorophyll fluorescence in *Emmenopterys henri* Oliv. under high light. Russian Journal of Plant Physiology 68 (3): 510–518. https://doi.org/10.1134/S1021443721030067

Kumar S, Singh R, Singh V, Singh MK, Singh AK. 2018. Effect of plant growth regulators on growth, flowering, yield and quality of tomato (*Solanum lycopersicum* L.). Journal of Pharmacognosy and Phytochemistry 7 (1): 41–44.

Li S, Hamani AKM, Si Z, Liang Y, Gao Y, Duan A. 2020. Leaf gas exchange of tomato depends on abscisic acid and jasmonic acid in response to neighboring plants under different soil nitrogen regimes. Plants 9 (12): 1674. https://doi.org/10.3390/plants9121674

Liu Y, Zhao Z, Si J, Di C, Han J, An L. 2009. Brassinosteroids alleviate chilling-induced oxidative damage by enhancing antioxidant defense system in suspension cultured cells of *Chorispora bungeana*. Plant Growth Regulation 59 (3): 207–214. https://doi.org/10.1007/s10725-009-9405-9

Maia JTLS, Martinez HEP, Clemente JM, Ventrella MC, Milagres CC. 2019. Growth, nutrient concentration, nutrient accumulation and visual symptoms of nutrient deficiencies in cherry tomato plants. Ciências Agrárias 40 (2): 585–598. https://doi.org/10.5433/1679-0359.2019v40n2p585

Moore S, Stein WH. 1954. A modified ninhydrin reagent for the photometric determination of amino acids and related compounds. Journal Biological Chemistry 221: 893–906.

R Core Team. 2023. R: A language and environment for statistical computing. R foundation for statistical computing, Vienna, Austria. https://www.R-project.org/

Riboldi LB, Araújo SHC, Murcia JAG, de Freitas ST, Castro PRC. 2018. Abscisic acid and 24-epibrassinolide regulate blossom-end rot (BER) development in tomato fruit under Ca^{2+} deficiency. Australian Journal of Crop Science 12 (9): 1440–1446. https://doi.org/10.21475/ajcs.18.12.09.pne1106

Riboldi LB, Gaziola SA, Azevedo RA, de Freitas ST, Castro PRC. 2019. 24-epibrassinolide mechanisms regulating blossom-end rot development in tomato fruit. Journal of Plant Growth Regulation 38 (3): 812–823. https://doi.org/10.1007/s00344-018-9892-x

Rouphael Y, Corrado G, Colla G, de Pascale S, Dell'Aversana E, D'Amelia LI, Fusco MG, Carillo P. 2021. Biostimulation as a means for optimizing fruit phytochemical content and functional quality of tomato landraces of the San Marzano area. Foods 10 (5): 926. https://doi.org/10.3390/foods10050926

Saure MC. 2014. Why calcium deficiency is not the cause of blossom-end rot in tomato and pepper fruit. A reappraisal. Scientia Horticulturae 174: 151–154. https://doi.org/10.1016/j.scienta.2014.05.020

Sergiev V, Alexieva A, Karanov E. 1997. Effect of spermine atrazine and combination between the monsome endogenous protective systems and stress markers in plants. Proceedings of the Bulgarian Academy of Sciences 51 (3): 121–124.

Shamshiri RR, Jones JW, Thorp KR, Ahmad D, Man HC, Taheri S. 2018. Review of optimum temperature, humidity, and vapour pressure deficit for microclimate evaluation and control in greenhouse cultivation of tomato: A review. International Agrophysics 32 (2): 287–302. https://doi.org/10.1515/intag-2017-0005

Sharma A, Kumar V, Shahzad B, Ramakrishnan M, Singh Sidhu GP, Bali AS, Handa N, Kapoor D, Yadav P, Khanna K, *et al*. 2020. Photosynthetic response of plants under different abiotic stresses: A review. Journal of Plant Growth Regulation 39 (2): 509–531. https://doi.org/10.1007/s00344-019-10018-x

SIAP (Servicio de Información Agroalimentaria y Pesquera). 2023. Cierre agrícola. Gobierno de México. Servicio de Información Agroalimentaria y Pesquera. Ciudad de México, México. https://nube.siap.gob.mx/cierreagricola/ (Retrieved: July 2025).

Steiner AA. 1984. The universal nutrient solution. Sixth International Congress on Soilless Culture. Wageningen, Netherlands, pp: 633–650.

Tepkaew T, Khamsuk O, Chumpookam J, Sonjaroon W, Jutamanee, K. 2022. Exogenous brassinosteroids regulate mango fruit set through inflorescence development and pollen fertility. Horticultural Science and Technology 40 (5): 481–495. https://doi.org/10.7235/hort.20220043

Trouwborst G, Sander WH, Harbinson J, Wim Van I. 2011. The influence of light intensity and leaf age on the photosynthetic capacity of leaves within a tomato canopy. The Journal of Horticultural Science and Biotechnology 86 (4): 403–407. https://doi.org/10.1080/14620316.2011.11512781

Verma PPS, Meena ML, Meena SK. 2014. Influence of plant growth regulators on growth, flowering and quality of tomato (*Lycopersicon esculentum* Mill.), cv. H-86. Indian Journal of Hill Farming 27 (2): 19–22.

Agrociencia

COFFEE INNOVATION: GLOBAL TRENDS AND FUTURE PERSPECTIVES

Marisol **Lima-Solano**[1], Victorino **Morales-Ramos**[1*], Fernando Carlos **Gómez-Merino**[2], Robert Hunter **Manson**[3], Adriana **Contreras-Oliva**[1], Ma. de Lourdes **Arévalo-Galarza**[2]

[1]Colegio de Postgraduados Campus Córdoba. Carretera Córdoba-Veracruz km 348, Manuel León, Amatlán de los Reyes, Veracruz, Mexico. C. P. 94953.
[2]Colegio de Postgraduados Campus Montecillo. Carretera México-Texcoco km 36.5, Montecillo, Texcoco, State of Mexico, Mexico. C. P. 56264.
[3]Instituto de Ecología A.C. Carretera Antigua a Coatepec 351, Colonia el Haya, Xalapa, Veracruz, Mexico. C. P. 91073.
* Author for correspondence: vicmor@colpos.mx

Citation: Lima-Solano M, Morales-Ramos V, Gómez-Merino FC, Manson RH, Contreras-Oliva A, Arévalo-Galarza ML. 2025. Coffee innovation: Global trends and future perspectives. **Agrociencia** 59(6): 857-871. https://doi.org/ 10.47163/agrociencia.v59i6.3207

Editor in Chief:
Dr. Fernando C. Gómez Merino

Received: February 16, 2025.
Approved: September 18, 2025.
Published in Agrociencia: September 22, 2025.

ABSTRACT

Coffee is the second most consumed beverage in the world, as well as one of the most valuable commodities, providing a livelihood for 25 million farmers in the tropics. The aim of this research was to analyze recent trends in coffee innovation. The documents for this review were extracted from the Scopus database in two separate searches. The first search registered 365 documents on coffee innovations between 1977 and April 2022, and the second flagged 138 documents on the life cycle analysis (LCA) of coffee, which was the primary innovation identified. Bibliometric methodologies in VOSviewer and the RStudio *bibliometrix* package were used for data processing. The results showed a growing number of articles on coffee innovations since 2010, with research focused on the areas of business, management, and accounting (14.1 %); environmental sciences (11.9 %); and agricultural and biological sciences (11.8 %). In terms of document production by country, the most prominent were the United States, Brazil, and the United Kingdom. The findings also revealed that the initial focus of coffee innovations was on issues related to dissemination, the human factor, and marketing. Since 2016, innovation trends have focused on sustainability evaluated through life cycle analysis originating mainly in producing countries as a response to climate change to ensure food security under a sustainable development approach.

Keywords: bibliometric analysis, sustainable development, climate change, food security.

INTRODUCTION

Coffee is one of the most traded commodities worldwide and provides a livelihood for millions of small-scale producers in tropical areas. Global coffee consumption during the 2021–2022 production cycle increased 4.2 %, or 175.6 million 60-kg bags (ICO, 2023). Due to its origin as an understory shrub in the mountains of East Africa with stable microclimates, coffee is vulnerable to climate variations. In countries such as Ecuador and Mexico, coffee farming has experienced a decline in yield due to limited

access to production system technologies for small-scale farmers (Duicela-Guambi *et al.*, 2018) and the high incidence of pests and diseases (Pham *et al.*, 2019). Given these challenges and the need to meet the growing demand for high-quality coffee, innovations have emerged throughout the coffee value chain.

Innovation is defined as the implementation of a new product, good, or service, or the improvement of a process or method, whether commercial or organizational (Nandal *et al.*, 2020). Innovation occurs as long as the people or organizations involved make a long-term commitment to increasing efficiency, competitiveness, and resilience to the problems they face (Kangogo *et al.*, 2020). Innovation is fostered when farmers adopt new agricultural products or processes, or when an exchange of knowledge allows for the development of new ideas or technological processes that generate economic, social, and environmental benefits (Cofré-Bravo *et al.*, 2019). When talking about innovation, a connection with improved processes can be inferred, which are not always product-related (Fernandez-Stark and Gereffi, 2019).

Although there are numerous studies on coffee, few use bibliometric methods. This type of analysis can help inform the scientific community of the trends and dynamism inherent in the research topic under consideration. In the case of coffee, scientific production and collaboration related to certification have been mapped (Cabrera *et al.*, 2020). In addition, over the last five years, sustainability in the sector has received significant attention in bibliometric research, including the use of technologies in precision coffee farming to strengthen the sector's competitiveness through operational efficiency (Santana *et al.*, 2021). The incorporation of technology in coffee cultivation has also been assessed with the use of remotely piloted aircraft systems (drones) to obtain timely and efficient aerial images (Bento *et al.*, 2023). Another study reported scientific data on the effect of caffeine on the general public and athletes resulting from coffee consumption (Contreras-Barraza *et al.*, 2021).

Bibliometric analyses on coffee using other approaches, such as the circular bioeconomy based on the use of organic residues (Ranjbari *et al.*, 2022), have boomed in the last 10 years. However, similar studies addressing trends in coffee innovations and covering aspects such as publication trajectories, country productivity, areas of knowledge, the most prolific journals and authors, the most relevant documents, the science map, the evolution of the topics addressed in publications, and cutting-edge topics are lacking. The main objective of this study was to address this gap by reviewing and reporting on trends in coffee innovation, covering the aforementioned aspects.

MATERIALS AND METHODS

Data collection

Analysis was conducted to examine the existing literature on innovations in coffee, to describe emerging trends in articles and journals, and to identify the most prolific authors and countries (Donthu *et al.*, 2021). The study was carried out in two stages

using searches in the Scopus database (Elsevier), recognized for its high quality and peer review.

In the first stage, the search criteria used the keywords "innovation" and "coffee" in the title, abstract, or keywords. Keywords in British English were standardized to American English, and plural words were changed into singular (Verma and Gustafsson, 2020). This resulted in a total of 365 documents generated between 1977 and April 22, 2022, when the search was conducted. These included: 216 articles, 57 conferences, 37 book chapters, 32 reviews, 10 conference reviews, six books, four notes, two short surveys, and one editorial.

All available documents were considered to obtain a broader overview of the development and evolution of innovation in the coffee sector. Data eligibility included all subject areas and languages used in the documents –mainly English (89.6 %), and a mix of French, German, Korean, Portuguese, Chinese, Russian, Slovak, and Spanish-.

Data analysis

The VOSviewer software version 1.6.20 was used to map the science and visualize the domain formed by the network of co-occurrences of coffee innovation keywords. The results are presented in network, overlay, and density cluster visualizations, which allow researchers to broaden their understanding of emerging research topics and the nature of the research, define the scope, or avoid bias in the source selection process (van Eck and Waltman, 2010). To generate the clusters, the association (S_{ij}) between elements *i* and *j* is estimated based on the distance between the nodes according to the following formula:

$$S_{ij} = \frac{C_{ij}}{W_i W_j}$$

where C_{ij} represents the number of occurrences of elements *i*, *j*, W_i, and W_j, the sum of the occurrences of elements *i* and *j*, or the sum of occurrences of pairs of these elements.

The scientific productivity of the authors was quantified based on Lotka's Law, which provides a platform for studying the variation between the actual and expected productivity patterns of authors in a subject area during a specific period (Tran and Aytac, 2021). This model establishes that the number of authors, A_n, who publish *n* research papers on a topic is inversely proportional to the square of *n*, according to the following formula:

$$A_n = \frac{A_1}{n^2}$$

where A_n is the number of publications corresponding to a given number of authors. A_1 represents the number of publications with a single author, and n^2 corresponds to the number of authors to be calculated using the exponential growth law squared.

Life cycle analysis

The first stage of analysis of publications showed that most innovations focused on sustainability as described in life cycle analyses (LCA). Therefore, another search was conducted to obtain more information on LCA as an element of innovation in coffee. To analyze the performance of publications on the LCA thematic map for coffee, documents were also collected from the Scopus search engine, using the keywords "life cycle analysis", "life cycle assessment", and "coffee" (TITLE-ABS-KEY). On this occasion, 138 documents were detected, spanning January 1996 to March 6, 2023. To illustrate the topics addressed in the various publications related to LCA, the *biblioshiny* library from the RStudio *bibliometrix* package was used, which allowed for network, data reduction, and correspondence analysis (Derviş, 2019).

RESULTS AND DISCUSSION

Publication timeline

The analysis of the evolution of publications on innovation in coffee yielded 21 documents during the period from 1977 to 1997, which suggested a lack of interest in the subject during this period. Around 2010, the topic of coffee innovation began to appear ever more frequently in publications, a trend that has continued to the present day (coefficient of determination $R^2 = 0.81$).

Country productivity

Research on coffee innovations was produced in more than 70 countries, with the 10 most prolific being the United States, Brazil, the United Kingdom, Indonesia, the Netherlands, Germany, Colombia, France, Italy, and Mexico, representing both the main consumers and the main producers of coffee worldwide, and accounting for 67.4 % of total publications, with the United States having the highest number of contributions with 14 %. In addition, the results revealed that the contribution of Indonesia, a coffee-producing country, has increased in recent years.

In coffee-importing countries (the United States, the United Kingdom, the Netherlands, Germany, France, and Italy), research has focused on the last two segments of the value chain (consumption and waste disposal). In contrast, LCA of coffee producing countries (Brazil, Indonesia, Colombia, and Mexico) address environmental issues and concerns.

Areas of knowledge, journals, and the most prolific authors

Analysis of the available scientific literature on innovations in coffee showed they are spread across six main areas of knowledge: business, management, and accounting

(14.1 %); agricultural and biological sciences (11.8 %); environmental sciences (11.9 %); engineering (8.2 %); economics, econometrics, and finance (7.3 %); and computer science (5.6 %). Documents were published in a total of 287 journals, of which the most prominent, with the highest number of publications related to innovations in coffee, were Earth and Environmental Science (4.1 %), Sustainability (2.2 %), Journal of Cleaner Production (1.4 %), ACM International Conference Proceeding Series (1.4 %), and Journal of Physics (1.4 %).

Most authors publish a small number of papers on a specific research topic. A small number of authors comprised the most prolific group, accounting for most of the available literature. The results of this research showed that 95 % of authors generated only one paper out of the total number of publications on coffee innovations, while 4 % wrote two, 0.41 % wrote three, and only 0.41 % wrote four or more publications. The main authors who published collectively were Drs. Bertrand, Etienne, Georget, and Montagnon.

Relevant documents

The most influential documents on coffee innovations, identified according to their impact on the academic community, received a total of 3920 citations, with an average of 17 citations per article (Table 1).

Table 1. The ten most cited articles on coffee innovations produced between 1977 and April 22, 2022.

Article	Description of the innovation	Citations	Average[1]
Campos-Vega *et al*. (2015), Trends in Food Science and Technology	Potential use of coffee residues, generated at any stage of the process, as functional ingredients in the food industry.	288	28.80
Notarnicola *et al*. (2017), Journal of Cleaner Production	The implementation of life cycle analysis (LCA) to assess and improve the environmental impacts of coffee production, identifying critical points and proposing solutions to reduce emissions and resource consumption.	241	30.13
Chua and Banerjee (2013), Journal of Knowledge Management	The use of social media to transform customers from passive recipients to active contributors of innovation, allowing them to propose and evaluate ideas for new products and services.	176	14.67

Table 1. Continuation

Article	Description of the innovation	Citations	Average[1]
Monaci and Palmisano (2004), Analytical and Bioanalytical Chemistry	The development of analytical methods for the detection of ochratoxin A in food, emphasizing biosensors, test strips, and molecularly imprinted polymers as alternatives to conventional chromatographic techniques.	153	7.29
Flood (2010), Food Security	The start-up Global Plant Clinic (GPC) takes a radical approach by offering plant health services to farmers, improving early detection of pests and diseases through plant health clinics run by "plant doctors" in rural areas.	116	7.73
Bray *et al*. (2002), Society and Natural Resources	The production of certified organic coffee in Mexico is driven by institutional transformation, organizational changes, and accumulated social capital among smallholder farmers.	108	4.70
Tscharntke *et al*. (2015), Conservation Letters	Linking existing certification mechanisms with landscape-scale ecosystem service management and conservation approaches for biodiversity conservation.	98	9.80
Matzler *et al*. (2013), Journal of Business Strategy	A capsule system design that combines high quality and convenience, creating an exclusive and premium experience for consumers.	97	8.08
Fuzi (2015), Regional Studies, Regional Science	Coworking spaces to promote creative interaction, facilitating entrepreneurship through support and adequate infrastructure.	85	8.50
Blackburn *et al*. (2008), Communications of the ACM	A new set of benchmarks and methodologies for assessing Java applications, using real applications and metrics to address the limitations of traditional benchmarks.	83	4.88

[1]Average number of citations per year.

Map of science

The construction of the keyword co-occurrence network revealed that, out of 2889 keywords, 33 met the minimum threshold of six co-occurrences. These were used to visualize the co-occurrence networks (Figure 1) between the concepts grouped into four clusters. A marketing cluster emphasized the importance of physical, chemical,

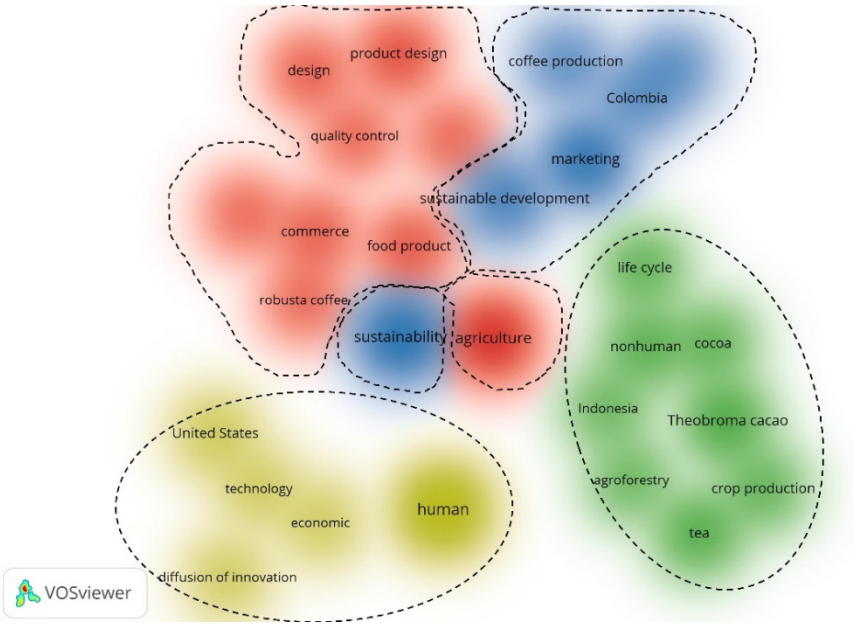

Figure 1. Keyword co-occurrence network of coffee innovation research, showing four thematic clusters (red: marketing and quality analysis; green: environmental sustainability; blue: social innovations; yellow: technology transfer.

and sensory analyses to guarantee the quality and traceability of coffee as elements for higher customer acceptance in an increasingly educated market, where not only quality is valued but also particular aspects associated with varieties and species, such as *Robusta* or *Arabica*. Another aspect that stood out in this cluster was the added value in product design, commercial aspects, and the way coffee is grown in various systems, with the use of technological innovations such as robots in the cultivation phase.

A second environment cluster brought together issues related to reducing greenhouse gases (GHG) based on an LCA in both coffee-producing and coffee-consuming countries. In the case of Indonesia, alternatives were considered to increase farmer income through the adoption of new commercial crops such as cocoa. In addition, innovations were oriented toward the production of coffee with protected origin designation and farmers' response to incentives derived from payments for environmental services.

A third cluster focused on social innovations based on collaboration between different actors in the coffee production chain, showed that educational resources have been used to develop entrepreneurial skills to promote economic development. One of the innovative strategies for adding value to coffee was the emergence of specialty coffee, targeting a specific market segment where consumers value flavor and aroma attributes. In addition, there are co-products from residues generated during coffee processing.

The final cluster was focused on technology transfer, and revealed that the United States has the greatest impact in this area, with research focused on the valorization of coffee spent grounds, commercialization, the nutritional compounds contained in the beverage, and the health benefits of coffee consumption. Likewise, technology has been used as a means to increase coffee production and consumption. In addition, the impact of the dissemination of innovations through mass media on the generation of economic benefits has been evaluated.

Trends in the topics covered in publications

From the publication of the first article on the subject of innovations in coffee until 2010, research focused on topics related to the promotion of innovations, specifically in the agroforestry area; afterwards, the topics addressed by academics were marketing and technology. Over time, the fields of research expanded to include themes related to economic factors and agricultural products, focusing on quality control and product design, such as blockchain, which emerged to meet the needs of a demanding market that makes use of technology. This allowed inclusive business models to be generated to ensure traceability, which results in greater confidence for end consumers of coffee (Miatton and Amado, 2020).

The thematic evolution was represented using colors on a plasma scale (Figure 2), ranging from purple to yellow. This visualization allows for easy identification of trends

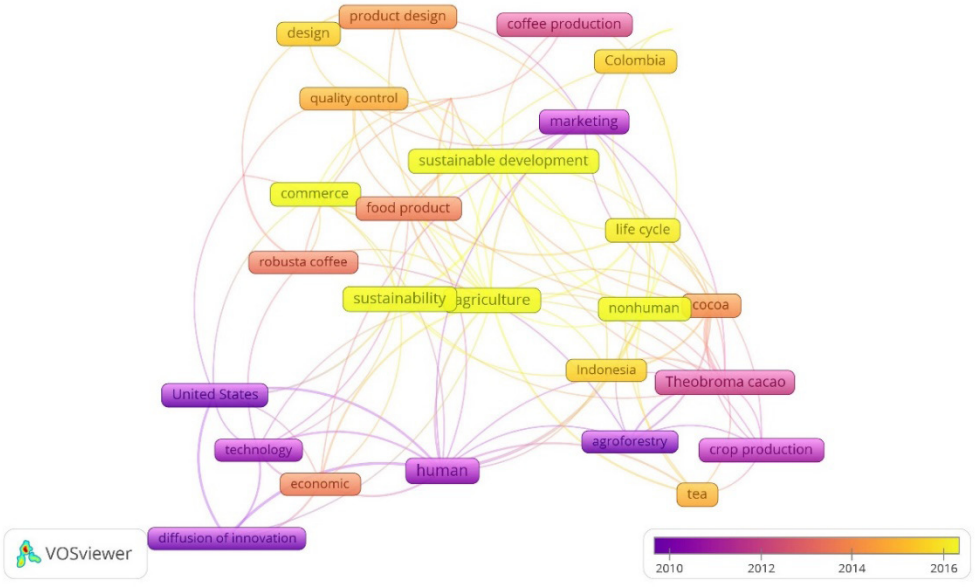

Figure 2. Keyword co-occurrence network of innovations in coffee by evolution of topics of interest, highlighting shifts in research focus over time. Older terms are represented in purple tones, while more recent terms appear in yellow.

and changes in research over time. Since 2016, authors have focused on sustainability, assessing the environmental impact at different stages of the coffee value chain, with the exporting stage being where the most GHG emissions (70 %) are released into the atmosphere (Nab and Maslin, 2020). For this reason, it is not surprising that research trends promote ventures with a focus on sustainable development to ensure food security, in accordance with the 2030 Agenda for Sustainable Development.

The evolution of the topics developed in different research projects related to innovations in coffee allowed the identification of innovations adopted by producers, whether to control weeds or manage plantations with varieties derived from Timor hybrids, due to their lower susceptibility to pests and diseases such as *Hemileia vastatrix* (Bertrand *et al.*, 2011). This also includes the adaptation of strategies to mitigate climate change with agroforestry systems (Camara *et al.*, 2012). Another example of studies related to environmental conservation is the transition process of the coffee value chain in pursuit of sustainability and the innovations this entails (González-Pérez and Gutiérrez-Viana, 2012).

The trend in recent years has focused on issues that facilitate technological development without neglecting economic, social, and environmental aspects, through the creation of new businesses. The European Union assessed the environmental impact of the consumption of products such as coffee, identifying through a life cycle analysis that the cultivation phase has the greatest impact and that farmers who use protected designation of origin have a higher level of technology adoption (Yamoah *et al.*, 2020). These trends set the stage for research on the adoption of innovations in coffee farming.

Another cutting-edge issue is sustainability which, in producing countries such as Costa Rica, has been analyzed for GHG reduction through the carbon neutrality certification process, based on an LCA assessment (Birkenberg *et al.*, 2021). Therefore, to protect the environment, innovations have been developed for the production of clean energy, generated through the alternative use of by-products such as coffee husks (Rajesh Banu *et al.*, 2020).

Commerce has also been a topic of interest for the scientific community since 2016. Consumer tastes and preferences represent a more knowledgeable and environmentally conscious market. Guiné *et al.* (2020) reviewed the factors influencing new product development in the food sector, emphasizing that consumer behavior and willingness to pay a premium for a higher quality coffee are decisive elements for product success.

Agricultural practices, particularly the use of fertilizers and other chemical inputs, are significant sources of GHG emissions, mainly carbon dioxide and nitrous oxide. Consequently, LCA has become a widely applied methodological tool, often combined with analyses of the carbon footprint, to evaluate the climate change impacts throughout the different stages of the coffee value chain.

Cutting-edge topics

The search conducted for LCA in coffee revealed that the distribution of documents was as follows: scientific articles (76 %), conferences (12.3 %), review articles (3.6 %), and book chapters (2.9 %), while the remaining percentage included other types

of documents. The countries with the most research on LCA in coffee are Italy, the United States, Colombia, the United Kingdom, Brazil, Spain, Germany, France, and Switzerland. Among all the research thematic areas, the main ones were environmental sciences (26.4 %), engineering (14.5 %), energy (12.9 %), agricultural and biological sciences (6.9 %), business, management, and accounting (6.6 %). The leading journals for publishing in this field are the International Journal of Life Cycle Assessment and the Journal of Cleaner Production.

The first document on LCA and coffee was published in 1996 in CIRP Annals Manufacturing Technology, entitled "Design for Disassembly and the Environment," which analyzed the environmental impacts of manufacturing a small coffee maker (Harjula *et al*., 1996). The most influential document was written by Notarnicola *et al*. (2017) from the University of Bari in Italy, in which they evaluated the environmental impacts of various products, including coffee consumed in the European Union. Considering that there are various coffee production systems and that one or more systems prevail in each producing country, it is recommended that the LCA be carried out by system and by country, in order to have a clearer picture of the environmental impact of coffee production.

The scope of an LCA can cover the entire coffee value chain (from cradle to grave) or certain segments (from cradle to door, door to door, or door to grave), considering only the activities that take place in each of the stages included in the assessment (Figure 3). For this reason, the carbon footprint metric is used for the calculation, considering the total GHG emissions to produce 1 kg of cherry, parchment, or green coffee, with the processing method as the functional unit (Figure 3). LCA studies in consumer countries have focused on the valorization of residues (Kookos, 2018), concentrating on the spent coffee grounds generated by the soluble industry and on residues from coffee consumed at home and in coffee shops, as well as its potential uses through recycling, recovery of compounds, or energy recovery (Mata *et al*., 2018).

Figure 3. Greenhouse gas (GHG) emission sources across all the segments of the coffee value chain, from production to consumption, based on life cycle assessment (LCA) boundaries and functional units.

Another way to capitalize on information related to environmental impact is via certification labels, which allow small and medium-sized enterprises to gain credibility and access to global markets through the European Union's product category rule, while also enabling promotional strategies for the domestic market (Rocha and

Caldeira-Pires, 2019). Consumers require reliable and easy-to-understand information, therefore technical units are proposed within the LCA to help them make decisions when choosing an environmentally friendly product (Vizzoto *et al.*, 2021). Carbon Neutrality is one of the certifications that provide this type of information, using the environmental indicator known as the carbon footprint (Birkenberg and Birner, 2018). The topics covered in publications related to the LCA of coffee have evolved to include issues that are currently relevant, such as the use of coffee by-products, GHG emissions, and their environmental impact (Figure 4). In coffee-producing countries such as Indonesia and Colombia, research conducted using LCA methodology has focused on technology transfer, certification at different steps in the production chain, profitability, and economic benefits. These efforts promote the development of topics such as the quantification of different environmental footprints at critical points, which helps to improve the efficiency of processes and identify ways to grow, process, and commercialize coffee with minimal environmental impact, for example, through product design with environmentally friendly packaging.

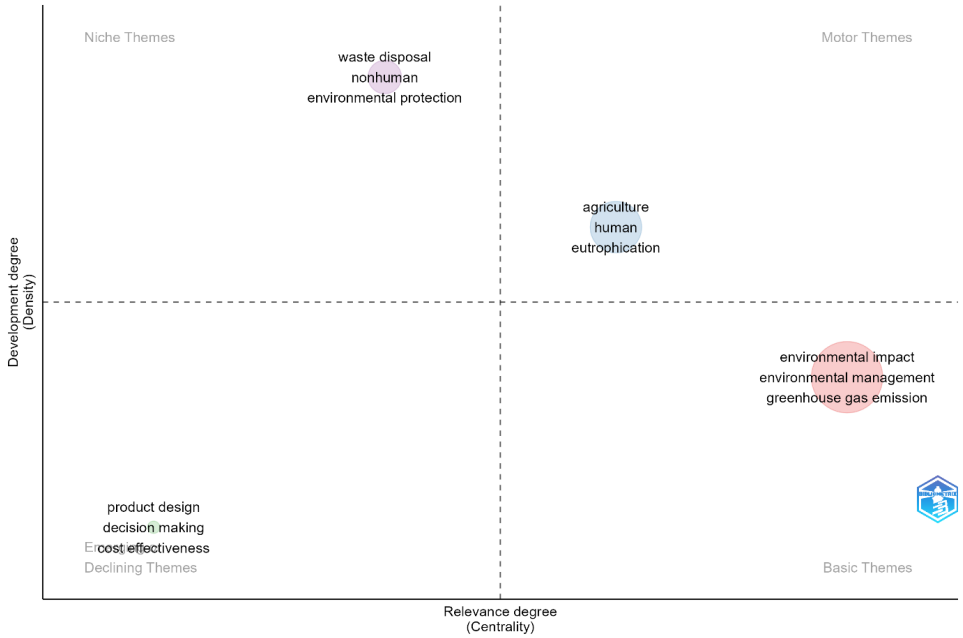

Figure 4. Thematic map of life cycle assessment (LCA) research in coffee, highlighting emerging environmental and sustainability topics across the value chain. The labels in grey indicate the names of the quadrants (types of themes), while the terms in black correspond to the most representative keywords of each cluster identified in the analysis.

CONCLUSIONS

This study provides an understanding of the evolution of the topics addressed in the various research studies on coffee innovation. In addition, the literature searches conducted revealed the growth potential of sustainable innovations focused on ensuring food security, reducing environmental impact, and making better use of resources and co-products. Since 2016, life cycle assessment (LCA) has gained prominence as a key methodological tool, positioning it as a valuable framework for guiding future research in the sector. In coffee-importing countries, research has focused on the last two steps in the value chain (consumption and end use). Coffee LCA ranked first among producing countries due to environmental concerns and the development of studies that help to solve environmental problems.

ACKNOWLEDGEMENTS

M.L.-S. thanks the Secretariat of Science, Humanities, Technology and Innovation (SECIHTI) for scholarship 932627 awarded for postgraduate studies at the Postgraduate College Córdoba Campus.

REFERENCES

Bento NL, Ferraz GAS, Santana LS, Silva MLO. 2023. Coffee growing with remotely piloted aircraft system: Bibliometric review. AgriEngineering 5 (4): 2458–2477. https://doi.org/10.3390/agriengineering5040151

Bertrand B, Alpizar E, Lara L, SantaCreo R, Hidalgo M, Quijano JM, Montagnon C, Georget F, Etienne H. 2011. Performance of *Coffea arabica* F1 hybrids in agroforestry and full-sun cropping systems in comparison with American pure line cultivars. Euphytica 181 (2): 147–158. https://doi.org/10.1007/s10681-011-0372-7

Birkenberg A, Birner R. 2018. The world's first carbon neutral coffee: Lessons on certification and innovation from a pioneer case in Costa Rica. Journal of Cleaner Production 189: 485–501. https://doi.org/10.1016/j.jclepro.2018.03.226

Birkenberg A, Narjes ME, Weinmann B, Birner R. 2021. The potential of carbon neutral labeling to engage coffee consumers in climate change mitigation. Journal of Cleaner Production 278: 123621. https://doi.org/10.1016/j.jclepro.2020.123621

Blackburn SM, McKinley KS, Garner R, Hoffmann C, Khan AM, Bentzur R, Diwan A, Feinberg D, Frampton D, Guyer SZ, *et al*. 2008. Wake up and smell the coffee: Evaluation methodology for the 21st century. Communications of the ACM 51 (8): 83–89. https://doi.org/10.1145/1378704.1378723

Bray DB, Sánchez JLP, Murphy EC. 2002. Social dimensions of organic coffee production in Mexico: Lessons for eco-labeling initiatives. Society and Natural Resources 15 (5): 429–446. https://doi.org/10.1080/08941920252866783

Cabrera LC, Caldarelli CE, da Camara MRG. 2020. Mapping collaboration in international coffee certification research. Scientometrics 124 (3): 2597–2618. https://doi.org/10.1007/s11192-020-03549-8

Camara AA, Dugué P, da Foresta H. 2012. Transformation of the mosaics of forest-savannas by agroforestry practices in sub-Saharan Africa (Guinea, Cameroon). CyberGeo 2012: 627. https://doi.org/10.4000/cybergeo.25588

Campos-Vega R, Loarca-Piña G, Vergara-Castañeda HA, Dave Oomah B. 2015. Spent coffee grounds: A review on current research and future prospects. Trends in Food Science and Technology 45 (1): 24–36. https://doi.org/10.1016/j.tifs.2015.04.012

Chua AYK, Banerjee S. 2013. Customer knowledge management via social media: The case of Starbucks. Journal of Knowledge Management 17 (2): 237–249. https://doi.org/10.1108/13673271311315196

Cofré-Bravo G, Klerkx L, Engler A. 2019. Combinations of bonding, bridging, and linking social capital for farm innovation: How farmers configure different support networks. Journal of Rural Studies 69: 53–64. https://doi.org/10.1016/j.jrurstud.2019.04.004

Contreras-Barraza N, Madrid-Casaca H, Salazar-Sepúlveda G, Garcia-Gordillo MÁ, Adsuar JC, Vega-Muñoz A. 2021. Bibliometric analysis of studies on coffee/caffeine and sport. Nutrients 13 (9): 3234–3248. https://doi.org/10.3390/nu13093234

Derviş H. 2019. Bibliometric analysis using bibliometrix an R package. Journal of Scientometric Research 8 (3): 156–160. https://doi.org/10.5530/jscires.8.3.32

Donthu N, Kumar S, Mukherjee D, Pandey N, Lim WM. 2021. How to conduct a bibliometric analysis: An overview and guidelines. Journal of Business Research 133: 285–296. https://doi.org/10.1016/j.jbusres.2021.04.070

Duicela-Guambi LA, Martínez-Soto ME, Loor-Solórzano RG, Morris-Díaz AT, Guzmán-Cedeño AM, Rodríguez-Monroy C, Chilán-Villafuerte WP. 2018. Gestión del conocimiento e innovación organizacional para reactivar la cadena productiva del café robusta, Ecuador. Revista Espamciencia 9 (1): 61–72.

Fernandez-Stark K, Gereffi G. 2019. Global value chain analysis: A primer. *In* Handbook on Global Value Chains. Edward Elgar Publishing: Cheltenham, UK, pp: 54–76. https://doi.org/10.4337/9781788113779.00008

Flood J. 2010. The importance of plant health to food security. Food Security 2 (3): 215–231. https://doi.org/10.1007/s12571-010-0072-5

Fuzi A. 2015. Co-working spaces for promoting entrepreneurship in sparse regions: The case of South Wales. Regional Studies, Regional Science 2 (1): 462–469. https://doi.org/10.1080/21681376.2015.1072053

Gonzale-Perez MA, Gutierrez-Viana S. 2012. Cooperation in coffee markets: the case of Vietnam and Colombia. Journal of Agribusiness in Developing and Emerging Economies 2: 57–73. https://doi.org/10.1108/20440831211219237

Guiné RPF, Florença SG, Barroca MJ, Anjos O. 2020. The link between the consumer and the innovations in food product development. Foods 9 (9): 1317. https://doi.org/10.3390/foods9091317

Harjula T, Rapoza B, Knight WA, Boothroyd G. 1996. Design for disassembly and the environment. CIRP Annals 45 (1): 109–114. https://doi.org/10.1016/S0007-8506(07)63027-3

ICO (International Coffee Organization). 2023. Coffee report and outlook. London, UK. 43 p. https://www.inter-reseaux.org/wp-content/uploads/Coffee_Report_and_Outlook_April_2023_-_ICO.pdf (Retrieved: May 2023).

Kangogo D, Dentoni D, Bijman J. 2020. Determinants of farm resilience to climate change: The role of farmer entrepreneurship and value chain collaborations. Sustainability 12 (3): 868. https://doi.org/10.3390/su12030868

Kookos IK. 2018. Technoeconomic and environmental assessment of a process for biodiesel production from spent coffee grounds (SCGs). Resources, Conservation and Recycling 134: 156–164. https://doi.org/10.1016/j.resconrec.2018.02.002

Mata TM, Martins AA, Caetano NS. 2018. Bio-refinery approach for spent coffee grounds valorization. Bioresource Technology 247: 1077–1084. https://doi.org/10.1016/j.biortech.2017.09.106

Matzler K, Bailom F, von den Eichen SF, Kohler T. 2013. Business model innovation: Coffee triumphs for Nespresso. Journal of Business Strategy 34 (2): 30–37. https://doi.org/10.1108/02756661311310431

Miatton F, Amado L. 2020. Fairness, transparency and traceability in the coffee value chain through blockchain innovation. 2020 International Conference on Technology and Entrepreneurship. https://doi.org/10.1109/icte-v50708.2020.9113785

Monaci L, Palmisano F. 2004. Determination of ochratoxin a in foods: State-of-the-art and analytical challenges. Analytical and Bioanalytical Chemistry 378 (1): 96–103. https://doi.org/10.1007/s00216-003-2364-5

Nab C, Maslin M. 2020. Life cycle assessment synthesis of the carbon footprint of *Arabica* coffee: Case study of Brazil and Vietnam conventional and sustainable coffee production and export to the United Kingdom. Geo: Geography and Environment 7 (2): e00096. https://doi.org/10.1002/geo2.96

Nandal N, Kataria A, Dhingra M. 2020. Measuring innovation: Challenges and best practices. International Journal of Advanced Science and Technology 29 (5): 1275–1285.

Notarnicola B, Tassielli G, Renzulli PA, Castellani V, Sala S. 2017. Environmental impacts of food consumption in Europe. Journal of Cleaner Production 140: 753–765. https://doi.org/10.1016/j.jclepro.2016.06.080

Pham Y, Reardon-Smith K, Mushtaq S, Cockfield G. 2019. The impact of climate change and variability on coffee production: A systematic review. Climatic Change 156 (4): 609–630. https://doi.org/10.1007/s10584-019-02538-y

Rajesh Banu J, Kavitha S, Yukesh Kannah R, Dinesh Kumar M, Atabani AE, Kumar G. 2020. Biorefinery of spent coffee grounds waste: Viable pathway towards circular bioeconomy. Bioresource Technology 302: 122821. https://doi.org/10.1016/j.biortech.2020.122821

Ramirez-Gomez CJ, Saes MSM, Silva VLS, Souza Piao R. 2022. The coffee value chain and its transition to sustainability in Brazil and Colombia from innovation system approach. International Journal of Agricultural Sustainability 20 (6): 1150–1165. https://doi.org/10.1080/14735903.2022.2065794Ranjbari M, Shams Esfandabadi Z, Quatraro F, Vatanparast H, Lam SS, Aghbashlo M, Tabatabaei M. 2022. Biomass and organic waste potentials towards implementing circular bioeconomy platforms: A systematic bibliometric analysis. Fuel 318: 123585. https://doi.org/10.1016/j.fuel.2022.123585

Rocha MSR, Caldeira-Pires A. 2019. Environmental product declaration promotion in Brazil: SWOT analysis and strategies. Journal of Cleaner Production 235: 1061–1072. https://doi.org/10.1016/j.jclepro.2019.06.266

Santana LS, Ferraz GAES, Teodoro AJS, Santana MS, Rossi G, Palchetti E. 2021. Advances in precision coffee growing research: A bibliometric review. Agronomy 11 (8): 1557. https://doi.org/10.3390/agronomy11081557

Tran CY, Aytac S. 2021. Scientific productivity, Lotka's Law, and STEM librarianship. Science and Technology Libraries 40 (3): 316–324. https://doi.org/10.1080/0194262X.2021.1907268

Tscharntke T, Milder JC, Schroth G, Clough Y, Declerck F, Waldron A, Rice R, Ghazoul J. 2015. Conserving biodiversity through certification of tropical agroforestry crops at local and landscape scales. Conservation Letters 8 (1): 14–23. https://doi.org/10.1111/conl.12110

van Eck NJ, Waltman L. 2010. Software survey: VOSviewer, a computer program for bibliometric mapping. Scientometrics 84 (2): 523–538. https://doi.org/10.1007/s11192-009-0146-3

Vegro CLR, de Almeida LF. 2020. Global coffee market: Socio-economic and cultural dynamics. *In* Coffee Consumption and Industry Strategies in Brazil. Elsevier: Amsterdam, Netherlands, pp: 3–19. https://doi.org/10.1016/B978-0-12-814721-4.00001-9

Verma S, Gustafsson A. 2020. Investigating the emerging COVID-19 research trends in the field of business and management: A bibliometric analysis approach. Journal of Business Research 118: 253–261. https://doi.org/10.1016/j.jbusres.2020.06.057

Vizzoto F, Testa F, Iraldo F. 2021. Towards a sustainability facts panel? Life Cycle Assessment data outperforms simplified communication styles in terms of consumer comprehension. Journal of Cleaner Production 323: 129124. https://doi.org/10.1016/j.jclepro.2021.129124

Yamoah FA, Kaba JS, Amankwah-Amoah J, Acquaye A. 2020. Stakeholder collaboration in climate-smart agricultural production innovations: Insights from the cocoa industry in Ghana. Environmental Management 66 (4): 600–613. https://doi.org/10.1007/s00267-020-01327-z

Agrociencia

Clavibacter michiganensis subsp. *michiganensis* MANAGEMENT STRATEGIES IN TOMATO (*Solanum lycopersicum* L.)

Valeria **Roldán-Guzmán**[1], Sergio **Aranda-Ocampo**[1*], Lauro **Soto-Rojas**[1], Joel **Pineda-Pineda**[2], Cristian **Nava-Díaz**[1]

[1]Colegio de Postgraduados Campus Montecillo. Carretera México-Texcoco km 36.5, Montecillo, Texcoco, State of Mexico, Mexico. C. P. 56230.
[2]Universidad Autónoma Chapingo. Carretera México-Texcoco km 38.5, Texcoco, State of Mexico, Mexico. C. P. 56230.
* Author for correspondence: arandasergio63@gmail.com

Citation: Roldán-Guzmán V, Aranda-Ocampo S, Soto-Rojas L, Pineda-Pineda J, Nava-Díaz C. 2025. *Clavibacter michiganensis* subsp. *michiganensis* management strategies in tomato (*Solanum lycopersicum* L.). **Agrociencia** 59(6): 872-883. https://doi.org/ 10.47163/agrociencia.v59i6.3089

Editor in Chief:
Dr. Fernando C. Gómez Merino

Received: February 10, 2025.
Approved: September 03, 2025.
Published in Agrociencia: September 18, 2025.

ABSTRACT

Clavibacter michiganensis subsp. *michiganensis* (Cmm) is the causal agent of bacterial canker, which is the most destructive disease of tomato (*Solanum lycopersicum* L.). This study compared the effectiveness of two nitrogen fertilization regimes, Steiner 100 % NO_3^- and Steiner 85/15 NO_3^-/NH_4^+, in supplying total nitrogen for tomato nutrition under greenhouse conditions. These treatments were tested in combination with the plant activators Romel (*Brevibacillus* sp.), Fungifree (*Bacillus* sp.), and Messenger Gold (Harpin protein αβ 3 %) to evaluate their effects on Cmm severity and yield in a completely randomized factorial experiment. Each fertilization regime was applied daily in drip irrigation, while plant activators were sprayed weekly. Inoculation of Cmm in plants was performed by cutting the petiole with scissors soaked in a suspension with 10^8 CFU mL^{-1}. Yield and severity were assessed by evaluating the nutrition and plant activator factors, as well as their interaction. A two-way analysis of variance (treatment and nutrition) and Tukey's comparison of means ($p \leq 0.05$) were performed. The Steiner 100 % NO_3^- nutrition regime showed significant differences ($p \leq 0.05$) in yield, fresh and dry weight of leaves, number of bunches, and number and diameter of fruits. Significant differences ($p \leq 0.05$) were found in the weighted percentage of leaf damage and whole-plant wilting severity; the highest severity was recorded with the Steiner 85/15 NO_3^-/NH_4^+ + Romel treatment and the lowest with Steiner 100 % NO_3^- + Messenger Gold. The application of Harpin protein and exclusive nitrogen fertilization with nitrates (NO_3^-) is an efficient management strategy that promotes higher yield and fruit quality while reducing the severity of Cmm under greenhouse conditions.

Keywords: Bacterial canker, Harpin protein, nitrate, ammonium, management.

INTRODUCTION

Clavibacter michiganensis subsp. *michiganensis* (Cmm) is an international quarantine pathogen by the European and Mediterranean Plant Protection Organization (EPPO). This microorganism causes bacterial canker in tomato (*Solanum lycopersicum* L.), which

is considered one of the most destructive diseases worldwide (Chalupowicz *et al*., 2016). It affects plants by causing wilting, necrosis, and canker on stems and petioles. This results in a nutritional imbalance and a decrease in physiological activity, which impacts fruit quality and yield (Kolomiiets *et al*., 2020). To date, there are no tomato varieties or hybrids with complete resistance to Cmm, making it difficult to control (Nandi *et al*., 2018).

The nutritional status of plants influences the plant-pathogen interaction (Ding *et al*., 2021). It has been demonstrated that the supply of nitrogen in the form of nitrate (NO_3^-) fertilization increases resistance through a hypersensitive response as a defense mechanism against pathogens and abiotic stress (Planchet, 2022). In tomato cultivation, fertilization with NO_3^- activates the salicylic acid pathway, inducing plant defense against the bacterial pathogens *Pseudomonas syringae* and *Ralstonia solanacearum* (Ding *et al*., 2021), while the supply of ammonium (NH_4^+) in fertilization acts as a cofactor for antioxidant enzymes and an activator of systemic acquired resistance as a defense response against *P. syringae* (González-Hernández *et al*., 2019).

Plant activators with commercial formulations based on species from the genera *Bacillus* and *Brevibacillus* as biocontrol agents, inducers of systemic resistance, and plant growth promoters have been extensively studied, inducing different defense responses in the plant against phytopathogens (Tiwari *et al*., 2019). Previous research has shown that the application of *Bacillus* species reduced the severity of diseases caused by bacterial pathogens such as *R. solanacearum* and *Xanthomonas perforans*; specifically, the application of *B. amyloliquefaciens* in tomato crops provides protection against infection by Cmm (Dame *et al*., 2021).

The Harpin protein is a plant activator used as an inducer of natural plant defenses, known as systemic acquired resistance against bacterial phytopathogens. It is also related to the promotion of plant growth and increased fruit yield and quality (Liu *et al*., 2020). Previous studies have concluded that the application of the PeBL1 protein induces a hypersensitive response and systemic resistance in *Nicotiana benthamiana* Domin against *P. syringae* pv. *tabaci* (Wang *et al*., 2015). The BAR11 protein obtained from *Saccharothrix yanglingensis* stimulated systemic resistance in *Arabidopsis thaliana* L. against *P. syringae* pv. *tomato* (Zhang *et al*., 2018).

In this study, it is assumed that nitrogen fertilization with NO_3^- or NH_4^+, combined with the spraying of plant activators, improves yield and reduces the severity of Cmm in greenhouse tomato crops. Therefore, the objective of this study was to evaluate the efficacy of two fertilization regimes in supplying total nitrogen, in combination with plant activators, on tomato yield and Cmm severity under greenhouse conditions.

MATERIALS AND METHODS

Location and plant material

The experiment was conducted in an overhead greenhouse located at the Postgraduate College, Montecillo Campus (19° 27′ 51′′ N, 98° 54′ 15′′ W) in Texcoco, State of Mexico,

Mexico. A total of 120 seedlings of the Cmm-susceptible hybrid tomato OptiMax (Sakata, Mexico) at the five-true-leaf phenological stage were used. Seedlings were transplanted into black plastic bags (25 × 25 cm) with 125 cm^3 of coarse tezontle at the base of the bags and a mixture of peat and perlite (2:1) as a substrate. Seedlings were maintained in the greenhouse with a relative humidity > 70 % and a temperature between 22 and 33 °C.

Nitrogen fertilization and plant activators

Two fertilization regimes were used to supply total nitrogen (N): 100 % Steiner NO_3^- and 85/15 modified Steiner NO_3^-/NH_4^+ (Table 1). Both regimes were applied daily via drip irrigation 5 d after transplant. Four 3-min irrigations were carried out daily until two months of vegetative development; then, irrigations were increased to 10-min irrigations until crop completion.

Table 1. Chemical composition (meq L^{-1}) of the Steiner 85/15 NO_3^-/NH_4^+ and Steiner 100 % NO_3^- fertilization regimes.

Nutrient solution	NO_3^-	$H_2PO_4^-$	SO_4^-	K^+	Ca^{2+}	Mg^{2+}	NH_4^+
Steiner 85/15 NO_3^-/NH_4^+	10.2	1	8.8	6.37	8.19	3.64	1.8
Steiner 100 % NO_3^-	12	1	7	7	9	4	0

Values expressed in milliequivalents per liter (meq L^{-1}). NO_3^-: nitrate; $H_2PO_4^-$: phosphate; SO_4^-: sulfate; K^+: potassium; Ca^{2+}: calcium; Mg^{2+}: magnesium; NH_4: ammonium.

For each fertilization regime, plant activators Romel (*Brevibacillus* sp., 2.5 mL L^{-1}) (Teza, Agricultura Sustentable S.A. de C.V., Mexico), Fungifree (*Bacillus* sp., 2.5 mL L^{-1}) (FMC Agroquímica, Mexico), and Messenger Gold (Harpin αβ protein 3 %, 1 g L^{-1}) (PHC, Mexico) were sprayed weekly at the doses recommended on the label.

Every two months, the variables evaluated were the number of bunches, fresh and dry leaf weight, number of small fruits, total number of fruits, fruit diameter, and kilograms of fruit per plant until harvest. Fresh and dry leaf weight (g) was determined using a D-Weight DGIT-01 analytical scale (Stay Elit), and fruit diameter (mm) using a None electronic vernier caliper (REXQualis). Fruit size was classified according to Mexican standard NMX-F-009-1982 (DOF, 1982).

Severity assessment

Cmm inoculation was performed by cutting petioles with scissors soaked in a bacterial suspension containing 10^8 colony-forming units per milliliter (CFU mL^{-1}) on the third apical leaf when more than 50 % of the plants had 15 true leaves. The pathogenic CP_Cmm-1 strain, previously identified as highly aggressive (Rivera-Sosa *et al*., 2022), was used. For the control, the cut was made with scissors soaked in sterile distilled water.

Since the first week of inoculation, severity was assessed using the weighted percentage of leaf damage (WPLD) and whole-plant wilting severity (WPWS) ratings. For WPLD, a severity scale was used, where 0 = healthy leaf; 1 = leaves with epinasty or loss of turgor; 2 = leaves with loss of turgor in half of the leaflet and the other half apparently healthy; 3 = wilting and browning in ¾ of the leaf; 4 = wilting and browning of the entire leaf and interveinal chlorosis; and 5 = presence of stem canker (Rivera-Sosa *et al*., 2022).

For WPWS, an arbitrary whole-plant wilting severity scale was used, where 0 = healthy plant, 1 = up to 20 % of the area shows wilting symptoms, 2 = 21 to 40 %, 3 = 41 to 60 %, 4 = 61 to 80 %, and 5 = more than 81 % of the area shows symptoms. The experiment ended 112 d after inoculation, when all fruits reached maturity Grade 6 according to the Mexican standard NMX-F-009-1982 (DOF, 1982).

Experimental design

The experiment was conducted using a completely randomized design with a factorial arrangement and 15 replicates. A first factor was represented by two nutrient solution regimes: the 100 % NO_3^- Steiner solution and the modified Steiner solution with an 85/15 NO_3^-/NH_4^+ ratio. Another factor was represented by four treatments applied by foliar spraying of plant activators: the application of Romel (*Brevibacillus* sp.), Fungifree (*Bacillus* sp.), Messenger Gold (3 % Harpin $\alpha\beta$ protein), and the spraying of sterile distilled water as a control. The experimental unit consisted of one tomato plant corresponding to each combination of fertilization regime and plant activator treatment.

Plant performance and canker disease severity were assessed by comparing the effects of nutrition and plant activator factors, as well as their interaction. Data were assessed using two-way analysis of variance (ANOVA) for treatment and nutrition; normality and homogeneity data were analyzed using the Shapiro-Wilks and Levene tests, and means were compared with the Tukey test ($p \leq 0.05$) using the R v4.2.1 programming language (https://www.R-project.org/).

Reisolation and identification of the pathogen

From plants with characteristic symptoms due to Cmm infection, vascular tissue samples (3 cm in length) were taken and macerated in sterile distilled water. Around 100 μL of the macerate was seeded in Petri dishes with nutrient agar culture medium (Difco, USA) and incubated at 28 °C for 48 h. Colonies with Cmm-like morphology were purified and characterized by Gram staining and infiltration of a suspension containing 10^8 CFU mL^{-1} on the underside of four-o'clock (*Mirabilis jalapa* L.) and tobacco (*Nicotiana tabacum* L.) leaves. The identity of the isolated strains was confirmed with the CMM5F-5′ and CMM6R-5′ primers specific for Cmm and PCR conditions described by Rivera-Sosa *et al*. (2022).

RESULTS AND DISCUSSION

Reisolation and identification of the pathogen

Yellow-orange, mucoid, Gram-positive bacterial colonies were isolated from plant tissue samples from each treatment with Cmm symptoms and used to induce hypersensitivity reactions on tobacco and four-o'clock leaves. The identity of the cultured Cp_Cmm-1 strain was confirmed by comparing the amplified product to the GenBank sequence. This demonstrated a 97 % identity with the *C. michiganensis* strain NCPBB 382 plasmid pCM2 (accession number AM711866.1).

Vegetative development and yield

At 78 d after transplant, results showed significant differences ($p \leq 0.05$) between treatments. Higher values were obtained with the Steiner 100 % NO_3^- nutrient solution regime for the variables fresh leaf weight ($F_{1, 14} = 5.7$, $p = 0.031$), dry leaf weight ($F_{1, 14} = 7.18$, $p = 0.017$), number of bunches ($F_{1, 14} = 7$, $p = 0.019$), number of fruits ($F_{1, 14} = 5.2$, $p = 0.038$), and fruit diameter ($F_{1, 16} = 9.77$, $p = 0.0065$), and had fewer small fruits ($F_{1, 16} = 16.98$, $p < 0.01$) (Table 2).

Table 2. Vegetative growth, fruit quality, and yield of the OptiMax tomato hybrid (*Solanum lycopersicum* L.) under two nitrogen fertilization regimes.

Nitrogen regime	FD *	NSF *	NB *	TNF *	FLW *	DLW *	Y *
Steiner 100 % NO_3^-	53.90 a	34.16 a	4.58 a	27.75 a	1286.17 a	77.51 a	00.76 a
Steiner 85/15 NO_3^-/NH_4^+	51.47 b	20.00 b	4.08 b	23.16 b	912.85 b	51.79 b	00.70 b
Pr(>F)	0.006	0.001	0.02	0.04	0.03	0.01	0.81

FD: fruit diameter; NSF: number of small fruits; NB: number of bunches; TNF: total number of fruits; FLW: fresh leaf weight (g); DLW: dry leaf weight (g); Y: yield (kg plant^{-1}). *Means followed by the same letter are not significantly different (Tukey, $p \leq 0.05$).

The results of this study are consistent with those reported by Nawarathna *et al*. (2021), who concluded that nitrate as a nitrogen source in tomato plants under greenhouse conditions increased plant biomass compared to ammonium supplementation. Biomass content is an indicator of nitrogen uptake in crops. The results suggest that nitrogen supplementation via nitrates in the OptiMax tomato hybrid is a better fertilization strategy than ammonium supply, promoting higher plant biomass content in terms of fresh/dry weight of leaves, number of bunches, and larger fruit diameter with export quality (62–71 mm in diameter) in accordance with the Mexican standard NMX-F-009-1982 (DOF, 1982).

Interaction between plant activator and nutrition

Plant activators showed differences between treatments for the variable small fruit size ($F_{7, 16} = 4.26$, $p = 0.007$). A greater number of small fruits were recorded with the Steiner 85/15 NO_3^-/NH_4^+ + Fungifree treatment and a lower number with Steiner 100 % NO_3^- + Fungifree (Table 3).

Table 3. Fruit quality and yield of the OptiMax tomato hybrid (*Solanum lycopersicum* L.) under different nitrogen fertilization regimes and plant activator applications.

Nitrogen regime	Plant activator	Number of small-sized fruits	*	Yield (kg plant^{-1})	*
Steiner 100 % NO_3^-	Romel	22.7	ab	2.3	a
	Fungifree	19.0	b	2.3	a
	Messenger Gold	22.7	ab	2.3	a
	Control	15.7	b	2.3	a
Steiner 85/15 NO_3^-/NH_4^+	Romel	38.7	ab	2.0	a
	Fungifree	43.3	a	2.1	a
	Messenger Gold	33.3	ab	2.2	a
	Control	21.3	ab	2.2	a
Pr(>F)		0.008		0.999	

*Means followed by the same letter are not significantly different (Tukey, $p \leq 0.05$).

These results highlight the influence of the nutrition regimes, since the only difference between treatments was the form of nitrogen supplied. It has been shown that most plants absorb and assimilate nitrogen better in the form of nitrate than ammonium (Boschiero *et al*., 2019). The effect of nitrogen nutrition on the yield of small-sized fruits (38–52 mm in diameter) in tomato crops is consistent with that reported by Carreras-Sempere *et al*. (2021), who concluded that nitrogen fertilization with ammonium nitrate promotes the production of a higher proportion of small fruits and, consequently, a lower yield of fruits with commercial quality.

Likewise, Howard *et al*. (2021) showed that fertilization with a nitrate/ammonium (NO_3/NH_4^+) combination also reduced the quality and size of tomato fruits. This was also observed in this research, as results suggest that fertilization with the nitrate/ammonium combination is not a cost-effective strategy for the OptiMax tomato hybrid, as it promotes the production of small-sized fruits over commercial-quality fruits. Other studies have shown that ammonium (NH_4^+) can affect plant development due to some toxicity, depending on the plant genotype and environmental conditions (Bittsánszky *et al*., 2015).

Ammonium has been shown to acidify the root zone and decrease the absorption of Ca^{2+} and Mg^{2+}. This could explain the effect on fruit size in treatments with the Steiner 85/15 NO_3^-/NH_4^+ fertilization regime, since these nutrients (Ca^{2+} and Mg^{2+}) promote the

development of larger fruits (Alcántar-González *et al*., 2016). However, the optimal nitrate/ammonium ratio for tomato cultivation in relation to the absorption of Ca^{2+} and Mg^{2+} differs, since it can be influenced by factors such as the plant genotype and the type of soil (Rivera-Espejel *et al*., 2014).

Severity of *Clavibacter michiganensis* subsp. *michiganensis*

The severity results at 78 d after inoculation showed significant differences in weighted percentage of leaf damage (WPLD) ($F_{5, 60}$ = 3.41, p = 0.0087) and whole-plant wilting severity (WPWS) scores ($F_{2, 60}$ = 5.43, p = 0.0067); the highest WPWS was recorded with the Steiner 85/15 NO_3^-/NH_4^+ + Romel treatment and the lowest with Steiner 100 % NO_3^- + Messenger Gold (Table 4). The source of nitrogen fertilization has implications for plant-pathogen interactions and varies depending on the pathogen and plant species (Ding *et al*., 2021). The results of this study are similar to those obtained by Gupta *et al*. (2013), who concluded that nitrate fertilization induced greater resistance against *Pseudomonas syringae* in tobacco.

Table 4. Whole-plant wilting severity (WPWS) caused by *Clavibacter michiganensis* subsp. *michiganensis* in the OptiMax tomato hybrid (*Solanum lycopersicum* L.) under different nitrogen fertilization regimes and plant activator applications.

Nitrogen regime	Plant activator	WPWS*	
Steiner 100 % NO_3^-	Romel	27.2	ab
	Fungifree	30.2	ab
	Messenger Gold	13.5	b
Steiner 85/15 NO_3^-/NH_4^+	Romel	42.8	a
	Fungifree	31.8	ab
	Messenger Gold	17	ab
	Pr(>F)	0.007	

*Means followed by the same letter are not significantly different (Tukey, $p \leq 0.05$).

Likewise, Zimerman-Lax *et al*. (2016) reported a significant reduction in the severity of *Acidovorax citrulli* in melon crops grown under greenhouse conditions. The contribution of nitrate as a source of nitrogen is reported to increase plant resistance by increasing the levels of salicylic acid and producing polyamines as defense signals, unlike ammonium, which increases the level of γ-aminobutyric acid that can be a food source for some pathogens (Mur *et al*., 2017).

The results of this study showed that the application of the Harpin protein (Messenger Gold), with the addition of nitrates in nutrition, significantly reduced WPLD ($F_{5, 60}$ = 3.41, p = 0.0087) and the severity of the plant disease caused by Cmm (Table 5).

The application of the Harpin protein (Messenger Gold) with nitrate supplementation resulted in higher yields and lower severity of bacterial canker disease. It also promoted

Table 5. Frequency distribution and weighted percentage of leaf damage (WPLD) caused by *Clavibacter michiganensis* subsp. *michiganensis* in the OptiMax tomato hybrid (*Solanum lycopersicum* L.) under different nitrogen fertilization regimes and plant activator applications.

		Severity scale							
Nitrogen regime	Plant activator	Grade 0	Grade1	Grade 2	Grade 3	Grade 4	Grade 5	WPLD	*
									
Steiner 100 % NO_3^-	Romel	13.33	6.67	20	53.33	6.67	0	13.4	ab
	Fungifree	6.67	6.67	20	20	26.67	20	18.7	ab
	Messenger Gold	13.33	60	26.67	0	0	0	5.2	b
Steiner 85/15 NO_3^-/NH_4^+	Romel	6.67	6.67	6.67	13.33	20	46.67	22.7	a
	Fungifree	13.33	6.67	6.67	20	13.33	40	17	ab
	Messenger Gold	13.33	46.67	6.67	13.33	13.33	6.67	6	b

*Means followed by the same letter are not significantly different (Tukey, $p \leq 0.05$).

better fruit set and filling and a higher proportion of fruits classified as medium and large. The Harpin protein induces plant defenses against different pathogens, in addition to promoting plant growth (Rajwade *et al*., 2020; Yuan *et al*., 2020). Its effect has been linked to the production and accumulation of salicylic acid and systemic acquired resistance (Nazarov *et al*., 2020; Sheikh *et al*., 2022). Fertilization in general influences the susceptibility response of tomato to Cmm and is reported to depend on factors such as genotype, growth stage, and amounts of fertilizer used in production systems (Brochu *et al*., 2023).

Likewise, differences in disease severity have been observed in tomato genotypes due to the inoculation of different Cmm strains, showing variability in virulence (Rivera-Sosa *et al*., 2022). To date, no research has addressed the direct relationship between the nitrogen source in fertilization and the degree of disease severity caused by Cmm in tomato crops. However, in this study, the exclusive nitrogen source with NO_3 and the application of the Harpin protein reduced severity after inoculating a strain identified as highly aggressive (Rivera-Sosa *et al*., 2022) in a susceptible tomato genotype (OptiMax). The above could suggest that the relationship between the nitrogen source in fertilization together with the application of the Harpin protein should be evaluated in genotypes with greater tolerance to Cmm infection to promote a better resistance response and reduce disease severity.

Plant activators formulated with *Bacillus* and *Brevibacillus* spp. showed higher degrees of severity (Grade 5) than the treatment with the application of the Harpin protein. Although species of the genera *Brevibacillus* and *Bacillus* are generally recognized for

their efficient and broad-spectrum antibacterial activity (Song *et al*., 2012; Dame *et al*., 2021), in this study, the formulation based on *Brevibacillus* sp. (Romel) resulted in the highest WPWS (Table 4, Figure 1) and WPLD (Table 5) scores. At severity Grade 5, plants in this treatment exhibited completely collapsed leaflets.

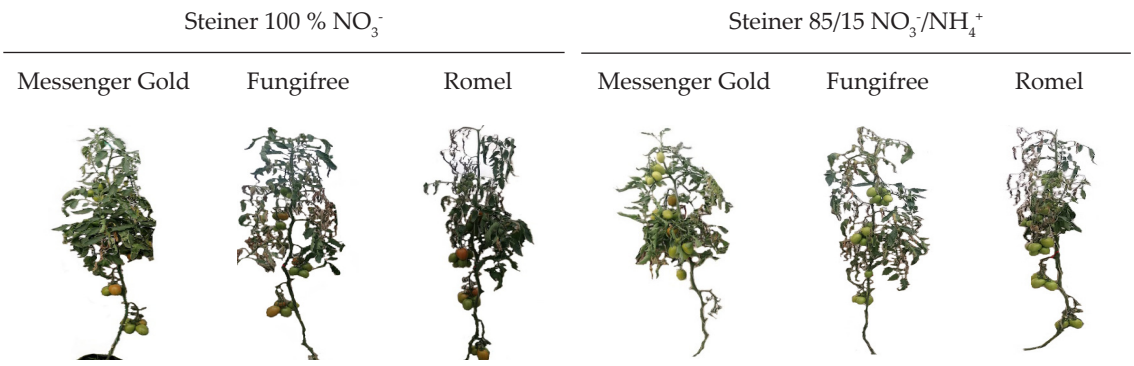

Figure 1. Whole-plant Grade 5 severity of *Clavibacter michiganensis* subsp. *michiganensis* in the OptiMax tomato hybrid (*Solanum lycopersicum* L.) under two nitrogen fertilization regimes and different plant activator treatments.

Biocontrol agent-plant-pathogen interactions are inherently complex. Several studies have demonstrated that *Brevibacillus* and *Bacillus* species can effectively reduce the severity of pathogen-induced diseases. However, commercial strains and formulations based on these biocontrol agents have also been reported as ineffective in certain pathosystems. This has been attributed to multiple factors, including the persistence of the agent in the phyllosphere over time and space (for foliar applications), inoculum concentration, frequency of application, and the genetic characteristics of the agent related to the production of metabolites involved in pathogen suppression. Additional factors include the plant species, its genotype, and susceptibility to the pathogen, the inoculation method, and the genetic variability and virulence of the pathogen itself (Lahlali *et al*., 2022; Mahapatra *et al*., 2022; Sedighian *et al*., 2025).

Treatments with the application of the Harpin protein resulted in the lowest severity, with photosynthetically active areas visible on the leaves and leaflets up to Grade 3. Plants receiving this treatment did not reach severity Grade 5 (Table 5). Across the whole plant, this treatment also exhibited lower overall severity (Figure 1) and better yields, producing fruits with larger diameters and better commercial quality. The Harpin protein induces a range of metabolic responses, including the natural expression of systemic acquired resistance (SAR) genes in response to pathogen infection (Nazarov *et al*., 2020; Sheikh *et al*., 2022). It also activates jasmonic acid/ethylene-dependent defense mechanisms as well as plant growth-related systems. These mechanisms have been extensively studied against various fungal and bacterial pathogens. To date, there are no reports of resistance induction in phytopathogens,

making the Harpin protein a promising strategy to enhance crop protection without causing adverse damage to the environment (Li *et al*., 2023).

CONCLUSIONS

The nitrogen fertilization regime influenced tomato fruit yield and quality. Under greenhouse conditions, the exclusive application of nitrate (NO_3^-) increased yield and fruit production within export quality standards, in contrast to the combined application of nitrate/ammonium (NO_3^-/NH_4^+). The application of plant activators formulated with *Bacillus* and *Brevibacillus* did not protect against infection by *Clavibacter michiganensis* subsp. *michiganensis* in the OptiMax tomato hybrid. The Harpin protein application and exclusive nitrogen fertilization with nitrates proved to be an efficient management strategy that promotes higher yield and fruit quality and reduces the severity of this pathogen under greenhouse conditions.

ACKNOWLEDGEMENTS

We would like to thank the Secretariat of Science, Humanities, Technology and Innovation (SECIHTI) and Postgraduate College's Program in Phytosanitary-Phytopathology, Montecillo Campus, for funding this research.

REFERENCES

Alcántar-González G, Trejo-Téllez LI, Gómez-Merino FC. 2016. Nutrición de cultivos (Segunda edición). Colegio de postgraduados: Ciudad de México, México. 443 p.

Bittsánszky A, Pilinszky K, Gyulai G, Komives T. 2015. Overcoming ammonium toxicity. Plant Science 231: 184–190. https://doi.org/10.1016/j.plantsci.2014.12.005

Boschiero BN, Mariano E, Azevedo RA, Trivelin PCO. 2019. Influence of nitrate-ammonium ratio on the growth, nutrition, and metabolism of sugarcane. Plant Physiology and Biochemistry 139: 246–255. https://doi.org/10.1016/j.plaphy.2019.03.024

Brochu AS, Durrivage J, Torres D, Pérez-López E. 2023. Diet and injection, important recommendations to characterize *Clavibacter michiganensis*-tomato interactions. Plant Health Progress 24 (4): 475–481. https://doi.org/10.1094/php-04-23-0040-rs

Carreras-Sempere M, Caceres R, Viñas M, Biel C. 2021. Use of recovered struvite and ammonium nitrate in fertigation in tomato (*Lycopersicum esculentum*) production for boosting circular and sustainable horticulture. Agriculture 11 (11): 1063. https://doi.org/10.3390/agriculture11111063

Chalupowicz L, Barash I, Reuven M, Dror O, Sharabani G, Gartemann KH, Eichenlaub R, Sessa G, Manuli-Sasson S. 2016. Differential contribution of *Clavibacter michiganensis* ssp. *michiganensis* virulence factors to systemic and local infection in tomato. Molecular Plant Pathology 18 (3): 336–346. https://doi.org/10.1111/mpp.12400

Dame ZT, Rahman M, Islam T. 2021. Bacilli as sources of agrobiotechnology: Recent advances and future directions. Green Chemistry Letters and Reviews 14 (2): 246–271. https://doi.org/10.1080/17518253.2021.1905080

Ding S, Shao X, Li J, Ahammed GJ, Ya Y, Ding J, Hu Z, Yu J, Shi K. 2021. Nitrogen forms and metabolism affect plant defense to foliar and root pathogens in tomato. Plant Cell and Environment 44 (5): 1596–1610. https://doi.org/10.1111/pce.14019

DOF (Diario Oficial de la Federación). 1982. Norma Mexicana NMX-F-009-1982. Productos alimenticios no industrializados, para uso humano–fruta fresca–determinación del tamaño en base al diámetro ecuatorial. Pliego de condiciones para el uso de la marca oficial México calidad suprema en tomate. Gobierno de México. Secretaría de Agricultura, Ganadería, Desarrollo Rural, Pesca, y Alimentación. Ciudad de México, México.

González-Hernández AI, Fernández-Crespo E, Scalschi L, Hajirezaei MR, von Wirén N, García-Agustín P, Camañes G. 2019. Ammonium mediated changes in carbon and nitrogen metabolisms induce resistance against *Pseudomonas syringae* in tomato plants. Journal of Plant Physiology 239: 28–37. https://doi.org/10.1016/j.jplph.2019.05.009

Gupta KJ, Brotman Y, Segu S, Zeier T, Zeier J, Persijn ST, Cristescus SM, Harren FJM, Bauwe H, Fernie AR, Kaiser WM, Mur LAJ. 2013. The form of nitrogen nutrition affects resistance against *Pseudomonas syringae* pv. *phaseolicola* in tobacco. Journal of Experimental Botany 64 (2): 553–568. https://doi.org/10.1093/jxb/ers348

Howard H, Häfner A, Karlowsky F, Schwarz SD, Krause A. 2021. Correction to: Evaluating recycling fertilizers for tomato cultivation in hydroponics, and their impact on greenhouse gas emissions. Environmental Science and Pollution Research 28 (42): 59304. https://doi.org/10.1007/s11356-020-11460-1

Kolomiiets Y, Grygoryuk I, Likhanov A, Butsenko L, Blume Y. 2020. Induction of bacterial canker resistance in tomato plants using plant growth promoting rhizobacteria. The Open Agriculture Journal 13 (1): 215–222. https://doi.org/10.2174/1874331501913010215

Lahlali R, Ezrari S, Radouane N, Kenfaoui J, Esmaeel Q, El Hamss H, Belabess Z, Barka EA. 2022. Biological control of plant pathogens: A global perspective. Microorganisms 10 (3): 596. https://doi.org/10.3390/microorganisms10030596

Li Z, Liu J, Ma W, Li, X. 2023. Characteristics, roles and applications of proteinaceous elicitors from pathogens in plant immunity. Life 13 (2): 268. https://doi.org/10.3390/life13020268

Liu Y, Zhou X, Liu W, Huang J, Liu Q, Sun J, Cai X, Miao W. 2020. HpaXpm, a novel Harpin of *Xanthomonas phaseoli* pv. *manihotis*, acts as an elicitor with high thermal stability, reduces disease, and promotes plant growth. BMC Microbiology 20 (1): 4. https://doi.org/10.1186/s12866-019-1691-4

Mahapatra S, Yadav R, Ramakrishna W. 2022. *Bacillus subtilis* impact on plant growth, soil health and environment. Journal of Applied Microbiology 132 (5): 3543–3562. https://doi.org/10.1111/jam.15480

Mur LAJ, Simpson C, Kumari A, Gupta AK, Gupta KJ. 2017. Moving nitrogen to the centre of plant defence against pathogens. Annals of Botany 119 (5): 703–709. https://doi.org/10.1093/aob/mcw179

Nandi M, Macdonald J, Liu P, Weselowski B, Yuan ZC. 2018. *Clavibacter michiganensis* ssp. *michiganensis*: Bacterial canker of tomato, molecular interactions and disease management. Molecular Plant Pathology 19 (8): 2036–2050. https://doi.org/10.1111/mpp.12678

Nawarathna KKK, Dandeniya WS, Dharmakeerthi RS, Weerasinghe P. 2021. Vegetable crops prefer different ratios of ammonium-N and nitrate-N in the growth media. Tropical Agricultural Research 32 (1): 95–104. https://doi.org/10.4038/tar.v32i1.8445

Nazarov PA, Baleev DN, Ivanova MI, Sokolova LM, Karakozova MV. 2020. Infectious plant diseases: Etiology, current status, problems and prospects in plant protection. Acta Naturae 12 (3): 46–59. https://doi.org/10.32607/actanaturae.11026

Planchet E. 2022. Nitric oxide production mediated by nitrate reductase in plants. *In* Nitric Oxide in Plant Biology. Academic Press: Cambridge, MA, USA, pp: 111–138. https://doi.org/10.1016/b978-0-12-818797-5.00001-7

Rajwade JM, Chikte RG, Paknikar KM. 2020. Nanomaterials: New weapons in a crusade against phytopathogens. Applied Microbiology and Biotechnology 104 (4): 1437–1461. https://doi.org/10.1007/s00253-019-10334-y

Rivera-Espejel EA, Sandoval-Villa M, Rodríguez-Mendoza MN, Trejo-López C, Gasga-Peña R. 2014. Fertilización de tomate con nitrato y amonio en raíces separadas en hidroponía. Revista Chapingo Serie Horticultura 20 (1): 57–70. https://doi.org/10.5154/r.rchsh.2012.12.069

Rivera-Sosa LM, Ramírez-Valverde G, Martínez-Yáñez B, Judith-Hernández A, Aranda-Ocampo S. 2022. Response of tomato (*Solanum lycopersicum*) varieties to *Clavibacter michiganensis* subsp. *michiganensis* infection. Mexican Journal of Phytopathology 40 (1): 18–39. https://doi.org/10.18781/r.mex.fit.2106-8

Sedighian N, Guineheux A, van der Wolf J, Déziel E. 2025. Ecofriendly control strategies against *Clavibacter michiganensis*, the causal agent of bacterial canker of tomato. *In* Plant Disease. The American Phytopathological Society: St. Paul, MN, USA. https://doi.org/10.1094/pdis-09-24-1931-fe

Sheikh TMM, Haider MS, Hanif A, Ali H, Khan AR, Li P, Zubair M, Farzand A, Tariq L, Ouyang X, Dong H, Zhang M. 2022. N-terminal HrpE from *Xanthomonas oryzae* pv. *oryzae* mediates the regulation of growth and photosynthesis in rice. Plant Growth Regulation 96 (3): 383–396. https://doi.org/10.1007/s10725-021-00790-w

Song Z, Liu Q, Guo H, Ju R, Zhao Y, Li J, Liu X. 2012. Tostadin, a novel antibacterial peptide from an antagonistic microorganism *Brevibacillus brevis* XDH. Bioresource Technology 111: 504–506. https://doi.org/10.1016/j.biortech.2012.02.051

Tiwari S, Prasad V, Lata C. 2019. *Bacillus*: Plant growth promoting bacteria for sustainable agriculture and environment. *In* New and Future Developments in Microbial Biotechnology and Bioengineering. Academic Press: Cambridge, MA, USA, pp: 43–55. https://doi.org/10.1016/b978-0-444-64191-5.00003-1

Wang H, Yan X, Guo L, Zen H, Qiu D. 2015. PeBL1, a novel protein elicitor from *Brevibacillus laterosporus* strain A60, activates defense responses and systemic resistance in *Nicotiana benthamiana*. Applied and Environmental Microbiology 81 (8): 2706–2716. https://doi.org/10.1128/aem.03586-14

Yuan X, Yu M, Yang CH. 2020. Innovation and application of the type III secretion system inhibitors in plant pathogenic bacteria. Microorganisms 8 (12): 1956. https://doi.org/10.3390/microorganisms8121956

Zhang Y, Yan X, Guo H, Zhao F, Huang L. 2018. A novel protein elicitor BAR11 from *Saccharothrix yanglingensis* Hhs.015 improves plant resistance to pathogens and interacts with catalases as targets. Frontiers in Microbiology 9: 700. https://doi.org/10.3389/fmicb.2018.00700

Zimerman-Lax N, Shenker M, Tamir-Ariel D, Perl-Treves R, Burdman S. 2016. Effects of nitrogen nutrition on disease development caused by *Acidovorax citrulli* on melon foliage. European Journal of Plant Pathology 145 (1): 125–137. https://doi.org/10.1007/s10658-015-0822-5

Agrociencia

FARMERS' AWARENESS OF DESERTIFICATION CAUSES IN AL-AFLAJ, SAUDI ARABIA

Bader Alhafi **Alotaibi***, Khalid **Alshabr,** Muhammad **Muddassir**

Department of Agricultural Extension and Rural Society. College of Food and Agriculture Science. King Saud University. Riyadh 11451, Saudi Arabia.
*Corresponding author: balhafi@ksu.edu.sa

Citation: Alotaibi BA, Alshabr K, Muddassir M. 2025. Farmers' awareness of desertification causes in Al-Aflaj, Saudi Arabia. **Agrociencia** 59(6): 884-898. https://doi.org/ 10.47163/agrociencia.v59i6.3453

Editor in Chief:
Dr. Fernando C. Gómez Merino

Received: March 19, 2025.
Approved: September 02, 2025.
Published in Agrociencia: September 10, 2025.

ABSTRACT

Desertification leads to land degradation, yield reduction, biodiversity loss, poverty, hunger, and adverse effects on the natural environment. Saudi Arabia has a desert climate, with some parts of the country, particularly in the southwest, maintaining semi-arid conditions. The current study aimed to understand farmers' awareness about desertification causes in Saudi Arabia. This knowledge is essential for designing and implementing effective interventions that promote sustainable agricultural practices to combat desertification. Data were collected from farmers in the Al-Aflaj governorate in Saudi Arabia, using a simple random sampling technique with the help of a pre-tested paper-based questionnaire. The findings showed that the majority of the farmers were highly aware of the causes of desertification. Farmers' age, education level, residence, and access to agricultural extension information all had a significant impact on their awareness of the causes of desertification. The study suggests that extension education programs, with the active participation of the ecology department, should be implemented to raise farmer awareness. Furthermore, the government must facilitate the adoption of sustainable agricultural practices and innovative measures to combat desertification.

Keywords: awareness, desertification, climate change.

INTRODUCTION

Desertification is an environmental problem in arid and semi-arid regions worldwide that has a negative impact on environmental sustainability. It is primarily driven by natural forces like wind erosion, human activities, urbanization, and food scarcity (Amin and Seif, 2019). Desertification is aggravated by soil salinity, vegetation cover removal, sand encroachment, urbanization, and eolian processes, all of which have a negative impact on the environment and socioeconomic development (Aldakheel, 2011; Allbed *et al.*, 2014; Alqarni *et al.*, 2018; Almadini and Hassaballa, 2019). Furthermore, climate change, land mismanagement, extreme grazing, and deforestation accelerate desertification.

Desertification can be mitigated through the adoption of sustainable practices such as high-carbon input techniques, the use of modern crop varieties, crop rotation, cover cropping, perennial cropping systems, integrated production approaches, crop

diversification, and agricultural biotechnology. Additional measures include balanced fertilizer application, precision nutrient management, reduced tillage intensity, and innovative water management strategies for both the drainage of waterlogged mineral soils and the irrigation of crops in arid and semi-arid regions (Smith *et al.,* 2020).

The global climate is experiencing several transformations, including rising temperatures, increased levels of carbon emissions, instabilities in ultraviolet radiation, and unpredictable changes in rainfall patterns caused by extreme weather events (Raza *et al.,* 2024). Saudi Arabia is highly vulnerable to climate change due to its arid climate and limited precipitation. Climate change poses a major challenge to sustainable agriculture and exacerbates food insecurity in the country. Increasing climate variability further intensifies drought and desertification, leading to reduced crop yields and heightened risks of food insecurity (Alotaibi *et al.,* 2023; Hasan *et al*., 2023). High temperatures could increase water loss through evapotranspiration by 10.3–27.4 % and alter the rainfall pattern for the northern regions (Ulllah *et al.,* 2024).

Saudi Arabia is the largest country in the Middle East, with a total area of approximately 2.25 million km^2. It encompasses various natural features, including mountains, plateaus, plains, valleys, and sand dunes. The country is predominantly characterized by an arid to semi-arid climate, with over 90 % of its territory classified as desert land. Furthermore, approximately 7 % of its land is highly vulnerable to desertification, posing significant threats to ecosystems and agricultural productivity, particularly by limiting plant growth (Abahussain *et al.,* 2002). In 2013, Saudi Arabia used more than 4.252 million ha of agricultural land, with 694 549 ha designated as invested agricultural lands and 3.558 million ha as non-invested lands. However, by 2018, the total cultivated area had decreased to 994 815 ha (MEWA, 2018).

The ongoing demand for water resources has accelerated desertification in Saudi Arabia, where the lack of perennial surface water requires dependency on groundwater for irrigation (Abahussain *et al*., 2002). Several villages are already experiencing desertification, while many others remain at high risk. The Al-Aflaj governorate, bordered by the Al Dahna and Rub' al-Khali deserts, is particularly vulnerable to desertification (Salih *et al.,* 2021) due to below-average rainfall in recent years. To address these challenges, soil scientists recommend strategies such as diversifying agricultural fertilizers and implementing careful irrigation management, which may help mitigate the adverse effects of desertification in the area (Al-Dosary, 2022).

Agricultural extensionists, who collaborate with farming societies at the local level, suggest that the dissemination of eco-friendly technologies in climate-prone regions of Saudi Arabia could minimize climate-related effects on agriculture (Alotaibi *et al.,* 2023). Innovative information dissemination to farmers is one of the primary goals of agricultural advisory services (Gao *et al.,* 2021). In many developing countries, the agricultural extension department is increasing awareness and adoption of sustainable agricultural practices that could mitigate climate effects and desert conditions (Ashraf *et al*., 2017; Raza *et al*., 2020).

Mitigation and control of desertification depend on key strategies, including sustainable agricultural and grazing practices, enhanced water management, and forest cultivation (Zhang and Huisingh, 2018). However, the effective implementation of these strategies requires evaluating farmer awareness of desertification causes, as low levels of awareness can hinder adoption and reduce their overall effectiveness. Although numerous studies have explored the biophysical aspects of desertification, there remains a notable gap in social research focusing on farmers' awareness of desertification causes.

The present study aims to analyze farmers' awareness of desertification causes in Al-Aflaj, Saudi Arabia. This could help with the development of policy and awareness programs that encourage the use of more sustainable practices to combat desertification. Awareness was assessed in relation to their socioeconomic characteristics, leading to the formulation of the following hypotheses: H1: Age, education, residence, occupation, farming experience, land tenure, and farm size influence farmers' awareness of desertification causes; H2: Information received from the agricultural extension department regarding desertification affects farmers' awareness.

MATERIALS AND METHODS

Description of the study area

The Al-Aflaj governorate is located in the southern part of the Najd Plateau, approximately 312 km from Riyadh. It is bounded to the west by the Tuwaiq Escarpment, the Al Dahna Desert to the east, Al-Kharj Province and Wadi Birk to the north, and Wadi Al Dawasir Province and the Al-Rub Al-Khali Desert to the south. The terrain transitions from plains in the east and forms plateaus along the western flank, adjacent to the Tuwaiq Escarpment. The region has natural water resources, including aquifers and deep groundwater in Al Minjur, Al Biyadh, and Al Wasia (Al-Dosary, 2022).

The land is arable and classified as appropriate for agricultural investments, with the majority of the population involved in farming. The area is ideal for seasonal grass, with approximately 30 % of the total land under cultivation. Major crops grown include wheat, barley, forage crops, vegetables, and a variety of seasonal fruits. Irrigation practices in Al-Aflaj primarily rely on drip systems, surface irrigation, and center-pivot irrigation (MEWA, 2018).

Research design and instrument development

The Al-Aflaj governorate was specifically selected due to its extensive agriculture (Al-Dosary, 2022). A simple random sampling technique was used to select 350 farmers from this region. Data was collected using a paper-based, structured questionnaire distributed to farmers in their native Arabic language. They were informed of the reason for the study and assured that the collected data would be used solely for

academic and research purposes. Out of the 350 farmers, 186 (82 %) returned the complete questionnaires, which were used for the final data analysis.

The questionnaire was reviewed and validated by a panel of researchers from the Department of Agricultural Extension and Rural Sociology at King Saud University, after which a pilot study was conducted to test the reliability of the Likert scale. Data were collected from 30 farmers, and Cronbach's alpha coefficient (α) was calculated to assess the internal consistency and reliability of the questionnaire (Bonett and Wright, 2015). A Cronbach's alpha value of 0.7 or higher is generally considered acceptable for further research (Cronbach, 1951; Schmitt, 1996). In this study, the coefficient was estimated at 0.79, indicating satisfactory reliability. Following these procedures, the field survey was carried out.

The questionnaire included three sections. The first focused on the socioeconomic characteristics of the respondents, including age, education, residence, occupation, farming experience, land tenure, farm size, and access to extension information on desertification, all measured on a nominal scale (0 = no; 1 = yes). Respondents' age was classified as young (18–42 years) or older (>42 years); education level as low (school) or high (college or university); farming experience as low (3–24 years) or high (>24 years); and farm size as small-scale (ownership of 2–240 ha) or large-scale (>240 ha).

The second section examined the irrigation systems used by farmers, distinguishing between drip irrigation, surface irrigation, and sprinkler systems, each measured on a nominal scale (0 = no; 1 = yes). The third section assessed farmers' awareness of the causes of desertification through a five-points Likert scale (1 = not aware at all; 2 = slightly aware; 3 = somewhat aware; 4 = moderately aware; 5 = extremely aware).

Data analysis

Data were analyzed using descriptive and inferential statistics. Socioeconomic characteristics were summarized with frequencies and percentages, while farmers' awareness of desertification causes was assessed using frequencies, means, and standard deviations. To determine differences in the farmers' awareness due to their personal demographics, parametric statistics were used. A principal component analysis (PCA) was used to reduce the dimensionality of large data sets. The Kaiser-Meyer-Olkin measure of sampling adequacy (KMO) was performed to measure the suitability of the survey response data. For the nominal variables with two categories (age, education level, farming experience, land tenure, residence, farm size, and source of information), the independent *t*-test was used. The Statistical Package for Social Sciences (SPSS version 28.0, IBM SPSS Statistics) was used for running the data analysis.

RESULTS AND DISCUSSION

Regarding age, the findings revealed that most of the respondents (52.2 %) were older, while 48 % were classified as young (18–42 years). In terms of education, the majority

(64.5 %) had a high level of education, holding a college degree or higher, whereas 36 % had only school-level education. Regarding residence, most of the respondents (59.1 %) lived in urban areas, while 41 % lived in rural areas. Most respondents (74 %) had limited farming experience, while 26 % had a high level of experience. Data showed that 83.3 % of respondents owned their agricultural land, whereas 16.7 % operated farms in partnership. Farm size distribution showed that 96 % managed small landholdings, while only 4.3 % cultivated large areas of 240 ha or more. Finally, in terms of access to information on desertification, the majority of respondents (83.3 %) did not seek advice from the Agricultural Extension Department, while only 16.7 % did on a regular basis (Table 1).

More than 70 % of the farmers used drip irrigation (Table 2). On the other hand, three-fifths used sprinkler irrigation, pivot sprinklers, or surface/flood irrigation systems on their farms.

Table 1. Frequency and percentage distribution of respondents' socioeconomic characteristics in Al-Aflaj, Saudi Arabia (n = 186).

Variables	Frequency (n)	Percentage
Age		
Young (18–42 years)	89	47.8
Older (>42 years)	97	52.2
Education		
Low (school degree)	66	35.5
High (college or university degree)	120	64.5
Residence		
Rural	76	40.9
Urban	110	59.1
Occupation		
Part time farming	155	83.3
Full time farming	31	16.7
Farming experience		
Low experience (3–24 years)	138	74.2
High experience (>24 years)	48	25.8
Land tenure		
Partnership	31	16.7
Ownership	155	83.3
Farm size		
Small scale farming (2–240 ha)	178	95.7
Large scale farming (>240 ha)	8	4.3
Information from the Agricultural Extension Department on desertification		
Does not receive information	155	83.3
Receives information	31	16.7

Table 2. Types and prevalence of irrigation systems used for agricultural purposes in Al-Aflaj, Saudi Arabia.

Irrigation systems	Yes (%)	No (%)
Drip irrigation	71	29
Sprinkler irrigation	17.2	82.8
Pivot sprinkler irrigation	22	78
Surface or flood irrigation	22.6	77.4

Farmers had relatively high awareness of the causes of desertification (Table 3). More than three-fifths extremely recognized high temperatures as a major driver, while half linked desertification to population growth, and 58.6 % identified creeping sand dunes as an important cause. In addition, over two-fifths showed strong awareness of other drivers, including land degradation (45.7 %), water depletion (48.7 %), lack of trees (48.9 %), the spread of unwanted weeds (41.4 %), bare sand accumulation (43.5 %), and tree cutting for firewood (40.9 %).

Table 3. Farmer awareness of the causes of desertification in Al-Aflaj, Saudi Arabia, expressed as percentages, mean scores, and standard deviations (SD) (n = 186).

Items	Not aware at all (%)	Slightly aware (%)	Somewhat aware (%)	Moderately aware (%)	Extremely aware (%)	Mean	SD
Creeping sand dunes	2.7	2.7	16.7	19.4	58.6	4.28	1.01
High temperatures	2.7	5.4	12.4	17.2	62.4	4.28	1.01
Lack of trees	4.8	10.8	15.1	20.4	48.9	3.98	1.23
Land degradation	5.4	9.1	16.1	23.7	45.7	3.95	1.21
Bare sand accumulation	5.9	10.8	16.7	23.1	43.5	3.88	1.24
Water depletion	10.2	8.1	16.7	16.7	48.4	3.85	1.37
Spread of unwanted weeds	5.4	10.8	18.3	24.2	41.4	3.85	1.22
Population growth	15.6	8.1	10.2	16.1	50.0	3.77	1.51
Increased number of animals for grazing	5.4	12.4	19.9	26.3	36.0	3.75	1.21
Increased irrigation	7.0	10.8	23.1	19.9	39.2	3.74	1.27
Soil exposure to gusts of wind	6.5	7.0	26.9	25.8	33.9	3.74	1.18
Low agricultural productivity	8.1	10.8	21.0	22.0	38.2	3.72	1.29
Increased water withdrawal	12.4	10.8	16.7	20.4	39.8	3.65	1.41
Vegetation cover removal	15.1	11.3	11.3	18.8	43.5	3.65	1.49
Tree cutting for firewood	15.1	9.7	14.5	19.9	40.9	3.62	1.47
Soil salinization	11.8	12.9	17.7	24.2	33.3	3.54	1.37
Lack of modern irrigation systems	10.8	13.4	21.5	25.3	29.0	3.48	1.32
Lack of rainfall	11.3	14.5	26.3	16.7	31.2	3.42	1.35
Soil erosion	10.2	11.8	32.8	19.4	25.8	3.39	1.26
Overgrazing	11.3	13.4	25.3	26.3	23.7	3.38	1.29
Presence of canyons and valleys	11.3	18.3	23.1	17.2	30.1	3.37	1.37
Overuse of fertilizers	9.1	19.9	28.0	22.0	21.0	3.26	1.25

Other contributing factors were also acknowledged, though to a slightly lesser extent (Table 3). More than 30 % of the farmers were extremely aware that low agricultural productivity, soil salinization, the presence of canyons and valleys, soil exposure to frequent gusts of wind, lack of rainfall, increased irrigation, increased number of animals for grazing, and increased water withdrawal can lead to desertification. In addition, less than 30 % of farmers were extremely aware that soil erosion, overgrazing, overuse of fertilizers, and lack of modern irrigation systems caused desertification. Less than 16 and 20 % were not aware at all and slightly aware about the causes of desertification, respectively. Less than 33 and 37 % were somewhat and moderately aware, respectively.

Results revealed that half of the farmers were extremely aware of the causes of desertification (Figure 1), while about two-fifths demonstrated moderate awareness. Fewer than 7 % reported having no awareness. Overall, the findings show that most respondents possessed a high level of awareness of the causes of desertification.

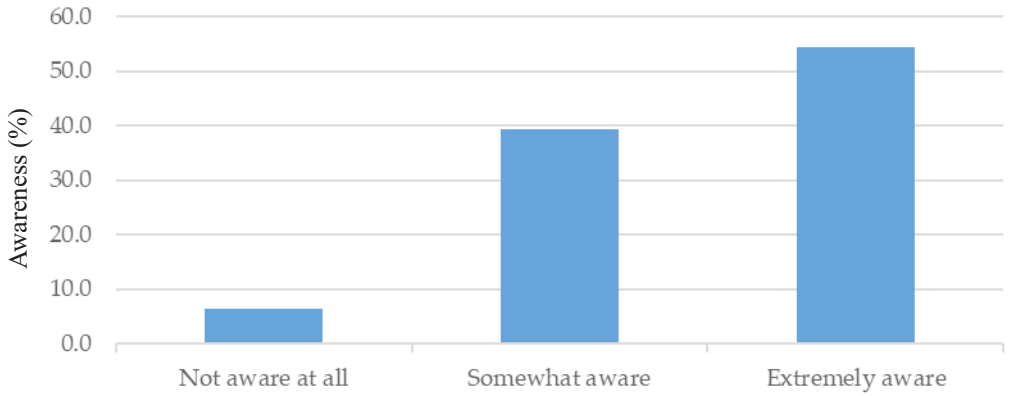

Figure 1. Overall farmer awareness levels of desertification in Al-Aflaj, Saudi Arabia.

These findings are consistent with Fekadu and Kumssa (2020), who reported that most farmers were highly aware of the causes of land degradation and desertification, citing factors such as population growth, over-tilling, soil erosion, rocky topography, poor agricultural practices, and poverty. Similarly, Owusu *et al*. (2024) found a high level of awareness among farmers in Ghana, which was attributed to agricultural extension programs, field demonstrations, and seminars that enhanced farmers' knowledge. In contrast, Yassin (2019) reported low awareness of desertification among Sudanese farmers, demonstrating the importance of awareness campaigns and technology transfer through active engagement of relevant institutions.

Higher awareness of the causes of desertification among farmers in the study area may be attributed to large-scale national and regional campaigns. The government of Saudi Arabia has actively communicated the severity of desertification as an environmental challenge for agriculture and land management. Several initiatives, including the

Saudi Green Initiative, the Green Riyadh Project, and the Middle East Green Initiative, have been launched to address this issue (UNDP, 2024). Additionally, the Ministry of Environment, Water, and Agriculture (MEWA) and the United Nations Convention to Combat Desertification (UNCCD) have organized workshops involving multiple stakeholders and experts to raise awareness (UNDP, 2024).

The Saudi Green Initiative has seen rapid progress at the community level, with villagers planting an estimated 250 000 trees and one million shrubs in desert areas. Furthermore, the Food and Agriculture Organization (FAO) and Saudi Arabia's National Center for Vegetation Development and Combating Desertification (NCVC) have provided technical guidance and remote training courses. The active participation of farming communities in these programs has likely played a crucial role in strengthening their awareness of the causes of desertification (UNDP, 2024; UNSDG, 2024).

To better understand farmers' awareness of desertification, specific factors were grouped using principal component analysis (PCA). Three factors were extracted, accounting for 60.8 % of the total variance (Table 4). Factor 1 includes human and

Table 4. Principal component analysis of farmers' awareness of desertification in Al-Aflaj, Saudi Arabia.

Items	Factor 1	Factor 2	Factor 3
	Explained variance		
	41.82 %	12.56 %	6.42 %
Land degradation		0.783	
Vegetation degradation		0.752	
Water depletion		0.819	
Low agricultural productivity		0.802	
Soil salinization		0.720	
Lack of trees		0.745	
Spread of unwanted weeds		0.760	
Bare sand accumulation		0.760	
Creeping sand dunes			0.755
High temperature			0.804
Soil erosion by torrential water	0.642		
Population growth	0.739		
Tree cutting for firewood	0.752		
Vegetation cover removal	0.761		
Overgrazing	0.631		
Overuse of fertilizers	0.616		
Increased irrigation	0.705		
Increased number of animals for grazing	0.780		
Increased water withdrawal from wells	0.831		
Lack of modern irrigation systems	0.797		

Factors explain 60.8 % of the variance. Kaiser-Meyer-Olkin measure of sampling adequacy (0.889), $p < 0.0001$).

agricultural pressures (10 items), which reflect anthropogenic drivers of desertification. Factor 2 (eight items) captures the ecological consequences of land misuse, while factor 3 (two items) represents natural and climate-related pressures.

Farmers' awareness according to their socioeconomic characteristics

Significant differences were observed according to age (t = -2.64, p < 0.001), education level (t = -5.23, p < 0.001), residence (t = 2.37, p = 0.01), and access to extension information (t = -2.23, p = 0.02). To assess the magnitude of these differences, effect sizes were calculated using Cohen's d (Table 5) (Lakens, 2013; Goulet-Pelletier and Cousineau, 2018).

Older farmers demonstrated higher awareness of desertification than younger farmers, although the mean difference indicated only a small effect (d = 0.38) (Table 5). It has been observed that the older the farmers are, the more agricultural experience they have and the better their ability to gain technical and meteorological knowledge

Table 5. Independent samples t-test results for differences in farmers' awareness of desertification by socioeconomic characteristics in Al-Aflaj, Saudi Arabia.

Variables	Mean	Standard deviation	t	p-value
		Age		
Young (n = 89)	32.25	7.56	-2.64	<0.001
Old (n = 97)	35.17	7.46		d = 0.38
		Education		
Low education (n = 66)	30.08	8.50	-5.23	<0.001
High education (n = 120)	35.80	6.27		d = 0.76
		Residence		
Rural (n = 76)	35.35	6.72	2.37	0.01
Urban (n = 110)	32.68	8.05		d = 0.36
		Farming experience		
Low experience (n = 138)	33.45	7.62	-0.98	0.32
High experience (n = 48)	34.70	7.67		
		Occupation		
Full time farming (n = 155)	33.88	7.78	0.42	0.67
Part time farming (n = 31)	33.24	6.95		
		Land tenure		
Partnership (n = 31)	32.27	6.85	-1.20	0.23
Ownership (n = 155)	34.07	7.76		
		Farm size		
Small scale farming (n = 178)	33.66	7.68	-0.96	0.33
Large scale farming (n = 8)	36.31	6.11		
		Information from extension about desertification		
No (n = 155)	33.22	7.76	-2.23	0.02
Yes (n = 31)	36.54	6.37		d = 0.46

of the causes of desertification. Older farmers seemed more inclined to adopt strategic measures against desertification (Tai *et al.,* 2020). Wei and Wang (2017) found that older farmers are usually responsible for their livelihood and have great ability to sense environmental risks such as climate change and desertification (Alotaibi *et al.,* 2020, 2024).

Highly educated farmers demonstrated significantly greater awareness of desertification than those with lower education (Table 5), with the difference in means reflecting a large effect (d = 0.76). This may be attributed to their greater access to diverse sources of information, such as scientific publications, magazines, and news articles, which facilitate continuous information updates (Geeson *et al*., 2015). In addition, MEWA has distributed more than 230 000 specialized educational materials during various agricultural events, covering topics such as logging and desertification, modern irrigation systems, red palm weevil control, fertilization, and the conservation of coral reefs and mangrove ecosystems (MEWA, 2024). Such initiatives may help explain the higher awareness levels among highly educated farmers compared to their less educated counterparts.

Educated farmers are more likely to participate in training programs and workshops related to desertification. Previous studies have shown that they also access information through multiple channels, including newspapers and magazines, which further enhances their knowledge base (Geeson *et al*., 2015; Mashi *et al*., 2022). Furthermore, highly educated respondents to this study reported significant agricultural production losses due to desertification, recounting experiences with land degradation, climate change, and drought. They also appeared more proactive in adopting nature-based solutions, such as tree planting and vegetation restoration, to rehabilitate degraded land.

Farmers residing in rural areas demonstrated relatively higher awareness of desertification compared to those living in urban areas (Table 5). Although the mean difference represented only a small effect (d = 0.36), this finding is understandable. Farmers who spend more time in rural environments often develop a deeper understanding of the interactions between humans and nature, the value of natural ecosystems, and the importance of environmental protection. Since most rural populations are directly engaged in agriculture, desertification-related projects and initiatives often target these communities. Rural communities also tend to participate more actively in discussions with development agencies and in training programs designed to enhance environmental knowledge (Chao *et al*., 2019).

Several initiatives illustrate the importance of community participation in combating desertification. For instance, the Ghana Environmental Management Project (GEMP) particularly aimed to strengthen institutions and empower rural communities to address desertification (Fuseini, 2014). In Saudi Arabia, the NCVC, in collaboration with FAO, organized a training course on climate change and desertification in 2022. These programs encouraged participants to discuss local conditions and challenges, thereby improving awareness and adaptive capacity. Farmers in the study area

may benefit from such opportunities by engaging in workshops and community discussions, which likely contributed to their relatively higher awareness levels (UN, 2022).

Farmers who received information about desertification from the extension department demonstrated higher awareness than those who did not (Table 5), with the difference in means reflecting a small effect (d = 0.46). Extension activities serve as important channels for technology transfer and the dissemination of innovative practices that enhance farmers' awareness and knowledge of environmental challenges (Alzahrani *et al*., 2023; Muddassir and Alotaibi, 2023).

Between 2015 and 2016, MEWA organized a wide range of activities to raise awareness of desertification and promote sustainable agronomic practices. These included 99 pilot fields, 23 public events, an agricultural extension forum, 175 extension lectures, 159 tours and field visits, and 69 extension meetings (MEWA, 2024). Furthermore, the Center for Desert Agriculture (CDA) at King Abdullah University of Science and Technology (KAUST), in collaboration with the NCVC, established the KAUST-NCVC Experiment Station and Ecological Observatory (KNESEO), which serves as a hub for agricultural and environmental research by providing experimental stations, infrastructure, technical expertise, and extension services. By granting access to advanced research and training, the center strengthens awareness of desertification, ecological conservation, water management, and sustainable food production (CDA, 2024).

The Saudi Green Initiative and KNESEO may encourage agricultural extension departments to provide more targeted training for farmers on the causes of desertification and eco-friendly practices. Active participation in extension activities, such as lectures, tours, field visits, and meetings, has the potential to significantly improve farmers' awareness of desertification drivers (Dabiah *et al*., 2023). Similar efforts have been observed in other regions. For example, the European Parliament has promoted awareness of desertification and sustainable agriculture through awareness-raising campaigns (Rossi, 2020).

The present study contributes to the existing literature in several ways. First, it provides empirical insights into farmers' awareness of the causes of desertification in the study area, offering a deeper understanding of how awareness levels differ across socio-economic characteristics. Second, the findings highlight the importance of establishing mechanisms through which agricultural departments and environmental agencies can design effective educational programs, training initiatives, and informational materials to promote sustainable agricultural practices as a means against desertification.

CONCLUSIONS

This study found that the majority of farmers in Al-Aflaj, Saudi Arabia, were aware of the causes of desertification. Farmers who belonged to older age groups, had higher education, resided in rural areas, and received information from agricultural

extension departments had a better understanding of the causes of desertification. The findings may have various policy implications. Agricultural extension services play an important role in raising awareness and promoting sustainable practices, emphasizing the need for stronger collaboration between government agencies and environmental institutions. Awareness can be further strengthened through targeted seminars, workshops, and training programs, as well as mass media campaigns, such as radio, television, and local newspapers, that communicate both the risks of desertification and the benefits of eco-friendly agricultural practices.

The study has some limitations. Since the sample was restricted to the Al-Aflaj governorate, the findings may not be representative of all farming regions in Saudi Arabia. Future research should be done in order to measure awareness and the adoption of sustainable practices in other areas, particularly those most vulnerable to desertification in Saudi Arabia, to provide broader evidence for national strategies aimed at environmental sustainability.

ACKNOWLEDGEMENTS

The authors declare financial support was received for the research, authorship, and/or publication of this article. This research was funded by the Ongoing Research Funding Program (ORF-2025-443), King Saud University, Riyadh, Saudi Arabia.

REFERENCES

Abahussain AA, Abdu AS, Al-Zubari WK, El-Deen NA, Abdul-Raheem M. 2002. Desertification in the Arab Region: Analysis of current status and trends. Journal of Arid Environments 51 (4): 521–545. https://doi.org/10.1006/jare.2002.0975

Aldakheel YY. 2011. Assessing NDVI spatial pattern as related to irrigation and soil salinity management in Al-Hassa Oasis, Saudi Arabia. Journal of the Indian Society of Remote Sensing 39 (2): 171–180. https://doi.org/10.1007/s12524-010-0057-z

Al-Dosary NMN. 2022. Evaluation of soil characteristics for agricultural machinery management and cropping requirements in Al-Aflaj Oasis, Saudi Arabia. Sustainability 14 (13): 7991. https://doi.org/10.3390/su14137991

Allbed A, Kumar L, Aldakheel YY. 2014. Assessing soil salinity using soil salinity and vegetation indices derived from IKONOS high-spatial resolution imageries: Applications in a date palm dominated region. Geoderma 230: 1–8. https://doi.org/10.1016/j.geoderma.2014.03.025

Almadini AM, Hassaballa AA. 2019. Depicting changes in land surface cover at Al-Hassa oasis of Saudi Arabia using remote sensing and GIS techniques. PLoS One 14 (11): e0221115. https://doi.org/10.1371/journal.pone.0221115

Alotaibi BA, Abbas A, Ullah R, Azeem MI, Samie A, Muddassir M, Dabiah AT, Raid M, Sadaf T. 2023. Dynamics and determinants of farmers' perceptions about causes and impacts of climate change on agriculture in Saudi Arabia: Implications for adaptation, mitigation, and sustainability. Atmosphere 14 (6): 917. https://doi.org/10.3390/atmos14060917

Alotaibi BA, Kassem HS, Nayak RK, Muddassir M. 2020. Farmers' beliefs and concerns about climate change: An assessment from southern Saudi Arabia. Agriculture 10 (7): 253. https://doi.org/10.3390/agriculture10070253

Alotaibi BA, Xu W, Shah AA, Ullah W. 2024. Exploring climate-induced agricultural risk in Saudi Arabia: Evidence from farming communities of Medina region. Sustainability 16 (10): 4245. https://doi.org/10.3390/su16104245

Alqarni S, Babiker A, Salih A. 2018. Detection, mapping and assessment change in urban and croplands area in Al-Hassa Oasis, eastern region in Saudi Arabia using remote sensing and geographic information system. Journal of Geographic Information System 10 (6): 659–685. https://doi.org/10.4236/jgis.2018.106034

Alzahrani K, Ali M, Azeem MI, Alotaibi BA. 2023. Efficacy of public extension and advisory services for sustainable rice production. Agriculture 13 (5): 1062. https://doi.org/10.3390/agriculture13051062

Amin A, Seif ESSA. 2019. Environmental hazards of sand dunes, South Jeddah, Saudi Arabia: An assessment and mitigation geotechnical study. Earth Systems and Environment 3 (2): 173–188. https://doi.org/10.1007/s41748-019-00100-5

Ashraf I, Khatam A, Mehmood CK, Saghir A, Hassan G. 2017. Effects of devolution on efficiency of agricultural extension in Khyber Pakhtunkhwa, Pakistan. Pakistan Journal of Agricultural Sciences 54 (4): 953–957. https://doi.org/10.21162/pakjas/17.5955

Bonett DG, Wright TA. 2015. Cronbach's alpha reliability: Interval estimation, hypothesis testing, and sample size planning. Journal of Organizational Behavior 36 (1): 3–15. https://doi.org/10.1002/job.1960

CDA (Center for Desert Agriculture). 2024. KAUST-NCVC Experiment Station and Ecological Observatory at Wadi Qadid National Park (KNESEO). King Abdullah University of Science and Technology. Thuwal, Saudi Arabia. https://cda.kaust.edu.sa/outreach-extension/kneseo (Retrieved: March 2025).

Chao W, Zhang C, Wang P. 2019. Urban and rural residents' willingness to pay for desertification prevention and control and its influencing factors. Nature Environment and Pollution Technology 18 (3): 935–940.

Cronbach LJ. 1951. Coefficient alpha and the internal structure of tests. Psychometrika 16 (3): 297–334. https://doi.org/10.1007/bf02310555

Dabiah AT, Alotibi YS, Herab AH. 2023. Attitudes of agricultural extension workers toward the use of electronic extension methods in agricultural extension in the Kingdom of Saudi Arabia. International Journal of Agriculture and Biosciences 12 (2): 104–109. https://doi.org/10.47278/journal.ijab/2023.050

Fekadu G, Kumssa T. 2020. Assessment of farmers perceptions on land degradation and desertification and its impact on wildlife in Dhera district, Oromia, Ethiopia. Journal of Entomology and Zoology Studies 8 (3): 970–974.

Fuseini O. 2014. Combating desertification in the Bawku West District of Ghana: Farmers' perception of desertification and project interventions. United Nations University. Land Restoration Training Programme Keldnaholt. Reykjavik, Iceland. 30 p.

Gao Q, Qiao J, Dong G, Yao Y. 2021. Organizational proximity, collaboration propensity, and cooperative performances: The case of Cooperative Agricultural Extension in China. Pakistan Journal of Agricultural Sciences 58 (1): 7–17.

Geeson N, Quaranta G, Salvia R, Brandt J. 2015. Long-term involvement of stakeholders in research projects on desertification and land degradation: How has their perception of the issues changed and what strategies have emerged for combating desertification? Journal of Arid Environments 114 (3): 124–133. https://doi.org/10.1016/j.jaridenv.2014.12.002

Goulet-Pelletier JC, Cousineau D. 2018. A review of effect sizes and their confidence intervals, Part I: The Cohen'sd family. The Quantitative Methods for Psychology 14 (4): 242-265. 10.20982/tqmp.14.4.p242

Hasan S, Abedullah, Kouser S. 2023. Economic evaluation of household firewood consumption and carbon footprints in Pakistan: Implication for climate change mitigations. Pakistan Journal of Agricultural Sciences 60 (4): 527–536. https://doi.org/10.21162/pakjas/23.77

Lakens D. 2013. Calculating and reporting effect sizes to facilitate cumulative science: a practical primer for t-tests and ANOVAs. Frontiers in psychology 4: 863. https://doi.org/10.3389/fpsyg.2013.00863

Mashi SA, Inkani AI, Oghenejabor OD. 2022. Determinants of awareness levels of climate smart agricultural technologies and practices of urban farmers in Kuje, Abuja, Nigeria. Technology in Society 70: 102030. https://doi.org/10.1016/j.techsoc.2022.102030

MEWA (Ministry of Environment, Water, and Agriculture). 2018. Statistical reports. Agriculture statistical year book. Government of the Kingdom of Saudi Arabia. Ministry of Environment, Water, and Agriculture. Riyadh, Saudi Arabia. https://www.mewa.gov.sa/ar/InformationCenter/Researchs/Reports/Pages/default.aspx (Retrieved: March 2025).

MEWA (Ministry of Environment, Water, and Agriculture). 2024. General Directorate of Agricultural Extension. Government of the Kingdom of Saudi Arabia. Ministry of Environment, Water, and Agriculture. Riyadh, Saudi Arabia https://www.mewa.gov.sa/en/Ministry/Agencies/AgencyofAgriculture/Departments/Pages/The%20Seeds%20Center.aspx (Retrieved: March 2025).

Muddassir M, Alotaibi BA. 2023. Farmers' awareness of improved maize cropping practices in Punjab, Pakistan. International Journal of Agriculture and Biosciences 12 (1): 8–17. https://doi.org/10.47278/journal.ijab/2022.039

Owusu AB, Fynn IEM, Adu-Boahen K, Kwang C, Mensah CA, Atugbiga JA. 2024. Rate of desertification, climate change and coping strategies: Insights from smallholder farmers in Ghana's Upper East Region. Environmental and Sustainability Indicators 23: 100433. https://doi.org/10.1016/j.indic.2024.100433

Raza A, Hassan A, Abbas S, Razzaq W, Hazoor S, Nosherwan M, Rehman A, Ali I. 2024. Effects of salinity on morpho-physiological traits in six maize hybrids at seedling stage. Agrobiological Records 18: 41–53. https://doi.org/10.47278/journal.abr/2024.036

Raza HA, Amir RM, Saghir A, Tahir M. 2020. Sugarcane production and protection constraints faced by the growers of Punjab, Pakistan with special focus on the role of agricultural extension worker in related mitigation. Pakistan Journal of Agricultural Sciences 57 (6): 1681–1688.

Rossi R. 2020. Desertification and agriculture. European Parliamentary Research Service. European Union. Brussels, Belgium. 12 p.

Salih A, Hassaballa AA, Ganawa E. 2021. Mapping desertification degree and assessing its severity in Al-Ahsa Oasis, Saudi Arabia, using remote sensing-based indicators. Arabian Journal of Geosciences 14 (3). https://doi.org/10.1007/s12517-021-06523-7

Schmitt N. 1996. Uses and abuses of coefficient alpha. Psychological Assessment 8 (4): 350–353. https://doi.org/10.1037//1040-3590.8.4.350

Smith P, Calvin K, Nkem J, Campbell D, Cherubini F, Grassi G, Korotkov V, Le Hoang A, Lwasa S, McElwee P, *et al*. 2020. Which practices co-deliver food security, climate change mitigation and adaptation, and combat land degradation and desertification? Global Change Biology 26 (3): 1532–1575. https://doi.org/10.1111/gcb.14878

Tai X, Lu L, Jiang Q, Chang D. 2020. The perception of desertification, its social impact and the adaptive strategies of ecological migrants in the desertification area, China. Chinese Journal of Population, Resources and Environment 18 (4): 324–330. https://doi.org/10.1016/j.cjpre.2020.05.001

Ulllah MI, Alsanhani A, Aldawdahi N. 2024. Farmer's perception of climate change: An assessment from Medina region, Saudi Arabia. Agrobiological Records 18: 12–17. https://doi.org/10.47278/journal.abr/2024.033

UN (United Nations). 2022. FAO conducts training to strengthening Saudi Forest and climate change action. United Nations Saudi Arabia. Riyadh, Saudi Arabia. https://saudiarabia.un.org/en/198797-fao-conducts-training-strengthening-saudi-forest-and-climate-change-action (Retrieved: March 2025).

UNDP (United Nations Development Programme). 2024. UNDP Saudi Arabia actively participates in the fight against desertification. New York, NY, USA. https://www.undp.org/saudi-arabia/press-releases/undp-saudi-arabia-actively-participates-fight-against-desertification (Retrieved: March 2025).

UNSDG (United Nations Sustainable Development Group). 2024. United for land: Saudi Arabia's local heroes combat desertification. New York, NY, USA. https://unsdg.un.org/latest/stories/united-land-saudi-arabias-local-heroes-combat-desertification (Retrieved: March 2025).

Wei HL, Wang GY. 2017. Analysis of correlation between the characteristics of farmers and their perceived risk of environmental disasters in desertification area—from the perspective of environmental justice. Journal of Natural Resources 32 (7): 1134–1144. https://doi.org/10.11849/zrzyxb.20160674

Yassin L. 2019. Combating desertification: Awareness, national mitigation and innovation. InfoNile. Kampala, Uganda. https://infonile.org/en/2019/03/combating-desertification-awareness-national-mitigation-innovation-2/ (Retrieved: March 2025).

Zhang Z, Huisingh D. 2018. Combating desertification in China: Monitoring, control, management and revegetation. Journal of Cleaner Production 182: 765–775. https://doi.org/10.1016/j.jclepro.2018.01.233

Agrociencia

IMPACT OF CLIMATE CHANGE ON MAIZE (*Zea mays* L.) PLANTING DATES IN THE EASTERN REGION OF PUEBLA, MEXICO

Rogelio **Bernal-Morales**[1], José Pedro **Juárez-Sánchez**[1*], Benito **Ramírez-Valverde**[1], Ignacio **Ocampo-Fletes**[1], María de los Ángeles **Velasco-Hernández**[2]

[1]Colegio de Postgraduados Campus Puebla. Boulevard Forjadores de Puebla 205, Santiago Momoxpan, San Pedro Cholula, Puebla, Mexico. C. P. 72760.
[2]Benemérita Universidad Autónoma de Puebla. Instituto de Ciencias. Boulevard Valsequillo y Avenida San Claudio, Edificio 112, Ciudad Universitaria, Colonia Jardines de San Manuel, Heroica Puebla de Zaragoza, Puebla, Mexico. C. P. 72570.
* Author for correspondence: pjuarez@colpos.mx

Citation: Bernal-Morales R, Juárez-Sánchez JP, Valverde-Ramírez B, Ocampo-Fletes I, Velasco-Hernández MA. 2025. Impact of climate change on maize (*Zea mays* L.) planting dates in the eastern region of Puebla, Mexico. **Agrociencia** 59(6): 899-914. https://doi.org/ 10.47163/agrociencia.v59i6.3311

Editor in Chief:
Dr. Fernando C. Gómez Merino

Received: April 23, 2025.
Approved: August 08, 2025.
Published in Agrociencia: August 12, 2025.

ABSTRACT

Climate change affects crop production, resulting in economic losses. One of the most significant changes caused by this phenomenon is a shift in the optimal planting date, so it is important to identify the optimal planting dates under the new climatic patterns, or at least appropriate ones that allow the selection of the indicated maize (*Zea mays* L.) variety (for example, short, intermediate, or late cycle genotype) that would be best to plant in order to obtain higher yields. Therefore, this research hypothesized that climate change would lead to shifts in the planting dates of rainfed maize. The objective was to assess the impact of climate change on planting dates in the eastern region of Puebla, Mexico. For this purpose, daily precipitation (PCP), as well as maximum and minimum temperature data from 13 climatological stations covering the period 1961–2020, were analyzed. Data quality was assessed using RClimDex software, and reference evapotranspiration (ETo) was estimated using the Penman–Monteith method. The optimal planting date was defined as the point when PCP ≥ 0.5 ETo, indicating sufficient water availability for seed germination. Results revealed that climate change increased variability in planting dates during the 1991–2020 period compared to 1961–1990. A spatially differentiated impact of climate change on planting dates was observed. In the 1991–2020 period, the earliest planting dates shifted toward the northwest, while the latest remained in the southern part of the region. These differentiated effects highlight the need for localized climate change adaptation strategies to support agricultural planning.

Keywords: Rainfed agriculture, evapotranspiration, climate variability.

INTRODUCTION

According to the United Nations Framework Convention on Climate Change (UNFCCC), climate change is defined as the "change in climate attributed directly or indirectly to human activity that alters the composition of the global atmosphere

and that is in addition to natural climate variability observed over comparable time periods." On the other hand, climate variability denotes variations in the mean state and other statistical characteristics, such as extreme events or standard deviations of climate, at all spatial and temporal scales (IPCC, 2018). Climate predictions indicate a warmer world over the next 50 years, with a 2 °C increase in temperature impacting yields of major crops (IPCC, 2014). Projections indicate that rainfed agricultural yields will decrease (Ureta *et al*., 2020).

By 2050, the world's population is projected to reach 9.3 billion inhabitants. To meet demand for food, annual production must increase by 5100 million Mg, implying a 60 % increase (FAO, 2015). In Mexico, rainfed maize (*Zea mays* L.) during the spring-summer cycle occupied the largest area planted in 2023, with 4 880 622.85 ha, representing 60 % of the total agricultural area, followed by beans (11 %). In the state of Puebla, the area planted to rainfed maize represented 78 % by 2023, and in the central-eastern part of Puebla, 88 % (SIAP, 2025).

In Mexico, the area planted with rainfed maize has decreased. In 2020, 5 439 354.2 ha were planted, and by 2023, 4 880 622.85 ha. Yields increased from 2.51 Mg ha^{-1} in 2020 to 2.75 Mg ha^{-1} in 2023. In 2023, the highest number of hectares lost was recorded (474 700.32 ha), followed by 2020 (303 292.21 ha), 2021 (134 270.67 ha), and 2022 (93 104.31 ha) (SIAP, 2025). Rainfed maize production is expected to increase by 11 % by 2030 compared to 2015, which is possible due to the increase in planted area (12 %) (Govaerts *et al*., 2019).

The increase in temperature and changes in precipitation distribution in the coming years will have a negative impact on the maize crops. In this regard, Han *et al*. (2022) found that high temperatures reduced yield; delayed planting significantly increased the risk of frost (>80 %) in mid- and high-latitude areas. Farmers struggle to establish their plantings due to the high spatial and temporal variability of precipitation, as well as its non-uniform distribution. In a projected warmer climate, the scheduling of agricultural practices will be affected, accelerating planting dates.

Climate change complicates determining the optimal planting date (Laux *et al*., 2008). Bigolin and Talamini (2024) evaluated climate change scenarios in a soybean-maize double cropping system and found a delay in the onset of the rainy season that delays planting. Producers define planting dates considering rain availability and the presence of frost. In this context, in northeast In China, adjusting planting dates is important to adapt to climate change, but there is little evidence on how well producers have done it (Zhu *et al.,* 2022). Hence, it is important to provide scientific evidence on the impact of climate change on planting dates to design adaptation strategies.

Climate change affects rainfed agricultural productivity, and its impact will depend on variations in climatic variables and seed sensitivity to these variables. For Lamichhane and Soltani (2020), an optimal sowing date contributes to having the best environmental conditions during their growth phases, which is reflected in higher yields. Furthermore, there is potential to increase crop productivity and adapt to warming (Huang *et al*., 2024). Choosing the right planting date is a strategy to

reduce the effects of climate change in agriculture, as the plant will not experience high temperatures and heat stress during its growth (Jafari *et al*., 2024). In this regard, Chassaigne-Ricciulli *et al*. (2021) studied the effect of four planting dates on hybrid maize seed yield and found that the earliest date achieved higher yields, since the grain filling period coincided with hot days and cool nights.

Some methodologies for assessing climate change impacts and planting dates use climate scenarios to quantify their effects on crop yields. In this context, Xu *et al*. (2024) considered climate projections based on CMIP6 models, reduced under four Shared Socioeconomic Pathways (SSP) scenarios. Alimagham *et al*. (2024) evaluated the potential impact of climate change on rainfed maize, millet, sorghum, and wheat using five global circulation models over three time periods (1995–2014 as baseline, 2040–2059, and 2080–2099) and two scenarios (SSP3-7.0 as typical and SSP5-8.5 as pessimistic).

The perception and strategies carried out by maize producers in the face of climate change have also been examined by using interviews, confirming that they have adjusted planting dates based on climatic conditions (Ramírez-Huerta *et al*., 2021). Tang *et al*. (2024) argue that water stress and planting dates have a significant impact on maize yield, based on a randomized complete block plot design in an experiment with five planting dates and six hybrids. The adoption of weather-resistant crop varieties plays a prominent role (Oriekhoe *et al*., 2024). Zimmermann *et al*. (2017) mention that farmers can adapt their sowing dates and crop thermal weather requirements to minimize yield losses.

Wang *et al*. (2024) argue that optimizing planting dates is a potential strategy to adjust maize production to climate change and increase yield. Meanwhile, Baum *et al*. (2020) indicate that sowing date and choice of crop variety are important factors in determining crop yield potential. However, there is a knowledge gap about how weather scenarios affect these choices, so selecting the best planting date can be used as an alternative to reduce these risks (Bigolin and Talamini, 2024). Therefore, the objective of the study was to identify the impact of climate change on planting dates of rainfed maize in the eastern region of Puebla. The hypothesis proposed was that with climate change a change in planting dates of rainfed maize is expected.

MATERIALS AND METHODS

The study region is located between 18° 37′ 30″ and 19° 20′ 29″ N and 97° 12′ 01″ and 97° 48′ 35″ W. It includes 11 municipalities in the eastern region of the state of Puebla (Figure 1) and is made up of plains, hills and mountains, with altitudes ranging from 1800 to 3200 m. Frosts occur frequently and unexpectedly; the season typically lasts from September to March, with an average of 90 days. The rainy season is from March to September, with an annual rainfall of 390 to 1200 mm (Juárez-Sánchez and Ramírez-Valverde, 2006). The most abundant soil type is ochric Regosol in 55.5 % of the territory, followed by ochric Andosol in 21.1 %, with Feozem and Rendzina in smaller proportions (Velázquez-López *et al*., 2019).

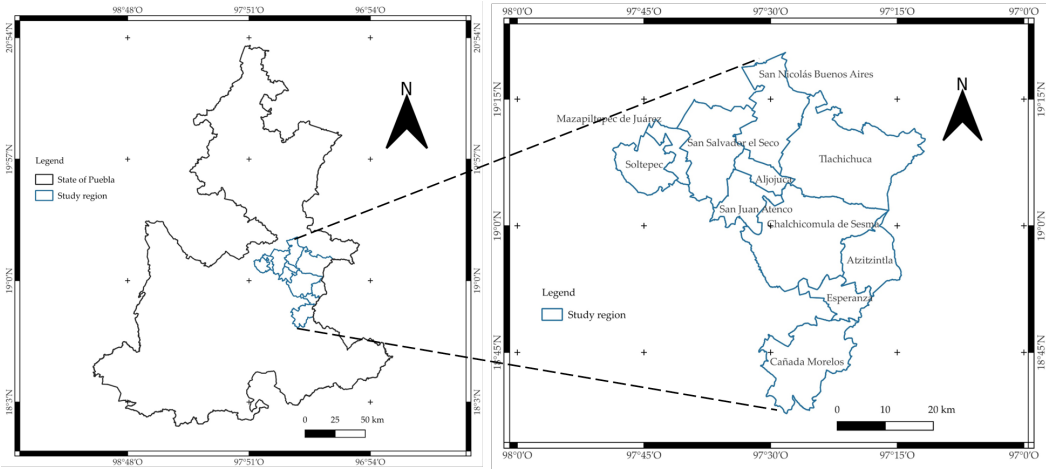

Figure 1. Municipalities comprising the study region in the state of Puebla, Mexico.

In 2023, 19 rainfed crops were planted in the region, with maize, beans, and grain barley accounting for 87.8 % (75 735 ha), 8.2 % (7081 ha), and 1.6 % (1148 ha), respectively, of the total rainfed area planted. Maize and beans are planted in all municipalities (SIAP, 2025). The optimal planting date is considered when precipitation (PCP) is ≥0.5 to the reference evapotranspiration (ETo), implying that the amount of water is sufficient for seed germination (FAO, 1997). The period from 1961 to 1990 has been maintained as the regulatory reference period for long-term climate change assessments (WMO, 2017). It is possible to determine whether climate change is present in the study region by comparing the normal (historical) daily values for PCP, ETo, and temperature from 1961–1990 to 1991–2020. These variables allow us to identify the dates of the beginning of the growing season for the periods evaluated.

For estimating evapotranspiration, the Penman-Monteith model stands out for its accuracy for different climatic conditions and regions. In this regard, Choque-Tarqui (2021) estimated evapotranspiration from satellite data, evaluating the Penman-Monteith, Thornthwaite, Hargreaves, Turc and Blaney, and Criddle methods, concluding that the Thornthwaite model has a very similar behavior to the Penman-Monteith model. Ortiz and Chile (2020) evaluated nine methods for estimating evapotranspiration, concluding that the best is the Penman-Monteith method.

Pipatsitee *et al*. (2023) used precipitable water vapor and temperature data derived from the Global Navigation Satellite System (GNSS-PWV), which proved to be suitable for daily evapotranspiration estimation and could be implemented for drought assessment and water resource management. Reyes-González *et al*. (2019) estimated evapotranspiration with remote sensing and validated it with *in situ* measurements, finding that both methods can be used to improve irrigation scheduling and preserve water resources in agriculture. Degano *et al*. (2024) estimated evapotranspiration with satellite and reanalysis data using the Google Earth engine and concluded that this method is a valid tool for estimating evapotranspiration.

To identify planting dates, daily precipitation (PCP), maximum temperature (*Tmax*), and minimum temperature (*Tmin*) data from 13 climatological stations from 1961 to 2020 (SMN, 2024) were used. The RClimDex software was used to analyze data quality, which allowed selecting climatological stations with less than 20 % of missing data and at least 10 years of uninterrupted data in the evaluated period. Reference evapotranspiration (ETo) was calculated on a daily scale with the Penman-Monteith method recommended by FAO (2006). The procedures and recommendations for limited climatic data were used, eliminating the need to use other methods and creating a consistent and transparent basis for a universal standardization of crop water requirement calculations.

ETo is calculated using daily data of *Tmax* and *Tmin*, actual vapor pressure (e_a), net radiation (R_n), and wind speed measured at 2 m (u_2). Missing humidity data were estimated assuming that the dew point temperature is similar to the daily minimum temperature using the following equation:

$$e_a = e^0(T_{min}) = 0.611exp\left[\frac{17.27T_{min}}{T_{min} + 237.3}\right]$$

where e_a is the actual vapor pressure, e^0 (*Tmin*) is the vapor saturation pressure and *Tmin* is the minimum temperature.

The solar radiation derived from thermal differences, i.e., the difference between *Tmax* and *Tmin*, was estimated and can be used to determine the fraction of extraterrestrial radiation reaching the earth's surface. The following equation was used for this purpose:

$$R_s = k_{R_s}\sqrt{(T_{max} - T_{min})R_a}$$

where R_s is the solar radiation [MJ m^{-2} d^{-1}], R_a is the extraterrestrial radiation [MJ m^{-2} d^{-1}], *Tmax* is the maximum temperature (°C), *Tmin* is the minimum temperature (°C), and k_{Rs} is the adjustment coefficient (0.16...0.19).

The adjustment coefficient is empirical and is differentiated for inland areas and coastal regions. For the former, the landmass dominates, and the air masses are not influenced by a large body of water, so $k_{Rs} \approx 0.16$. For coastal locations, situated near a large body of water, the air masses are influenced by a nearby body of water, so $k_{Rs} \approx 0.19$. In case of unavailability of wind data within the same region, a value of 2 m s^{-1} can be used as a temporal estimate. This value is the average of 2000 meteorological stations worldwide (FAO, 2006).

Once the optimal planting date (PCP ≥ 0.5 ETo) was estimated for each of the climatological stations, the QGIS geographic information system was used to interpolate the information using the weighted inverse distance method. During

interpolation, sample points are weighted so that the influence of one point relative to the others decreases as the distance from the unknown point being created increases. The weighting is assigned to the sample points by using a weighting coefficient that controls how the influence of the weighting decays as the distance to the new point increases. The larger the weighting coefficient, the less effect the points will have if they are far from the unknown point during the interpolation process. As the coefficient increases, the value of the unknown points approaches the value of the closest observation point (QGIS, 2023).

RESULTS AND DISCUSSION

The results show a change in sowing dates when comparing the base period (1961–1990) with the recent period (1991–2020). During the base period, Chalchicomula de Sesma recorded the earliest average planting date, occurring on Julian day 121 (May 1). This was followed by Mazapiltepec de Juárez and San Juan Atenco, where sowing typically occurred on Julian day 132 (May 12), and by Aljojuca, Soltepec, and San Salvador el Seco on Julian day 133 (May 13). In Tlachichuca, sowing dates were more variable, occurring on Julian days 133, 139 (May 19), and 143 (May 23). Similarly, in San Nicolás Buenos Aires, planting began on Julian days 135 (May 15) and 139 (May 19). The municipalities with the latest sowing dates were Atzitzintla, with dates recorded on Julian days 133, 138 (May 18), and 141 (May 21); Esperanza, on Julian days 138, 140 (May 20), and 146 (May 26); and Cañada Morelos, on Julian days 141, 145 (May 25), and 147 (May 27) (Figure 2). Precipitation and temperature are fundamental for estimating evapotranspiration. The changes in dates in the base period are due to the fact that in the areas with the earliest planting dates, climatic conditions for seed germination are established first.

In relation to the planting dates of the recent period, the earliest planting dates were registered in San Juan Atenco, on average, on Julian day 128 (May 8), followed by Soltepec on Julian days 134 (May 14) and 140 (May 20), Mazapiltepec on Julian day 141 (May 21), and San Salvador el Seco on Julian days 138 (May 18), 141, and 143 (May 23). In Chalchicomula, planting dates began on Julian days 133 (May 13), 135 (May 15), 138, and 143. In San Nicolás Buenos Aires, they began on Julian days 132 (May 12), 138, 144 (May 24), and 150 (May 30); in Tlachichuca on Julian days 134, 140, 143, 147 (May 27), and 153 (June 2); in Atzitzintla on Julian day 143; and in Esperanza on 145 (May 25) and 147, while the latest dates continued to occur in Cañada Morelos, beginning on Julian days 148 (May 28), 153, and 158 (June 7) (Figure 3).

Changes in the sowing dates of the 1961–1990 period compared to 1991–2020 are due to the decrease in precipitation and the increase in maximum temperature, which is reflected in a higher daily evapotranspiration. Therefore, more days are required to have sufficient water for seed germination, considering that the optimal sowing date occurs when PCP ≥ 0.5 ETo. The climatological station 21026 Ciudad Serdán, located in the municipality of Chalchicomula de Sesma, was used to compare both periods

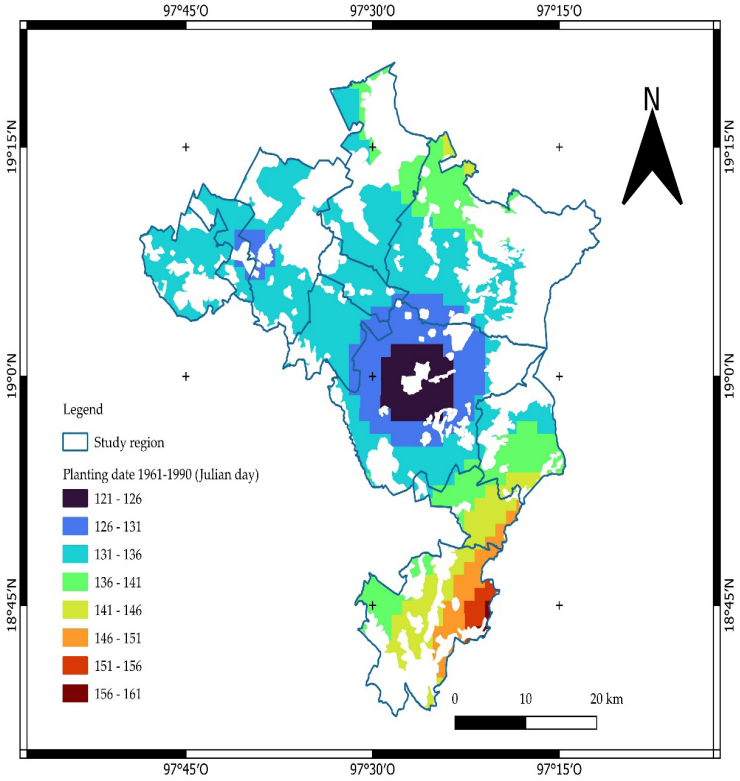

Figure 2. Optimal planting dates recorded during the base period (1961–1990) in the evaluated municipalities of the state of Puebla, Mexico. The colored areas represent rainfed agricultural areas, where maize (*Zea mays* L.) represents 87.8 % (75 735 ha) of the total. Areas in white represent other land uses.

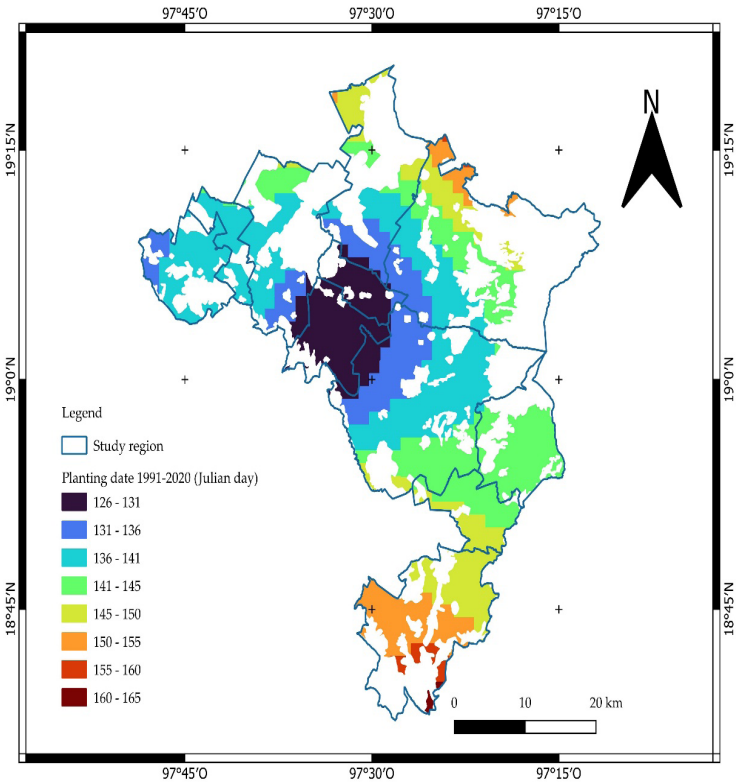

Figure 3. Optimal planting dates for the most recent period evaluated (1991–2020) in the evaluated municipalities of the state of Puebla, Mexico. The colored areas represent rainfed agricultural land, where maize (*Zea mays* L.) represents 87.8 % (75 735 ha) of the total. The areas in white represent other land uses.

to the same planting date. For 1961–1990, it began on Julian day 121 (May 1), and the final growth date was considered to be September 30, because growers expect the first frosts on this date. During the growing season, there was a PCP of 660.8 mm, a *Tmax* of 22.5 °C and an ETo of 716.8 mm.

When comparing the climatic values for the period 1991–2020 with the same dates from May 1 to September 30, PCP values of 458.4 mm, *Tmax* of 24.7 °C, and ETo of 744.8 mm were observed, indicating a decrease in PCP of 202.4 mm, an increase in *Tmax* of 2.2 °C, and an increase in ETo of 27.6 mm during the growing season. ETo values would go from 4.7 to 4.9 mm per day, which causes a higher average evapotranspiration. More PCP is now required to establish the ideal conditions for planting, resulting in an average of 10 days to move planting dates in the recent period.

When comparing the recent period of station 21026, which lasted from Julian day 121 (May 01) to 131 (May 10), the PCP was 438.5 mm, *Tmax* was 24.6 °C, and ETo was 727.4 mm per day. When comparing these climatic values of the base period growing season, a decrease in precipitation of 222.3 mm, an increase in *Tmax* of 2.1 °C, and an increase in ETo of 10 mm per day were found, so that the daily ETo went from 4.7 to 5.1 mm per day. For the most recent period, climate change has had a differentiated impact in the study region in terms of planting date shifts, as there are areas where planting dates are later and areas where they are earlier (Figure 4).

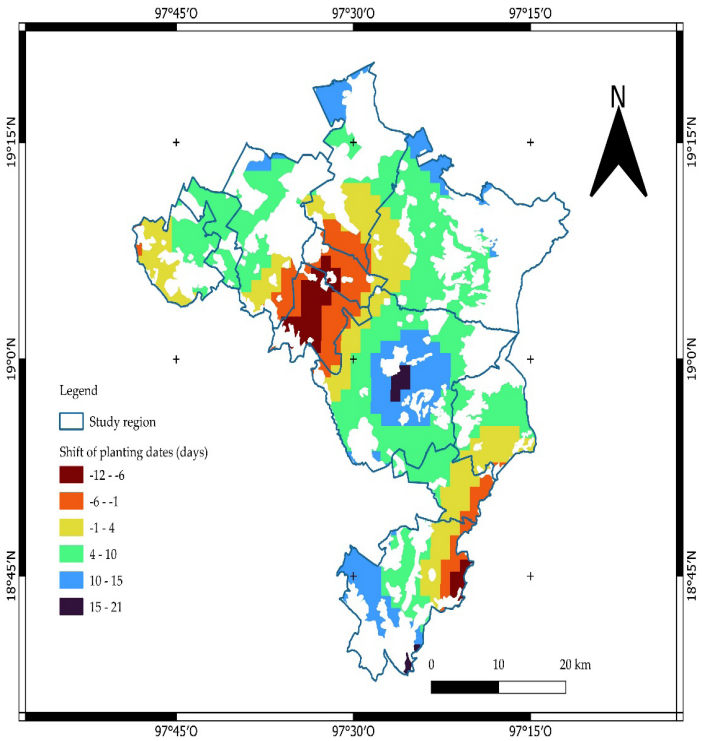

Figure 4. Shift of planting dates for the period 1991–2020 versus 1961–1990 in the evaluated municipalities of the state of Puebla, Mexico. The colored areas represent rainfed agricultural land, where maize (*Zea mays* L.) represents 87.8 % (75 735 ha) of the total. The areas in white symbolize other land uses.

During the base period, ideal conditions for seed germination occurred in the central zone, Chalchicomula, extending to the north through San Juan Atenco, Aljojuca, San Salvador el Seco, Mazapiltepec, Soltepec, the southern zone of Tlachichuca, and San Nicolás Buenos Aires, then in the northern zone of San Nicolás Buenos Aires, Tlachichuca, and Atzitzintla, and finally in the southern zone of Atzitzintla, Esperanza, and Cañada Morelos. From 1991 to 2020, the ideal conditions for seed germination moved to the northwest, starting in San Juan Atenco and Aljojuca and extending to the municipalities of Soltepec, Mazapiltepec, San Salvador el Seco, and the northwest zone of Chalchicomula, then to the northern zone of San Nicolás Buenos Aires, the northeast of Tlachichuca, Atzitzintla, and Esperanza, to finally settle in Cañada Morelos.

There is no research work that identifies planting dates using the approach used, laying the groundwork for what may be expected in the future when analyzing planting dates using climatic scenarios. The changes in sowing dates identified confirm the strategies that producers have carried out due to the delay in rainfall, which leads to a shift in sowing dates (Pérez-Magaña *et al*., 2021). Ramírez-Huerta *et al*. (2021) indicate that some producers advanced planting dates due to earlier than normal rainfall. On the other hand, Osorio-García *et al.* (2012) mention that the farmers' argument for the adoption of intermediate planting dates (before May 15) is due to changes in the rainfall pattern in the region, which have caused production systems under residual moisture (early plantings) to become increasingly scarce. According to Navarro-Hinojoza *et al*. (2023), in many localities in the country's north, weather conditions such as rainfall patterns, amount of precipitation, and climatic variations are causing the development of strategies to counteract uncertainty, such as changing planting dates and using short-cycle seeds to avoid yields being affected by frosts expected in late September and early OctoberWhen quantifying the impact of the change in planting date, in the particular case of the study region, a field trip was carried out on September 28, 2025. A farmer in the community of San Juan Arcos Ojo de Agua carried out a 10-day differentiated planting, and the result was that the first planting did not have enough water, which caused the maize crop (cacahuazintle) to be damaged by the presence of red spider mite. In comparison to the crop that was planted 10 days later, it was predicted it would have a good yield. In this sense, Bigolin and Talamini (2024) indicate that a delay in the planting date translates into fewer days of rain to complete its cycle, so it is important to plant varieties of a shorter genotype so that the production of the maize crop is not affected.

The most significant changes in planting dates were recorded in Chalchicomula, where planting is increasingly late and takes up to 21 days, followed by Tlachichuca and San Salvador el Seco, which have late dates of up to 15 days, and Atzitzintla, where late dates are up to 10 days later. Mazapiltepec has later dates ranging from 4 to 10 days. The municipalities with the earliest plantings are San Juan Atenco and Aljojuca, with dates ranging from 1 to 12 days earlier. Cañada Morelos has areas with earlier dates up to 12 days earlier and later dates of up to 15 days. In San Nicolás Buenos Aires, there are earlier dates of up to 6 days before and later dates of up to 15 days, while

Esperanza and Soltepec have earlier dates of up to 6 days before and later dates of up to 10 days.

In terms of the impact of climate change on planting dates in both periods, there was less variability in 1961–1990, indicating that producers sowed systematically almost on the same date, whereas there is greater variability in 1991–2020 (Figure 5), causing problems for farmers who must wait for favorable moisture conditions to be established before beginning the agricultural cycle. An analysis of variance was performed to determine if the variability in both periods is the same or has changed, with a significance level of 0.05. A *p*-value of 7.5714×10^{-11} was obtained, indicating significant statistical differences between both periods, with greater variability in the recent period and showing that the region is being affected.

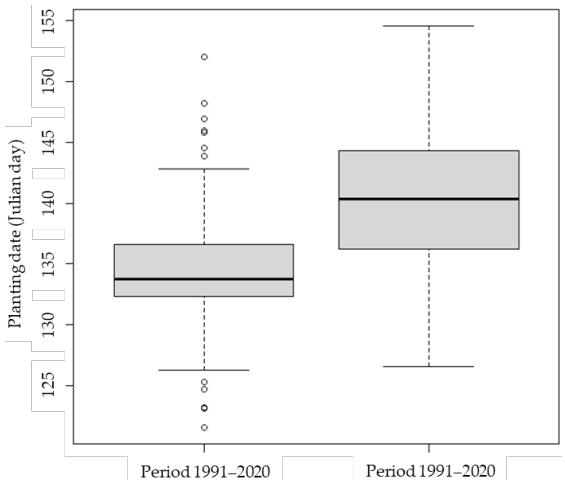

Figure 5. Variability of the planting date of the base period (1961–1990) compared to the most recent period (1991–2020) in the evaluated municipalities of the state of Puebla, Mexico.

Chassaigne-Ricciulli *et al.* (2021) recommend differential sowing dates based on information on the degree days (°D) of development. Given this, once the optimal date was identified, the degree days for the period 1991–2020 were calculated in relation to the reference period for each climatological season, and September 30 was considered as the final date of the growing season. The DegDay software (Snyder, 2002) was used for this purpose. There is a differentiated impact on the dynamics of thermal capacity in the growing season in the period 1991–2020 in relation to the base period (Figure 6). According to the Neild and Newman (1987) variety classification of maize genotypes, the accumulated degree days during the growing season require 1150 to 1315, 1315 to 1590, and 1590 to 1760 °D for short-, intermediate-, and long-cycle genotypes, respectively. In the study region, short-cycle genotype varieties are required, since the

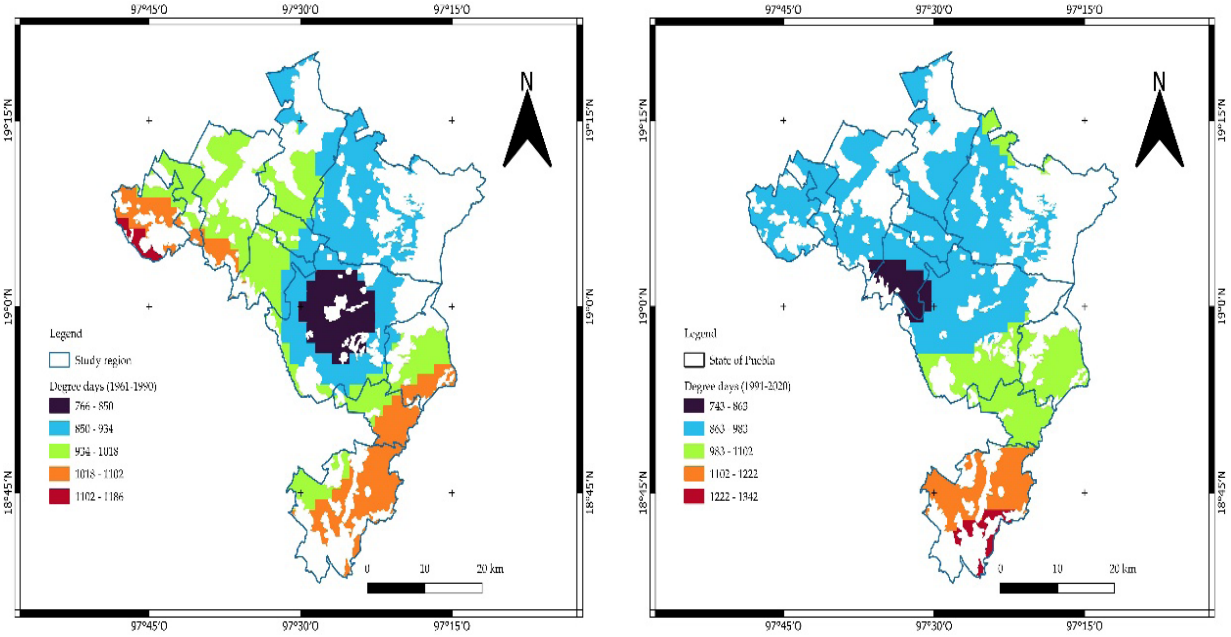

Figure 6. Degree days (°D) of maize (*Zea mays* L.) crop development during the period 1961–1990 (left) compared to the period 1991–2020 (right) in the evaluated municipalities of the state of Puebla, Mexico.

highest degree days accumulated during the growing season are 1342 °D, relatively above the upper limit of the requirements for a short-cycle genotype. Degree days are another important climatic variable that should be considered for planning agricultural activities, so it would be important to quantify the degree day requirements of the different Criollo seeds.

The findings show that degree days have increased, but they have also decreased in certain areas. In Soltepec, Mazapiltepec, San Salvador el Seco, and San Juan Atenco, values ranged from 28 to 248 °D, while in Chalchicomula they have decreased/increased from -138 to 193 °D. In Tlachichuca and Esperanza, they have decreased/increased from -28 to 193 °D; in Atzitzintla, they have decreased/increased from -28 to 83 °D; in San Nicolás Buenos Aires and Aljojuca, they have decreased/increased from -138 to 83 °D; and in Cañada Morelos, they have the largest increases, ranging from -28 to 303 °D (Figure 7). As a result of the decrease in precipitation and increase in temperature during the growing season, it is concluded that short-cycle and drought-resistant genotypes must be used in the study region.

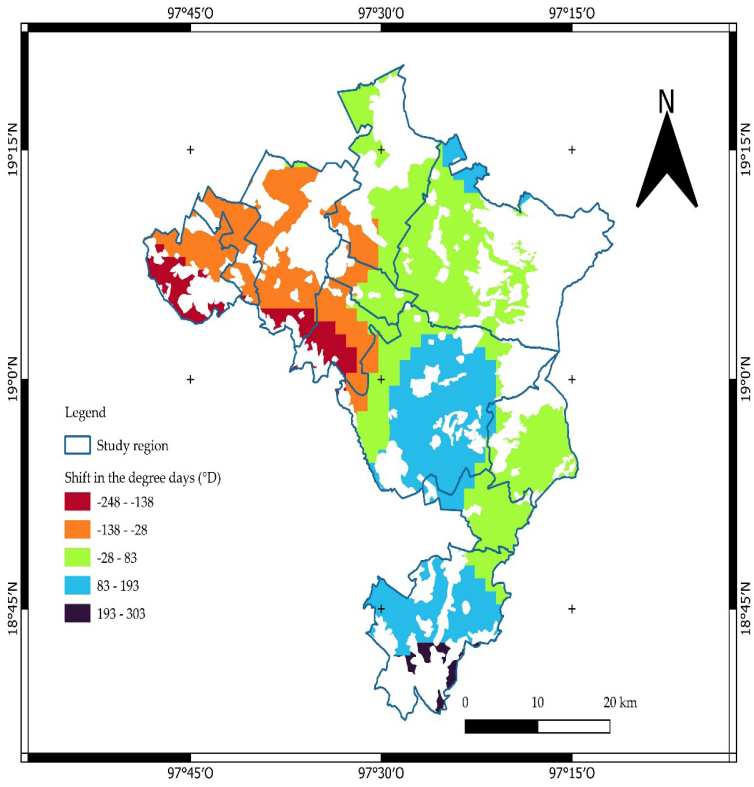

Figure 7. Changes in the dynamics of the degree days (°D) of maize (*Zea mays* L.) crop development in the period 1991–2020 compared to the period 1961–1990 in the evaluated municipalities of the state of Puebla, Mexico.

CONCLUSIONS

A significant impact of climate change on planting dates was identified during the recent period (1991–2020) compared to the reference period (1961–1990). The increased climatic variability observed in recent decades has made it difficult for producers to determine optimal or favorable dates to initiate the agricultural cycle, as temperature and humidity conditions become less predictable. This differentiated impact has caused a spatial displacement of planting dates, since the earliest planting dates tend to be located towards the northwest, while the latest ones persist in the southern part of the study region. As a result, producers are forced to adopt shorter-cycle varieties to avoid early frost damage.

It is essential to validate the planting dates estimated in this study with those actually used by producers in order to evaluate the degree of current adaptation to the new climatic conditions. Understanding these adjustments will allow the design of more effective local adaptation strategies to climate change. Finally, it is recommended

that future studies and planning tools consider probable rainfall values instead of 30-year historical averages for the estimation of planting dates or the beginning of the growing season, as this would provide greater precision in the face of increasing climatic variability.

ACKNOWLEDGEMENTS

We wish to thank the Postgraduate College Campus Puebla and the Secretariat of Science, Humanities, Technology, and Innovation (SECIHTI) for the scholarship granted to Rogelio Bernal-Morales for his doctoral studies.

REFERENCES

Alimagham S, van Loon MP, Ramírez-Villegas J, Adjei-Nsiah S, Baijukya F, Bala A, Chikowo R, Silva JV, Soulé AM, Taulya G, *et al.* 2024. Climate change impact and adaptation of rainfed cereal crops in sub-Saharan Africa. European Journal of Agronomy 155: 127137. https://doi.org/10.1016/j.eja.2024.127137

Baum M, Licht M, Huber I, Archontoulis S. 2020. Impacts of climate change on the optimum planting date of different maize cultivars in the central US corn belt. European Journal of Agronomy 119: 126101. https://doi.org/10.1016/j.eja.2020.126101

Bigolin T, Talamini E. 2024. Impacts of climate change scenarios on the corn and soybean double-cropping system in Brazil. Climate 12 (3): 42. https://doi.org/10.3390/cli12030042

Chassaigne-Ricciulli AA, Mendoza-Onofre LE, Córdova-Téllez L, Carballo-Carballo A, San Vicente-García FM, Dhliwayo T. 2021. Effective seed yield and flowering synchrony of parents of CIMMYT three-way-cross tropical maize hybrids. Agriculture 11 (2): 161. https://doi.org/10.3390/agriculture11020161

Choque-Tarqui CE. 2021. Estimación de la evapotranspiración a partir de datos satelitales para la región de Alto Beni, Norte de La Paz. Revista de Investigación e Innovación Agropecuaria y de Recursos Naturales 8 (1): 45–53. https://doi.org/10.53287/dmrt8855uy51u

Degano MF, Rivas RE, Bayala MI. 2024. Determinación de la evapotranspiración con datos satelitales y de reanálisis utilizando Google Earth Engine. Tecnología y Ciencias del Agua 15 (4): 137–193. https://doi.org/10.24850/j-tyca-2024-04-04

FAO (Food and Agriculture Organization of the United Nations). 1997. Zonificación agro-ecológica: guía general. Boletín de suelos No. 73. FAO. Rome, Italy. http://fao.org/4/w2962s/w2962s00.htm (Retrieved: June 2024).

FAO (Food and Agriculture Organization of the United Nations). 2006. Evapotranspiración del cultivo. Guías para la determinación de los requerimientos de agua de los cultivos. Rome, Italy. 298 p.

FAO (Food and Agriculture Organization of the United Nations). 2015. Construyendo una visión común para la agricultura y alimentación sostenibles. Rome, Italy. 50 p.

Govaerts B, Cárdenas-Chávez XF, Fernández A, Vega D, Vázquez O, Pérez M, Carvajal A, Ortega P, López P, Rodríguez R, *et al.* 2019. Maíz para México - plan estratégico 2030. Ciudad de México, México. 144 p.

Han X, Dong L, Cao Y, Lyu Y, Shao X, Wang Y, Wang L. 2022. Adaptation to climate change effects by cultivar and sowing date selection for maize in the Northeast China Plain. Agronomy 12 (5): 984. https://doi.org/10.3390/agronomy12050984

Huang N, Liang J, Lun F, Jiang K, Long, B, Chen X, Gao R, Zhou Y, Men J, Bi P, Pan Z. 2024. Quantifying the sensitivity of maize production to long-term trends in fertilization and regional climate in China. Journal of Agriculture and Food Research 15: 101015. https://doi.org/10.1016/j.jafr.2024.101015

IPCC (Intergovernmental Panel on Climate Change). 2014: Summary for policymakers. Climate change 2014: Impacts, adaptation, and vulnerability. Part A: Global and sectoral aspects. Cambridge University Press: Cambridge, UK. 34 p.

IPCC (Intergovernmental Panel on Climate Change). 2018: Anexo I: Glosario. *In* Calentamiento global de 1,5 °C. Informe especial del IPCC sobre los impactos del calentamiento global de 1,5 ºC con respecto a los niveles preindustriales y las trayectorias correspondientes que deberían seguir las emisiones mundiales de gases de efecto invernadero, en el contexto del reforzamiento de la respuesta mundial a la amenaza del cambio climático, el desarrollo sostenible y los esfuerzos por erradicar la pobreza. Geneva, Switzerland, pp: 73–94.

Jafari A, Bihamta M, Moghbel M, Soufizadeh S, Bazgeer S, Karimi M. 2024. Effect of planting date and cultivar on growth stages, morphological traits and growth indices of corn in Karaj City. Journal of Crops Improvement 26 (1): 17–34. https://doi.org/10.22059/jci.2023.345619.2727

Juárez-Sánchez JP, Ramírez-Valverde B. 2006. El Programa de Subsidios Directos a la Agricultura (Procampo) y el incremento de la producción de maíz en una región campesina de México. Ra Ximhai 2 (2): 373–391. https://doi.org/10.35197/rx.02.02.2006.04.jj

Lamichhane JR, Soltani E. 2020. Sowing and seedbed management methods to improve establishment and yield of maize, rice and wheat across drought-prone regions: A review. Journal of Agriculture and Food Research 2: 100089. https://doi.org/10.1016/j.jafr.2020.100089

Laux P, Kunstmanna H, Bárdossy A. 2008. Predicting the regional onset of the rainy season in West Africa. International Journal of Climatology 28 (3): 329–342. https://doi.org/10.1002/joc.1542

Navarro-Hinojosa E, Fuentes E, Flores-Estrada MS. 2023. Estrategias de sobrevivencia ante contextos de vulnerabilidad socioambiental en pequeños agricultores de zonas semiáridas del noreste mexicano. Revista Perspectivas Rurales 21 (42): 1–21. http://doi.org/10.15359/prne.21-42.6

Neild RE, Newman JE. 1987. Nch-40 growing season characteristics and requirements in the corn belt. National Corn Handbook. Purdue University, West Lafayette, IN, USA. https://www.extension.purdue.edu/extmedia/nch/nch-40.html (Retrieved: September 2024).

Oriekhoe OI, Adisa O, Ilugbusi BS. 2024. Climate change and food supply chain economics: a comprehensive analysis of impacts, adaptations, and sustainability. International Journal of Applied Research in Social Sciences 6 (3): 267–278. https://doi.org/10.51594/ijarss.v6i3.885

Ortiz RS, Chile M. 2020. Métodos de cálculo para estimar la evapotranspiración de referencia para el Valle de Tumbaco. Siembra 7 (1): 70–79. https://doi.org/10.29166/siembra.v7i1.1450

Osorio-García N, López-Sánchez H, Gil-Muñoz A, Ramírez-Valverde B, Gutiérrez-Rangel N, Crespo-Pichardo G, Montero-Pineda A. 2012. Utilización, oferta y demanda de tecnología para producción de maíz en el Valle de Puebla, México. Agricultura, Sociedad y Desarrollo 9 (1): 55–69.

Pérez-Magaña A, Méndez-Cadena ME, Martínez-Corona GB. 2021. Representaciones sociales sobre el cambio climático por productores agrícolas de la Sierra Nevada de Puebla. *In* Rivera-

Ramírez JM, Becerra-Espinosa H. (coords.), Teoría y Educación Ambiental. Reflexiones en Tiempo de Pandemia. Universidad Autónoma de Chapingo: Puebla, México, pp: 51–66.

Pipatsitee P, Ninsawat S, Tripathi NK, Shanmugam M, Chitsutti P. 2023. Estimating daily potential evapotranspiration using GNSS-based precipitable water vapor. Heliyon 9 (7): e17747. https://doi.org/10.1016/j.heliyon.2023.e17747

QGIS (Quantum Geographic Information System). 2023. Una introducción fácil a los SIG. https://docs.qgis.org/3.28/es/docs/gentle_gis_introduction/spatial_analysis_interpolation.html (Retrieved: March 2024).

Ramírez-Huerta M, Juárez-Sánchez JP, Ramírez-Valverde B. 2021. Estrategias de adaptación en el cultivo del maíz ante la variabilidad climática, Puebla, México. Revista Geográfica Venezolana 62 (2): 368–380.

Reyes-González A, Reta-Sánchez DG, Sánchez-Duarte JI, Ochoa-Martínez E, Rodríguez-Hernández K, Preciado-Rangel P. 2019. Estimación de la evapotranspiración de maíz forrajero apoyada con sensores remotos y mediciones *in situ*. Terra Latinoamericana 37 (3): 279–290. https://doi.org/10.28940/terra.v37i3.485

SIAP (Servicio de Información Agroalimentario y Pesquero). 2025. Producción agrícola. Gobierno de México. Servicio de Información Agroalimentario y Pesquero. Ciudad de México, México. https://nube.agricultura.gob.mx/cierre_agricola/ (Retrieved: April 2024).

SMN (Servicio Meteorológico Nacional). 2024. Información estadística climatológica. Gobierno de México. Servicio Meteorológico Nacional. Ciudad de México, México. https://smn.conagua.gob.mx/es/climatologia/informacion-climatologica/informacion-estadistica-climatologica (Retrieved: June 2024).

Snyder RL. 2002. DegDay version 1.01 written March 2002. University of California. Department of Land, Air and Water Resources, Atmospheric Science. Davis, CA, USA.

Tang H, Xie X, Zhang L, Liu C. 2024. Assessing the influence of planting dates on sustainable maize production under drought stress conditions. Sustainability 16 (11): 4571. https://doi.org/10.3390/su16114571

Ureta C, González EJ, Espinosa A, Trueba A, Piñeyro-Nelson A, Álvarez-Buylla ER. 2020. Maize yield in Mexico under climate change. Agricultural Systems 177: 102697. https://doi.org/10.1016/j.agsy.2019.102697

Velázquez-López J, Juárez-Sánchez JP, Ramírez-Valverde B, del Valle-Sánchez M, Jiménez-Morales J, Taboada-Gaytán OR. 2019. Regionalización de la producción de maíz de temporal en el Estado de Puebla, México. Cuadernos Geográficos 58 (2): 152–167. https://doi.org/10.30827/cuadgeo.v58i2.7531

Wang X, Liu F, Zhao N, Du X, Yin P, Li T, Lan T, Feng D, Kong F, Yuan J. 2024. Optimizing sowing dates increase solar radiation to mitigate maize lodging and yield variability: A five-year field study. Journal of Integrative Agriculture. Journal Pre-proof. https://doi.org/10.1016/j.jia.2024.03.078

WMO (World Meteorological Organization). 2017. Directrices de la Organización Meteorológica Mundial sobre normales climáticas (OMM-N° 1203). Edición de 2017. Geneva, Switzerland. 21 p.

Xu Q, Liang H, Wei Z, Zhang Y, Lu X, Li F, Wei N, Zhang S, Yuan H, Liu S, Dai Y. 2024. Assessing climate change impacts on crop yields and exploring adaptation strategies in Northeast China. Earth's Future 12 (4): e2023EF004063. https://doi.org/10.1029/2023EF004063

Zhu G, Liu Z, Qiao S, Zhang Z, Huang Q, Su Z, Yang X. 2022. How could observed sowing dates contribute to maize potential yield under climate change in Northeast China based

on APSIM model. European Journal of Agronomy 136: 126511. https://doi.org/10.1016/j.eja.2022.126511

Zimmermann A, Webber H, Zhao G, Ewert F, Kros J, Wolf J, Britz W, Vries W. 2017. Climate change impacts on crop yields, land use and environment in response to crop sowing dates and thermal time requirements. Agricultural Systems 157: 81–92. https://doi.org/10.1016/j.agsy.2017.07.007

Agrociencia

SUCTION IRRIGATION IN ORNAMENTAL PLANTS: ANALYSIS OF WATER CONSUMPTION IN *Dimorphotheca ecklonis* DC. AND *Graptopetalum paraguayense* (N.E.Br.) E. Walther

María Magdalena **Nevárez-Favela**[1], Abel **Quevedo-Nolasco**[1*], J. Cruz **García-Albarado**[2], Martin Alejandro **Bolaños-González**[1], Adolfo **López-Pérez**[1], Moisés **Márquez-Velázquez**[3], Ruben **Esparza-Orozco**[1]

[1]Colegio de Postgraduados Campus Montecillo. Postgrado en Hidrociencias. Carretera México-Texcoco km 36.5 Montecillo, Texcoco, State of Mexico, Mexico. C. P. 56264.
[2]Colegio de Postgraduados Campus Córdoba. Postgrado en Paisaje y Turismo Rural. Carretera Córdoba-Veracruz km 348, Manuel León, Amatlán de los Reyes, Veracruz, Mexico. C. P. 94953.
[3]Colegio de Postgraduados Campus Montecillo. Postgrado Edafología. Carretera México-Texcoco km 36.5 Montecillo, Texcoco, State of Mexico, Mexico. C. P. 56264.
* Author for correspondence: abcdqn@gmail.com

Citation: Nevárez-Favela MM, Quevedo-Nolasco A, García-Albarado JC, Bolaños-González MA, López-Pérez A, Márquez-Velázquez M, Esparza-Orozco R. 2025. Suction irrigation in ornamental plants: Analysis of water consumption in *Dimorphotheca ecklonis* DC. and *Graptopetalum paraguayense* (N.E.Br.) E. Walther. **Agrociencia** 59(6): 915-928. https://doi.org/ 10.47163/agrociencia.v59i6.3381

Editor in Chief:
Dr. Fernando C. Gómez Merino

Received: February 16, 2025.
Approved: September 19, 2025.
Published in Agrociencia: September 25, 2025.

ABSTRACT

Suction irrigation in ornamental species provides only the amount of water required by the soil-plant-atmosphere system, reducing water losses due to evaporation, runoff, and percolation. In this work, an experiment was conducted in subdivided plots arranged in randomized blocks to evaluate the daily and cumulative water consumption of *Dimorphotheca ecklonis* DC. and *Graptopetalum paraguayense* (N.E.Br.) E. Walther. Two substrate mixtures were used: tezontle (3–4 mm) with peat (2:1) and tezontle (4–6 mm) with peat (2:1), with suction heights of 8 and 15 cm (H8 and H15). The results showed significant statistical differences ($p < 0.05$) in cumulative water consumption, suction height, and plant type. The ornamental species showed significant statistical differences in terms of water consumption (daily and cumulative), plant height, cover, and total fresh and dry matter production, where *D. ecklonis* recorded the highest values, while *G. paraguayense* maintained higher substrate moisture. These findings show that suction irrigation is an efficient water supply option in green infrastructure systems because water consumption is self-regulating.

Keywords: porous capsules, water use efficiency, self-supply, naturation, substrates.

INTRODUCTION

Freshwater resources are increasingly scarce, and their availability is under growing pressure from population growth, urbanization, and climate change (van Iersel *et al.*, 2016). Agriculture, which includes ornamental horticulture, is the main consumer of water resources globally, accounting for nearly 80 % of total use (Velasco-Muñoz *et al.*, 2018). The ornamental horticulture industry is on the rise, requiring the implementation

of strategies to use water efficiently and minimize its environmental impact (van Iersel *et al.*, 2016). Ornamental production in Mexico before 1994 relied mainly on rainfed agriculture. After that year, the number of ornamental species cultivated under irrigation increased to more than 58, while in rainfed systems, the number rose only from 28 to 32 (LaFevor, 2022). Therefore, research and adoption of irrigation systems that promote efficient water use are indispensable.

Suction irrigation using ceramic porous emitters, commonly applied in small-scale vegetable production in arid regions, also has potential for ornamental plant cultivation (Peña-Casadevalls and Vargas-Rodríguez, 2018). The shapes of ceramic porous emitters are diverse. Early models were shaped as pans, pots (Cai *et al.*, 2018) and cylinders but changed to spheres. Olguín-Palacios (1975) used truncated cone-shaped emitters made of brick-colored clay with a capacity of 300 cm^3. In contrast, Quevedo-Nolasco *et al.* (2023) used spherical emitters of white kaolinite ceramic, connected to the water source by a 5 mm internal diameter flexible plastic tube, and operated under suction. Zhang *et al.* (2009) tested cylindrical ceramic emitters with dimensions of 15 cm in length, 4 cm external radius, and 3 cm internal radius, a saturated hydraulic conductivity of 0.012 cm d^{-1}, and operation under both positive and negative pressure. Similarly, Liu *et al.* (2023a) worked with cylindrical white clay emitters with a 1 cm internal radius, a 2 cm external radius, and a 7 cm length, operated at hydraulic loads ranging from 0 to 100 cm. Cai *et al.* (2021) also used cylindrical white clay emitters but with dimensions of 7 cm length, 4 cm external radius, and 2 cm internal radius.

Currently, porous emitters are typically buried, leading some researchers to classify them as a form of subirrigation (Cai *et al.*, 2018). Subsurface irrigation with ceramic emitters provides a continuous supply of water and nutrients at a constant low rate that maintains soil moisture and reduces evaporative water losses (Liu *et al.*, 2023b). Subsurface irrigation has economic and ecological advantages compared to surface irrigation, such as savings in labor, energy, water, and nutrients, as well as having more uniform plant growth, lower air humidity, fewer foliar diseases, and fewer environmental problems due to nutrient and chemical leaching (Qiaosheng *et al.*, 2007).

Irrigation with porous emitters is performed with both positive and negative charges (suction) (Olguín-Palacios, 1975; Zhang *et al.*, 2009). The water output of porous emitters used in suction irrigation depends on the size and pore percentage of the emitter and its surface, in addition to the height from which the water is absorbed, the suction gradient generated (depending on the evapotranspirative demand and soil type), and the thermal and osmotic gradient (Olguín-Palacios, 1975).

Irrigation with porous emitters is used in the production of crops such as tomato, goji berry, apple, bean, strawberry, corn, ornamental plants (geranium, petunia, and gazania), and pitahaya, among others. However, its application in ornamental horticulture is poorly documented. Therefore, the objective of this work was to analyze the water consumption of two species of ornamental plants by suction irrigation in two substrates and two suction heights, in pots. The effects of suction height (H),

substrate type (S), and plant species (P) on response variables, including daily and cumulative water consumption as well as biophysical traits, were evaluated using a split-plot design in randomized blocks, under the hypothesis that at least one factor influences water consumption in the studied species.

MATERIALS AND METHODS

The experiment was carried out in a greenhouse at the Postgraduate College Campus Montecillo, in Texcoco, State of Mexico (19° 27′ 37.1′′ N and 98° 54′ 12.12′′ W), at an altitude of 2240 m, where the climate is semi-dry temperate with summer rains. The species assessment period was from May 9 to July 27, 2023.

An experimental design with plots subdivided into randomized blocks was established. Suction heights of 8 and 15 cm (H8 and H15, respectively) were measured in the large plot, substrate combination (S) in the medium plot, and plant type (P) in the small plot. The suction height represents the difference in level between the center of the capsule and the water level of the source. The substrate mixture consisted of tezontle and peat in a 2:1 (v/v) ratio. A coarse substrate (Sg) with tezontle particle diameters between 4 and 6 mm and a fine substrate (Sf) with tezontle particle diameters between 3 and 4 mm were used. The plants (P) were used *Dimorphotheca ecklonis* DC. (Pd) and *Graptopetalum paraguayense* (N.E.Br.) E. Walther (Pg). A total of eight treatments (2H × 2S × 2P) and four replicates were used, giving a total of 32 experimental units. Each pot was used as an experimental unit, which had a volume of 6 L (23.5 cm top diameter and 20 cm height) and a porous emitter (capsule) substrate-plant with storage as a water source.

The suction irrigation system consisted of a porous kaolinite capsule, 12 cm in diameter, equipped with two opposing tubes of 4 mm internal diameter. One tube was used to fill the capsule and subsequently sealed, while the other was connected to the water source (Figure 1). To evaluate the ability of the emitters to yield water, a sorptivity analysis was performed according to the methodology of Quevedo-Nolasco *et al.* (2023). This irrigation system does not require an external source of energy but takes advantage of the suction gradient, or differences in water matrix potential, that operates between a continuously dried soil due to the evapotranspiration of a crop and a porous body communicated with the water source, which allows a continuous, efficient, and localized supply only in the crop root zone (Olguín-Palacios, 1975). In order to differentiate each mixture, the water retention curve (de Boodt *et al.*, 1974) and bulk density were determined at the Soil Physics Laboratory of the Postgraduate College.

Graptopetalum paraguayense, commonly known as mother-of-pearl or ghost plant, is a Mexican species of the Crassulaceae family. Its rosettes reach 15–20 cm in diameter, and it exhibits crassulacean acid metabolism (CAM). In addition to its ornamental use, it is used medicinallly for liver disorders, diuretic effects, diabetes, hypertension, and pain relief in China (Ai *et al.*, 2017). *Dimorphotheca ecklonis* (Cape daisy or polar star)

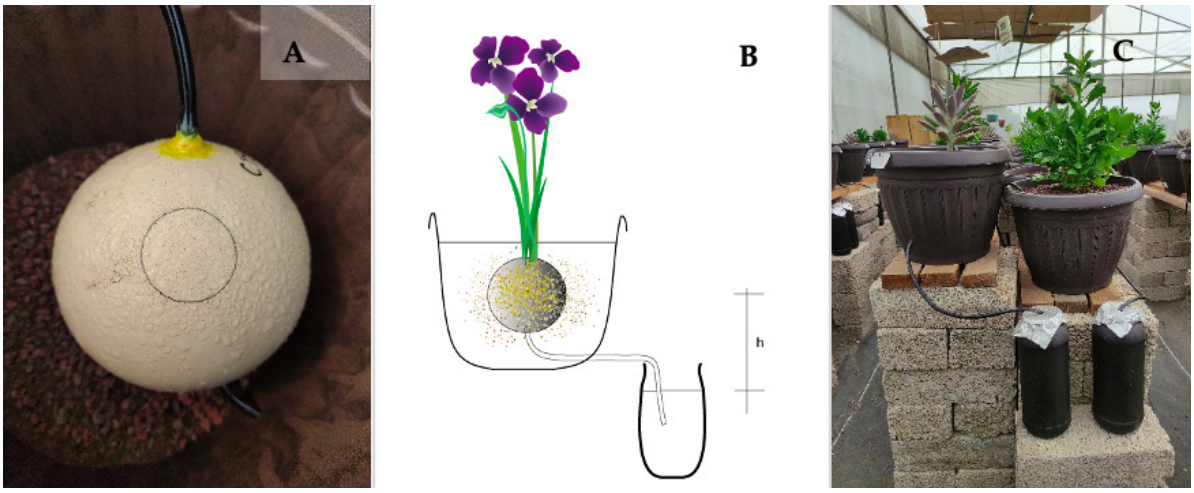

Figure 1. Suction irrigation system used for the evaluation of water consumption. A: porous capsule releasing water; B: suction irrigation scheme with porous emitter; C: suction irrigation on ornamental species.

is an ornamental African species of the Asteraceae family with abundant white, pink, purple, or salmon flowers measuring 5–8 cm (Khalil and Seleem, 2019). These plants were selected for their availability in nurseries, size, low maintenance requirements, and adaptability to the climate of the evaluation site. Prior to transplanting, both were acclimatized in the greenhouse for three weeks, reaching average heights of 7 cm and 6 cm and diameters of 8.5 cm and 6 cm, respectively.

Well water (pH 6.9 and electrical conductivity of 276 mS cm^{-1}) was used as the base for preparing the nutrient solution, following the formulation of Steiner (1984). The solution had an electrical conductivity of 0.5 dS m^{-1}, with 3 NO_3^-, 0.25 $H_2PO_4^-$, 1.75 SO_4^{2-}, 1.75 K^+, 2.25 Ca^{2+}, and 1 Mg^{2+} milliequivalents per liter (mEq L^{-1}) and an osmotic pressure of 0.018 MPa. The following nutrient sources were used: calcium nitrate ($Ca(NO_3)_2$), potassium nitrate (KNO_3), monopotassium phosphate (KH_2PO_4), potassium sulfate (K_2SO_4), magnesium sulfate ($MgSO_4$), and sulfuric acid (H_2SO_4), in addition to micronutrients (Rovensa Next, Mexico), with iron (Fe^{2+}), manganese (Mn^{2+}), zinc (Zn^{2+}), boron (H_3BO_3), copper (Cu^{2+}), and molybdenum (MoO_4^{2-}). The nutrient solution was placed in a 1.1 L black container with a lid to avoid algae proliferation.

During the experiment, daily water consumption (DWC) was measured, which started on May 9 by adding the volume consumed on the previous day by means of a test tube at 8:00 am. Daily consumption was transformed to daily irrigation lamina by dividing the daily water consumption (cm^3) by the exposed area of the pot (430 cm^2). The daily water consumptions were summed to obtain the cumulative water consumption (CWC). Moisture variations in the substrates were recorded and calculated using the gravimetric method at a distance of 2 cm from the emitter.

Daily evaporation was measured using a tub placed inside the greenhouse. In addition, plant height (cm), canopy cover (%), and substrate volumetric moisture content (v/v) were recorded weekly. Volumetric moisture represents the ratio of water volume to soil volume and is dimensionless. Moisture was calculated by the gravimetric method from the start of the experiment until July 5. To avoid damage to the roots of *D. ecklonis*, samples of 40 cm^3 of substrate were obtained at a distance of 1.5 cm from the capsule. At the end of the experiment, on July 27, 2023, total fresh matter (TFM) was measured by destructive sampling (aerial and root biomass) and total dry matter (TDM). Additionally, water use efficiency (WUE) was calculated by dividing TDM by the cumulative water consumption in lamina.

Analysis of variance (ANOVA) was performed for response variables ($p < 0.05$). The assumptions of normality of residuals were examined with the Shapiro-Wilk test ($p > 0.05$). Data independence was analyzed graphically, and for homogeneity of variances, Bartlett's test was used ($p > 0.01$). When significant differences between means were found, Tukey's test was performed. Statistical analysis was performed with the RStudio program (R Core Team, 2024).

RESULTS AND DISCUSSION

Characteristics of the porous capsules and substrates

The sorptivity values of the porous capsules had a mean of 0.576 mm $s^{-1/2}$, a standard deviation of 0.033, and 5.71 % coefficient of variation. As for the substrates, the bulk density was 0.59 g cm^{-3} for Sf and 0.56 g cm^{-3} for Sg. On water retention, the fine substrate (Sf) retained slightly more water compared to the coarse substrate (Sg) at water column suction heights of 0, 10, and 50 cm (Table 1). Also, Sf presented greater pore space, aeration capacity, readily available water, and reserve water.

Table 1. Volumetric water content of fine (Sf) and coarse (Sg) substrates at different suction (water column) values.

Suction (CCA)	Fine substrate (v/v)	Coarse substrate (v/v)
0	0.49	0.38
10	0.22	0.14
50	0.16	0.11
100	0.09	0.09

CCA: centimeters of water column; v/v: volumetric moisture content (dimensionless). Fine substrate (Sf) consisted of tezontle (3–4 mm) mixed with peat (2:1), and coarse substrate (Sg) consisted of tezontle (4–6 mm) mixed with peat (2:1).

Water release capacity of the porous capsules

The volume of water released to suction varied between 21 and 442 mL d^{-1}, with a mean of 110 mL d^{-1}, which depended on several factors such as the hydraulic characteristics of the emitters, including suction height, crop, and environmental conditions (Quevedo-Nolasco *et al.*, 2023). In tomato with suction irrigation, Vargas-Rodríguez *et al.* (2010) reported irrigation doses between 180 and 390 mL d^{-1} $plant^{-1}$. Similarly, Peña-Casadevalls and Vargas-Rodríguez (2018) reported water consumptions between 200 and 330 mL d^{-1}. Although the operating conditions, type of crop, environment, porous media, and suction height are not the same, it should be emphasized that the suction irrigation system meets the water demand.

Several irrigation systems operate using porous emitters. Abu-Zreig *et al.* (2006) found leakage rates of 125–1020 mL d^{-1} operating at positive pressure in an irrigation system with porous pots (pitchers). Liu *et al.* (2023b) observed irrigation laminae below 5 mm d^{-1} in a tomato crop irrigated with porous emitters operating at positive hydraulic loads between 0.1 and 0.5 m. Unlike these systems, suction irrigation allows precise control of water delivery, providing water exactly when needed and minimizing losses due to infiltration.

Daily water consumption by factors

In the experimental units, lamina water consumption varied between 1 and 8 mm d^{-1}, with a behavior similar to water evaporation that depends on atmospheric weather elements. The suction heights of 15 and 8 cm (H15 and H8, respectively) and plant species (Pg and Pd) factors influenced water consumption (Figures 2A and 2C). However, the substrate (Sg and Sf) had no effect (Figure 2B), so despite minor variations in terms of water retention, there were no significant differences.

Daily water consumption varied between 1.7 and 5.5 mm (mean 3 mm) at a suction height of 8 cm and between 1.1 and 3.7 mm (mean 2.1 mm) at 15 cm. By substrate, the coarse substrate (Sg) averaged 2.6 mm (1.5–5.5 mm), while the fine substrate (Sf) averaged 2.5 mm (1.1–4.2 mm). For plant species, Pg consumed 1.1–2.3 mm and Pd 2.2–5.5 mm, with a mean of 1.7 and 3.4 mm, respectively.

Cumulative water consumption by factors

At the end of the experiment, the established species had a water consumption of 236.7 mm at 8 cm suction height compared to 170.9 mm obtained at 15 cm due to less force to recover water from the source and lower negative pressure (Figure 2D). In irrigation with porous emitters, the applied hydraulic load determines the amount of water available to the soil, plant, and atmospheric system (Liu *et al*., 2023a). In this type of irrigation, ceramic porous emitters operate both at negative pressure or suction (Olguín Palacios, 1975; Quevedo-Nolasco *et al.*, 2023) and positive pressure (Liu *et al.*, 2023b).

Cumulative water consumption per substrate was similar, with values of 198.7 mm for Sf and 208.9 mm for Sg (Figure 2E). This should be interpreted with caution, since water

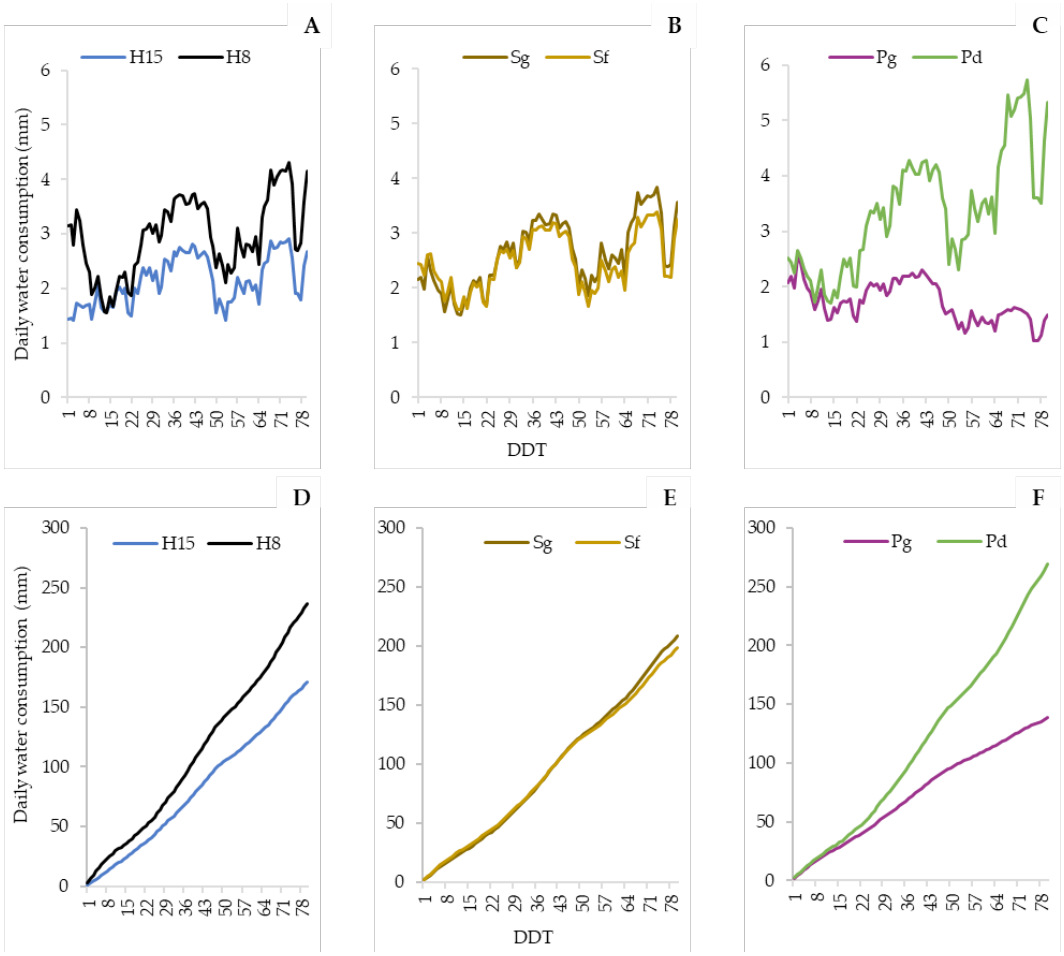

Figure 2. Daily (A–C) and accumulated (D–F) water consumption of ornamental species under suction irrigation, showing effects of suction height (H15, H8), substrate type (Sg, Sf), and plant species (Pg, Pd). H15: suction height of 15 cm; H8: suction height of 8 cm; Sg: tezontle (4–6 mm)-peat 2:1 (v/v); Sf: tezontle (3–4 mm)-peat 2:1 (v/v); Pg: *Graptopetalum paraguayense* (N.E.Br.) E. Walther; Pd: *Dimorphotheca ecklonis* DC.; DDT: days after transplanting.

movement in soil (or growth medium) is influenced by its physical characteristics (Ma *et al.*, 2022), where differences between substrates in terms of water retention were minimal (Table 2).

In terms of plant type, the cumulative water consumption of *D. ecklonis* and *G. paraguayense* was 269.4 and 138.2 mm, respectively (Figure 2F). The difference in cumulative water consumption is consistent with FAO (2006), which indicates that different species can have different levels of evapotranspiration, even under the same environmental conditions, due to differences in transpiration resistance, height, foliage roughness, albedo, orientation, soil cover, and root characteristics.

Table 2. Volumetric distribution of water, air, and solids in fine (Sf) and coarse (Sg) substrates composed of tezontle-peat mixtures (de Boodt *et al*., 1974).

Variable	Sf (v/v)	Sg (v/v)
Solid material	0.51	0.62
Total pore space	0.49	0.38
Aeration capacity	0.28	0.25
Water readily available	0.06	0.03
Reserve water	0.06	0.02
Water hardly available	0.09	0.08

/v: volumetric content (dimensionless). Fine substrate (Sf): tezontle 3–4 mm + peat 2:1 (v/v); Coarse substrate (Sg): tezontle 4–6 mm + peat 2:1 (v/v).

Daily and cumulative water consumption by treatment

In the first 10 d after transplanting, the daily water consumption of all treatments depended on the suction height. The lower the height (lower negative pressure), the higher the water consumption and vice versa (Figure 3A), which was statistically validated. Seedlings acclimatized during the early stages, but as transpiration increased, so did water consumption. This period of increased water consumption during the first days of the establishment of the porous capsule irrigation system was also observed by Liu *et al.* (2023b) in a tomato crop irrigated with positive pressure porous emitters.

Treatments with *D. ecklonis* (Pg), regardless of substrate particle size and suction height, consumed a greater amount of water compared to *G. paraguayense* (Pd). As noticed by Durhman *et al.* (2007) and Khalil and Seleem (2019), both species exhibit distinct morphological and physiological characteristics. In particular, *D. ecklonis* showed faster growth than *G. paraguayense*, which was reflected in a higher water demand.

The average cumulative water consumption (expressed in mm) per treatment, in descending order, was as follows: H8SgPd (348), H8SfPd (286.9), H15SfPd (234.3), H15SgPd (208.2), H8SgPg (156), H8SfPg (155.8), H15SgPg (123.1), and H15SfPg (117.8) (Figure 3B). These water consumption values are comparable with those reported by Yang *et al.* (2024), who documented water consumptions between 300 and 450 mm in tomato crops irrigated with porous emitters at a pressure of 20 cm. Similarly, Liu *et al.* (2023a), also employing porous emitters, observed water consumptions of 85 and 110 mm in open-grown goji bushes under pressures of 40 and 80 cm, respectively, which also took advantage of a cumulative rainfall of 269.1 mm.

Substrate moisture

The volumetric moisture ratio (v/v) in the substrates remained between 0.09 and 0.19, with maximum moisture retention values of 0.38 and 0.49 for Sg and Sf, respectively.

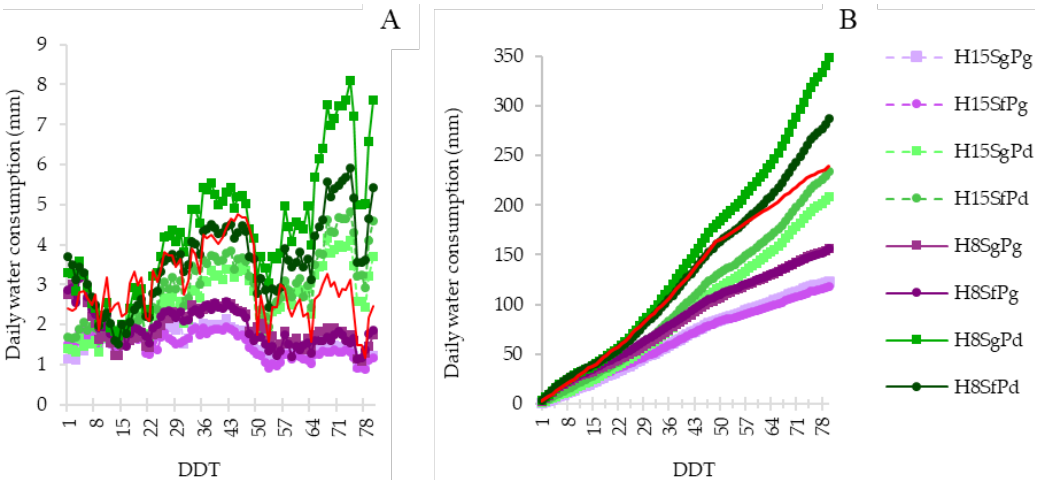

Figure 3. Daily (A) and cumulative (B) water consumption of treatments as influenced by suction height, substrate, and plant species. H15: suction height of 15 cm; H8: suction height of 8 cm; Sg: tezontle (4-6 mm)-peat mixture 2:1 (v/v); Sf: tezontle (3-4 mm)-peat mixture 2:1 (v/v); Pg: *Graptopetalum paraguayense* (N.E.Br.) E. Walther; Pd: *Dimorphotheca ecklonis* DC; DDT: days after transplanting.

The distribution of moisture in the substrate depends, in part, on the location of the sampling point in relation to the emitter, since more distance, both vertically and horizontally, results in a decrease in moisture content (Siyal *et al.*, 2009). This peripheral distribution of water around the emitter is influenced by the particle size of the substrate and the water demand of the crop.

In previous studies, Zhang *et al.* (2009) reported volumetric soil moisture values of up to 0.43 at depths of 30–40 cm when using suction irrigation (30–50 cm) with porous emitters buried at a 20 cm depth; however, this moisture decreased over the course of days. Similarly, Liu *et al.* (2023b) observed soil moisture values between 0.17 and 0.22 when using porous emitters with pressures from 10 to 50 cm in tomato crops.

Suction height

Higher water uptake was observed at lower suction height (8 cm), registering a value of 236.7 ± 95 mm in H8 versus 170.9 ± 59.4 mm in H15. This uptake was inversely proportional to moisture content in the substrates, which was also higher at lower suction height (H8: 18.8 ± 2.5) compared to H15 (16.3 ± 2.6). The higher water availability in H8 allowed for superior plant development, evidenced by higher plant height, cover, total fresh matter, and total dry matter (Table 3). These results coincide with those reported by Ma *et al.* (2022), who emphasize that water availability directly influences the morphological and physiological characteristics of plants.

Table 3. Effects of suction height, substrate, and plant species on water consumption, substrate moisture, and evaluated plant growth variables.

Factors	DWC	CWC	Substrate moisture	Plant height	Soil cover	TFM	TDM	WUE
	(mm d^{-1})	(mm)	(v/v)	(cm)	(%)	(g)	(g)	(g TDM cm^{-1} H_2O)
H8	3.0 ± 0.7[a]	236.7 ± 95[a]	18.8 ± 2.5[a]	17.8 ± 8.8[a]	48.7 ± 43.3[a]	193.6 ± 111.2[a]	31.9 ± 27.7[a]	1.1 ± 0.7[a]
H15	2.1 ± 1.2[b]	170.9 ± 59.4[b]	16.3 ± 2.6[b]	14.1± 5.0[b]	34.0 ± 21.1[b]	139.4 ± 48[b]	17.7 ± 11.9[b]	0.9 ± 0.4[a]
p-value	0.0006	0.0006	0.028	0.0343	0.0305	0.028	0.0018	0.1846
Sg	2.6 ± 0.9[a]	208.8 ± 23.8[a]	18.4 ± 2.5[a]	16.1 ± 8.3[a]	47.8 ± 42.8[a]	175.3 ± 99.7[a]	27.1 ± 25.6[a]	1.1 ± 0.6[a]
Sf	2.5 ± 1.2[a]	198.7 ± 76[a]	16.8 ± 2.9[a]	15.8 ± 6.3[a]	34.9 ± 22.7[a]	157.8 ± 78.3[a]	22.5 ± 18.7[a]	1.0 ± 0.5[a]
p-value	0.4977	0.4977	0.1272	0.8123	0.052	0.4348	0.2249	0.4482
Pd	3.4 ± 0.3[a]	269.9 ± 71.3[a]	16.3 ± 2.5[b]	21.0 ± 7.2[a]	66.0 ± 33.8[a]	220.3 ± 96.6[a]	41.4 ± 20.5[a]	1.5 ± 0.5[a]
Pg	1.7 ± 0.9[b]	138.2 ± 24.6[b]	18.8 ± 2.6[a]	10.9 ± 1.7[b]	16.7 ± 2.4[b]	112.7 ± 27[b]	8.2 ± 2.3[b]	0.6 ± 0.2[b]
p-value	<0.0001	<0.0001	0.0235	<0.0001	<0.0001	0.0003	<0.0001	<0.0001

Values indicate mean ± standard deviation. Different letters represent significant differences (Tukey, $p < 0.05$). DWC: daily water consumption; CWC: cumulative water consumption; TFM: total fresh matter; TDM: total dry matter; WUE: water use efficiency; H15: suction height of 15 cm; H8: suction height of 8 cm; Sg: tezontle (4–6 mm)-peat mixture 2:1 (v/v); Sf: tezontle (3–4 mm)-peat mixture 2:1 (v/v); Pg: *Graptopetalum paraguayense* (N.E.Br.) E. Walther; Pd: *Dimorphotheca ecklonis* DC.

In this context, several authors have recommended the use of positive pressure with ceramic emitters for crop production in intensive farming systems. Pressure loads of 30, 40, and 70 cm (Liu *et al.*, 2023c), as well as ranges between 20 and 50 cm (Cai *et al.*, 2018), have been proposed. When applying pressurized water, the irrigation supply depends on both the hydraulic load and the operation mode of the system. Self-regulation of water supply in these systems is based on the hydraulic characteristics of the emitter, substrate type, emitter size, shape, and suction height, as well as the water requirements of the crop and environmental conditions.

Substrates

No significant differences were detected between substrates (S) in total daily water consumption or in the other variables analyzed. The retention of readily available water was 0.06 and 0.03 (v/v) for the respective substrates, according to Tukey's test. However, previous studies have reported contrasting findings. For example, Quevedo-Nolasco *et al*. (2023) observed substrate-related differences in water consumption using Duncan's test. Similarly, Wang *et al*. (2019) indicated that the physical characteristics of soils or growth media affect water movement, where the matrix suction influences water availability and, consequently, plant development. In line with this, Pacheco-Hernández *et al*. (2016) reported significant differences in height, leaf area, and dry matter in poinsettia cultivated in different substrate mixtures under suction irrigation.

Likewise, A'saf *et al*. (2020) documented variations in morphology, physiology, growth, and flower quality in three ornamental species grown across six substrate combinations.

Ornamental species

Both plant species presented significant differences in daily water consumption (CAD), cumulative water consumption (CWC), substrate moisture, plant height, cover, total fresh matter (TFM), total dry matter (TDM), and water use efficiency (WUE). In general, the highest values were recorded in *D. ecklonis*, with the exception of substrate moisture. Similarly, Quevedo-Nolasco *et al.* (2023) reported differences in cumulative water consumption in three ornamental species (gazania, petunia, and geranium) under suction irrigation for 80 days, with values ranging from 11.2 to 18.6 cm. These results highlight how different species can present differentiated patterns of water consumption depending on their specific characteristics.

Efficient use of water

No significant differences in water use efficiency (WUE) were found in relation to the suction height (H) of the emitters, registering values of 0.9 and 1.1 g TDM cm^{-1} H_2O for suction heights of 8 and 15 cm, respectively. Similarly, substrate type (S) did not show significant differences in terms of WUE, with values of 1.1 and 1.0 g TDM cm^{-1} H_2O for coarse (Sg) and fine (Sf) substrates, respectively. In contrast, significant differences were indeed observed as a function of species type (P), with WUE values of 1.5 and 0.6 g TDM cm^{-1} H_2O for *G. paraguayense* and *D. ecklonis*, respectively. This difference is congruent with the phenological and genomic differences existing between both species.

The study of water use efficiency in ornamental plants by suction irrigation with porous emitters is still limited. Zhang *et al.* (2009), in an experiment conducted with tomato crop, evaluated irrigation with porous emitters at different pressures (0, -30, and -50 cm H_2O column). The results showed that WUE was inversely proportional to yield. At a pressure of 0 cm H_2O, the highest yield was obtained, with 1.17 kg per pot and WUE of 24.9 kg m^{-3}, while at -50 cm H_2O, the lowest yield was recorded, with 0.95 kg per pot and WUE of 32.8 kg m^{-3}. Similar results were observed in greenhouses in Israel and Spain, where AD values between 25 and 33 kg m^{-3} of tomato (30–40 L kg^{-1}) were reported (Salazar-Moreno *et al.*, 2014). These findings indicate that the suction irrigation system can change both WUE and yield depending on the suction height, substrate type, and, possibly, plant species grown.

In contrast, under pressure subirrigation conditions with porous emitters, Liu *et al.* (2023a) evaluated Goji berry production, finding WUE values of 1, 1.01, and 0.85 kg m^{-3} for pressure loads of 40, 60, and 80 cm, respectively. These results show how variations in irrigation pressure can influence water use efficiency, depending on the management of the system. Suction irrigation has the advantage of self-regulation of water from ceramic emitters, which represents a beneficial potential in terms of water efficiency.

CONCLUSIONS

Statistically significant differences were found in relation to suction height, understood as the difference between the source and the centroid of the irrigation emitter. At lower heights, the highest values were achieved in daily and cumulative water consumption, substrate moisture, plant height, coverage, total fresh matter, and total dry matter. No statistically significant differences were identified between substrate mixtures, probably due to the minimal differences in their physical characteristics (particle size), which are related to water retention.

Among the ornamental species evaluated, statistically significant differences were found in the parameters of daily and cumulative water consumption, height, coverage, and total fresh and dry matter production. *Dimorphotheca ecklonis* showed the highest values for these parameters, while *G. paraguayense* showed a higher level of moisture in the substrate. Both the objective and the hypothesis were validated, demonstrating that the factors of suction height and type of ornamental species significantly influenced the response variables evaluated.

ACKNOWLEDGEMENTS

To the Secretariat of Science, Humanities, Technology, and Innovation (SECIHTI) for awarding M.N.N.F. a scholarship to further his studies and research, as well as to the Postgraduate College Montecillo Campus, Postgraduate Program in Hydro Sciences.

REFERENCES

A'saf TS, Al-Ajlouni MG, Ayad JY, Othman YA, St. Hilaire R. 2020. Performance of six different soilless green roof substrates for the Mediterranean region. Science of the Total Environment 730: 139182. https://doi.org/10.1016/j.scitotenv.2020.139182

Abu-Zreig MM, Abe Y, Isoda H. 2006. The auto-regulative capability of pitcher irrigation system. Agricultural Water Management 85 (3): 272–278. https://doi.org/10.1016/j.agwat.2006.05.002

Ai L, Chung YC, Jeng KCG, Lai PFH, Yeh SC, Lee KC, Lin SY, Xia Y, Wang G, Cui SW. 2017. Antioxidant hydrocolloids from herb *Graptopetalum paraguayense* leaves show anti-colon cancer cells and anti-neuroinflammatory potentials. Food Hydrocolloids 73: 51–59. https://doi.org/10.1016/j.foodhyd.2017.06.027

Cai Y, Wu P, Zhang L, Zhu D, Wu S, Zhao X, Chen J, Dong Z. 2018. Prediction of flow characteristics and risk assessment of deep percolation by ceramic emitters in loam. Journal of Hydrology 566: 901–909. https://doi.org/10.1016/j.jhydrol.2018.07.076

Cai Y, Wu P, Zhu D, Zhang L, Zhao X, Gao X, Ge M, Song X, Wu Y, Dai Z. 2021. Subsurface irrigation with ceramic emitters: An effective method to improve apple yield and irrigation water use efficiency in the semiarid Loess Plateau. Agriculture, Ecosystems and Environment 313: 107404. https://doi.org/10.1016/j.agee.2021.107404

De Boodt M, Verdonck O, Cappaert I. 1974. Method for measuring the water release curve of organic substrates. Acta Horticulturae 37: 2054–2063. https://doi.org/10.17660/actahortic.1974.37.20

Durhman AK, Rowe DB, Rugh CL. 2007. Effect of substrate depth on initial growth, coverage, and survival of 25 succulent green roof plant taxa. HortScience 42 (3): 588–595. https://doi.org/10.21273/hortsci.42.3.588

FAO (Food and Agriculture Organization). 2006. Evapotranspiración del cultivo. Guías para la determinación de los requerimientos de agua de los cultivos. Estudios FAO Riego y Drenaje 56. Roma, Italia. http://www.fao.org/3/x0490s/x0490s00.htm (Retrieved: December 2023).

Khalil SE, Seleem FM. 2019. Role of biochar soil amendment for alleviation of adverse effects of water stress on *Dimorphotheca ecklonis* plants. Bioscience Research 16 (2): 1337–1353.

LaFevor MC. 2022. Spatial and temporal changes in crop species production diversity in Mexico (1980–2020). Agriculture 12 (7): 985 https://doi.org/10.3390/agriculture12070985

Liu X, Han M, Zhang L. 2023a. A new subsurface ceramic emitter for smallholders without pumps: design, hydraulic performance, and field application. Irrigation Science 41 (6): 835–845. https://doi.org/10.1007/s00271-023-00877-4

Liu X, Zhang L, Liu Q, Yang F, Han M, Yao S. 2023b. Subsurface irrigation with ceramic emitters: optimal working water head improves yield, fruit quality and water productivity of greenhouse tomato. Scientia Horticulturae 310: 111712. https://doi.org/10.1016/j.scienta.2022.111712

Liu X, Zhang L, Zhang C, Sun Y, Yang X. 2023c. Optimization algorithm for determining working water head of subsurface irrigation with ceramic emitters based on soil wetting patterns. Computers and Electronics in Agriculture 212: 108069. https://doi.org/10.1016/j.compag.2023.108069

Ma Y, Liu H, Yu Y, Guo L, Zhao W, Yetemen O. 2022. Revisiting soil water potential: Towards a better understanding of soil and plant interactions. Water 14 (22): 3721. https://doi.org/10.3390/w14223721

Olguín-Palacios, C. 1975. Suction irrigation; description of the method and advances in investigation. First drip irrigation seminar. Colegio de Postgraduados: Texcoco, Mexico.

Pacheco-Hernández P, López-Martínez V, Andrade-Rodríguez M, Alia-Tejacal I, de Jesús Sainz-Aispuro M, Villegas-Torres OG, Arteaga-Ramírez R, Vázquez-Peña MA. 2016. Cuantificación microlisimétrica del consumo de agua residual tratada en la nochebuena (*Euphorbia pulcherrima* Willd. ex Klotzsch). Tecnología y Ciencias del Agua 7 (6): 179–186.

Peña-Casadevalls MS, Vargas-Rodríguez P. 2018. Suction irrigation technology for the production of tomato (*Lycopersicon esculentum)* under controlled conditions. Revista Ciencias Técnicas Agropecuarias 27 (2).

Qiaosheng S, Zuoxin L, Zhenying W, Haijun L. 2007. Simulation of the soil wetting shape under porous pipe sub-irrigation using dimensional analysis. Irrigation and Drainage 56 (4): 389–398. https://doi.org/10.1002/ird.290

Quevedo-Nolasco A, Herrera-Gómez SS, Zamora-Morales BP, Rodríguez-Cruz E. 2023. Water consumption of three ornamental species with the suction irrigation system. Agro Productividad 16 (5): 3–15. https://doi.org/10.32854/agrop.v16i5.2354

R Core Team. 2024. R: A language and environment for statistical computing. R Foundation for Statistical Computing, Vienna, Austria. URL https://www.R-project.org/

Salazar-Moreno R, Rojano-Aguilar A, López-Cruz IL. 2014. La eficiencia en el uso del agua en la agricultura controlada. Tecnología y Ciencias del Agua 5 (2): 177–183.

Siyal AA, van Genuchten MT, Skaggs TH. 2009. Performance of pitcher irrigation system. Soil Science 174 (6): 312–320. https://doi.org/10.1097/SS.0b013e3181a97532

Steiner AA. 1984. The universal nutrient solution. Proceedings of the Sixth International Congress on Soilless Culture: Wageningen, Netherlands, pp: 633–650.

van Iersel MW, Chappell MR, Thomas PA. 2016. Optimizing growth, quality, and profits through precision irrigation in ornamental plant production. Acta Horticulturae 1131: 57–64. https://doi.org/10.17660/ActaHortic.2016.1131.8

Vargas-Rodríguez P, Peña-Casadevalls M, García-Victoria K, Roble-de la Rosa D, Álvarez-Andión R. 2010. Sistema de riego con emisores porosos para la producción de tomate con ahorro de agua y energía: propuesta de diseño. Ingeniería Hidráulica y Ambiental 31 (1): 34–42.

Velasco-Muñoz JF, Aznar-Sánchez JA, Belmonte-Ureña LJ, Román-Sánchez IM. 2018. Sustainable water use in agriculture: A review of worldwide research. Sustainability 10 (4): 1084. https://doi.org/10.3390/su10041084

Wang JJ, Long HY, Huang YF, Wang XL, Cai B, Liu W. 2019. Effects of different irrigation management parameters on cumulative water supply under negative pressure irrigation. Agricultural Water Management 224: 105743. https://doi.org/10.1016/j.agwat.2019.105743

Yang F, Wu P, Zhang L, Wei Y, Tong X, Wang Z. 2024. Effects of subsurface irrigation types on root distribution, leaf photosynthetic characteristics, and yield of greenhouse tomato. Scientia Horticulturae 328: 112883. https://doi.org/10.1016/j.scienta.2024.112883

Zhang J, Saito H, Kato M. 2009. Study on subsurface irrigation using ceramic pitcher on tomato cultivation in greenhouse. Journal of Arid Land Studied 19 (1): 265–267.